DISSERTATION

TUGGING ON THE *HEARTSTRINGS*: DETERMINING THE FUNCTION OF *TBX5* IN EARLY CARDIAC DEVELOPMENT

Submitted by

Lindsay E. Parrie

Department of Biology

In partial fulfillment of the requirements

For the Degree of Doctor of Philosophy

Colorado State University

Fort Collins, Colorado

Spring 2012

Doctoral Committee:

Advisor: Deborah Garrity

Gerrit Bouma
Donald Mykles
ASN Reddy

ABSTRACT

TUGGING ON THE *HEARTSTRINGS*: DETERMINING THE FUNCTION OF *TBX5* IN EARLY CARDIAC DEVELOPMENT

During cardiac morphogenesis, the vertebrate heart acquires a characteristic three dimensional shape well-suited for efficient function. The morphology of the developing cardiac organ reflects a series of changes in the cardiomyocytes themselves, which must become specified, migrate, proliferate, grow in size, alter their shape and adhesive properties, and develop ultrastructure, among other differentiated characteristics. Mutation of the T-box transcription factor *tbx5* leads to embryonic lethal cardiac phenotypes and forelimb malformations in vertebrate models. Haploinsufficiency of Tbx5 results in Holt-Oram Syndrome (HOS), a human congenital disease characterized by cardiac and forelimb defects. Homozygous mutation of zebrafish *tbx5a* in *heartstrings* (*hst*) embryos also leads to lethal defects in cardiac looping morphogenesis and prevents initiation of pectoral fin formation. Here I describe a new *hst* mutant allele ($tbx5a^{s296}$) which encodes a premature stop codon within the *tbx5a* T-box region, a location likely to generate a full loss-of-function allele. Data from comparative genetics and immunoblot analyses indicate that both alleles are null. I find that mutants completely lacking Tbx5a generated normal cardiomyocyte numbers in early chamber morphogenesis stages. Moreover, in situ hybridization data and functional assays support the idea that venous

differentiation is not seriously impaired in zebrafish mutants, in contrast to mouse. However, cardiac cell size was significantly smaller in both chambers of *tbx5a* mutants. Hearts stalled early in the process of cardiac looping, but cell shape changes associated with chamber ballooning surprisingly still occurred. These studies point to a critical role for Tbx5a in growth-related aspects of cardiac differentiation, and suggest that morphologic events of cardiac looping morphogenesis and chamber ballooning are genetically separable. A second zebrafish *tbx5* paralog was recently described, termed *tbx5b*, which showed a lower amount of sequence conservation than is typical for a T-box gene. Based on overlapping expression patterns within the embryonic heart, I hypothesized that functional redundancy between *tbx5a* and *tbx5b* might reduce the severity of cardiac phenotypes for *tbx5a* mutant embryos. I here report that the cardiac phenotypes in *tbx5b*-depleted fish were similar, but not identical, to those of homozygous *tbx5a* mutants. In addition, *tbx5b*-depletion led to defects in the timing and morphogenesis of pectoral fin outgrowth. Somewhat surprisingly, simultaneous depletion of both Tbx5 gene paralogs did not lead to more severe cardiac phenotypes, and injection of wild-type mRNA was not sufficient to cross-rescue the phenotypes of the paralogous gene. In the heart, *tbx5a* and *tbx5b* appear to have related essential functions that are nevertheless independently required. In the fin, *tbx5a* alone was required for fin bud initiation, but both genes are independently required for patterning and morphogenesis. Therefore, this work demonstrates a functional divergence between the two zebrafish *tbx5* paralogs.

ACKNOWLEDGMENTS

I would like to thank Amelia Striegel, Cory Harrell, Donna Clayton, Drew Neavin, Erin Renfrew, John Fitts, Kathy Cosenza, Michael DeMiranda Jr., and Dr. Yelena Chernyavskaya for all of the help through the years. Many thanks to everyone in the Garrity lab (including all of the wonderful undergraduate members), for creating a wonderful research environment.

Thank you Drs. David Towle, David Feldman, Derek Dimcheff, Don Cass, John Portis, and Marshal Bloom for supporting me in my early research and academic endeavors.

Finally, I would like to acknowledge all of the overwhelming support from my friends and family; I would never have made it without you. I love and appreciate you all.

TABLE OF CONTENTS

CHAPTER 1. *Introduction* 1

Zebrafish and Developmental Biology. 2

Taxonomic Classification. 2

Natural History 2

Zebrafish as a Model Organism 7

Zebrafish Genome. 8

Aquarium/Laboratory Strains. 8

Importance of Heart Development 10

Cardiomorphogenesis 10

T-box genes in Development 14

Tbx5 in Development 17

Role of Tbx5 in higher animals 18

Loss of Tbx5 function 22

Role of Tbx5 in zebrafish 23

Targets of *tbx5* regulation 25

Thesis Aims 27

CHAPTER 2. *Zebrafish* tbx5a *is Dispensable in the Heart for Cardiomyocyte Number, but Required for Cell Growth*

Introduction 30

Results 32

Discussion. 50

Materials and Methods 58

CHAPTER 3. *Cell Morphology in Embryonic Hearts Lacking Tbx5a*

Introduction 62

Results and Discussion 68

Materials and Methods 74

CHAPTER 4. *Zebrafish* tbx5 *Paralogs are Not Functionally Redundant in Cardiac or Pectoral Fin Development.*

Introduction 76

Results 79

Discussion 110

Materials and Methods 116

REFERENCES. 125

APPENDIX I. *Determining Critical Tbx5 Expression in Early Cardiac Development*

Introduction 144

Results / Discussion. 147

Materials & Methods 164

Figures 168

APPENDIX II. *Alternative* tbx5a *mRNA Splicing and Promoter Element Search.*

Introduction 179

Results / Discussion 181

Materials and Methods 188

Figures 190

LIST OF ABBREVIATIONS 194

LIST OF TABLES

Table 1.1: Zebrafish taxonomic classification 2

Table 1.2: Selected morphological events in zebrafish development 11

Table 1.3: Tbx5a target genes 27

Table 2.1: Analysis of Mendelian inheritance patterns of embryos resulting from wildtype and mutant intercrosses 34

Table 4.1: Quantitative PCR primer sequences 122

LIST OF FIGURES

Fig. 1.1: The habitat of wild zebrafish includes slow moving, shallow rivers and swamps on the Indian Subcontinent 3

Fig. 1.2: Adult Zebrafish morphology 4

Fig. 1.3: Closely related species that cohabitate with wild *Danio rerio* 6

Fig. 1.4: Early zebrafish cardiac development 12

Fig. 1.5: Relative percent identities of Tbx5a proteins 19

Fig. 1.6: *tbx5* expression in zebrafish and mouse embryos 21

Fig. 1.7: Cardiac and pectoral fin abnormalities in 72 hpf *hst* mutant embryos 24

Fig. 2.1: Cardiac deformities in *tbx5a* mutant larvae 33

Fig. 2.2: Sequencing of the zebrafish *tbx5a*^{s296} allele 35

Fig. 2.3: Absence of functional *tbx5a* results in a lack of cardiac looping 38

Fig. 2.4: Chamber and myocardial differentiation in *tbx5a* mutant embryos and larvae. 40

Fig. 2.5: Pectoral fin development is absent in *tbx5a*^{s296} mutant embryos 43

Fig. 2.6: Mutations in Tbx5a represent null alleles 45

Fig. 2.7: *tbx5a* is not required for regulation of cardiomyocyte number 47

Fig. 2.8: Cardiomyocyte size is reduced in 48 hpf *hst* embryos 49

Fig. 3.1: Classical model for the assembly of mature myofibrils 67

Fig. 3.2: Cell adhesion is not reduced in *hst* cardiomyocytes 69

Fig. 3.3: Adhesion of 48 hpf *hst* mutant cardiomyocyte nuclei is not altered 71

Fig. 3.4: Myofibrillogenesis is not altered in *hst* hearts 73

Fig. 4.1: The zebrafish Tbx5b protein sequence is not highly conserved 80

Fig. 4.2: Alignment and schematic comparison of zebrafish Tx5a and Tbx5b protein sequences and genomic structure 82

Fig. 4.3: Confirmation of *tbx5b* morpholino knock-down using GFP-tagged mRNA containing the *tbx5b*MO target site 85

Fig. 4.4: Lack of functional Tbx5a or Tbx5b results in dysmorphic cardiac formation. . 86

Fig. 4.5: *tbx5* deficient embryos display similar cardiac looping angles and heart rates at 48 hpf. 88

Fig. 4.6: Chamber specification is normal in *tbx5a* mutant and *tbx5b* morphant embryos 90

Fig. 4.7: Differential expression of putative target genes in *tbx5a* mutants versus *tbx5b* morphants 91

Fig. 4.8: Loss of Tbx5a or Tbx5b differentially affects the expression of conserved Tbx5 target genes 96

Fig. 4.9: Depletion of *tbx5b* delays pectoral fin initiation and reduces fin outgrowth . . 98

Fig. 4.10: Differential phenotypes observed in fin differentiation in *tbx5a* mutants and *tbx5b* morphants 100

Fig. 4.11: Cardiac and pectoral fin development are sensitive to *tbx5a* and *tbx5b* overexpression. 102

Fig. 4.12: mRNA injection rescue studies suggest *tbx5a* and *tbx5b* are not functionally redundant in cardiac development 104

Fig. 4.13: *tbx5a* and *tbx5b* are not functionally redundant in pectoral finbud outgrowth 107

Fig. 4.14: Cardiac cell number is not affected by a lack of functional Tbx5a or Tbx5b 109

Fig. AI.1: First method of creating transgenic zebrafish embryos via I-SceI meganuclease 168

Fig. AI.2: Genotyping *hsp701:tbx5a*-GFP F1 generation by PCR amplification 169

Fig. AI.3: Second method for creating transgenic zebrafish: the Gateway approach . . .170

Fig. AI.4: The pIhsp70:tbx5a-GFP and hps701:tbx5a-GFP (#1) constructs both express GFP and are inducible 171

Fig. AI.5: Sub-cloning scheme required to create the 3' entry vector for the 3rd method: vSlick- modified Gateway 172

Fig. AI.6: LR recombination required to create the Injection Construct #4 for the third method: modified vSlick-Gateway 173

Fig. AI.7: Wildtype *tbx5a* fused with GFP does not fluoresce 174

Fig. AI.8: Schematics of Injection Constructs used in attempts at creating viable transgenic animals 175

Fig. AI.9: Schematic of construct #6 cardiac-specific induction system 176

Fig. AI.10: Confirmation that the Drive Line construct is inducible and stimulates construct #6 to encode cardiac specific GFP (vSlick Method) 177

Fig. AI.11: Confirmation of doubly- inducible *tbx5b*-v2a-GFP (construct #8), demonstrating cardiac- and lens-specific GFP expression 178

Fig. AII.1: Alternative splicing occurs in the 5' region of *tbx5a* 190

Fig. AII.2: T-box Binding Elements (TBEs) are present in the promoter regions of candidate downstream genes 191

Fig. AII.3: Identifying the necessary *cis*-regulatory domains upstream of *tbx5a* 192

Fig. AII.4: Use of Gateway technology increases specificity and level of transient expression of *tbx5a*UE-GFP transgenes 193

CHAPTER 1: INTRODUCTION

Organogenesis involves a complex series of steps, including spatio-temporal regulation of gene expression and protein function, progenitor cell differentiation, and organized cell movement, that combine to create a complex, specialized, functional tissue. Transcription factors (TFs) play an essential role in organogenesis by regulating embryonic gene expression essential for embryonic patterning, cell specification, differentiation, and morphogenesis. Tbx5, a T-box transcription factor, is a positive regulator of gene expression and is critical in vertebrate heart and forelimb formation. The heart is the first organ to function in development, and for many vertebrates it is critical that it function even before morphogenesis has completed (Bakkers 2011). Haploinsufficiency of Tbx5 can cause Holt-Oram Syndrome, a human congenital disease characterized by cardiac and forelimb defects. Homozygous mutation of zebrafish *tbx5a* in *heartstrings* (*hst*) embryos also leads to lethal defects in cardiac looping morphogenesis and prevents initiation of pectoral fin formation. Conservation of gene functions with mammals means that zebrafish provide an excellent model system for human disease. Investigation of zebrafish gene function with both forward and reverse genetic tools provides novel insights into human cardiovascular disease mechanisms that ultimately translate into a broader understanding of human diseases. The overarching aim of this project is to determine the functional role of Tbx5 in zebrafish cardiac development.

Zebrafish and Developmental Biology

Taxonomic classification

Table 1.1: Zebrafish taxonomic classification (see www.itis.gov: *Danio rerio*). At the 1993 Zebrafish Meeting at Cold Spring Harbor Laboratory a consensus vote determined that the official zebrafish name would be changed from *Brachydanio rerio* to *Danio rerio* (Westerfield 1995). The name Danio derives from the Bengali name "dhani," meaning "of the rice field" (Spence *et al.* 2008).

Kingdom	Animalia	multicellular organisms
Phylum	Chordata	
Subphylum	Vertebrata	
Class	Actinopterygii	Class of ray-finned fish
Subclass	Neopterygii	
Infraclass	Teleostei	bony fishes
Superorder	Ostariophysi	
Order	Cypriniformes	Order of cyprins, minnows, suckers
Superfamily	Cyprinoidea	
Family	Cyprinidae	carps and minnows
Genus	*Danio*	
Species	*rerio*	
common name	zebra danio	

Zebrafish Natural History

Zebrafish are small, bony fish that belong to the Teleostei infraclass along with pufferfish, trout, and carp (Gu *et al.* 2002). The natural habitat of zebrafish is warm, freshwaters of the Indian subcontinent (Fig. 1.1) (Engeszer *et al.* 2007, Spence *et al.* 2008). Adult zebrafish are generally smaller than two inches in length and have a striped appearance, although pigmentation can vary widely (Fig. 1.2). Zebrafish are moderately sexually dimorphic, with the males having a more fusiform, linear shape and pinker coloration, while the females develop a protruding belly at sexual maturity. The breeding

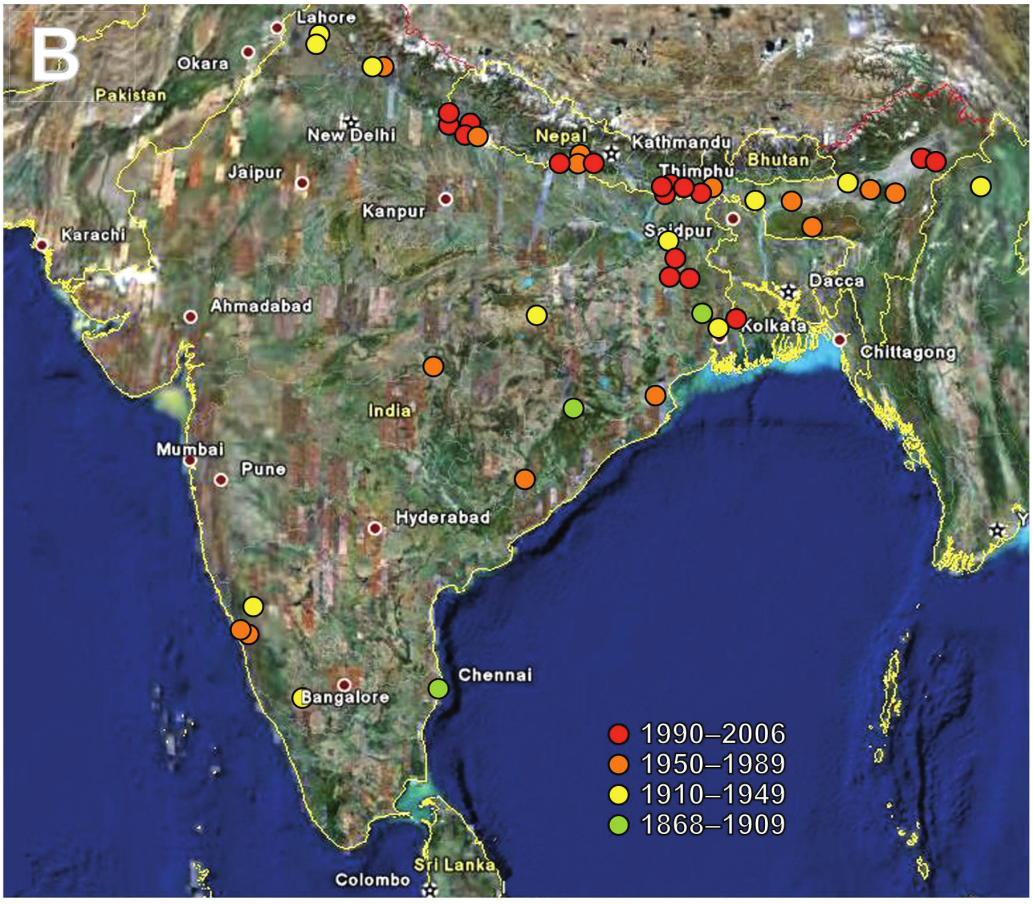

Fig. 1.1: The habitat of wild zebrafish includes slow moving, shallow rivers and swamps on the Indian Subcontinent. A. Seinpoh stream in Meghayala is an example of a high elevation, slow moving meadow stream habitat. **B**. Historical zebrafish range on the Indian subcontinent (reproduced / adapted with permission Engeszer *et al.* 2007).

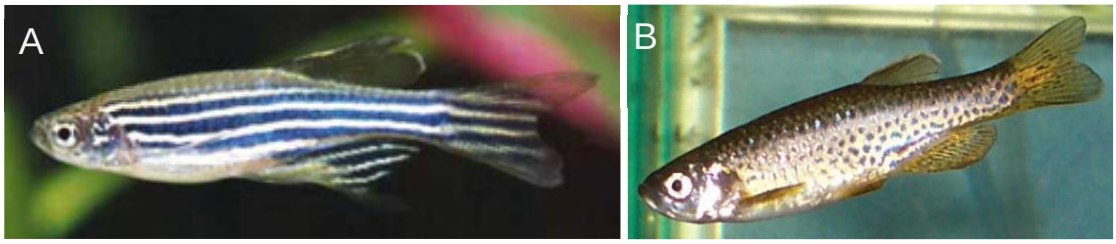

Fig. 1.2: Adult zebrafish morphology. **A**. An example of a "typical" wildtype zebrafish female; i.e. rounded white belly and dark blue pigment stripes on a white background color. (www.diszhal.info) **B**. Pigment polymorphism demonstrated in a "leopard" male, where the pigment is distributed in spots along the body. Note the pinker background color is that of a wild-type male.
(http://aquainfo.dk/images/showthumb_db.html?ii=495&wd=500).

season for these fish extends from April to August, during which time they congregate in shallow rice paddies to spawn. Zebrafish spawn in early morning, when they undergo a ritualized mating dance in which the male rapidly pursues a female, attempting to nudge her sides. If the female is receptive she will release eggs which the males will then fertilize. The fertilized embryos sink to the silty substrate, away from potentially predatory adults, and begin a period of rapid development. After roughly 48 hours post fertilization (hpf) embryos hatch out of a protective, optically opaque chorion and begin feeding by 5 days post fertilization (dpf) (Kimmel *et al.* 1995). For the first few days of their development, embryonic zebrafish survive on their yolk mass and acquire necessary oxygen by diffusion until heart function develops sufficiently to deliver oxygen to all tissues.

Zebrafish are omnivorous, eating primarily insects, larvae, zooplankton, and phytoplankton (Spence *et al.* 2008). Because zebrafish feed in both the water column and surface it is possible that they are beneficial for mosquito control (Dutta 1993). Natural predators of adult zebrafish include larger fish such as snakeheads (*Channa*) (Fig. 1.3) and catfish as well as predatory birds like herons (Engeszer *et al.* 2007). The average lifespan of wild zebrafish is unknown, but in a laboratory setting they live an average of 42 months (Gerhard 2002). After two years they tend to develop symptoms of senescence including a curved spine, lethargy and even muscle degeneration. Because wild zebrafish do not demonstrate these symptoms of old age, it appears that they may die at younger ages, before these symptoms can develop (Spence *et al.* 2007). The oldest known zebrafish reared in captivity died at an amazing 66 months (Gerhard *et al.* 2002).

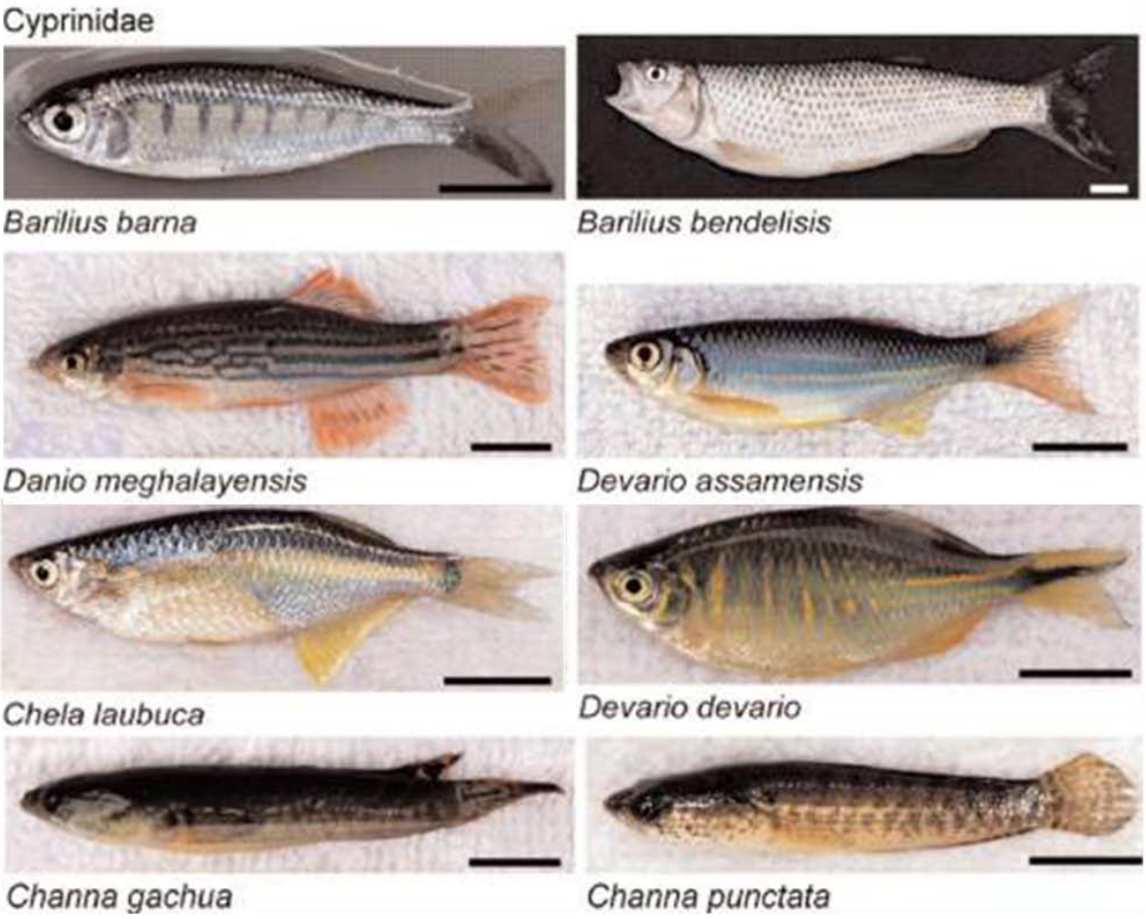

Fig. 1.3: Closely related species that cohabitate with wild *Danio rerio*. *Danio meghalayensis* displays similar sexual dimorphic traits as *D. rerio*. *Channa* are known zebrafish predators. Reproduced/adapted with permission, Engeszer *et al.*, 2007.

Zebrafish as a model organism

Because zebrafish naturally school in shallow freshwater pools, they readily adapt to a laboratory environment where many fish can be maintained in relatively small areas. The ability of females to produce large clutches of eggs, upwards of 200 eggs per batch, is ideal for many biological studies. An additional trait that lends itself to laboratory use is that because zebrafish undergo external fertilization, egg and sperm can be isolated from individual fish and used for in vitro fertilization (Westerfield 1995). Zebrafish were only occasionally used as a model organism for decades before becoming prevalent in molecular genetics and cell differentiation studies (Streisinger *et al.* 1981, Kimmel *et al.* 1989, 1990). With the advent of new tools and techniques, zebrafish are now a powerful model organism relevant for many biological fields including developmental biology, genetic models of human disease, regeneration, neurophysiology, and even behavior (Li *et al.* 1997, Nguyen 2001, Yelon 2001, Dooley *et al.* 2008, Brittijn *et al.* 2009, Palastra *et al.* 2010, Ebarasi *et al.* 2011, Pavlidis *et al.* 2011, Shao *et al.* 2011).

Zebrafish is the ideal system for use in my studies for several reasons. First, *ex utero* development in transparent eggs allows for easy observation of cardiac development *in situ*. Second, due to their small size, zebrafish are well-suited for studying cardiovascular disorders because they do not initially depend on a functional circulatory system to facilitate gas exchange. Furthermore, there are several cardiac mutant lines available, thereby facilitating study of cardiac development. Finally, the ease of creating transgenic animals along with new technologies to drive tissue-specific expression of fluorescently labeled proteins is also a distinct advantage.

Zebrafish genome

The zebrafish genome is comprised of 25 chromosomes and totals 1.7 gigabases in size (Nusslein-Volhard *et al.* 2002). To put this in perspective, the human genome is 3.2 Gb, while the smallest vertebrate genome (0.39 Gb) belongs to the *Tetraodon nibroviridis* pufferfish, and the largest belongs to another fish: the marbled lungfish's genome is an impressive 130 Gb. Although a genome-wide duplication event occurred in the teleost lineage, it was followed by a rapid divergence and loss of genes, so that only roughly 20% of zebrafish genes are duplicated. Thus, paralogs of zebrafish genes are often highly diverged, making it relatively easy to study individual gene function (Jaillon *et al.* 2004). Interestingly, several genes that arose from individual gene duplication events prior to genome-wide duplications have remained clustered in vertebrate genomes including zebrafish, human, and mouse. One example occurs in the T-box transcription factor family, where Tbx2 and Tbx4 are tightly linked and closely related genes Tbx3 and Tbx5 are similarly linked on a separate chromosome. These clusters appear to have resulted from a duplication of an ancestral gene and/or unequal cross-over more than 600 million years ago (Agulnik *et al.* 1995, Agulnik *et al.* 1996).

Aquarium/Laboratory strains:

The following is a list of critical zebrafish strains and transgenic lines used in my studies.

Tubingen long fin (TL): Homozygous for two genes: *leo*1, a recessive mutation causing spotting in adult fish, and *lof dt2* a dominant homozygous viable mutation causing long

fins. This is not the line used in the Sanger zebrafish sequencing project. It is genetically different from TU because it was not bred as stringently (i.e. not sufficiently backcrossed to remove embryonic lethal mutations). Therefore, this strain retains more polymorphisms than TU, but fewer than the WIK line.

WIK: Derived from wild catch in India; used for genome mapping (Spence *et al.*, 2008).

Tg(myl7:GFP)f1: Formerly: Tg(*cmlc2*:GFP), *Tg(myl7:GFP)*. The *myl7* promoter drives GFP expression throughout the cardiomyocytes of both chambers. Although the GFP localization in these transgenics is not consistent (it varies with age and chamber), it is useful for identifying cardiac-specific tissue.

Tg(myl7:EGFP-HsHRAS): Formerly: *Tg*(*cmlc2*:Ras-GFP). This construct contains the last 20 amino acids from the C-terminus of human HRAS fused to the C-terminal end of enhanced green fluorescent protein (EGFP). It is a useful line for visualizing cardio-myocyte morphology as the GFP is localized to the membrane through the RAS tag.

Tg(-5.1myl7:nDsRed2): This line was formally Tg(*cmlc2*:DsRed-nuc), a transgenic line in which DsRed2 is expressed in cardiomyocyte nuclei of both chambers, visible after 48 hpf. This line is useful for quantification of total cardiomyocytes, and is best used with Tg(*myl7*:GFP) for ease of visualization.

For additional details on mutant lines see http://zfin.org.

Cardiac Development

Importance of heart development

The heart is critical for survival and yet, despite its importance, we still lack basic understanding of mechanisms regulating its formation. Understanding cardiac development is valuable because anomalies in cardiac formation are one of the leading causes of prenatal and infant mortality (Kochanek *et al.* 2004). The patterning, differentiation and morphogenesis of the heart tube, as well as its assimilation of rhythm, involve complex processes requiring large numbers of genes. Dysregulation or mutation of cardiac genes often results in a loss of form and/or function of the heart (Olson 2006). A complete understanding of the contributions of individual genes in creating the functional heart requires researchers to synthesize insights obtained from more than one model system (Bryson-Richardson and Currie 2008, Chien *et al.* 2008).

Cardiac morphogenesis

In both mammals and fish heart formation begins during early segmentation stages when bilateral cardiac precursors are specified within the lateral plate mesoderm (LPM) (Table 1.2) (Yutzey and Bader 1995, Yelon *et al.* 2002). In zebrafish, atrial and ventricular precursors are distinct prior to heart tube formation (Fig. 1.4) (Stainier and Fishman 1992, Bakkers 2011). At the 6-8 somite stage, expression of the homeobox transcription *nkx2.5* is required for the continued development of cardiomyocytes (Thomas *et al.* 2008). Nkx2.5 plays a role in determining the size of the bilateral heart fields. If *nkx2.5* expression is altered (either increased or decreased), through modulation of one of its

regulators, the resulting heart size is also similarly altered (Reiter *el al*. 1999, Marques *et al*. 2008). Three of the known positive regulators of *nkx2.5* expression include fellow transcription factor *gata5*, and paracrine factors *fgf8*, and *bmp2b*. Increasing the expression of any of these four genes in zebrafish results in a larger heart field and, ultimately, a larger heart (Reiter *et al.* 2001).

Table 1.2: Selected morphological events in zebrafish development

11-12 hpf	Bilateral cardiac precursors are being specified
18 hpf	Cardiac progenitor cells migrate to midline; fuse to create a linear heart tube
22-36 hpf	Rhythmic contractions of cardiomyocytes begin; chambers differentiating
28 hpf	Nascent pectoral fin bud observed
36-40 hpf	Circulation begins; heart tube "loops" (the tube folds back on itself, to bring the two chambers adjacent to one another)
48+ hpf	Unidirectional blood flow is robust; *hst* cardiac phenotypes observed; cardiac function progressively worsens until mutant embryos die ~7 dpf.

The bilateral precursor populations migrate to the embryonic midline and fuse to form a heart cone (zebrafish, Bakkers 2011) or cardiac crescent (mammal, Moorman *et al.* 2003). The cells within the heart cone have already established positions to aid in the chamber formation, where atrial myocytes mantle the ventricular and endocardial cells (see Fig. 1.4D; orange cells surround the purple and green cells). Cardiomyocyte differentiation begins even before the bilateral precursor cells fuse to form the heart cone (Yelon *et al.* 1999). Atrial cells are determined later, with expression of atrial myosin heavy chain beginning at the 19 somite stage (Berdougo *et al.* 2003). Between 22 and 24 hpf the heart cone elongates, acquires a left-of-center displacement (termed "jogging") as influenced by *bmp4* (Chen *et al.* 1997). Cardiac contractions are initially peristaltic and

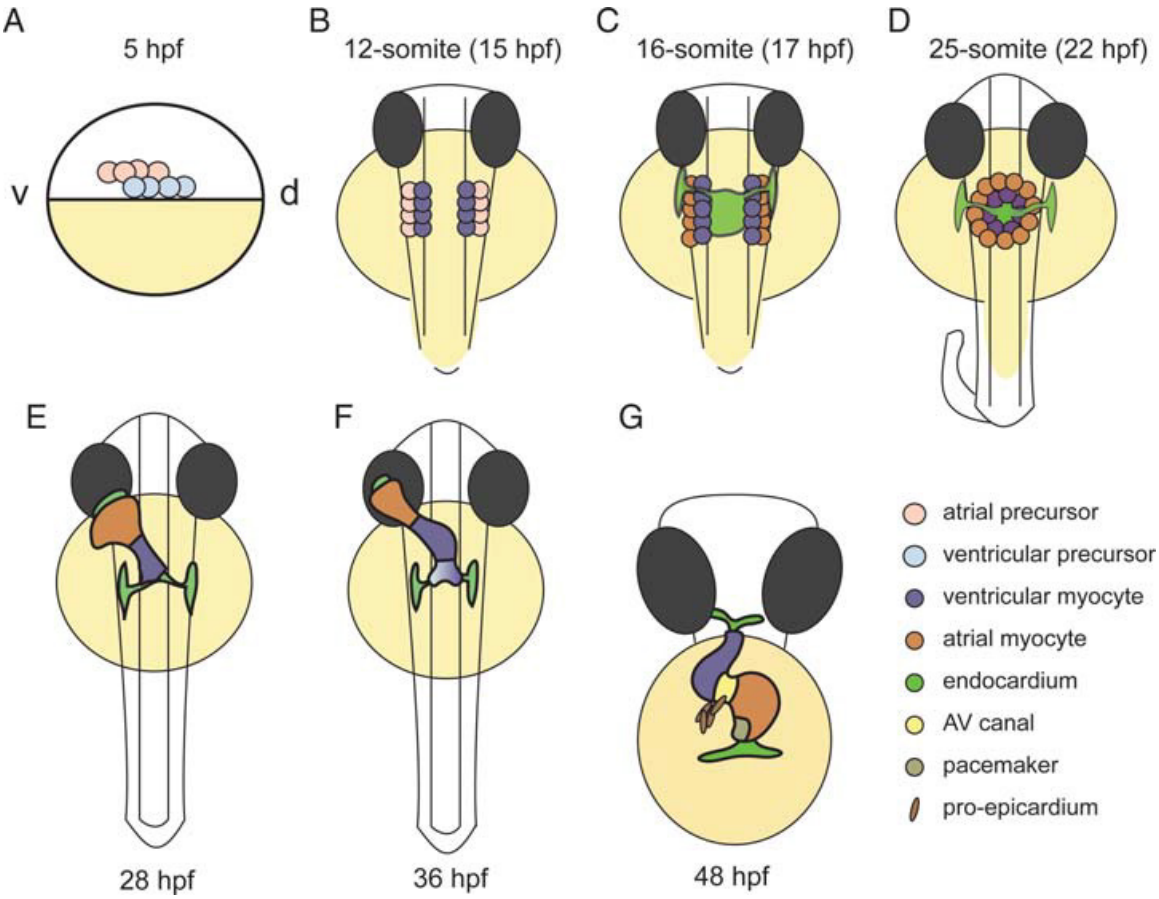

Fig. 1.4: Early zebrafish cardiac development. A. Just prior to gastrulation the heart progenitor cells are located on lateral regions of the embryo. **B**. After involution, these cells converge towards the embryonic axis and reach their destination at the level of the future hindbrain by the five-somite stage. Two rows of cells are represented at this stage, with ventricular myocytes (dark blue) present most medially and the atrial precursors most laterally (pink). **C**. By the 16-somite stage, the atrial myocytes have differentiated and endocardium is now present (green). **D**. Starting at 19 hpf, the myocardial precursors merge posteriorly to form a horseshoe-shaped structure. By 19.5 hpf, as anterior cells migrate medially, the horseshoe transforms into a cone with the ventricular cells (dark blue) at its center, and the atrial cells (orange) at its base. The endocardial cells (green) line the inside of the cone. **E**. Next, the cone telescopes out to form a tube. The ventricular end of the heart tube assembles first, followed by the atrial end. **F**. By 36 hpf, visibly distinct ventricular and atrial chambers have begun to form, and the heart begins to undergo looping morphogenesis **G**. After 48 hpf, valuve cushions begin to form at the AV canal. (Figure reproduced/adapted with permission from Bakkers 2011, text modified from Stainier 2001).

then functions as a pump as the heart tube undergoes chamber morphogenesis (Bakkers 2011). Around 36 hpf, the chambers begin the process of cardiac looping at 36 hpf, in which the atrium migrates anteriorly to lay adjacent to the ventricle. Contributions of cells from the second heart field, which migrate from the pharyngeal mesoderm, add to the heart tube at either the arterial or venous poles (de Pater *et al.* 2009, Dyer and Kirby 2009, Greulich *et al.* 2011, Lazic *et al.* 2011). Additionally, chamber ballooning (regional differentiation and expansion of cardiomyocytes) is an important morphological change that ensures the correct size and placement of chambers during formation (Christoffels *et al.* 2000, Forouhar *et al.* 2006). The specific effects of cell morphogenesis on chamber development will be discussed in later chapters. Ultimately, valves differentiate from endocardial cushion tissue, facilitating unidirectional circulation (Bartman *et al.* 2004). The heartbeat continues to increase in force and frequency over the next few days (Beis *et al.* 2005, Yelon 2001).

Several differences exist among vertebrates regarding cardiac formation. The most obvious difference is that zebrafish hearts are comprised of two chambers, while human hearts contain four chambers (Thisse 2002). Therefore, blood flow is abridged in zebrafish. In fish, low-oxygen blood is pumped through the atrium to the ventricle, which pumps the blood to the gills for gas-exchange before it flows out to the rest of the body (Isogai *et al.* 2001). In contrast, mammals utilize two separate sets of chambers, one exclusively pumps deoxygenated blood to the lungs, the other for circulation to the body. During one cardiac cycle, low-oxygen blood is returned to the right atrium and is pumped out of the right ventricle to the lungs for gas exchange. Oxygen-rich blood returns to the

left atrium, and the powerful left ventricle pumps blood out to the head and body (Harvey 1889). Because zebrafish hearts have fewer chambers, they do not undergo septation and are therefore not a viable model for septation disorders seen in humans (Li 1997, Basson *et al.* 1997, Schott 1998, Sakata *et al.* 2002). Despite these differences, many of the major morphogenetic events in cardiac development, such as chamber formation, cardiac looping and onset of rhythm, occur in parallel with tetropods and in many instances the genes regulating these events are conserved (Thisse and Zon 2002).

T-box Genes in Developmental Biology

T-box genes

Genes of the T-box superfamily are present throughout nearly all of the Animal Kingdom, from Cnidarians (including *Hydra* and jellyfish) through the highest Chordates (Agulnik *et al.* 1995, Technau and Bode 1999). They are so named because the original "T" transcription factor, isolated from the Brachyury mouse, contained a region important for binding DNA (Kispert and Herrmann, 1993). This "T-box," known as the proteins "T-domain," is found in the N-terminus of T-box genes of 20+ genes including (but not limited to): TBR1, TBX1-6, TBX10, TBX15, TBX18, TBX19, TBX20-22, no-tail (ntl), and VegT (Naiche *et al.* 2005). T-box genes are classified into 5 subfamilies: Brachyury, T-brain1, Tbx1, Tbx2 and Tbx6 (Papaioannou 2001). Members of the same family are more related in sequence, and most likely arose from duplication events throughout evolution. As found in other gene families, the intron-exon boundaries of T-box homologs are conserved throughout evolution, but intron length varies between

species (Wattler *et al.* 1998). Most T-box family members encode a single transcript that is not subjected to alternative splicing (Wilson and Conlon *et al.* 2002). One exception is the VegT gene in *Xenopus*, which encodes alternate 3' splice forms that are either maternally or zygotically expressed (Stennard *et al.* 1999). Additional regions of T-box genes essential for transcriptional regulation include the transcriptional activation domain, located in the C-terminus of T-box proteins (Zaragoza *et al.* 2004), and the interaction domain in the N-terminus, upstream of the T-domain (Wilson and Conlon 2002). The C-terminus of T-box genes are important for the strength an induction response, but not for the specificity (Marcellini *et al.* 2002). Specificity arises from interactions of the T-box protein with other transcriptional regulators and is regulated by the interaction domain (Wang *et al.* 2011, Wilson and Conlon 2002).

T-box genes are significant to developmental biology because T-box genes have diverse and critical functions in development, beginning with regulation of gastrulation (and thereby anterior-posterior (AP) axis formation) and organ development. A general theme among T-box genes is that they are all required for specification of the tissue in which they are expressed (Smith 1997, Stennard 2005). T-box genes have been associated with human disorders including Holt-Oram Syndrome, DiGeorge syndrome, and small-patella syndrome (SPS), among others (Greulich *et al.* 2011, Smith 1997). T-box genes may even play a role in metastasis of certain cancers, possibly by promoting epithelial-mesenchymal transition. Moreover, expression of Brachyury in early tumor stages predicts poor patient prognosis (Kilic *et al.* 2011, Naiche *et al.* 2005, Suzuki *et al.* 2011).

In cardiac development, members of two T-box subfamilies are required for normal heart formation (Hoogars *et al.* 2007, Plageman and Yutzey 2005). Tbx1, Tbx18 and Tbx20 of the Tbx1 subfamily, and Tbx2, Tbx3 and Tbx5 of the Tbx2 subfamily are expressed in cardiac development (Greulich *et al.* 2011). With the exception of Tbx2, Tbx3, and Tbx20, T-box genes are primarily activators of gene expression (Carreira *et al.* 1998). Within the Tbx1 subfamily, Bmp/SMAD1 directly regulates *tbx20* expression in cardiac development (Mandel *et al.* 2010). In turn, Tbx20 negatively regulates *tbx2* (which consequently negatively regulates chamber-specific genes) (Singh *et al.* 2009). Therefore, *tbx20* plays a role in chamber specification. *tbx1* and *tbx18* are required for the elongation of the heart tube. *tbx1* is expressed in the pharyngeal mesoderm and promotes the proliferation of mesenchymal precursor cells that contribute to the secondary heart field. Therefore, Tbx1 ensures elongation of the outflow tract (Greulich *et al.* 2011). For proper formation of the inflow area, *tbx18* expression is required in the sinus venosus and is a marker of proepicadium.

Members of the Tbx1 subfamily are associated with human disorders. Mutations in *tbx20* are associated with congenital heart defects, including dilated cardiomyopathy (DCM), atrial septal defects (ASD), and mitral valve disorders (Kirk *et al.* 2007). Tbx1 has been associated with DiGeorge Syndrome, in which affected individuals display thyroid, facial, cardiac outflow tract, and vertebrae abnormalities (Jerome *et al.* 2001, Lindsay *et al.* 2001, Merscher *et al.* 2001).

Within the Tbx2 subfamily, Tbx2 interacts with the Nkx2-5 and Gata4 transcription factors to bind to the mouse Nppa (natriuretic peptide type A, formerly Anf) promoter, thereby blocking Tbx5 activation (Habets *et al.* 2002). Overexpression of *tbx2* leads to ectopic formation of cardiac jelly, leading to an expansion of cushion tissue, and thus affects valve formation in mice (Shirai *et al.* 2009). Tbx2 and its close homolog Tbx3 are both expressed in the margins of both fore- and hind-limb buds (Chapman *et al.* 1996b). Tbx3 regulates limb formation through repression of osteoblast differentiation and promoting cell proliferation (Govoni *et al.* 2009). In mouse heart development, Tbx3 controls the formation of the sinoatrial node as well as specifying the location of the pacemaker within the atrium (Hoogars *et al.* 2007). Loss of Tbx3 increases second heart field proliferation, thereby negatively affecting outflow tract morphogenesis and heart tube extension (Mesbah *et al.* 2008). Overall, Tbx2 and Tbx3 are important for repression of chamber myocardial genetic programs, thereby promoting the alternative fates of valve, septa, and conduction system formation (Wilson and Conlon 2002). Tbx2 is also upregulated in some types of breast cancers (Jacobs *et al.* 2000). Mutations in Tbx3 can result in human ulnar-mammary syndrome (Bamshad *et al.* 1997, He *et al.* 1999).

Tbx5 in Development

Significance:

The organogenic functions of the Tbx5 T-box transcription factor (a Tbx2 subfamily member) in cardiac development and forelimb formation are conserved among vertebrates (Basson *et al.* 1999, Showell *et al.* 2004). Based on Pairwise Alignment

Scores of RefSeq protein sequences, zebrafish Tbx5a shares 74.6% overall amino acid identity to human TBX5 isoform 1 (see Fig. 1.5). Despite the relative lack of overall protein sequence conservation, the Tbx5 T-box domain is highly conserved across species, with over 95% similarity between human TBX5 and zebrafish *tbx5a* T-box protein sequences (Tamura *et al.* 1999).

Role of Tbx5 in higher animals:

Tbx5 plays a role in the formation of the embryonic heart, limb, eye, and pro-epicardium (PE, a collection of progenitor cells that contributes to the venous pole of the heart and also forms the epicardium (Serluca 2008)). Prior to heart tube formation, *tbx5* is expressed in the cardiac mesoderm (Camarata *et al.* 2010, Chapman *et al.*, 1996; Bruneau *et al.*, 1999; Horb and Thomsen, 1999). One of the earliest roles of Tbx5 is to regulate PE formation; in zebrafish, *tbx5a* is required in early segmentation stages for proper PE morphogenesis and may regulate migration of PE cells to the epicardium (Liu and Stainier 2010). Also during somite stages, *tbx5a* expression in the anterior lateral plate mesoderm confers competence to later *bmp* signaling which is required for proper cardiac differentiation and ventricular formation (Liu and Stainier 2010). During heart tube formation, *tbx5a* functions to promote myogenic and conduction system gene programs (Greulich *et al.* 2011, Moorman and Christoffels 2003).

By the completion of cardiac looping in chick, mouse, and frog, *tbx5* mRNA is expressed as a gradient, with the highest levels in the posterior heart, including the two atria and the left ventricle (Li *et al.* 1997, Bruneau *et al.* 1999, Horb and Thomsen 1999, Christoffels

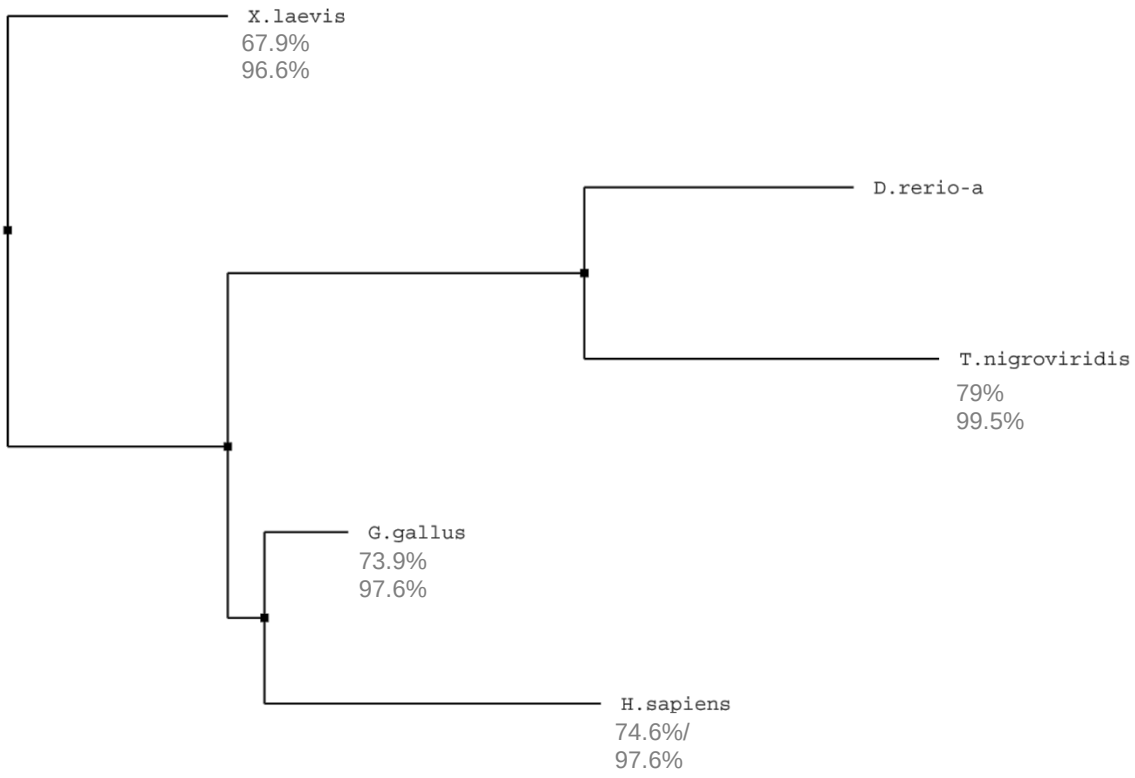

Fig. 1.5: Relative percent identities of Tbx5a proteins. Relationship tree created using the neighbor joining method indicating percent identity. Although this tree is not intended to infer evolutionary relationship, it is useful for diagraming that zebrafish Tbx5a sequence is most similar to that found in the green spotted puffer fish (*T. nigroviridis*). Percents given are overall identities (top number) and T-box identities (bottom number) as compared to *D. rerio*.

et al..2000, Hatcher *et al.* 2000, Liberatore *et al.* 2000). A similar *tbx5a* mRNA expression gradient is present in the nascent heart tube at 26 hpf in zebrafish (Fig. 1.6), but then appears to reverse and is present primarily in the ventricle by 48 hpf (Begemann and Ingham 2000, Garrity *et al.* 2002). It may be that graded *tbx5a* expression functionally contributes to the definition or implementation of the anterior/posterior axis of the vertebrate heart. Consistent with this hypothesis, others have noted that, in mice, graded *tbx5* expression plays a role in chamber differentiation and valve formation, and that *tbx5* expression levels remained high in the caudal region (atria) through later stages of embryonic development (Bruneau *et al.* 1999). While previous work suggested that precise levels of *tbx5* mRNA expression within the heart tube are important for general morphology (Bimber *et al.* 2007, Garrity *et al.* 2002, Horb and Thomsen 1999), no studies have so far reported how slight alterations in *tbx5* levels impact expression of target genes in the heart, or affect cardiomyocyte growth or morphology.

Tbx5 also displays dynamic changes in cellular localization during development. As expected for a transcription factor, initial expression is restricted to the nucleus (Hatcher *et al.* 2000). Remarkably, studies in chick indicate that Tbx5 protein is dynamically localized in either the nucleus or the cytoplasm depending on the developmental stage and individual cardiac cell type (Bimber *et al.* 2007). The cytoplasmic localization is due to an association with structural PDZ-LIM protein Pdlim7 and the actin cytoskeleton, and is hypothesized to sequester *tbx5a* away from the nucleus to promote atrioventricular junction (AVJ) cell fates (Camarata *et al.* 2006, Kulisz and Simon 2008). At these later stages of chamber morphogenesis *tbx5* is expressed in the cardiac trabeculae but not the

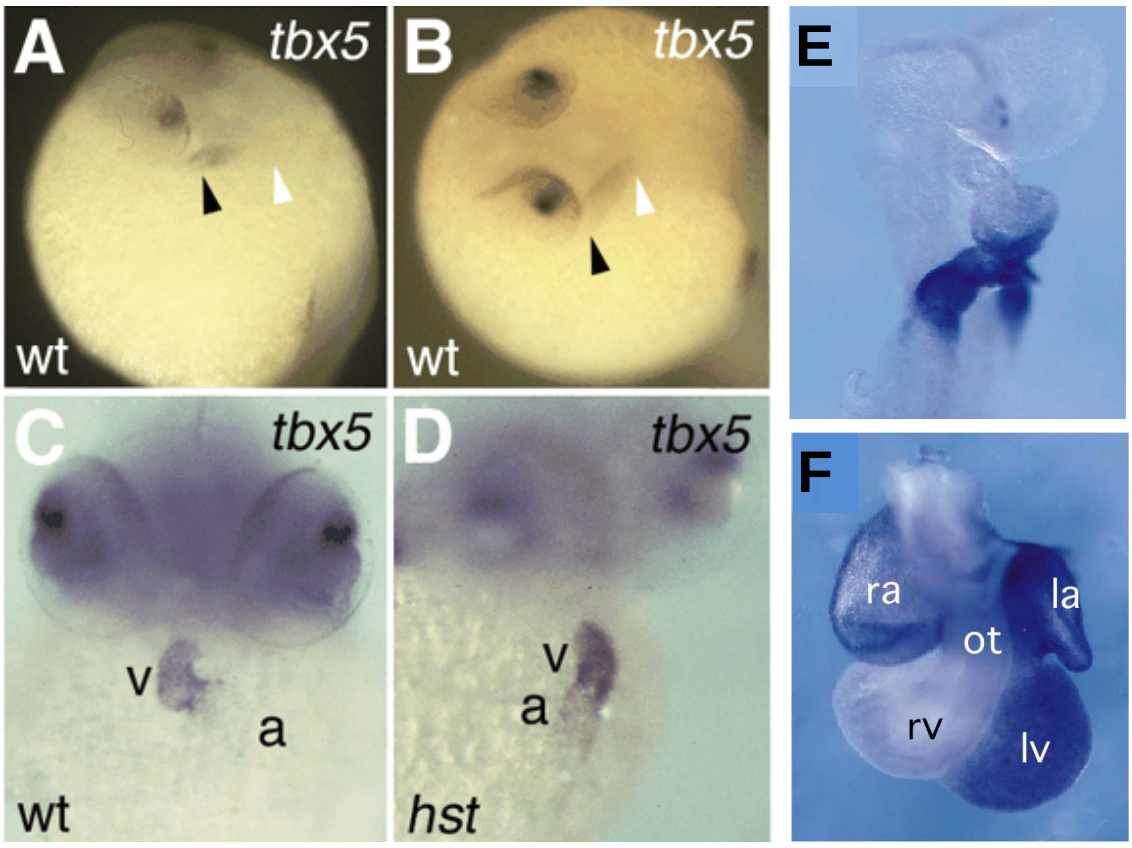

Fig. 1.6: *tbx5* expression in zebrafish and mouse embryos. Whole mount *in situ* hybridization illustrating the presence of *tbx5a* mRNA in **A**, **B**) 26hpf zebrafish embryos eye and heart tube; **C**, **D**) 48hpf zebrafish larvae and Tbx5 mRNA in **E**) E8.5 mouse nacent heart, **F**) E11.5 mouse heart. For panels A-D) black arrowhead or "a": atrium; white arrowhead or "v": ventricle. In panel F) ra = right atrium, la = left atrium, rv = right ventricle, lv = left ventricle, and ot = outflow tract. Reproduced/modified with permission from Garrity *et al*. 2002 and Bruneau *et al*. 1999, with permission from Elsevier.

compact layer of the ventricular myocardium (Bruneau *et al.* 1999). Although *tbx5* is expressed throughout cardiac development, it is still unknown at which developmental timepoints Tbx5 function is most critical for later cardiac function. Nor is it understood how disrupting the graded expression in the heart tube may affect expression or distribution of downstream target genes.

Loss of Tbx5 function:

Mutation of Tbx5 in mammals produces dominant phenotypes affecting cardiac septation as well as electrophysiological defects including atrioventricular conduction block (Newbury-Ecob *et al.* 1996, Bruneau *et al.* 2001). Mice with targeted mutations in *tbx5* display a retardation of growth and morphogenesis in the inflow tract and atria; in many cases the left ventricle shows a decrease in the total cardiac cell number (Bruneau *et al.* 2001). Mutations in human *tbx5* lead to Holt-Oram Syndrome (HOS), a disease characterized by congenital heart defects as well as malformed upper limbs (Basson *et al.* 1999, Li *et al.* 1997). Haploinsufficient effects of Tbx5 mutations in mammals suggest that Tbx5 functions are sensitive to dose (Basson *et al.*, 1999, Bruneau *et al.*, 2001). Interestingly, both loss- and gain-of-function mutations in *tbx5* can result in HOS (Hatcher and Basson 2001, Postma *et al.* 2008, Vaughan and Basson 2000). The extent of limb deformity can range from mild distortion of the fingers to nearly complete absence of the arm (Basson *et al.* 1994, Newbury-Ecob *et al.* 1996, Simon 1999). These hypo- and hypermorphic *tbx5* phenotypes hint that small changes in Tbx5 dose might dramatically impact morphology of the embryonic heart and limb. Overexpression of

tbx5 through the use of the beta-myosin heavy chain promoter in mice results in decreased ventricular development and embryonic lethality (Liberatore *et al.* 2000).

Role of Tbx5 in zebrafish:

The zebrafish is an ideal system for cardiac development studies for several reasons: 1) zebrafish cardiac development is rapid, with formation of the heart tube completed by 26 hpf. Embryos that lack a functional heart, such as *hst*, do not die from heart failure until roughly 7 dpf, because embryos acquire oxygen by diffusion from the surrounding water (Bakkers 2011). Therefore, zebrafish embryos with lethal cardiac malformations may be evaluated without secondary complications due to hypoxia. 2) Zebrafish provide superb experimental access to the developing heart since embryos develop externally to the mother. One may observe severe cardiac defects at developmental timepoints not readily accessible in other models (Thisse and Zon 2002). 3) Efficient transgenesis tools for zebrafish exist. 4) The zebrafish *heartstrings*/*tbx5a* mutant line is published (Garrity *et al*. 2002). The *hst* loss-of-function phenotype (see Fig. 1.7) results from a nonsense mutation in *tbx5a* that likely creates a null allele. This mutation results in overtly normal heart tube formation, accompanied by a slight bradycardia. Several early cardiac markers were expressed normally at 16 hpf in *hst* embryos, indicating that myocardial tissue specification occurred despite the absence of functional Tbx5a. Despite overtly normal heart tube formation, the *hst* heart later failed to loop and progressively deteriorated morphologically. The *hst* mutation is homozygous lethal due to heart failure, but heterozygous fish appear fully wildtype (Garrity *et al.* 2002). An apparently independent phenotype of *hst* embryos is the complete lack of pectoral fins. Forelimb phenotypes also

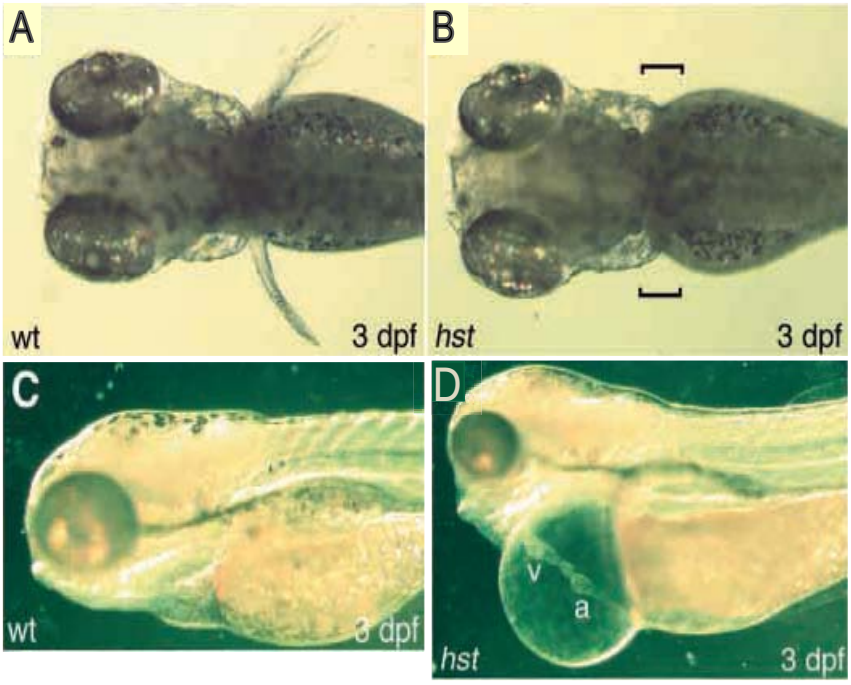

Fig. 1.7: Cardiac and pectoral fin abnormalities in 72 hpf *hst* mutant embryos. (A,C) Wildtype embryos; (B,D) homozygous *hst* mutant siblings have mild to severe pericardial edema and an unlooped, dysmorphic heart. (A) Wildtype pectoral fins elongate, but (B) *hst* mutant embryos lack pectoral fin buds (brackets). (A,B) dorsal views. (C-D) Lateral views; a, atrium, v, ventricle. Reproduced/modified with permission from Garrity *et al*. 2002.

feature in human HOS and in mouse models (Basson *et al.* 1994, Bruneau *et al.* 2001). Using a conditional knockout strategy in mouse, homozygous deletion of Tbx5 in the developing forelimb resulted in a complete lack of forelimb bud formation (Rallis *et al.* 2003). A newly discovered zebrafish *tbx5* paralog, *tbx5b*, is also expressed in lateral plate mesoderm in development (Albalat *et al.* 2010), but no experiments have yet identified functions for this gene.

Targets of Tbx5 regulation:

The transcription factor Tbx5 regulates a number of downstream targets. T-box transcription factors interact with their DNA target genes by binding a conserved site termed the T-box Binding Element (TBE), found in the promoter sequences of target genes (Kispert and Herrmann 1993, Ghosh *et al.* 2001). Mutation of TBEs found in the promoter of atrial natriuretic factor (ANF), fibroblast growth factor 10 (Fgf10) and connexin40 (Cx40), as well as gel shift and transfection assays, provided evidence that these sites mediate the direct regulation by Tbx5 (Bruneau *et al.* 2001, Hiroi *et al.* 2001, Koshiba-Takeuchi *et al.* 2006, Plageman and Yutzey 2004, Showell *et al.* 2004). Molecular genetic studies provide evidence that Tbx5 acts synergistically in vivo and in vitro with other transcription factors, including Nkx2.5, GATA4, MEf2c, Sall4, TAZ, and Myocardin to bind to target TBEs and activate cardiac gene expression (Garg *et al.* 2003, Ghosh *et al.* 2009, Hiroi *et al.* 2001, Koshiba-Takeuchi *et al.* 2006, Plageman and Yutzey 2004, Wang *et al.* 2011).

Tbx5 binds individual TBEs as a monomer (Bruneau *et al.* 2001, Hiroi *et al.* 2001). Wang *et al.* (2011) tested whether Tbx5 binds with Myocardin (Myocd), a transcriptional co-activator of myocyte differentiation, via electrophoretic mobility shift assay (EMSA) to determine that Myocd and Tbx5 do not form a stable ternary complex on the TBE. However, Myocd does form such a complex with CArG and Serum Response Factor to regulate smooth muscle expression (via CArG boxes) (Wang *et al.* 2001). Interestingly, of known Tbx5 mutations that result in HOS, only the G80R mutation within the T-box abolished synergistic interaction with Myocd, further supporting that the Tbx5-Myocd protein interaction is mediated by the T-box region of *tbx5*. These studies also suggest that additional co-factors are needed for binding of *tbx5* to the TBE (Wang *et al.* 2011).

Additional known target genes of Tbx5 include other transcription and paracrine factors such as *bone morphogenic protein 4* (*Bmp4*) and *hairy/enhancer-of-split related with YRPW motif 2* (*Hey2*) (Mori *et al.* 2006; Plageman and Yutzey 2006) and *N-myc downstream-regulated gene* (*Ndrg4*). *Ndrg4*, a novel member of the NDRG family, is thought to regulate the proliferation and growth of cardiomyocytes during zebrafish development. As assayed by *in situ* hybridization, *Ndrg4* mRNA is down-regulated in *hst* mutant embryos (Qu *et al.* 2008). Although *Ndrg4* has been identified by *in situ* studies as a downstream target of Tbx5, no quantitative studies have been completed on its expression in *hst* embryos during development. Microarray experiments using cardiac-derived mice cell line (1H) identified several genes with altered expression in response to induced Tbx5 expression (Table 1.3) which include genes that would make good targets for further quantitative analysis.

Table 1.3: Tbx5a target genes. A list of putative downstream targets of Tbx5 was identified by a literature search, including microarray data of *tbx5* mutants[1]. As positive controls, we included genes with known altered expression in *tbx5* mutants. We will investigate expression patterns of these genes by both quantitative PCR and *in situ* hybridization techniques. TF: Transcription Factor. PC: Paracrine Factor. E: Enzymatic activity. *Tbx5 shows evidence of autoregulation.

Possible Targets:	Function:	Known Targets:	Function:
Tbx2b	chamber morphogenesis; TF	***Nppa***	chamber myocardium; PF
Tbx3b	conduction system; TF	***Hey2***	ventricular septation; TF
Tbx5	chamber morphogenesis; TF,*	***Bmp4***	cardiac cushion formation; PF
MEST	unknown; up-regulated in microarray[1]	***Fgf10***	limb bud outgrowth; PF
		Ndrg4	cardiac morphogenesis; E?

Thesis Aims:

Based on the previous discussion, an outstanding question in the field of Tbx5 biology remains as to how and when Tbx5 is required to create a functional heart. In this thesis, I exploit the zebrafish model system to examine the cellular basis of *tbx5* cardiac phenotypes. In particular, I determine the phenotypic effects of a nonsense mutation with the T-box of *tbx5a*, I investigate the impact of a lack of Tbx5b on heart and fin development, and I address the potential for genetic redundancy between the two paralogous Tbx5 genes. This work tests the overarching hypothesis that Tbx5 is dispensable for early cardiac morphogenesis (cardiomyocyte specification and migration), but operates in an essential, dose-responsive fashion from the heart tube stage onward to facilitate volumetric growth of cardiomyocytes, thereby affecting cardiac looping.

Chapter 2: To test the hypothesis that Tbx5a activity is critical in morphogenetic events occurring after heart tube formation.

Homozygous mutation of zebrafish *tbx5a* in *heartstrings (hst)* embryos leads to lethal defects in looping morphogenesis. The *tbx5a*^{m21} *hst* allele encodes a stop codon within the C-terminal region, downstream of the T-box DNA-binding domain. In Chapter 2, I describe a new *hst* mutant allele (*tbx5a*^{s296}) which encodes a premature stop codon within the *tbx5a* T-box, a location likely to generate a full loss-of-function allele. Specifically: 1) I use immunoblot technology to investigate whether these alleles generate truncated proteins, or encode null alleles; and I determine whether zebrafish *tbx5a* regulates 2) cardiomyocyte cell number or 3) volumetric growth.

Chapter 3: To test the hypothesis that the cardiac dysgenesis observed in hst *embryos results from decreased cell adhesion and/or myofibrillogenesis during early chamber morphogenesis stages.*

Mutation of *tbx5* leads to embryonic lethal cardiac phenotypes in vertebrate models. I systematically investigate the cellular basis for *tbx5a* cardiac phenotypes using the zebrafish *hst* mutant line, which is informative for the etiology of HOS. In Chapter 3, I investigate the effects of *tbx5a* mutation at chamber morphogenesis stages on 1) cell adhesion using transgenic zebrafish lines, and 2) myofibril formation, using fluorescent microscopy.

Chapter 4: To elucidate the role of Tbx5b in cardiac and pectoral fin development.

The goal of Chapter 4 is to describe the loss-of-function phenotype of the newly discovered *tbx5b* gene. Because there is substantial overlap in the gene expression patterns between *tbx5a* and *tbx5b*, I hypothesize that functional redundancy exists between these zebrafish paralogs. I take several experimental approaches: 1) I characterize the loss-of-function phenotypes for *tbx5b*; 2) I test whether it is possible to rescue, or even cross-rescue morpholino knockdown phenotypes by co-injection of the cognate or paralogous mRNA; 3) I investigate whether zebrafish development is sensitive to *tbx5b* over-expression.

The study of congenital cardiac diseases is significant because more than 1% of live births are affected by congenital heart defects (CHD) (Clark *et al.* 2006). Although HOS accounts for only a fraction of these birth defects (1 in 100,000, Mori and Bruneau 2004), the disease is useful as a model for characterizing how mutations in transcription factors active early in cardiac development lead to heritable defects. HOS is also a useful model for the study of progressive cardiac conduction disease. Ultimately, a better understanding of the genetic control of Tbx5 during cardiac development will positively impact therapeutic approaches. Animal models of HOS in mouse and zebrafish (including the *tbx5a* mutant *heartstrings/hst*) indicate an essential role for *tbx5* in cardiac morphogenesis (Bruneau *et al.* 2001, Garrity *et al.* 2002).

CHAPTER 2: ZEBRAFISH TBX5A IS DISPENSABLE IN THE HEART FOR NORMAL CARDIOMYOCYTE NUMBER BUT REQUIRED FOR CELL GROWTH.

Introduction

The patterning, differentiation and morphogenesis of the heart tube, as well as its assimilation of rhythm, is a complex process requiring large numbers of genes. Understanding cardiac formation is important because anomalies in heart development are one of the leading causes of prenatal and infant mortality (Minino *et al.*, 2007). Many of the major events in vertebrate cardiac morphogenesis, such as chamber formation, cardiac looping and onset of rhythm, occur in parallel and in several instances the genes regulating these events are conserved (Bakkers, 2011, Dahme *et al.*, 2009, MacRae and Fishman, 2002, Thisse and Zon, 2002). Members of the T-box family of transcription factors share a highly conserved DNA-binding motif, known as the T-domain, containing about 200 amino acid residues. T-box genes are expressed in a variety of tissues during embryogenesis, and mutations in several T-box genes are associated with human developmental disorders (Greulich *et al.*, 2011, Hoogaars *et al.*, 2007). T-box genes with roles in the heart include *tbx1, tbx2, tbx3, tbx5, tbx18* and *tbx20* (Hoogaars *et al.*, 2007). Haploinsufficiency for Tbx5 can cause Holt-Oram Syndrome (HOS), a human congenital disease (reviewed in (Mori and Bruneau, 2004, Piacentini *et al.*, 2007)). HOS is characterized by cardiac and forelimb morphological defects, and progressive cardiac conduction disease (Basson *et al.*, 1997, Basson *et al.*, 1999, NewburyEcob *et al.*, 1996).

Heterozygous mutation of Tbx5 in mice produces dominant phenotypes remarkably similar to HOS, including deficiencies in cardiac septation as well as electrophysiological defects such as atrioventricular conduction block (Bruneau *et al.*, 2001). Homozygous mutation of Tbx5 in mice led to lethal defects in cardiac morphogenesis, especially affecting the posterior domain of the heart (Bruneau *et al.*, 2001) and prohibited forelimb outgrowth (Hasson *et al.*, 2007). In zebrafish two *tbx5* genes, designated *tbx5a* and *tbx5b*, have remained in the genome since a teleost-specific genome duplication approximately 300 million years ago (Albalat *et al.*, 2010, Hurley *et al.*, 2007, Jaillon *et al.*, 2004). Homozygous mutation of zebrafish *tbx5a* in *heartstrings (hst)* embryos led to lethal defects in looping morphogenesis, heart morphology and early function, and blocked the initiation of pectoral fins (Garrity *et al.*, 2002). While heterozygous *hst* fish appeared fully wildtype, graded morpholino knockdown studies indicated *tbx5a* is also required for pectoral fin outgrowth (Ahn *et al.*, 2002, Garrity *et al.*, 2002). Functions for *tbx5b* have not yet been described.

The multiple mechanisms by which the Tbx5 transcription factor functions as a key morphogenetic driver in heart development are still being defined. Retinoic acid appears to restrict the expression of Tbx5 primarily to the posterior portion of the heart tube (Sirbu *et al.*, 2008). Hence, graded levels of Tbx5 may serve as cues for positional information along the anterior-posterior cardiac axis (Liberatore *et al.*, 2000). Tbx5 interacts with a variety of transcription factors and co-factors to differentially regulate expression of target genes including *Nppa, Chisel, Hey2* and *Cx40* to promote chamber myocardial cell fates (Bruneau *et al.*, 2001, Hiroi *et al.*, 2001, Ieda *et al.*, 2010, Takeuchi

and Bruneau, 2009). Tbx5 has additional functions in the endocardium and epicardium (Hoogaars *et al.*, 2007).

Here we describe a new *hst* mutant allele (*tbx5a*^{s296}) which encodes a premature stop codon within the T-box region of the *tbx5a* gene, a location likely to generate a complete loss-of-function allele. A previously described allele, *tbx5a*^{m21}, encodes a stop codon within the C terminal domain at amino acid 316 out of 485 (Garrity *et al.*, 2002). We present a comparative molecular genetic analysis of embryos homozygous for either mutant allele, and determine the status of both alleles as null alleles. We find that (surprisingly) Tbx5a was dispensable for establishing cardiac cell number and for differentiation of the venous pole of the heart. Mutants lacking Tbx5a were still able to initiate the process of chamber ballooning by altering cell shape in atrium and ventricle. Conversely, our data underscore that Tbx5a is needed for cell growth. Cardiomyocytes lacking Tbx5a were smaller in both ventricle and atrium at early chamber morphogenesis stages. Since *tbx5a* mutant hearts never complete looping, but do undergo cell shape changes, our studies further suggest that the processes leading to chamber ballooning are genetically separable from processes underlying cardiac looping.

Results:

Identification of a new tbx5a *mutant allele*

We identified an ENU-induced mutant (s296) in a large-scale screen for recessive lethal mutations that disrupt cardiac function. Homozygous mutant embryos have severe cardiac deformities, a complete absence of pectoral fin bud initiation (Fig. 2.1H-K), and

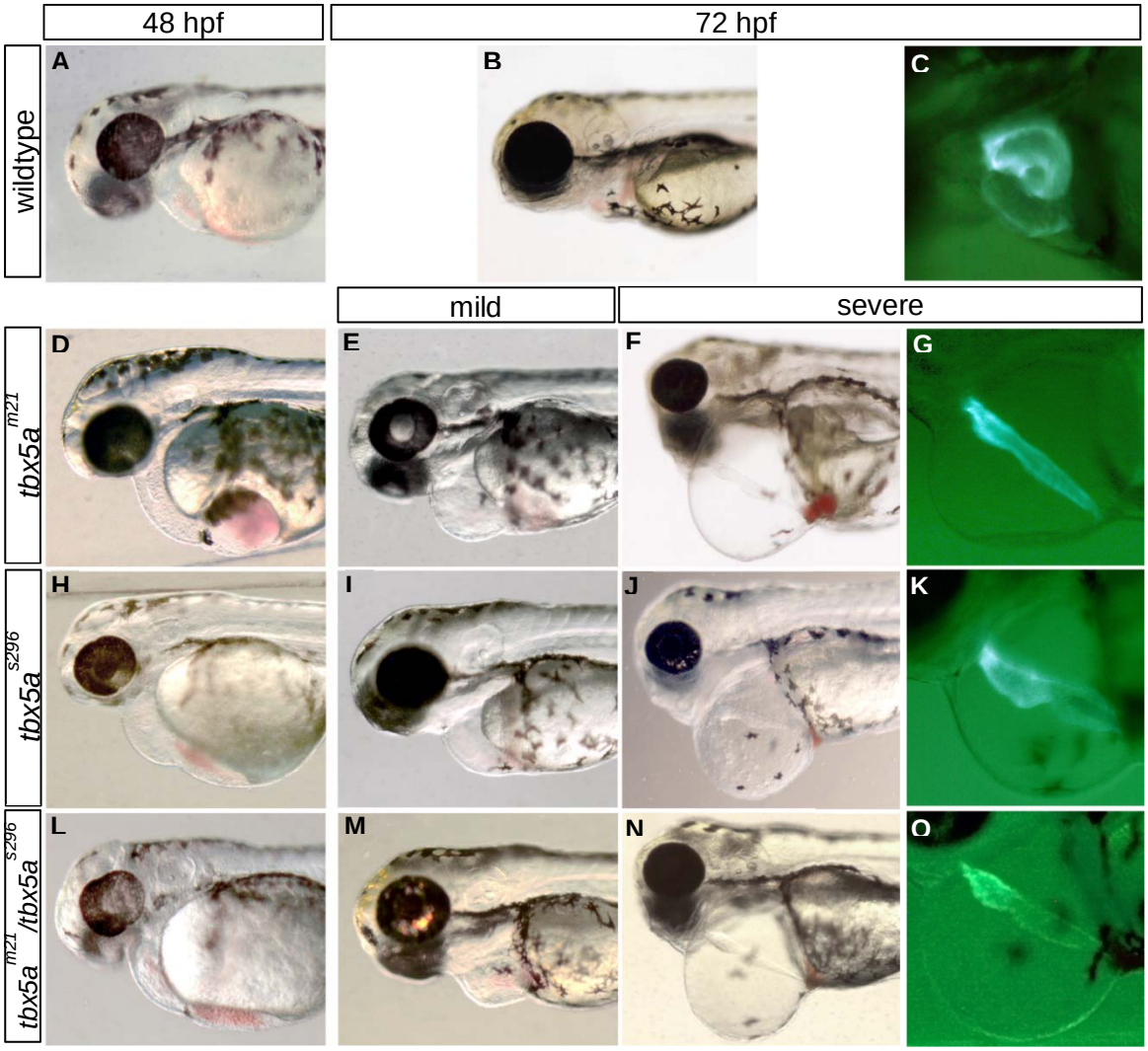

Fig. 2.1: Cardiac deformities in *tbx5a* mutant larvae. Wildtype larvae. (**D-G**) Homozygous mutant *tbx5a*^{m21} (**H-K**) or *tbx5a*^{s296} larvae. (**L-O**) *tbx5a*^{m21}/*tbx5a*^{s296} mutant larvae. As indicated, larvae displayed either a "mild" or "severe" *heartstrings* phenotype at 72 hpf. (**C, G, K, O**) Fluorescent hearts of *Tg(myl7:EGFP-HsHRAS)* embryos, demonstrating the dysmorphic form of hearts in the mutants.

die between 6 and 8 days post-fertilization (dpf). Heterozygous embryos have normal anatomy, and adults are viable as well as fertile. Because these phenotypes strongly resembled those seen in homozygous *hst* mutant embryos (Fig. 2.1D-G), we performed a complementation test by intercrossing heterozygous fish from the s296 and *tbx5a*^{m21} lines to determine if the s296 mutation is allelic to *tbx5a*^{m21}. Complementation failed to occur (Fig. 2.1L-O), with 24.9% of resulting embryos demonstrating *hst*-like cardiac and pectoral fin phenotypes and 75.1% of resulting offspring appearing completely wildtype (see Table 2.1). Failure to complement indicates that the m21 and s296 mutations are allelic.

Table 2.1: Analysis of Mendelian inheritance patterns of embryos resulting from wildtype and mutant intercrosses. Phenotypes were assessed at 72 hpf to determine presence of pectoral fins and status of cardiac looping. The number and relative proportion (%) of offspring are given per genotype.

Genotype:	# of mutants observed/clutch size	Percent of embryos with *hst* phenotype
m21/m21	54/215	25.1%
m21/s296	58/233	24.9%
s296/s296	48/204	23.5%

Sequencing of tbx5*^{s296} *allele reveals a nonsense mutation

To determine the molecular location of the *tbx5a*^{s296} mutation we cloned and sequenced cDNA from homozygous *tbx5a*^{s296} embryos. Sequencing revealed a G to A transition at basepair 527, which would introduce a nonsense mutation at amino acid 120 within the T-box region of the coding sequence (Fig. 2.2). If translated, the predicted Tbx5a^{s296} mutant protein would include only the first half of the T-box DNA-binding domain. In contrast, the previously described *tbx5a*^{m21} mutation was located in the carboxyl-terminus

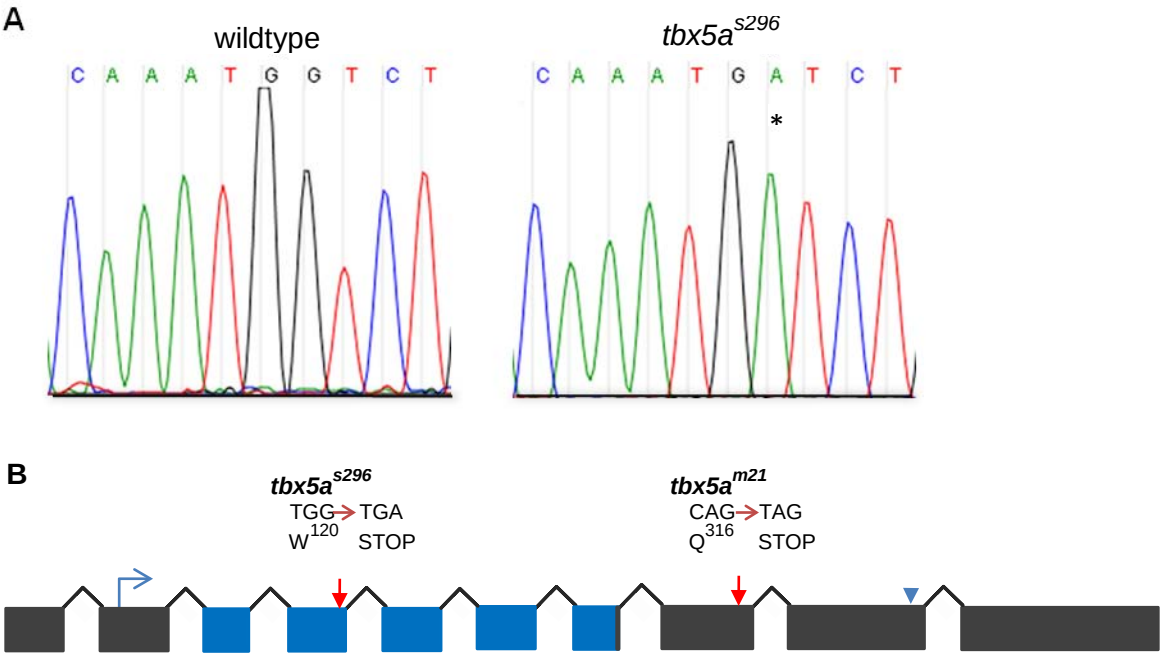

Fig. 2.2: Sequencing of the zebrafish *tbx5a*^{s296} allele. (**A**) Sequencing of *tbx5a* cDNA indicated a G to A nucleotide change at base pair 527 in *tbx5a*^{s296} mutant embryos. The *tbx5a*^{s296} mutation changes residue 120 (tryptophan) to a premature stop codon within the T-box DNA binding domain. (**B**) A schematic diagram of the *tbx5a* transcript showing exons, including the locations of the start and stop sites (blue arrow and arrowhead respectively) and the two *hst* nonsense mutations (red arrows). Blue boxes indicate the region encoding the T-box domain.

(Garrity *et al.*, 2002), a region that in mammals contains elements that positively regulate DNA binding (Hiroi *et al.*, 2001). Therefore, the potential existed that each allele could encode truncated proteins with unique cellular interactions or dominant-negative effects.

To investigate whether dominant-negative effects occurred, we examined the percentage of affected offspring obtained from a *tbx5a*^{s296} heterozygous cross. At 72 hpf, 23.5% of embryos displayed the *hst* phenotype, while 76.5% were completely wildtype (Table 2.1). This ratio indicated a lack of dominant-negative effects. Dominant negative effects were likewise not observed for homozygous *tbx5a*^{m21} mutant embryos (Garrity *et al.*, 2002).

Comparison of* tbx5a *mutant phenotypes

In order to investigate the relative severity of the *tbx5a*^{m21}and *tbx5a*^{s296} alleles, we compared the phenotypes of homozygous *tbx5a*^{m21}*/tbx5a*^{m21}, *tbx5a*^{s296}*/tbx5a*^{s296} or *tbx5a*^{m21}*/tbx5a*^{s296} embryos. In all three *hst* genotypes, the formation and contractility of the heart tube in mutant embryos at 24-26 hours post fertilization (hpf) was indistinguishable from wildtype (data not shown). By 48 hpf, mutant hearts of all three *hst* genotypes had failed to loop and fluid began to accumulate in the pericardium (Fig. 2.1D,H,L). *tbx5a*^{s296}*/tbx5a*^{s296} or *tbx5a*^{m21}*/tbx5a*^{s296} mutant embryos within a clutch exhibited variable expressivity similar to that previously reported for *tbx5a*^{m21}*/tbx5a*^{m21} embryos (Fig. 2.1) (Garrity *et al.*, 2002). “Mild” homozygous *hst* embryos showed moderate defects in cardiac looping and reduced blood flow (Fig. 2.1E,I,M), whereas “severe” homozygous *hst* embryos developed an enlarged pericardial edema, an extended heart tube, and completely lacked blood flow (Fig. 2.1F,G,J,K,N,O). Lethality occurred

for all *hst* embryos by approximately 7 dpf, whether the cardiac phenotypes were mild or severe. Looping morphogenesis was quantified in homozygous *tbx5a*^{m21}or *tbx5a*^{s296} mutant larva by measuring the angle of the AVJ relative to the anterior/posterior axis of the larva; we term this rubric the "looping angle" (Fig. 2.3). Wildtype larvae demonstrated an average looping angle of 13° by 48 hpf. In contrast, both homozygous *tbx5a*^{m21} hearts and *tbx5a*^{s296} hearts showed average looping angles greater than 50°, indicating that significantly less looping had occurred relative to wildtype hearts ($p<0.05$ for both mutants). Indeed, looping angles for *hst* mutant hearts at 48 hpf were similar to those of 34 hpf wildtype hearts (48° ± 2.5 SEM; Chernyavskaya and Garrity, unpublished data), suggesting that, on average, *hst* mutant hearts barely initiate looping, if at all. Thus, overt cardiac and fin phenotypes appeared indistinguishable among *tbx5a*^{m21}*/tbx5a*^{m21}, *tbx5a*^{m21}*/tbx5a*^{s296} or *tbx5a*^{s296}*/tbx5a*^{s296} embryos. Moreover, *tbx5a* morpholinos described by us and others have produced the identical phenotype (Ahn *et al.*, 2002, Garrity *et al.*, 2002, Ghosh *et al.*, 2009). These data indicate that both the *tbx5a*^{m21}and *tbx5a*^{s296} mutations generate strong loss-of-function alleles.

Chamber specification is unaffected in tbx5a^{s296}*embryos*

To more rigorously test our hypothesis that *tbx5a*^{m21}and *tbx5a*^{s296} represent equivalently strong alleles, we performed molecular studies to examine specification and differentiation in the heart and fins of homozygous embryos by whole mount *in situ* hybridization. In vertebrate species such as mice, chick and frog, *tbx5* plays an important role in the assignment of chamber formation fates (Bruneau *et al.*, 2001, Goetz *et al.*, 2006, Liberatore et al., 2000). In zebrafish, atrial and ventricular cell myocardial lineages

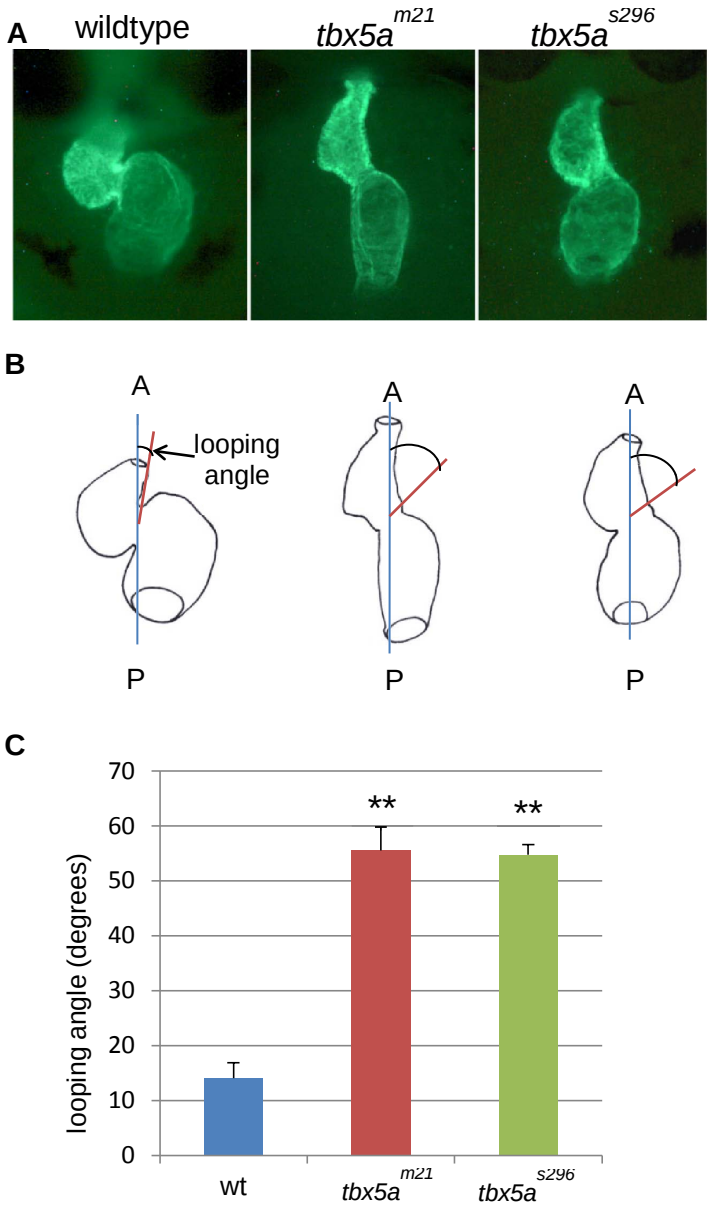

Fig. 2.3: Absence of functional *tbx5a* results in a lack of cardiac looping. (**A**) 48 hpf hearts in wildtype or *tbx5a* mutant *Tg(myl7:EGFP-HsHRAS)* embryos. (**B**) Diagram outlining chamber looping, in which the "looping angle", representing the degrees between the embryonic A/P axis (blue line) and the plane of the AVJ (red line), was calculated. (**C**) The mean looping angle ± SEM (n=14-15 hearts per genotype). Angles for wildtype and mutant hearts were compared by Student's *t*-test (*p <0.05).

can be distinguished with molecular markers well before the chambers become morphologically discrete. To investigate the proportion and specification of chambers as they formed within the heart tube, we examined the expression of *atrial-specific myosin heavy chain* (*amhc*) and *ventricle-specific myosin heavy chain* (*vmhc)* (Berdougo *et al.*, 2003, Yelon *et al.*, 1999). At 30 hpf, the presumptive atrium expresses *amhc* just under the left eye. Early atrium specification proceeded normally in both *tbx5a*^{m21}and *tbx5a*^{s296} homozygous mutant embryos as seen by appropriate *amhc* expression (Fig. 2.4A-C). At 42 hpf, wildtype, *tbx5a*^{m21} and *tbx5a*^{s296} embryos all expressed *vmhc* in the ventricle only (Fig. 2.4D-F). One previous report describing a morpholino-targeted *tbx5a* phenotype indicated that *vmhc* can show ectopic expression within the presumptive atrium of the heart tubes at 36 hpf (Lu *et al.*, 2008), but here we find that homozygous *tbx5a*^{m21} and *tbx5a*^{s296} mutant embryos expressed *vmhc* in a region strictly similar to wildtype by the onset of chamber ballooning (~42 hpf). Endocardial specification occurred normally in *hst* embryos as indicated by the expected *fli1* expression in the heart at 48 and 72 hpf (data not shown) (Brown *et al.*, 2000). While the initial steps of chamber formation were normal, *tbx5a*^{s296} mutant embryos did show later defects in cardiac differentiation. In wildtype embryos, *versican* (*vcana*) expression becomes restricted to the atrioventricular (AV) boundary after 37 hpf ((Thisse *et al.*, 1993), Fig. 2.4G) and *bmp4* to the same region by 48 hpf (Fig. 2.4J). However, in both homozygous *tbx5a*^{m21} and *tbx5a*^{s296} embryos, restriction of these markers did not occur (Fig. 2.4H, I, K, L) but remained expanded throughout the entire ventricle. Therefore, cells of the first heart field segregate normally into atrial and ventricular precursors in *tbx5a*^{m21}and *tbx5a*^{s296} mutant embryos, but by 48 hpf have arrested or slowed further differentiation.

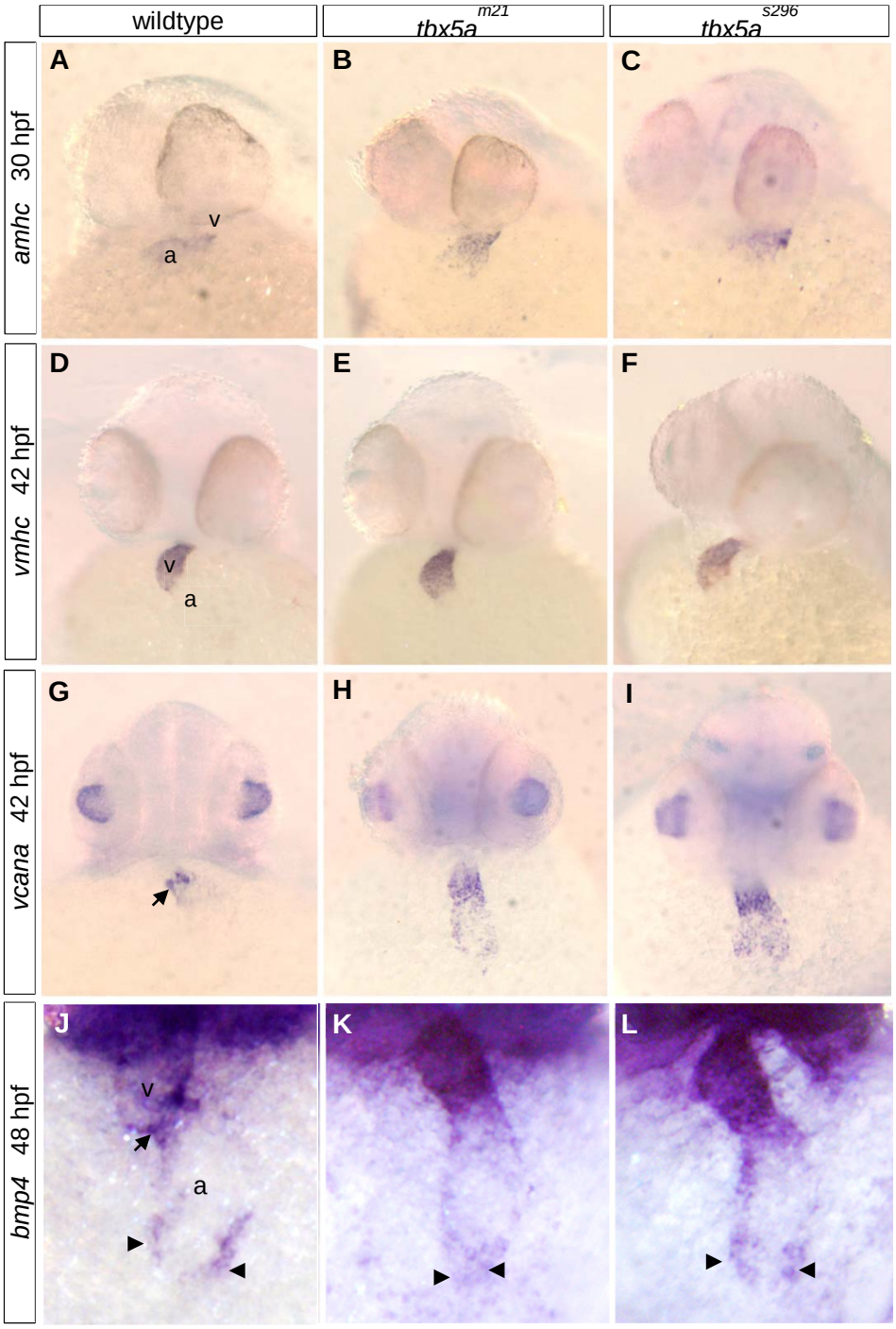

Fig. 2.4: Chamber and myocardial differentiation in *tbx5*a mutant embryos and larvae. A developmental series of *in situ* hybridization experiments examining (**A-C**) atrial-specific *amhc* expression (30 hpf), (**D-F**) ventricular-specific *vmhc* expression (42 hpf), (**G-I**) *vcana* expression after the onset of cardiac looping (42 hpf), and (**J-L**) *bmp4* cardiac expression at 48 hpf in wildtype and *tbx5a* mutant embryos. a: atrium; v: ventricle; arrows: gene expression restricted to the atrial-ventricular junction; arrowhead: sinus venosus.

Venous differentiation in* hst *embryos

Within the vertebrate heart, *tbx5* may play a key role in recruitment or expansion of the population of sinoatrial precursors. For example, Tbx5 regulates the expression of *myosin heavy chain 6,* a gene required for development of the sinoatrial region (Ching *et al.*, 2005). To investigate the potential impairment of sinoatrial development in zebrafish embryos lacking *tbx5a,* we employed *in situ* hybridization and functional studies. Wildtype embryos express BMP4 in a population of cells marking the sinus venosus (SV) at 48 hpf. In contrast, *islet-1* mutants, which show reduced differentiation at the venous pole, failed to express BMP4 in the venous region of the heart (de Pater *et al.*, 2009). In addition, mutation of the Bmp type 1 receptor *alk8* in *laf* embryos led to hearts with a reduced atrium but normal-sized ventricle, further supporting the role of BMP signaling in differentiation of the venous pole of the heart (Chocron *et al.*, 2007; Marques and Yelon, 2009). We therefore selected *bmp4* as an appropriate marker for evaluating differentiation of posterior (venous) cell fate in the 48 hpf heart tube. Homozygous *tbx5a*^{m21}and *tbx5a*^{s296} embryos did not differ from wildtype in that both expressed a similar patch of *bmp4* at the venous pole at this stage (Fig. 2.4J-L), suggesting differentiation was normal in this region.

Like mice, zebrafish mutant for *tbx5a* exhibit bradycardia (Garrity *et al.*, 2002), but it is uncertain whether this was due specifically to sinoatrial defects. To investigate the function of the sinus venosus region, we visually examined hearts of *tbx5a*^{m21} and *tbx5a*^{s296} mutants in live embryos from 30-72 hpf for arrhythmias indicative of pacemaker dysfunction. Bradycardia was noted in both mutants, but no evidence of sinus

pauses, AV block or other arrhythmia was found (n = 30 mutant embryos per allele). Thus, both gene expression and functional assays suggest that during early chamber formation stages, posterior SHF cells were added to the heart tube and sinoatrial function was not severely defective in *hst* mutants.

Pectoral fin outgrowth is absent in homozygous tbx5a^{s296} embryos

Along with cardiac defects, pectoral fin dysgenesis is a hallmark of Tbx5a depletion in zebrafish (Ahn *et al.*, 2002, Garrity *et al.*, 2002). Wildtype embryos begin differentiating pectoral fin tissue by 28 hpf, and limb buds are easily identifiable by 32 hpf (Gibert *et al.*, 2006). Small fins with defined proximal/distal axes are observed by 72 hpf (Fig. 2.5G). As reported for *tbx5a^{m21}* mutants, we find homozygous mutant *tbx5a^{s296}* embryos at 72 hpf completely lacked morphological evidence of pectoral buds or fins (Fig. 2.5H, I). Investigation by *in situ* hybridization confirms that homozygous *tbx5a*^{s296} mutant embryos did not express the early fin field marker *bmp4* by 36 hpf (Fig. 2.5A-C) nor the later fin fold marker, *vcana*, by 48 hpf (Fig. 2.5D-F). Taken together, these molecular data on cardiac and fin phenotypes confirm our initial impression of equivalently strong loss-of-function phenotypes for the *tbx5a^{m21}* and *tbx5a^{s296}* alleles.

The m21 and s296 mutations in tbx5a encode null alleles

A possibility remained that the *tbx5a^{m21}*and *tbx5a^{s296}* alleles encoded proteins that retained at least some residual Tbx5a function. For accurate interpretation of phenotypes, it was important to definitively test whether *tbx5a^{m21}*and *tbx5a^{s296}* encoded null alleles. Therefore, protein extracts from mutant embryos were assayed by immunoblot analysis

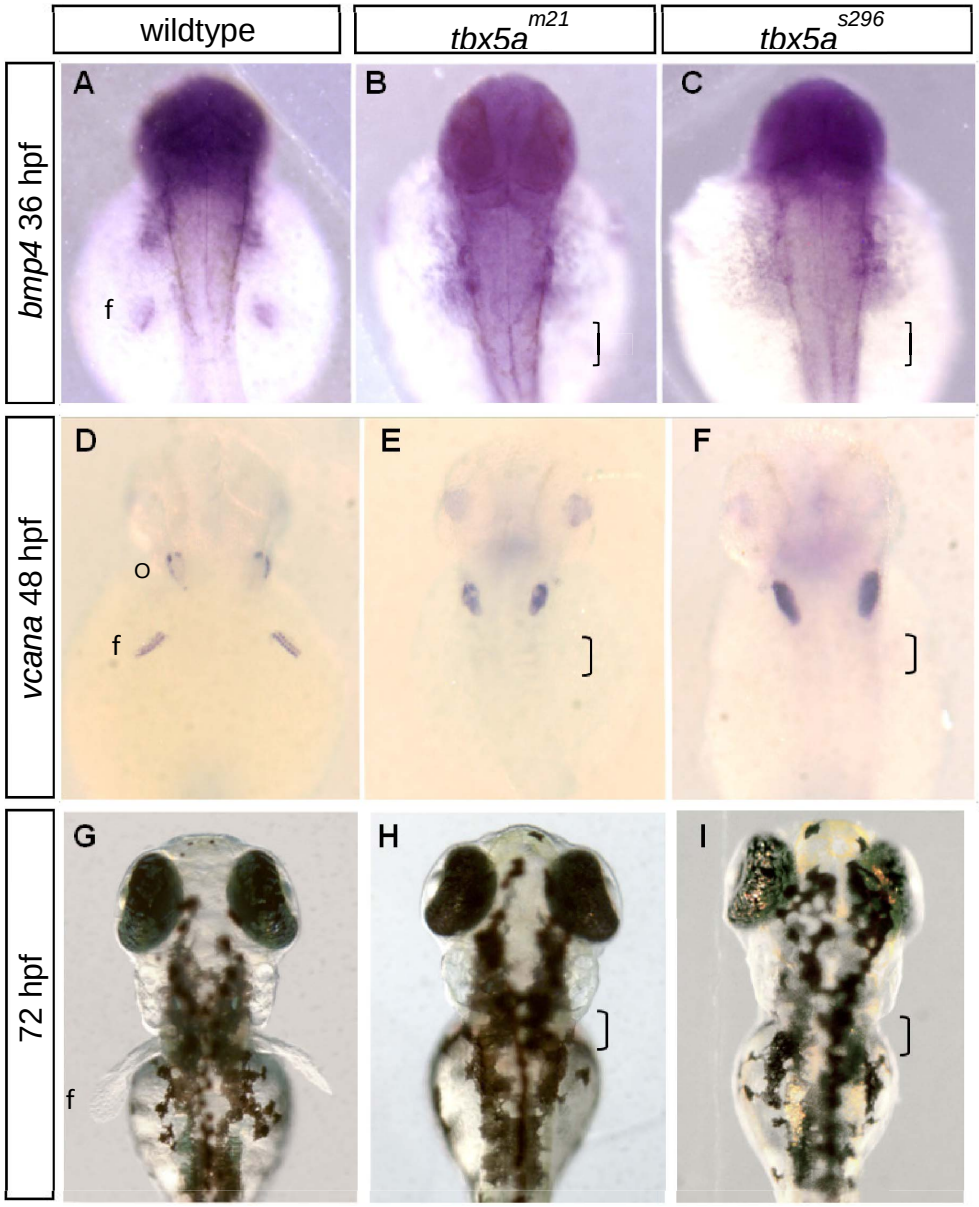

Fig. 2.5: Pectoral fin development is absent in *tbx5a*^{s296} mutant embryos. A developmental series of *in situ* hybridization experiments examining fin initiation. (**A-C**) Mutants do not express *bmp4* in the fin field at 36 hpf. Normal expression in pharyngeal arches provides an internal control. (**D-F**) Mutants do not express the apical fin fold marker *vcana* at 48 hpf, but show normal expression in the otic placodes. (**G-I**) Brightfield images taken at 72 hpf indicate the absence of pectoral fins even at this later stage. o:otic placode. Brackets indicate the location where expression of fin markers or pectoral fin outgrowth was expected.

using an antibody against zebrafish Tbx5a (Fig. 2.6). The predicted size of wildtype Tbx5a is 54 kDa. If translated, the *tbx5a*^{m21} allele would encode a 31 kDa truncated protein, and *tbx5a*^{s296} allele would encode a 15 kDa truncated protein. Tbx5b, a paralogous zebrafish T-box protein, has a predicted size of 47.4 kDa. Because the antibody used in this analysis is a polyclonal antibody targeted to the first 15 amino acids of the zebrafish *tbx5a* sequence, and the Tbx5a and Tbx5b proteins are only 20% similar in this region, it is unlikely the antibody will cross-react with Tbx5b. This expectation was confirmed with the detection of a ~54 kDa protein for wildtype Tbx5a, but no protein of 47 kDa. No proteins were detected in *tbx5a*^{m21}*/tbx5a*^{m21}or *tbx5a*^{s296}*/ tbx5a*^{s296} samples, indicating that both constitute protein null alleles (Fig. 2.6). This finding is consistent with genetic data including a lack of stronger phenotypes obtained via several different zebrafish *tbx5a* morpholinos (Ahn *et al.*, 2002, Garrity *et al.*, 2002, Ghosh *et al.*, 2009).

Tbx5a is not required for regulation of cardiomyocyte number, nor addition to the arterial pole

One important physiological activity of Tbx5 is its regulation of cardiomyocyte proliferation (Brown *et al.*, 2005, Hatcher and McDermott, 2006). With confirmed null alleles in hand, we therefore investigated the effects of *tbx5a* depletion on cardiomyocyte number in zebrafish. To assess cardiac cell number, we intercrossed the *tbx5a* mutant lines with a transgenic line in which the nuclear DsRed reporter gene is driven by the heart-specific *myl7* (formerly *cmlc2*) promoter (*Tg(myl7:nDsRed2/myl7:EGFP)*(Mably *et al.*, 2003)). Cardiomyocytes were quantified by counting the total number of DsRed-positive nuclei in 48 hpf transgenic fish of several genotypes, including homozygous

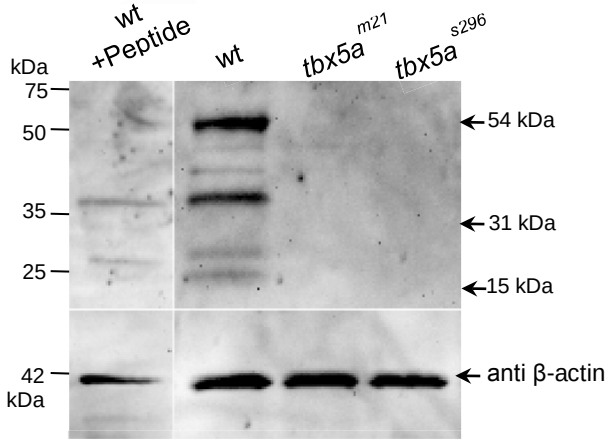

Fig. 2.6: Mutations in Tbx5a represent protein null alleles. Immunoblot analysis was performed on protein extracts isolated from wildtype or homozygous *tbx5a*^{m21} or *tbx5a*^{s296} embryos. The blot was probed with a polyclonal antibody against zebrafish *tbx5a*. Wildtype Tbx5a is predicted to be 54 kDa. The faint bands between 54 and 31 kDa are most likely degradation products that were consistently observed in other wildtype protein preparations. The Tbx5a^{m21}mutant protein has a predicted size of 31 kDa, while the Tbx5a^{s296} mutant protein has a predicted size of 15 kDa. As a control for specificity of the Tbx5a antibody, *tbx5a* antibody pre-incubated with the original immunizing peptide was tested on wildtype extracts. Bands in this control lane indicate non-specific bands. To control for protein loading the blot was reprobed for beta-actin.

wildtype, homozygous mutant *tbx5a*^{m21}, homozygous mutant *tbx5a*^{s296}, phenotypically wildtype siblings (the offspring of a cross of *tbx5a*^{m21} heterozygotes), and *tbx5a* morphant embryos (Fig. 2.7). We observed no significant differences in total cardiomyocyte numbers at 48 hpf among any of these fish (p=0.399).

Cardiomyocyte size is reduced in* hst *embryos

In order to determine if *tbx5a* plays a role in growth and differentiation of individual cardiomyocytes, we measured the size and shape of *hst* cardiomyocytes in the heart during the chamber ballooning stages. Regional cell shape changes play an important role in determining overall morphology of the developing heart tube (Auman *et al.*, 2007). As the ventricle undergoes chamber morphogenesis, the cells located within the outer curvature of the chamber (OC) elongate perpendicular to the direction of blood flow, while cells in the inner curvature (IC) retain a smaller, cuboidal shape (Auman *et al.*, 2007). In both atrium and ventricle, OC cells continue to express the marker *natriuretic peptide precursor A* (*nppa*), whereas IC cells lose this expression of *nppa* (Auman *et al.*, 2007). In mice and chick, cells of the OC grow to a larger size than the IC (Manasek *et al.*, 1972, Meilhac *et al.*, 2004). Therefore, following the precedent of Auman and colleagues, we defined the ventricular OC as the region of cells that retain *nppa* expression and the IC as the region of cells that are not expressing *nppa*. To quantify cell size and shape in zebrafish hearts, we used ImageJ software and the *Tg(myl7:EGFP-HsHRAS)* line (Chi *et al*., 2008), in which cardiomyocytes express GFP at the cell periphery (Fig. 2.8). ImageJ software was used to calculate the size (that is, the surface area) and the circularity of cardiomyocytes in each region. Although Auman and

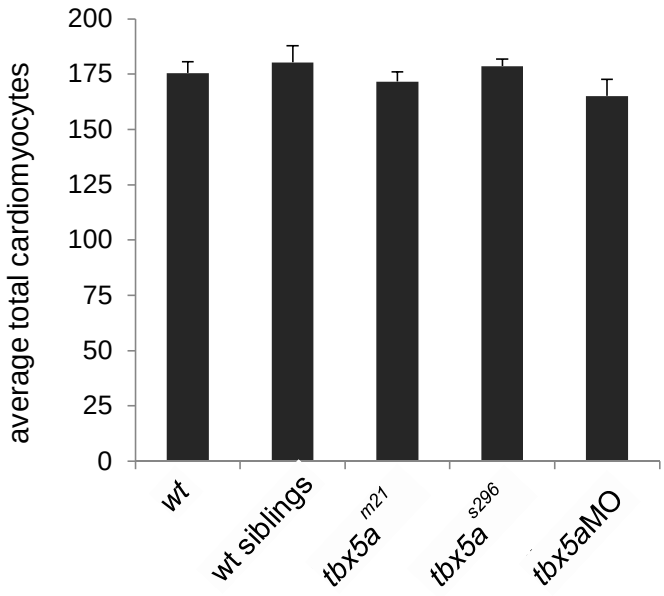

Fig. 2.7: *tbx5a* is not required for regulation of cardiomyocyte number. Quantification of total cardiomyocyte numbers in homozyogous wildtype embryos, phenotypically wildtype siblings from a cross of two *hst* heterozygotes, or homozygous *tbx5a* mutant or morphant embryos at 48 hpf. Cardiomyocytes were identified by quantifying nuclei from inverted fluorescent images of *Tg(myl7:nDsRed2)* embryonic hearts. Data are expressed as means ± SEM (*p<0.05). n=20 for WT, n=12 for WT siblings, n=11 for *tbx5a*^{m21}, n=7 *tbx5a*^{s296}, n= 17 for *tbx5a* morphant embryos.

colleagues reported that by 52 hpf OC cells are larger than IC cells (Auman *et al.*, 2007), a difference in wildtype ventricular OC and IC cell size was not yet apparent by 48 hpf ($p=0.87$). In the atrium at 48 hpf, OC cells were already notably larger than IC cardiomyocytes ($p<0.001$) (Fig. 2.8C). Upon examining *tbx5a*^{m21} mutants, we find that cells of IC and OC were statistically smaller in both chambers relative to the cognate region in wildtype controls (Fig. 2.8C). The cell size reduction was not due to general developmental delay as wildtype and *hst* mutant embryos show equivalent expression of markers in non-*tbx5a* expressing tissues such as the otic placodes and pharyngeal arches (Fig. 2.5D-I) (Garrity *et al.*, 2002). Moreover, this phenotype is not likely to be a secondary consequence of altered blood flow, since circulation in *hst* mutants remains relatively robust prior to 48 hpf, although it typically decreases substantially over the following 24 hpf. Instead, the overall smaller size of cells in both chambers of *hst* mutants appears to indicate a block in continued cell growth and differentiation of chamber cardiomyocytes by 48 hpf. Dampened or arrested cardiomyocyte cell growth is consistent with the deteriorating cardiac function observed for the zebrafish *hst* heart at 72 hpf, which includes a collapsed ventricle, lesions in atrial tissue, decreased contractility of the heart, and loss of circulation in the more severe *hst* mutants (Garrity *et al.*, 2002).

Assessment of cell shape changes associated with chamber ballooning

As measured in the ImageJ program, "circularity" is a measure of cell shape, with a value of 1.0 indicating a perfect circle and smaller values indicating an increasingly elongated polygon. Circularity values indicated that in wildtype ventricles, OC cells became more

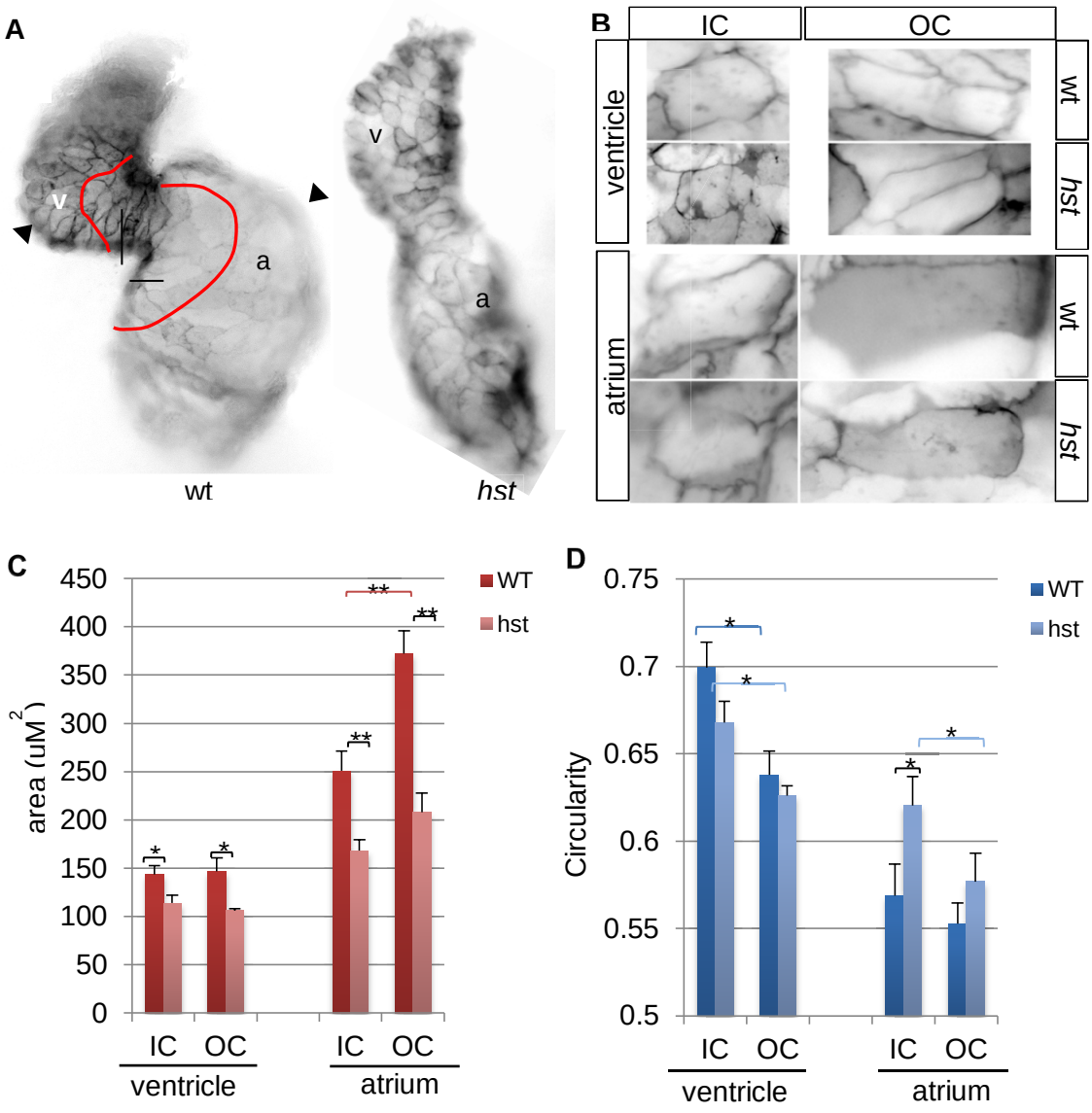

Fig. 2.8: Cardiomyocyte size is reduced in 48 hpf *hst* embryos. (**A**) Hearts from *Tg(myl7:EGFP-HsHRAS)* wildtype and *tbx5a*^{m21} embryos were imaged *in situ* to quantify cardiomyocyte dimensions. IC and OC were determined as described in Auman *et al.* (2007). (**B**) Representative images of cardiomyocytes taken at 400x magnification, selected from each chamber to illustrate their relative size and shape. (**C**) Quantification of cardiomyocyte size in the ventricle or atrium, based on the surface area of individual cells. (**D**) Quantification of cardiomyocyte shape for each chamber, in which higher numbers indicate a more circular shape. Data are expressed as means ± SEM (*p<0.05, **p<0.001). n=10 wildtype embryos 369 total cells, n=10 for *hst* embryos with 337 total cells. IC = Inner Curvature, OC = Outer Curvature cells. Red lines in (A) denote the boundary for scoring cells as IC or (arrowhead) OC.

elongated than IC by 48 hpf (p=0.002)(Fig. 2.8B,D), a change associated with chamber ballooning (Auman *et al.*, 2007). In *tbx5a*^{m21} mutant hearts, the ventricular OC cells showed typical elongation whereas IC cells remained rounded. Compared to wildtype, no significant differences were detected in the circularity values for *tbx5a*^{m21} ventricular OC cells (p=0.12) or ventricular IC cells (p=0.11). Therefore, the ventricles of *tbx5a*^{m21} mutants appear to be undergoing normal chamber ballooning.

Cells of the wildtype atrium also undergo changes in cell shape as ballooning proceeds. In this chamber, both IC and OC cells became elongated, and displayed circularity values even smaller than the ventricular OC cells (Fig. 2.8D). At 48 hpf, IC and OC were equally elongated (p=0.55), although OC cells were already substantially larger than IC cells (Fig. 2.8C). In *tbx5a*^{m21} mutants, atrium OC cells were elongated to the same degree as wildtype (p=0.37). However, *tbx5a*^{m21} mutant atrium IC cells showed a more rounded phenotype compared to wildtype atrium IC cells (p=0.027). This difference identifies the atrial IC as one region of the heart that may especially require Tbx5a activity for continued differentiation of cell shape. Overall, these data suggest that although looping morphogenesis remains stalled in *hst* embryos, most cell shape changes associated with chamber ballooning still proceed normally in both chambers.

Discussion:

Here we describe a new mutant *hst/tbx5a* allele in zebrafish, termed *tbx5a*^{s296}. This nonsense allele encodes a stop codon within the T-box region, compared to the more C-

terminal location of the mutation in *tbx5a*^{m21}previously described. Our phenotypic studies using these two null *hst* mutants support the findings that *tbx5a* is not required for cardiac cell number during chamber morphogenesis stages, for differentiation of the venous pole of the heart, or for the correct proportion of atrial versus ventricular cells. However, Tbx5a is required for cardiomyocytes of both chambers to attain their normal size by chamber ballooning stages. Examination of the atrium as it enters chamber ballooning indicated that both IC and OC cells of this chamber normally undergo a substantial elongation in cell shape. By contrast, previous studies showed that ventricle OC cells elongate substantially more than IC cells during this period (Auman *et al.*, 2007). Tbx5a appears to influence cell shape changes within the atrium IC, but does not affect atrium OC, nor within the ventricle. While the hearts of *hst/tbx5a* mutants never complete looping morphogenesis, they nevertheless display characteristic changes associated with chamber ballooning (with the exception of the atrium IC), suggesting that chamber ballooning and looping morphogenesis are not interdependent processes.

Four lines of evidence support the conclusion that both the *tbx5a*^{s296} and *tbx5a*^{m21} alleles are null and that neither exerts any dominant-negative effects. First, biochemical evidence indicates the absence of signal on an immunoblot, indicating these mutations encode null alleles. Second, homozygous *tbx5a*^{m21}and *tbx5a*^{s296} embryos do not represent more than 25% of progeny in a monohybrid cross, indicating the phenotype is fully recessive. Moreover, homozygous *tbx5a*^{m21} and *tbx5a*^{s296} embryos are phenotypically identical in their cardiac and fin phenotypes, and age of lethality. Finally, the phenotypes of a transheterozygous embryo (*tbx5a*^{m21}*/tbx5a*^{s296}) are indistinguishable from a

homozygote of either allele, providing genetic evidence that both are equivalently strong alleles. The capacity of Tbx5 to demonstrate dominant-negative activity has been observed for mutations in human Tbx5 that yield a truncated protein lacking the 3' end of the T-box (Basson *et al.*, 1999, Herrmann and Kispert, 1994, Kispert and Herrmann, 1993, Kispert *et al.*, 1995, Li *et al.*, 1997, Muller and Herrmann, 1997). In zebrafish, however, *tbx5a* transcripts can be weakly detected by whole-mount *in situ* hybridization for only a few hours after the expected onset of transcription, but are non-detectable beyond 26 hpf (Garrity *et al.*, 2002). Nonsense-mediated mRNA decay (NMD) is a cellular fidelity mechanism which prohibits the translation of mRNAs with premature stop codons or incorrect splicing (Hentze and Kulozik, 1999). NMD, a conserved mechanism found in all eukaryotes, may help ensure that aberrant proteins which could have dominant-negative or deleterious gain-of-function activities are not produced (Chang *et al.*, 2007, Cheng *et al.*, 1994, Zhang *et al.*, 1998). For both *tbx5a*^{m21} and *tbx5a*^{s296} transcripts, the location of the premature stop codon within an internal exon located more than 50 basepairs upstream of the end of the last spliced exon suggests that these transcripts are candidate targets for NMD (Fig. 2.2). Thus, NMD is likely mechanism that could account for the observed lack of Tbx5a protein in these mutants. Alternatively, the truncated Tbx5a proteins may be extremely unstable and thus undetectable by immunoblot.

We find that *tbx5a* is not essential for determining normal cardiomyocyte number in zebrafish during early chamber morphogenesis. It is therefore likely that *tbx5a* is dispensable for functions regulating cardiomyocyte proliferation in zebrafish, although

we have not yet tested this directly. In contrast, depletion of TBX5 by morpholino in *Xenopus* resulted in a ~30-40% decrease of total cardiac cells in hearts undergoing early chamber formation (stage 37), indicating that TBX5 positively regulates cardiomyocyte proliferation in this system (Brown *et al.*, 2005, Goetz *et al.*, 2006). Decreased numbers were due to a delay or arrest in G1/S-phase, which was followed later by an increase in apoptotic cells (Goetz *et al.*, 2006). On the other hand, overexpression of wildtype TBX5 in chick (beginning at HH 17-18, early cardiac looping stages) also reduced cardiomyocyte proliferation by 40% (Hatcher *et al.*, 2001). These data support a model in which TBX5 functions as a growth arrest signal that negatively regulates cardiomyocyte proliferation. At a somewhat later stage in human development (10-15 weeks), Hatcher *et al.*, noted a reciprocal relationship of TBX5 expression with proliferating cell nuclear antigen (PCNA), an indicator of mitotic activity, providing additional support for the idea that TBX5 functions as a growth arrest signal (Hatcher *et al.*, 2001). Overall, genetic studies of Tbx5 in various organisms have emphasized that embryos are quite sensitive to Tbx5 dosage and that alterations leading to increases or decreases relative to the normal amount are associated with phenotypes. In addition, the timing of depletion or over-expression of Tbx5 may affect the phenotypic outcome, especially if Tbx5 has a dual role as an activator in early stages and a growth arrest signal in later stages, as has been proposed (Goetz *et al.*, 2006). Indeed, studies of cardiac T-box factor *tbx2* have demonstrated the principle that the same T-box gene can have either activating or repressive effects on cardiomyocyte proliferation depending on the developmental timing and context (Hoogaars *et al.*, 2007, Sedletcaia and Evans, 2011).

Mice lacking Tbx5 showed pronounced defects in the formation of the posterior end of the heart, including hypoplastic sinoatrial structures (Bruneau *et al.*, 2001). Our experiments here examining zebrafish posterior cardiac differentiation and pacemaker functionality suggested that sinoatrial structures were not severely affected in *tbx5a* mutants. In zebrafish, the cells of the first heart field (FHF) form the linear heart tube, to which cells derived from the second heart field (SHF) are later added, both at the arterial and venous poles (de Pater *et al.*, 2009; Hami *et al.*, 2011; Lazic and Scott, 2011). While total FHF proliferation in the heart tube is proposed to be low over the 24-48 hpf period (de Pater *et al.*, 2009), contributions from the SHF may equal as much as one-third of the ventricle cell number (Lazic and Scott, 2011). Thus, our observation of equivalent numbers of cardiomyocytes in *tbx5a* mutant heart tubes suggests that SHF addition to the arterial pole was not substantially affected in these mutants.

In vertebrates, the venous pole of the heart develops pacemaker function (Arrenberg *et al.*, 2010; Moorman and Christoffels, 2003). Functional defects in pacemaker activity can result in sick-sinus syndrome, leading to sinus pauses or arrest, bradycardia, and other types of arrhythmia (Dobrzynski *et al.*, 2007). Sinus dysfunction phenotypes were noted in adult heterozygous tbx5 mice, which were reported to exhibit over 100 sinus pauses per hour, as well as primary and secondary atrioventricular block (AVB) (Bruneau *et al.*, 2001). Due to embryo transparency, arrhythmias can be easily detected in zebrafish embryos from a young age (Ebert *et al.*, 2005; Milan and MacRae, 2008). Mutants such as Islet-1 (*isl1*), that are defective in cardiomyocyte differentiation specifically at the venous pole, also showed sinus dysfunction phenotypes including bradycardia and

frequent sinus pauses (de Pater *et al.*, 2009). The *hst* phenotypes were mild in this regard, with no detectable change in a marker of sinus venosus development, and no evidence of sinus pauses or AV block, or sporadic arrhythmia. Bradycardia, which can be associated with sinoatrial dysfunction, was observed, but was not nearly as severe as in *isl-1* mutants which have known defects in venous differentiation (de Pater *et al.*, 2009; Garrity *et al.*, 2002), and might be due to any of several factors. Bradycardia itself can be a sign of sinus dysfunction, yet mice defective in any of several genes required for normal pacemaker activity usually show bradycardia in combination with some other type of arrhythmia (Dobrzynski *et al.*, 2007), but this was never observed for *hst* mutant embryos.

The zebrafish genome contains two paralogous *tbx5* genes (Albalat *et al.*, 2010), *tbx5a* and *tbx5b*. Therefore, the potential remains that *tbx5b* paralog could share a redundant function with *tbx5a* in modulating cardiac cell number in early chamber morphogenesis stages, and that this function masks a cell proliferation phenotype in *hst* mutants. *tbx5b* is expressed in the embryonic eye and heart, but not in the pectoral fins (Albalat *et al.*, 2010). Testing the hypothesis of genetic redundancy awaits functional studies of *tbx5b*. However, it is clear that alteration of cardiac cell number is not a primary defect contributing to the *hst* cardiac phenotype by chamber morphogenesis stages. The specification of an adequate population of cardiac precursors comprising the first heart field occurs in vertebrates at early gastrulation and somitogenesis stages (Marques and Yelon, 2009, Zaffran and Frasch, 2002). Although cardiomyocytes do continue to divide once the heart tube is established, rates of division during this period are not high (de Pater *et al.*, 2009, Lazic and Scott, 2011). Thus, the normal number of cells detected in 48

hpf *hst* heart tubes appears to indicate that these embryos appropriately specify an adequate pool of cardiac progenitors, and that the extent of apoptosis in the heart tube prior to ballooning is not prohibitive. The neutrality of the *tbx5a* mutants with regard to cardiomyocyte numbers makes an interesting contrast to the phenotypes described for one of Tbx5's conserved binding partners, Nkx2.5. Simultaneous depletion of zebrafish *nkx2.5* and its paralog *nkx2.7* by led to a surplus of atrial cells and a depletion of ventricular cell numbers (Targoff *et al*., 2008). Knockdown of only one of these genes led to much milder phenotypes, suggesting a probable compensatory function by the paralog.

Recently it has become appreciated that continued differentiation of cardiomyocytes derived from the secondary heart field serves to elongate the zebrafish heart tube at both the venous and arterial poles (de Pater *et al.*, 2009, Hami *et al.*, 2011, Lazic and Scott, 2011). Based on the hypoplastic phenotype of mouse hearts at the venous pole, we investigated potential phenotypes associated with this region in the zebrafish. The *hst* phenotypes were mild in this regard, with no detectable change in a marker of sinus venosus development, and no evidence of sinus pauses or AV block, or sporadic arrhythmia. Bradycardia, which can be associated with sinoatrial dysfunction, was observed, but was not nearly as severe as in *isl-1* mutants which have known defects in venous differentiation (de Pater *et al.*, 2009, Garrity *et al.*, 2002), and might be due to any of several factors. Bradycardia itself can be a sign of sinus dysfunction, yet mice defective in any of several genes required for normal pacemaker activity usually show bradycardia in combination with some other type of arrhythmia (Dobrzynski *et al.*, 2007), but this was never observed for *hst* mutant embryos.

Cardiac looping is a dynamic process that begins roughly as early as 30 hpf zebrafish and continues through about days 5 post-fertilization. Concomitantly, as early as 36 hpf, cells of the future ventricular OC begin to show differences in F-actin distribution relative to cells of the future ventricular IC (Deacon *et al.*, 2010). Genetic studies suggest that F-actin cytoskeletal rearrangements are necessary to drive the regional changes in cell size and shape that culminate in chamber ballooning (Deacon *et al.*, 2010, Latacha *et al.*, 2005, Taber, 2006). Regional changes in cells shape and alignment have been proposed as a mechanism that mediates cardiac looping in vertebrates (Latacha *et al.*, 2005, Manasek *et al.*, 1972, Taber, 2006), but have also been proposed as a key determinant of chamber ballooning (Auman *et al.*, 2007). The *hst* mutants provide new insight into this question. Embryos lacking Tbx5a stall early in looping morphogenesis, yet still are able to initiate several cardiomyocyte cell shape changes in a fashion consistent with chamber ballooning in both atrium and ventricle. An exception is that cells of the *hst* atrium IC remained more rounded than their wildtype counterparts, indicating a requirement for Tbx5a function specifically in this region. Overall, our data argue against a model in which looping morphogenesis is an essential prerequisite for chamber ballooning, and point instead to separable mechanisms driving each process. Cell shape changes in that occurred normally in the IC and OC were not sufficient to mediate looping to any significant degree.

Our data support an essential role for Tbx5a in the sustained growth of cardiomyocytes of both chambers. This phenotype is not likely to be a secondary consequence of altered blood flow, since circulation in *hst* mutants remains relatively robust prior to 48 hpf,

although it typically decreases substantially over the following 24 hpf. Previous reports in zebrafish and other vertebrates have similarly indicated that cell size is an important factor influencing cardiac morphogenesis (Soufan *et al.*, 2006).

In summary, the *hst* null alleles provide a valuable genetic model for dissecting exactly how Tbx5 contributes mechanistically to the forming heart. Comparative analyses of Tbx5 function using different model systems is advantageous given that each model has its own limitiations, and the task of ascertaining primary versus secondary phenotypes is often far from simple. Because this study identifies Tbx5a as a critical regulator of cell growth, follow-up studies examining growth factor signaling, MAPK/ERK signaling pathways, or cell cycle regulation in *tbx5a* mutants will be of interest.

Materials & Methods:

Zebrafish husbandry

Zebrafish were raised and staged as described previously (Westerfield, 1995, Nusslein-Volhard and Dahm, 2002) and as per Colorado State University Animal Care and Use Protocols. Developmental time at 28.5°C was determined from the morphological features of the embryo as described by (Kimmel *et al.*, 1995).

Identification of **tbx5a^{s296}** *allele*

The *tbx5a^{s296}* mutation was recovered in a screen for ENU-induced mutations on a TL background, as described previously (Beis *et al.*, 2005). Mutant alleles were maintained by outcrossing to the WIK wild-type line.

tbx5a^{s296} ***allele cloning and sequencing***

mRNA from *tbx5a^{s296}* homozygous mutant embryos was extracted using the Trizol method (Chomczynski and Sacchi, 1987). Reverse transcription and polymerase chain reaction was performed as described (Ebert *et al.*, 2005). Resulting cDNA was TA-cloned into the pCRII vector (Invitrogen) and sequenced using m13 universal primers, and deposited in Genbank (*ID pending, to be provided by final submission*).

In situ hybridization

Embryos were fixed in 4% paraformaldehyde solution in PBS (PFA) and prepared for whole mount *in situ* hybridization as described (Thisse *et al.*, 1993). The digoxigenin-labled (Roche) riboprobe for *tbx5b* was prepared as described (Albalat *et al.*, 2010) with the following additions: the cDNA was cloned into pCRII (Invitrogen), linearized with ApaI restriction enzyme, and synthesized using T7 RNA polymerase. Other RNA probes used include *amhc*, *versican*, *bmp4*, and *dhand*. Presence of mRNA expression was visualized in whole mount using NBT/BCIP chromogenic reagents (Roche).

Zebrafish Imaging

Live larvae (48 and 72 hpf) were immobilized using MESAB and placed on agarose injection plates for imaging. To quantify cardiac looping, wildtype and mutant lines were crossed with *Tg(myl7:EGFP)* to allow for cardiac-specific fluorescence. Looping angles were determined by measuring the angle of the AV junction or the chamber offset angle as compared to the anterior/posterior axis of the embryo. All samples were visualized using a Spot Insight IN1120 digital camera on an Olympus SZX12 fluorescent stereo-

microscope. Post-processing was done using Adobe Photoshop software. Hearts of embryos were scored visually at least three times from the onset of contraction (~26 hpf) through 72 hpf in order to assess the incidence of arrhythmias of types previously reported in zebrafish, including atrial fibrillation, sporadic irregular contractions, 2:1 atrioventricular block, or sinus pauses (Ebert *et al*., 2005; Kopp *et al*., 2005; Langheinrich *et al*., 2003; Peal *et al.*, 2011; Rottbauer *et al*., 2001).

Immunoblot analysis

Immunoblot analysis was performed as previously described (Mizuno *et al.*, 2001). For separation of whole protein lysate, 60 mg of total protein was loaded into 4-12% Tris–acetate gradient gels (Lonza) and electrophoresis accomplished at 150 V for approximately 1.5 h. Following separation, the proteins were transferred to a 0.45 µm nitrocellulose membrane (Sigma) in a submerged transfer apparatus according to the instructions provided by the manufacturer (Enduro, Labnet Intl). Membranes were blocked in 1×TBST (1×TBS with 0.1% Tween-20) and 5% non-fat dry milk (NFDM) for 1 hr at 25°C before incubation with primary antibodies. Membranes were incubated with commercially available antibodies in 1×TBS: Zebrafish Tbx5a-NT (1:500 dilution, Anaspec) and Human beta-actin (1:3000, Pierce). For blocking control anti-Tbx5a-NT was incubated with 2x blocking peptide (Anaspec) for 30 min at room temperature before use. Membranes were incubated with primary antibodies for 1 h at 25°C then washed twice quickly and three times for 10 min with 1×TBST. An anti-rabbit conjugated goat HRP secondary antibody (1:5000, Thermo Scientific) was used to detect both primary antibodies. Membranes were incubated in secondary diluted in block solution (1×TBST

and 5% NFDM) for 1 h at 25°C before washing three times for 10 min with 1×TBST. The blots were incubated with Dura Chemiluminescence Reagent Plus (Fisher) as described by the distributor and imaged using UVP for up to 30 min. Signal comparisons were made as described in the text.

Cardiomyocyte quantification

The number of cardiomyocytes in the heart was quantified in wildtype and mutant embryos crossed into a *Tg(myl7:nDsRed2/myl7:EGFP)* homozygous background. At 48 hpf, embryos were pressed between a glass coverslip and slide to gently flatten the heart. Intact flattened hearts were immediately imaged using a Leica 5500 microscope. Differences in the means were analyzed by Student's *t*-test.

Assay of cardiomyocyte morphology

To investigate volumetric cell growth, we crossed the mutant *tbx5a* lines with a GFP-transgenic line (*Tg(myl7:EGFP-HsHRAS*) in which the reporter gene product is associated with the plasma membrane, thereby clearly outlining cell shape. We quantified cardiomyocyte shape directly in 48 hpf embryos (n=10 each WT and *tbx5a*^{m21}) and evaluated cell size/volume using imaging software (Image J) (Abramoff *et al.*, 2004, Auman *et al.*, 2007).

CHAPTER 3: CELL MORPHOLOGY IN EMBRYONIC HEARTS LACKING TBX5A

Introduction

Mechanisms affecting chamber morphogenesis

During cardiac morphogenesis, the vertebrate heart acquires a characteristic three-dimensional shape well-suited for efficient function. The morphology of the developing cardiac organ reflects a series of changes in the cardiomyocytes. These cells must become specified, migrate, proliferate, grow in size, alter their shape and adhesive properties, and develop ultrastructure (myofibrils), among other differentiated characteristics. Three levels of regulation ultimately affecting cardiac size: 1) spatio-temporal regulation of specification of cardiac precursors, 2) rate of cell division, or rate of apoptosis within the developing heart, and finally 3) amount of volumetric growth of individual cardio-myocytes (Bryant and Simpson 1984, Conlon & Raff 1999, Day and Lawrence 2000).

Specification of cardiac precursors occurs early in zebrafish development. During the blastula stage, between 256- and 540-cell stages, mesodermal cells are still able to contribute to future ventricle or atrial cell fates (see Stainier *et al*. 1993). However, after the mid-blastula transition (i.e. the onset of zygotic transcription, which occurs at approximately the 1000-cell stage), individual mesodermal cells can only contribute to either the ventricular or the atrial precursor population (Stainier *et al.* 1993).

Although the timing of specification is known, the signaling pathways that produce this initial chamber precursor assignment are still not well understood. Several genes are expressed throughout early development, and their functions can change depending on the timing and region of expression (Zhou *et al.* 2008, Sedletcaia and Evans 2011).

One gene family whose signals are important in establishing cardiac chamber proportionality is the bone morphogenic protein (Bmp) group (Marques and Yelon 2009). Bmps belong to the transforming growth factor-beta (TGF-β) superfamily of signaling molecules, and play roles in controlling cell proliferation, differentiation, and laterality (van Wijk *et al.* 2007). Bmps regulate dorsal/ventral patterning in early embryonic development. In early cardiac development, *bmp2* influences activation of *nkx2.5* signaling (Prall *et al.* 2007). Ectopic expression of *bmp2* (and the resulting increase in *nkx2.5*) is associated with increased cardiac progenitor specification, but also a decrease in cardiomyocyte proliferation, ultimately resulting in smaller hearts. Elimination of *bmp2* expression results in cessation of cardiac formation (Marques and Yelon 2009). Another important Bmp molecule for cardiac formation is *bmp4*, which plays an important role in laterality and is known to interact with Tbx5a in segmentation stages (Liu and Stainier 2010). *bmp4* is expressed throughout both chambers until chamber cushions are specified in the atrioventricular junction (AVJ), starting after 36 hpf (Beis *et al.* 2005). At this time *bmp4* expression begins to restrict to the area surrounding the AVJ. Evidence that *bmp4* contributes to AVJ formation includes lack of *bmp4* results in valve and septation defects in mice (Jiao *et al.* 2003) and AV canal differentiation is dependent upon Bmp4-Has2 signaling in zebrafish (Patra *et al.* 2011).

Another pervasive morphogen regulator of cell proliferation and specification is *fgf8*, a growth factor expressed in the bilateral heart fields before fusion (Marquest *et al.* 2008). Fgf8 functions in a spatio-temporal specific manner: if *fgf8* is reduced prior to cardiomyocyte specification, both chambers exhibit a reduction in total cardiomyocytes. However, if *fgf8* is depleted after 19 hpf, cardiomyocyte reduction is only observed in the nascent ventricle. Additionally, if *fgf8* is overexpressed, total cardiomyocyte number increases, but only if expression is begun before chamber specification (Marques *et al.* 2008).

Molecular genetic studies in chick and mouse have examined the effects of *tbx5* mutation on cell proliferation, migration, and specification as mechanisms to account for defects in chamber formation (Hatcher and Basson 2001, Hiroi *et al.* 2001, Hatcher *et al.* 2004). However, our studies of the *hst* mutant showed that bilateral cardiac precursors correctly expressed several markers of early specification, and that they successfully migrated to the midline to generate a linear heart tube of normal morphology (see Chapter 2). Therefore, as specification and migration are not detectably altered, consideration of other potential mechanisms is warranted to explain the *hst* phenotype.

Mechanisms regulating cell growth

Importance of cellular adhesion in cardiomorphogenesis

Development of tissues into organs is dependent upon cells forming and maintaining connections with neighboring cells as well as to the extracellular matrix (ECM). Intercellular connections are especially important for organs such as the heart, which

undergoes expansion/contraction movements, nearly from the moment it is formed. In cardiac development, cardiomyocytes additionally must withstand the added mechanical force of blood flow on intracellular connections. Blood flow and contractility independently influence ventricular cell shape, ultimately affecting chamber morphology (Auman *et al.* 2007). One mechanism that tissues use to maintain integrity is the cellular connections achieved through adherens junctions. In cardiomyocytes, a primary molecular component of adherens junctions is the calcium-dependent N-cadherin, which is connected intracellularly to the sarcomere (Noorman *et al.* 2009). Therefore, contracting sarcomeres transduce force to the adherens junctions, but also to the ECM through connections to integrins via costameres (Samarel 2005). An additional, important function of adherens junctions is that they are able to transduce signals, via secondary messenger molecules, to regulate cellular differentiation (Chopra *et al.* 2011). Defects in adherens junctions can also result in congenital cardiac defects (Bagatto *et al.* 2006).

In experiments conducted for Chapter 2 and 4 we observed an increase in expression of *vcana* and *hand2* in *hst* mutant lines (Fig. 2.4, 4.7). *vcana*, a large proteoglycan important in cell adhesion, migration, and proliferation, also interacts with zebrafish ECM (called "cardiac jelly" in heart development). *vcana* binds hylauronan, a polysaccharide molecule that contributes to restriction of cardiac cushion formation (Lagendijk *et al.* 2011, Matsumoto *et al.* 2003). In zebrafish, *hand2* is required for polarization of myocytes and regulates the expression of *fibronectin1* (*fn1*), thereby controlling ECM formation (Trinh *et al.* 2005, Yin *et al.* 2010). *fn1* is downregulated in *hand2* mutants, leading to loss of epicardial integrity (Barnes *et al.* 2011). Interestingly, *hand2* is also essential for gut-

looping in zebrafish embryogenesis (Yin *et al.* 2010), which demonstrates a role for *hand2* in tissue movement. These genetic studies provide ample evidence that transcription factors and cytoskeletal structures can impact development.

Myofibrillogenesis

The heart is the first organ to function in an embryo (Lyons 1996). Zebrafish provide a useful model for studying the generation of myofibrils, as they develop *ex utero* and myocytes develop in a monolayer. In zebrafish, cardiomyocytes begin contracting by 24 hpf, as the heart tube is still assembling (Bakkers 2011). Cardiomyocytes contract by the use of myofibrils, comprised of sarcomeres which are the functional subunits in striated muscle (Tokuyasu and Maher 1987). The sarcomere is comprised of many proteins, including α-actinin, titin and actin (Fig. 3.2). There is contention as to how, exactly, these multiple components ultimately assemble into the complex myofibril structure (reviewed in Ono 2010). For example, in chick cardiomycocyte myofibrillogenesis no premyofibrils were observed, and instead all sarcomere proteins appropriately localized prior to onset of contractions (Ehler *et al.* 1999). However, zebrafish myocytes appear to utilize premyofibrils associated with the cell membrane (Fig. 3.1) in the process of myofibrillogenesis. A newly identified zebrafish mutant, *futka* (*ftk*), demonstrates abnormalities in cardiac myofibrillogenesis (Sultana *et al.* 2008). The mutation is located in an early cardiac connexin (Cx36.7/Ecx), which functions upstream of *nkx2.5*, as demonstrated by rescue of the *ftk* phenotype by *nkx2.5* expression, although the mechanism for this signaling is not yet identified. The cardiac homeobox protein Nkx2.5 is known to physically interact with Tbx5 and thereby induce cardiomyocyte

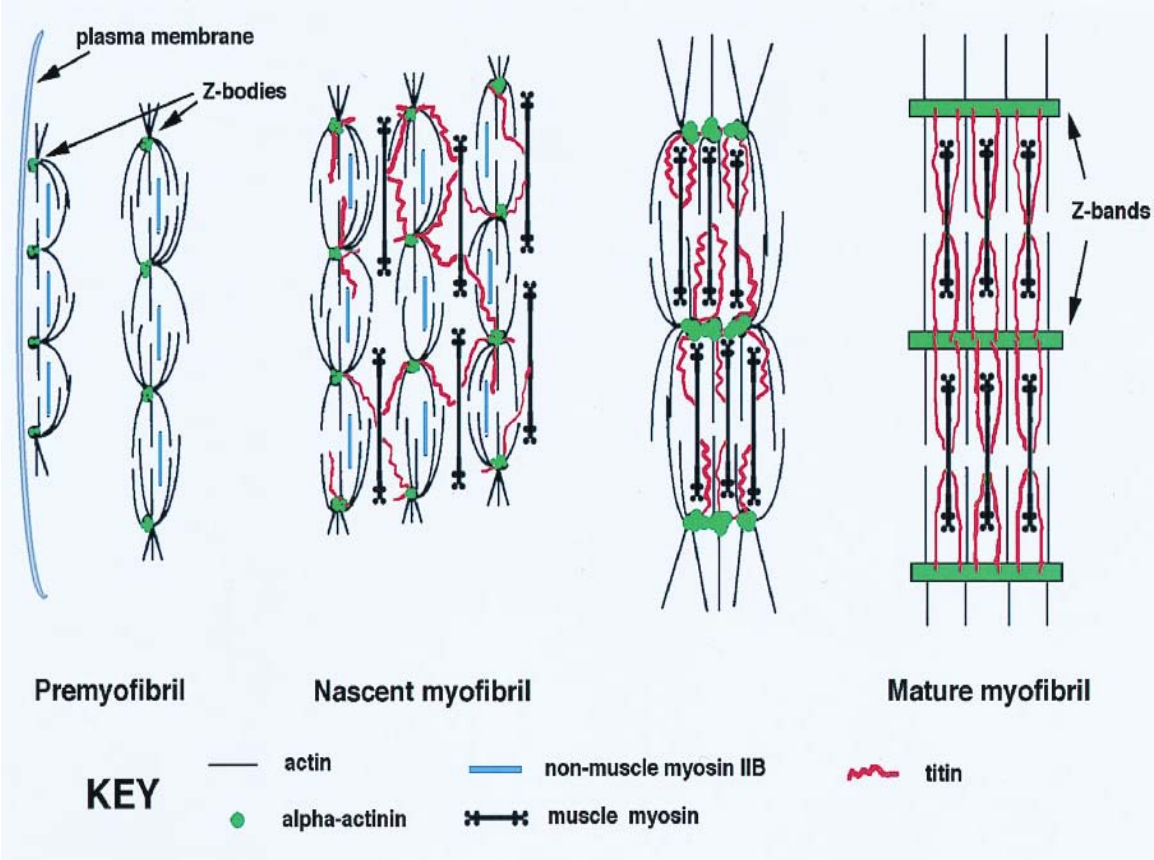

Fig. 3.1: Classical model for the assembly of mature myofibrils. The position of alpha-actinin (green circles) relative to actin, myosin II, nonmuscle myosin IIB, and titin is shown for each stage of myofibril development. Near the spreading edge of the cell (far left), a-actinin is found in mini-sarcomeric arrays in the premyofibrils. In the nascent myofibril, the a-actinin-rich Z-bodies have begun to laterally associate, possibly through interaction with titin. Overlapping muscle myosin II filaments bound to titin are present at this stage. In the mature myofibril the a-actinin containing Z-bodies fuse to form the wide lateral arrays of mature Z-bands; nonmuscle myosin IIB is lost, whereas muscle myosin filaments are now aligned into A-bands. From Dabiri *et al.* 1997 (Copyright 1997 National Academy of Sciences, USA).

differentiation (Hiroi *et al*. 2001). Therefore, myofibril structure may also be altered in *hst* mutant embryos.

Lu *et al*. (2008) found that decreased levels of zebrafish *tbx5a* expression lead to decreased expression of cardiac-specific genes, including several components of sarcomeres. These results would predict that myofibril structure would be disrupted in *hst* embryos. Therefore, in this chapter, I assay for myofibrillar ultrastructure by fluorescent methods. In addition, I investigate whether a zebrafish *tbx5a* loss-of-function mutation affects volumetric cell growth by a decrease in cell-cell adhesion or by defects in F-actin structures. The goal of this study is to investigate the cellular basis of *tbx5* cardiac phenotype.

Results and Discussion

Cardiomyocyte adhesion is not reduced in hst *mutant embryos:*

To investigate whether *tbx5a* mutation disrupted intercellular adhesion within hearts undergoing chamber morphogenesis and looping, I evaluated the integrity of heart tubes subjected to modest pressure provided by the weight of a cover slip laid upon them (a process known as "pressing"). Under these conditions, wildtype hearts maintain their integrity and all cardiomyocytes remain intact within their respective chambers (Fig. 3.2). I observed no difference in cardiomyocyte cell adhesion or heart tube morphology in presses of *hst* versus wildtype larvae at 48 hpf, indicating that there is no reduction in intercellular adhesion in embryos lacking functional *tbx5a*. As a "reduced-integrity"

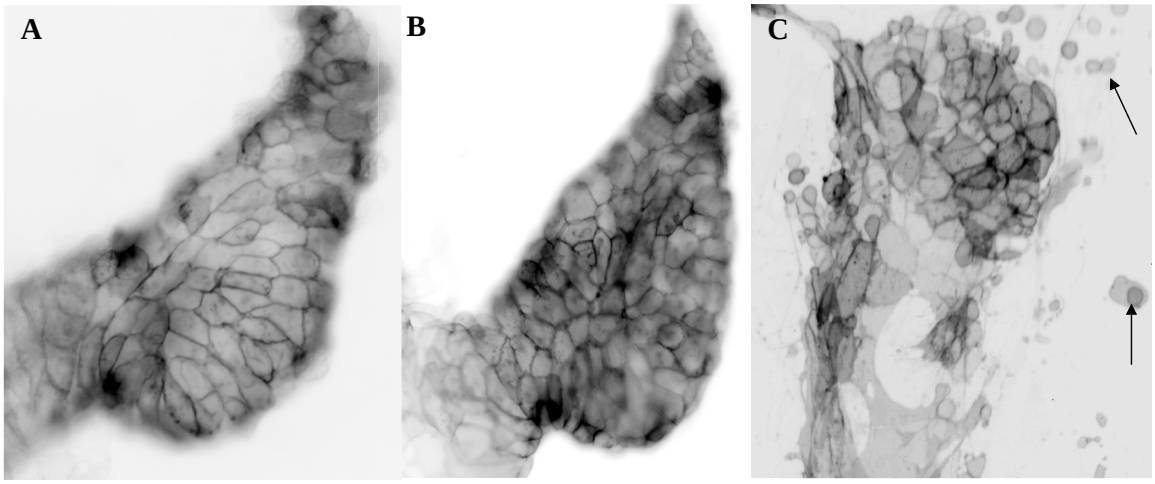

Fig. 3.2: Cell adhesion is not reduced in *hst* cardiomyocytes. Inverted fluorescent images of hearts from 48 hpf *Tg(myl7:EGFP-HsHRAS)* embryos: (**A**) wildtype, (**B**) *hst*, or (**C**) injected with morpholino (MO) against the calcium channel CACNB2 subunit. Loss of CACNB2 function decreases cardiomyocyte adhesion and is used here as a positive control. Arrows: detached, rounded cardiomyocytes in MO hearts provide contrast with the well-connected, trapezoidally shaped wildtype or *hst* cells.

control in this assay, calcium channel CACNB2 morphant *Tg(myl7:EGFP-HsHRAS*) embryos were similarly pressed. As previously shown in the lab, knock-down of CACNB2 reduced integrity of intercellular adhesion and, under slight pressure, individual cardiomyocytes readily dissociated from the heart tube, leading to a breakdown in organ structure (see Fig. 3.2, arrows).

Another characteristic of loss of intercellular integrity in CACNB2 morphants was a deformation of nuclear shape in pressed heart tubes. We therefore assayed *hst* embryos to determine whether this abnormality was detectable. To examine nuclear shape, we pressed wildtype, *hst*, and CACNB2 morphant *Tg(myl7:nDsRed2/myl7:EGFP)* 48 hpf embryos. Pressed nuclei from both wildtype and *hst* embryos maintained their normal, rounded shape, indicating that the *hst* mutation does not affect intracellular integrity. However, cardiomyocyte nuclei in CACNB2 morphant *Tg(myl7-dsRed2)* hearts were elongated or even detached from the mass of heart tube cells (Fig. 3.3C), consistent with reduced intercellular or intracellular integrity within these heart tubes (Chernyavskaya *et al*. 2012). These data suggest that overall adhesion of cardiomyocytes is normal in *hst* embryos. It is important to note that presses only assay for a decrease in integrity and cannot illuminate structural organization.

Myofibril structure is not altered in* hst *hearts

In order to determine if cardiomyocyte morphology differences observed at 48 hpf in Chapter 2 resulted from myofibril defects, we examined cardiomyocyte ultrastructure at 46-48 hpf (Fig. 3.4). Phalloidin-labeling in wildtype cardiomyocyte showed regular,

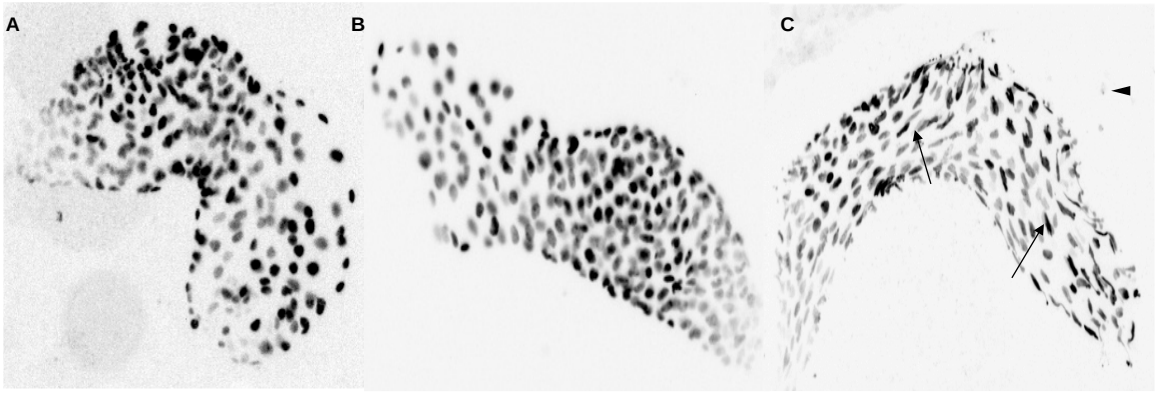

Fig. 3.3: Adhesion of 48 hpf *hst* mutant cardiomyocyte nuclei is not altered. Inverted fluorescent images of hearts from (**A**) wildtype, (**B**) *hst*, (**C**) or CACNB2 MO-injected *Tg(myl7:nDsRed2/myl7:EGFP).* Hearts were pressed for morphological comparison. Arrows: elongated nuclei; arrowhead: detached cell.

organized sarcomere structure (Fig. 3.4A, B). This regular pattern was observed in *hst* ventricles and atria, regardless of the severity of the cardiac phenotype (Fig. 3.4C-E, see Chapter 2 for explanation of mild and severe *hst* phenotypes). Although it is apparent that cell shape is altered, myofibrillogenesis still occurred in the absence of functional Tbx5a, and myofibrils strongly resemble wildtype myofibril structure. Our results support the model present by Dabiri *et al.* (1997) in which dense Z-bodies form near the periphery of the cell (see Fig. 3.4C'). Huang *et al.* (2010) also observed that thin filaments associate with the zebrafish cardiomyocyte membrane at 48 hpf, indicating that, in zebrafish, myofibrillogenesis may occur via premyofibril formation.

Alternate hypothesis for role of tbx5 *in cardiomyocyte growth and differentiation*

An alternative mechanism for regulation of cell morphology is controlling presence of adhesion molecules at the cell surface (Takeichi 2011). Junctional polarization is responsible in early development for specification of epithelium versus mesenchyme (whose adherens junctions (AJ) are dispersed randomly) (Nishioka *et al.* 2009). Cells respond to mechanical forces, such as blood flow, by remodeling their adherens junction composition (Taguchi *et al.* 2011). Maintenance of tension at the junction appears to be a major factor in proper junction formation. F-actin-stabilizing proteins may function as the mechanosensitive regulator for this process (Taguchi *et al.* 2011). Absence of *fn1*, a major component of ECM, results in aberrant AJ formation, suggesting that myocardial function is dependent on epithelial organization and integrity in heart tube formation (Trinh and Stainier 2004). ECM proteins are also important for the promotion of adhesion-dependent cell growth. Because *hand2* and *vcana*, genes with roles in ECM

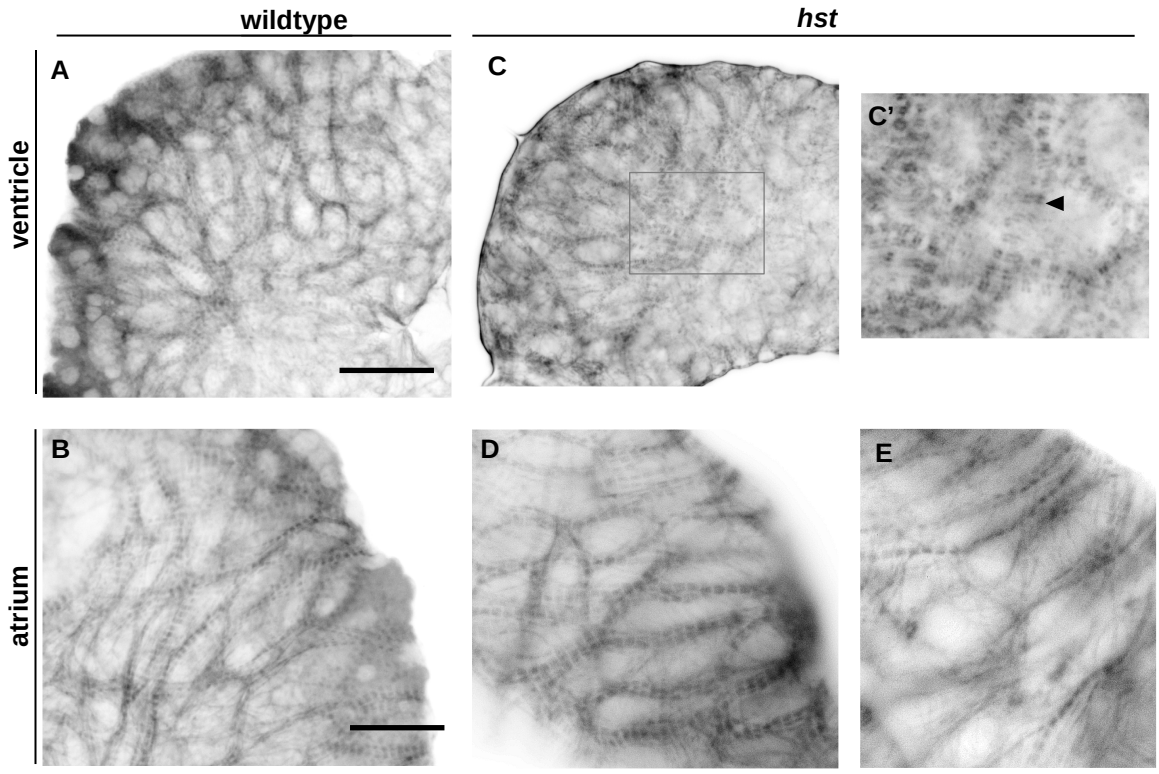

Fig. 3.4: Myofibrillogenesis is not altered in *hst* hearts. Hearts of 72 hpf *Tg(myl7:HsHRas-EGFP)* embryos: (**A**,**B**) wildtype and (**C-E**) *hst* homozygous embryos. (**A**, **C**) Ventricular F-actin was visualized using rhodamine-labeled phalloidin. (**C'**) A representative area showing sarcomere structure magnified from (**C**). (**B**) Wildtype atrial F-actin. F-Actin from a phenotypically 'severe' *hst* atrium (**D**), as compared to a phenotypically 'mild' *hst* atrium (**E**). Arrowhead: putative Z-body, located adjacent to the cell membrane. Scale bar = 20um.

organization and mediation of intracellular signaling, are ectopically expressed in *hst* embryos, investigation into the role of ECM would facilitate our understanding of mechanisms that contribute to cardiac looping.

In summary, we have determined that *hst* cardiomyocyte morphology deficiencies do not result from a decrease in cell adhesion or altered myofibril structure at chamber morphogenesis stage. Future investigation into the role of ECM or AJ molecules and their signaling may be valuable in understanding the cellular changes exhibited in *hst* mutant embryos. An additional area of exploration that may prove fruitful is examination of cellular morphology, adhesion, and myofibrillogenesis in *tbx5b*MO embryos to determine possible functional redundancy. These studies may help to determine if *tbx5b* also plays a role in cell growth and elucidate mechanisms for these changes.

Materials and Methods

Raising and Staging of Embryos

Developmental time at 28.5°C was determined from the morphological features of the embryo as described by Kimmel (1990).

Assay of cardiomyocyte adhesion

To investigate a possible reduction in intercellular adhesion, I crossed the mutant *hst* line with the *Tg(myl7:EGFP-HsHRAS*) line, in which the reporter gene product is associated with the plasma membrane, thereby clearly outlining cell shape. The integrity of

cardiomyocyte nuclei was assayed in wildtype, *hst*, or CACNB2 morphant embryos crossed into a *Tg(myl7:nDsRed2/myl7:EGFP)* homozygous background. At 48 hpf, embryos were pressed between a glass coverslip and slide to gently flatten the heart (n=10 embryos each wt, *hst*, and MO). Flattened hearts were immediately imaged using a Leica 5500 microscope.

Assay for myofibrillar structure

Cardiomyocytes were visualized by removing hearts from wildtype or *hst* embryos fixed in 4% PFA. The hearts were washed in PBSTx, blocked for one hour, and incubated in a 1:100 dilution of rhodamine-labeled phalloidin (Invitrogen) for 30 minutes prior to visualization on a Leica 5500 microscope.

CHAPTER 4: ZEBRAFISH *TBX5* PARALOGS ARE NOT FUNCTIONALLY REDUNDANT IN CARDIAC OR PECTORAL FIN DEVELOPMENT.

Introduction

Genes of the T-box superfamily of transcription factors are present throughout nearly all of the animal Kingdom, from primitive invertebrates (including *Hydra* and jellyfish) through all tetrapods (Agulnik *et al*. 1995, Technau and Bode 1999). T-box genes encompass 5 subfamilies: Brachyury, T-brain1, Tbx1, Tbx2 and Tbx6 (Papaioannou 2001). Members of the same subfamily most likely resulted from duplication events throughout evolution. T-box genes have diverse functions in development, including regulation of gastrulation, patterning of body axes, morphogenesis and organ development (Stennard and Harvey 2005). In general, T-box genes help specify the tissue in which they are expressed (Gruelich *et al*. 2011, Naiche *et al*. 2005). T-box genes are associated with human disorders including DiGeorge syndrome and cancer, among others (Naiche *et al*. 2005). They may play a role in metastasis of certain cancers by promoting epithelial-mesenchymal transition. Moreover, recent studies indicate that expression of Brachyury in early tumor stages predicts poor patient prognosis (Kilic *et al*. 2011, Naiche *et al*. 2005, Suzuki *et al*. 2011). All genes of this family include a highly conserved "T-box" region that encodes a DNA binding domain that regulates expression of target genes. The transcriptional activation domain of T-box proteins is typically located in the

C-terminus, outside of the T-domain (Zaragoza *et al*. 2004). The C-terminus is important for the strength of an induction response, but not for the specificity (Marcellini *et al*. 2002). The specificity of T-box proteins is conferred in part by their interactions with other transcriptional regulators, and in some cases involves an N-terminal interaction domain distinct from the T-domain itself (Wilson and Conlon 2002).

Tbx5 is one of the earliest genes to be expressed in the cardiac field during embryonic development (Bruneau *et al*. 1999). Mutation of mammalian Tbx5 produces dominant phenotypes affecting cardiac septation as well as electrophysiological defects including atrioventricular conduction block, (Bruneau et al., 2001). Holt-Oram Syndrome (HOS) is a human congenital disease that results from mutations in Tbx5 (Mori and Bruneau, 2004, Piacentini *et al*. 2007). HOS is characterized by cardiac and forelimb morphological defects, and progressive cardiac conduction disease. Mammalian models of HOS indicate an essential role for *tbx5* in cardiac morphogenesis (Basson *et al*., 1999), Showell *et al.* 2004). In zebrafish, the *tbx5a* gene is expressed in the embryonic heart, dorsal optic cup, and pectoral fins (Begemann and Ingham 2000). The *tbx5a/heartstrings (tbx5a*) mutant displays a loss-of-function phenotype that recapitulates aspects of HOS in both the heart and forelimb (Garrity *et al.*, 2002). Homozygous *tbx5a* mutation prevents initiation of pectoral fin formation, and conditional deletion of mouse Tbx5 in the forelimb buds similarly results in a complete lack of forelimb bud formation (Garrity *et al.* 2002, Rallis *et al.* 2003). Despite overtly normal heart tube formation and slight bradycardia, the hearts of homozygous *tbx5a* mutant embryos later fail to loop and progressively deteriorate, leading to heart failure and lethality. Although embryonic

lethal, the cardiac phenotypes in *tbx5a* mutants differ somewhat from those reported for Tbx5 mutation in the mouse, which particularly affect formation of the venous end of the developing heart (Bruneau *et al.* 2001, Ghosh *et al.* 2009, Parrie *et al.* in press).

Recently, a second zebrafish *tbx5* paralog has been described, termed *tbx5b* (Albalat *et al.* 2010). Because a *tbx5b*-like gene is present in all known teleost genome sequences, this gene likely arose during the teleost-specific genome duplication event approximately 300 million years ago (Hurley *et al*. 2007). Based on *in situ* hybridization (ISH) studies, Albalat *et al*. (2010) reported that zebrafish *tbx5b,* similar to *tbx5a,* is expressed in the embryonic eye and heart. However, within the eye, *tbx5b* expression is expanded as compared to *tbx5a,* to include a majority of the dorsal side. ISH was not sufficient to detect *tbx5b* expression in either the caudal-most portion of the lateral plate mesoderm which contributes to pectoral fin mesenchyme, or within the forming pectoral fins themselves (Albalat *et al*. 2010).

Based on the overlapping expression patterns of *tbx5a* and *tbx5b* in the embryonic heart, we hypothesized that functional redundancy between these two paralogs might ameliorate the cardiac phenotype in *tbx5a* mutant embryos. To address this question, we first re-visited the status of *tbx5b* as an authentic *tbx5* paralog, as opposed to a divergent *tbx5*-like gene. Second, we determined the embryonic functions of *tbx5b* during development using a morpholino knockdown approach. We report here that depletion of *tbx5b* is embryonic lethal due to heart failure. The cardiac phenotypes in *tbx5b*-depleted fish were similar, but not identical, to those of *tbx5a* mutants. Although *tbx5b* expression was not

detectable by ISH in the fins, we find that *tbx5b*-depletion led to defects in the timing and morphogenesis of pectoral fin development. Somewhat surprisingly, depletion of both gene products did not lead to more severe phenotypes. Overall, our data do not indicate that substantial genetic redundancy exists between the two genes. In the heart, *tbx5a* and *tbx5b* appear to have related essential functions that are nevertheless independently required. In the fin, *tbx5a* alone was required for fin bud initiation, but both genes are independently required for patterning and morphogenesis.

Results

Genetic Analysis

We isolated and sequenced full-length *tbx5b* mRNA from WIK wildtype *Danio rerio* embryos (Fig. 4.1; GenBank Accession number: HQ822122). The predicted Tbx5b protein is 430 aa in length, 55 residues shorter than *D. rerio* Tbx5a. The zebrafish Tbx5b amino acid sequence was aligned with other vertebrate Tbx5 proteins (*Gallus gallus*, *Homo sapiens*, *Xenopus leavis*) as well as to both Tbx5 paralog genes in three other teleost species (*Gasterosteus aculeatus*, *Oryzias latipes*, and *Tetraodon nigroviridis*) (Fig. 4.1). As with other T-box genes (Papaioannou 2003) *D. rerio* Tbx5b was most similar to the other Tbx5 proteins within the T-box region (87.5% conserved with *H. sapiens*, for example). The degree of conservation within the *D. rerio* Tbx5b T-domain was thus lower than reported for other T-box gene family members, which typically display 95-99% amino acid identity within this region (Bamshad *et al.* 2007, Bruneau *et al.* 2001, Holland *et al.* 1995, Horb and Thomsen 1999).

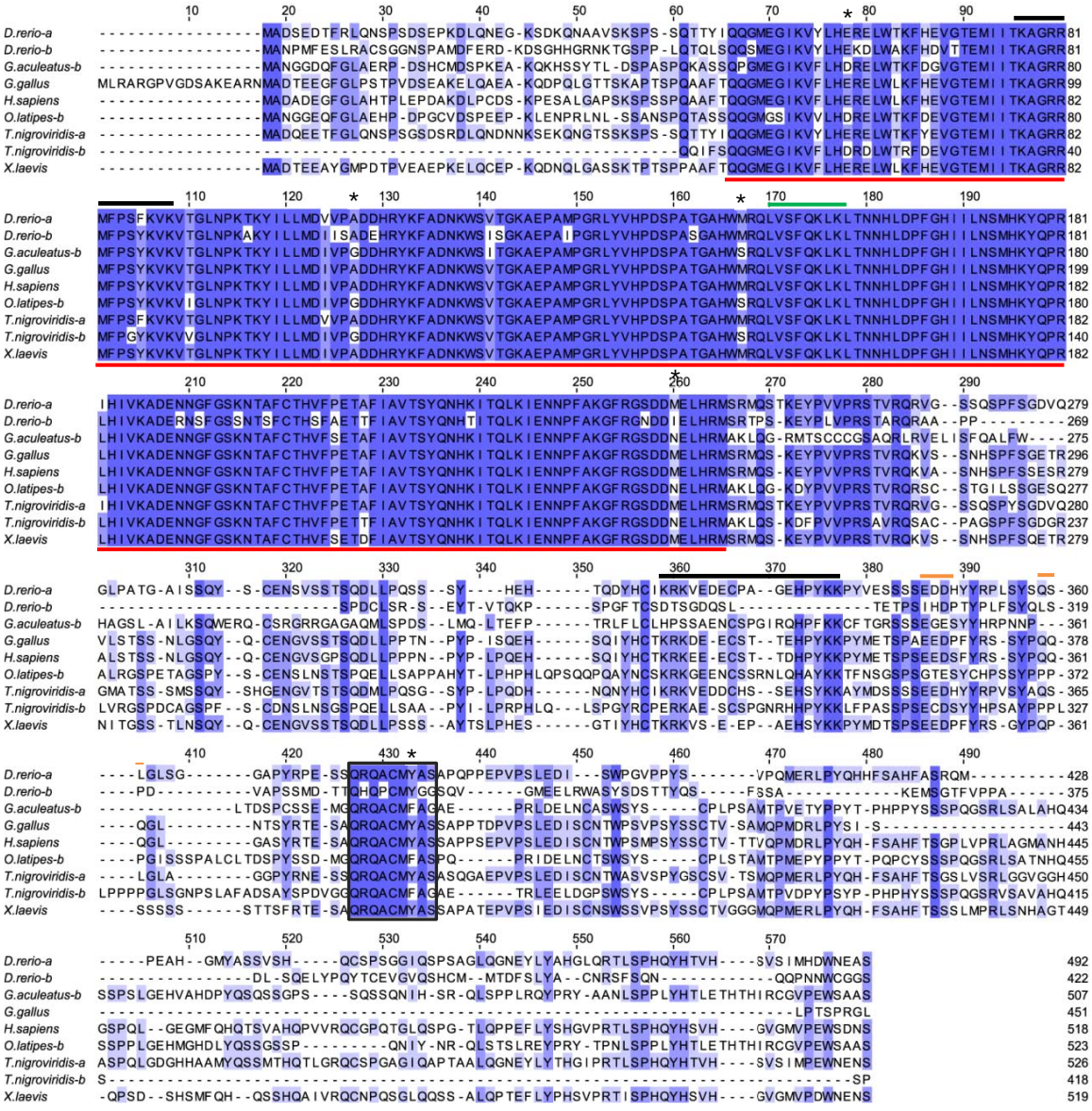

Fig. 4.1: The zebrafish Tbx5b protein sequence is not highly conserved. Comparison of Tbx5 proteins. Alignment of the predicted Tbx5 protein sequences from vertebrates *G. gallus*, *X. leavis*, and *H. sapiens* with the predicted Tbx5a and Tbx5b protein sequences from teleost species *D. rerio*, *G aculeatus*, *O. latipes*, *T. nigroviridis*. Amino acids that are identical are highlighted in blue. Red line underscores the T-box DNA binding domain. Asterisks indicate residues *D. rerio* Tbx5b does not share with other teleost Tbx5b proteins. Boxed region highlights a 9-amino acid conserved Tbx5-specific motif of unknown function. Black lines mark the two nuclear localization signals. Green line indicates the nuclear export signal. Orange lines denote the transactivation signal. The Genbank accession number for the zebrafish *tbx5b* mRNA sequence is HQ822122.

Interestingly, alignment of vertebrate Tbx5 amino acid sequences identified a highly conserved 9 amino acid motif within the C-terminus. Teleost Tbx5a genes encode QRQACMYAS, a motif that by BLASTP analysis shows 100% conserved in at least 26 other vertebrate species (Fig. 4.1, box; and data not shown). In Tbx5b genes, three teleost species encode a closely related motif: QRQACMFA[S/G]. However, *D. rerio* Tbx5b encodes QHQPCMYGG, which contains 4 conservative amino acid substitutions, making it the most divergent Tbx5 gene in this motif relative to Tbx5a or the other Tbx5b sequences (Fig. 4.1, Fig. 4.2). This motif is predicted to encode a beta-sheet secondary structure. It has not been reported so far for any other gene and although its function is unknown, it is near the activation signal reported by Zaragoza *et al*. (2004) (Fig. 4.1), and may therefore play a role in Tbx5a transactivation. A BLASTP search against the NCBI Reference Sequence database using only the 9 amino acid motif was sufficient to return exclusively Tbx5 of multiple vertebrate species as the top several hits, suggesting that the motif may be unique to the Tbx5 gene. Overall, this divergence of *D. rerio* Tbx5b may indicate that it has lost classical functions or evolved novel roles as compared to other Tbx5 proteins. This may also indicate a higher rate of evolution for *D. rerio* Tbx5b than found in the other teleost species.

Although *D. rerio* Tbx5a and Tbx5b are proposed paralogs (Albalat *et al.* 2010), the degree of diversity in Tbx5b relative to other T-box genes made us re-visit this hypothesis. We directly compared the zebrafish Tbx5 genes in terms of amino acid sequence, genomic structure, and examined the position of *D. rerio* within the broader Tbx5 evolutionary family. Overall, the zebrafish *tbx5a* gene shows 74.6% amino acid

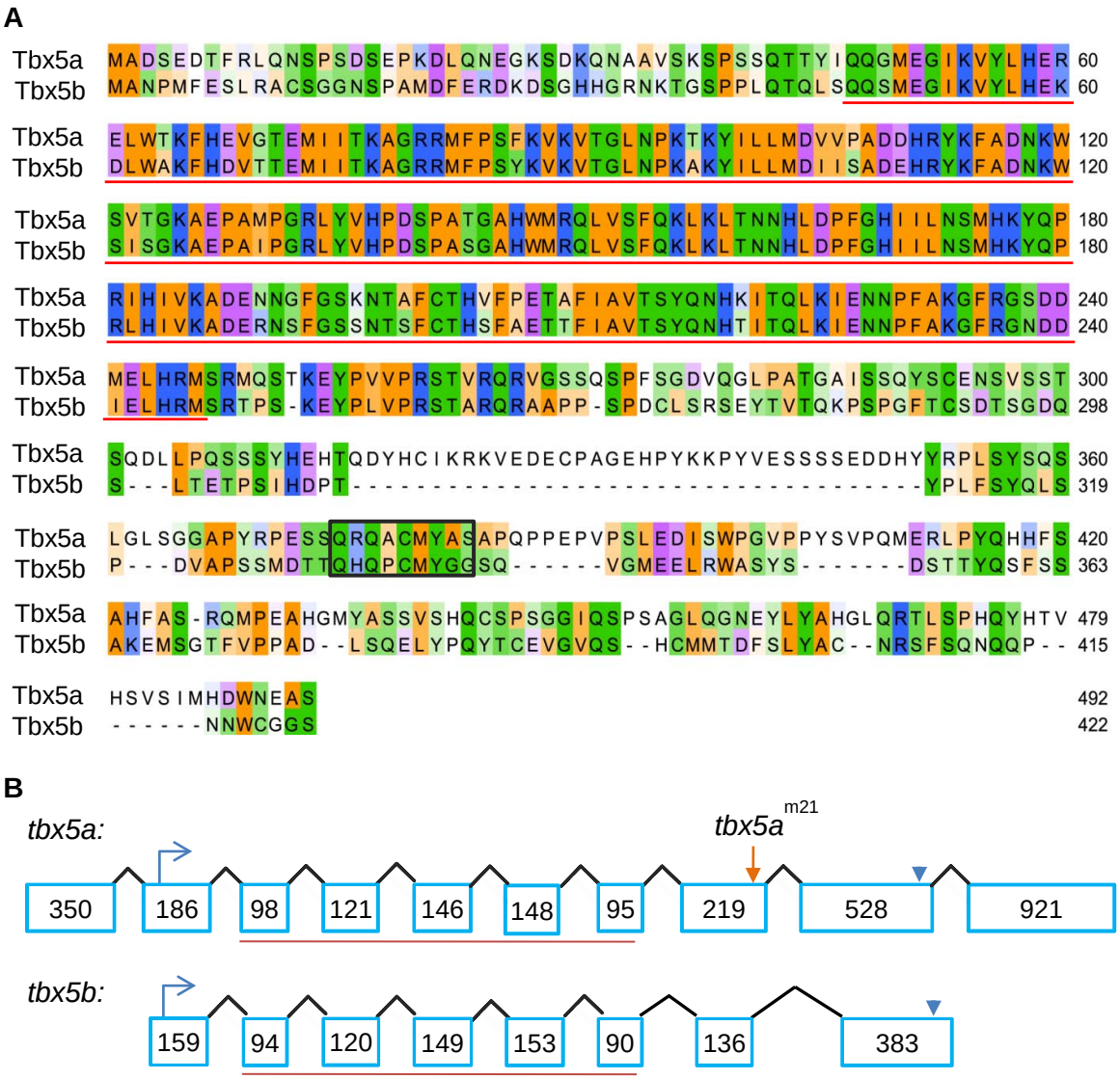

Fig. 4.2: Alignment and schematic comparison of zebrafish Tx5a and Tbx5b protein sequences and genomic structure. (**A**) The Tbx5b T-box (aa 52-250, underlined in red) was highly conserved (86.5%), but the paralogs showed an overall amino acid identity of only 55.2%. Colors indicate similar types of amino acids: green = polar, orange = nonpolar, blue = basic, purple = acidic. Box denotes the conserved 9-amino acid motif, also identified in Fig. 1. (**B**) Schematic comparison of genomic structure of the zebrafish *tbx5* paralogs. Numbers in blue boxes are exon sizes in basepairs. Blue arrow denotes the location of the start codon. Blue arrowheads indicate location of wildtype termination signal. Red underline identifies the region encoding the T-box DNA-binding domain. Orange arrow indicates the location of the nonsense mutation in the *tbx5a*^{m21} allele.

identity with human TBX5, whereas *tbx5b* is substantially more divergent, sharing only 59% amino acid identity. While the length and sequence of N-terminal domain and T-box domains were reasonably similar between Tbx5a and Tbx5b, the latter protein has a substantially shorter, highly diverged C-terminus (Fig. 4.2A). The T-box DNA binding region was moderately conserved between the two genes, with identity in 174 out of 210 aa (83%). Next, a comparison of the genomic structure showed that the two *tbx5* genes both had five exons within the T-box region, all of which were nearly identical in size (Fig. 4.2). This finding was consistent with a general trend that exons comprising the T-box tend to be of similar size and number throughout evolution, although intron length varies between species (Wattler *et al*. 1998). Outside of the T-box domain, the number and sizes of exons was substantially different between the two genes, with *tbx5b* having fewer, smaller exons (Fig. 4.2B). These disparities suggested that Tbx5b may be either a rapidly evolving paralog, or that it was a T-box family member but not a true Tbx5 paralog. To resolve this, we compared *tbx5b* with other vertebrate T-box genes, including conservation signaling domains specific to each T-box family. Analysis reveals that the *tbx5b* is more similar to *tbx5a* than other T-box genes including *tbx4*, *tbx2*, and *tbx3* (data not currently shown).

Morpholino Knockdown and Analysis of Cardiac Phenotypes

To test the hypothesis that Tbx5b performs unique functions in zebrafish development, a translation-blocking morpholino (*tbx5b*MO) was designed for *tbx5b* knockdown. To validate the efficacy of *tbx5b*MO, we created a Tester mRNA consisting of the *tbx5b* morpholino target sequence fused to sequence encoding the GFP reporter. Whereas

embryos injected with 1000 ng/µl of capped Tester mRNA displayed green GFP fluorescence, 87% of embryos co-injected with Tester mRNA along with 100 uM of *tbx5b*MO lacked any detectable GFP fluorescence by 24 hpf, indicating that *tbx5b*MO efficiently targeted the expected mRNA sequences (Fig. 4.3). By 48 hpf, 79% (121/153) of embryos injected with 100 uM of *tbx5b*MO alone exhibited cardiac phenotypes, including defective cardiac looping, reduced contractility, and abnormal chamber morphology (Fig. 4.4C,G,K). By 72 hpf, cardiac phenotypes for *tbx5b* morphant embryos overtly resembled those of homozygous *tbx5a* mutants (Fig. 4.4B,F,J and Garrity *et al.* 2002), including a collapsed, dysmorphic heart surrounded by pericardial edema. Depletion of Tbx5b was lethal by 6-7 days post-fertilization.

To determine if double knockdown of *tbx5a* and *tbx5b* would result in more severe cardiac defects, such as a reduction in cardiac tissue or absence of circulation, as was previously described for double knockdown of *Xenopus* Tbx5 and Tbx20 (Brown *et al.* 2005), we injected *tbx5b*MO into *tbx5a* mutants or co-injected *tbx5b*MO and *tbx5a*MO. The end-stage cardiac phenotypes of zebrafish *tbx5a/tbx5b* double knockdown embryos overtly resembled those of both *tbx5a* mutant and *tbx5b* morphant embryos displaying a dysmorphic, weakly contracting heart surrounded by pericardial edema (Fig. 4.4D,H,L).

Next, we used additional tools to examine the *tbx5b* morphant and *tbx5a/tbx5b* double knockdown embryos to determine whether there were more subtle phenotypic differences from *tbx5a* mutants, which could support a hypothesis of independent function within the heart. To examine the extent of cardiac looping defects, we utilized a transgenic line

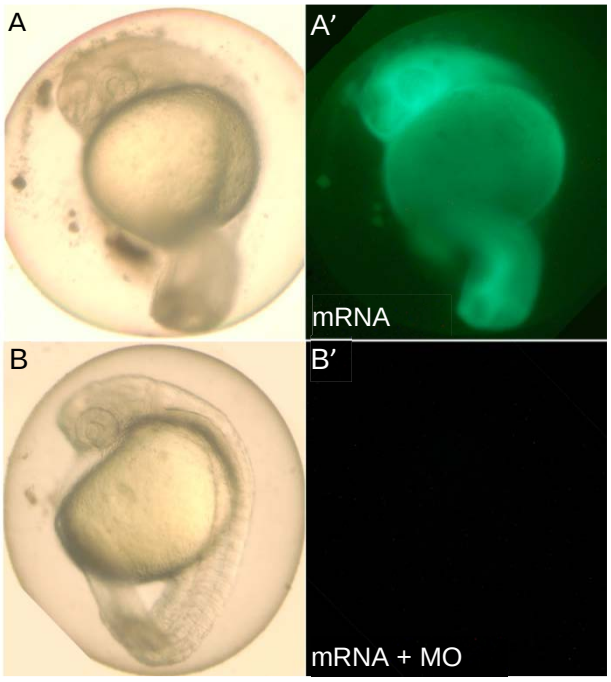

Fig. 4.3: Confirmation of *tbx5b* morpholino knock-down using GFP-tagged mRNA containing the *tbx5b*MO target site. The efficacy of *tbx5b* morpholino knock-down was confirmed using a Tester mRNA constructed by inserting the tbx5b MO target site cloned in front of EGFP coding sequences. (**A**, **A'**) 30/30 embryos injected with 1000 ng/µl Tester mRNA displayed normal body morphology and expressed GFP. (**B**) Embryos co-injected with 100 µM morpholino and 1000 ng/µl Tester mRNA displayed normal body morphology, but (**B'**) 26/30 failed to detectably express GFP, indicating that the *tbx5b*MO efficiently targeted the expected binding site.

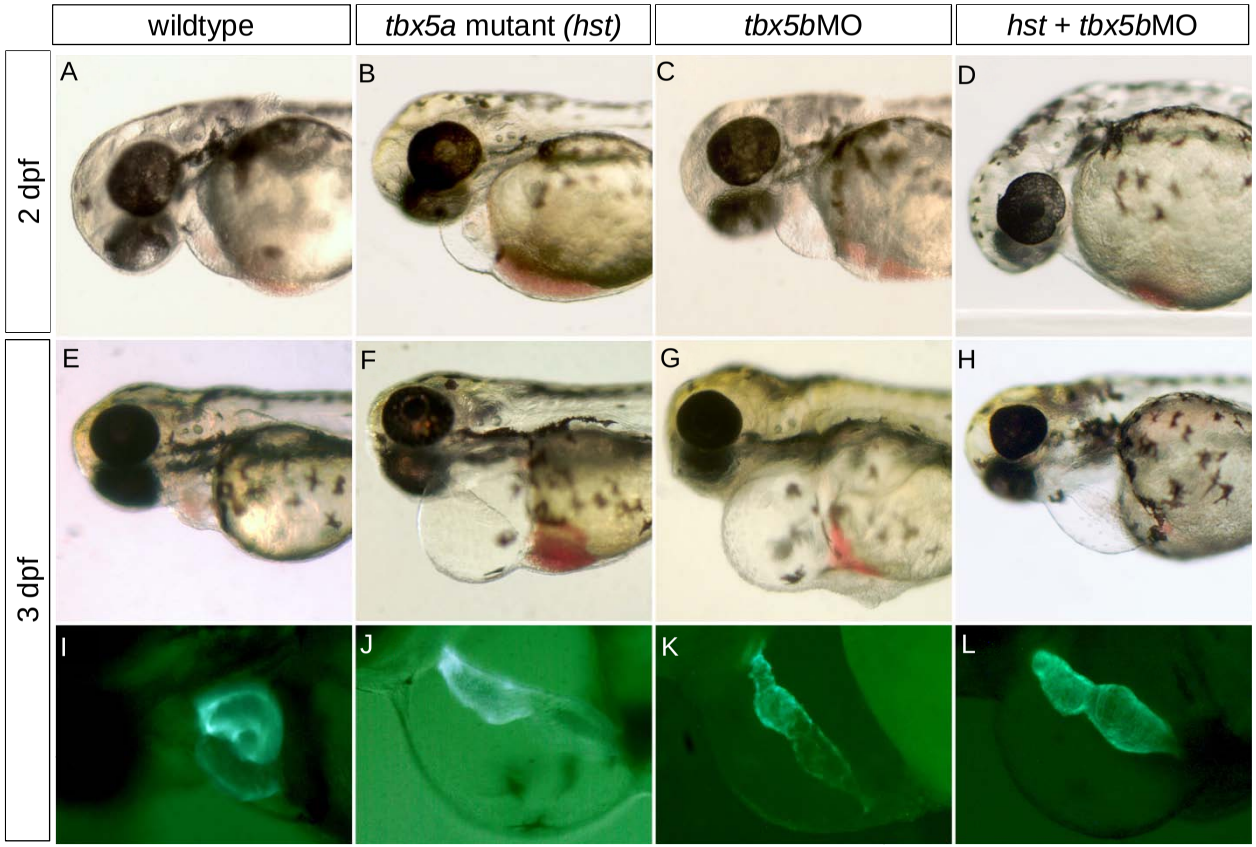

Fig. 4.4: Lack of functional Tbx5a or Tbx5b results in dysmorphic cardiac formation. (**A**, **E**) Control hearts completed looping by 48 hpf and unidirectional blood flow was secured by 72 hpf. (**B**, **F**) In homozygous *tbx5a (heartstrings)* mutant embryos, blood began pooling at the venous end of the heart by 48 hpf, and cardiac edema was enlarged by 72 hpf. (**B-D**, **F-H**) In *tbx5a* mutant, *tbx5b* morphant embryos, and *tbx5a* mutant embryos injected with *tbx5b*MO, similar dysmorphic cardiac phenotypes were observed. (**I-L**) *Tg(myl7:GFP)* embryos were used to visualize cardiac shape at later timepoints.

expressing GFP in the heart. Hearts in live *Tg(myl7:EGFP-HsHRAS)* embryos injected with *tbx5b*MO were visualized at 48 hpf (Fig. 4.5). The cardiac cardiac "looping angle" has been defined as the angle created between the plane of the cardiac atrioventricular junction (AVJ) and the embryo A/P axis, as diagrammed (Fig. 4.5B, Chernyavskaya *et al.* 2012). Near the onset of looping, 34 hpf wildtype hearts showed an average looping angle of 47° ± 4 (Chernyavskaya *et al.* 2012). By 48 hpf, wildtype larvae undergoing normal morphogenesis have reduced the average looping angle to 14° (Fig. 4.5). As previously reported, homozygous *tbx5a* mutant larvae demonstrated an average looping angle of 54° (Parrie *et al.* submitted). Note that although the chambers in mutant hearts frequently remain linearly aligned, or only slightly displaced, the plane of the AVJ still shows tilting in the direction expected for normal looping. Hearts of *tbx5b* morphants exhibited an average looping angle of 58°, indicating greatly reduced looping. The looping angle for embryos with depleted for both *tbx5a* and *tbx5b* was 57°, indicating no difference from loss of either *tbx5* alone. Next, to address cardiac function, we quantified heart rate at early chamber morphogenesis stage (42 hpf), chosen as the optimal time for balancing maximal cardiac function prior to end-stage degeneration. At 42 hpf, heart rates of *tbx5b* morphant embryos are significantly reduced as compared to controls, but not significantly different from *tbx5a* mutants or knockdown of *tbx5b* in *tbx5a* mutant embryos (Fig. 4.5D). Thus, based on both a morphological (heart looping) and a functional (heart rate) parameter, knockdown of both zebrafish *tbx5* paralogs together did not result in a more severe cardiac phenotype than observed for singly depleted embryos. Together, these data demonstrate that Tbx5b is required for cardiac development.

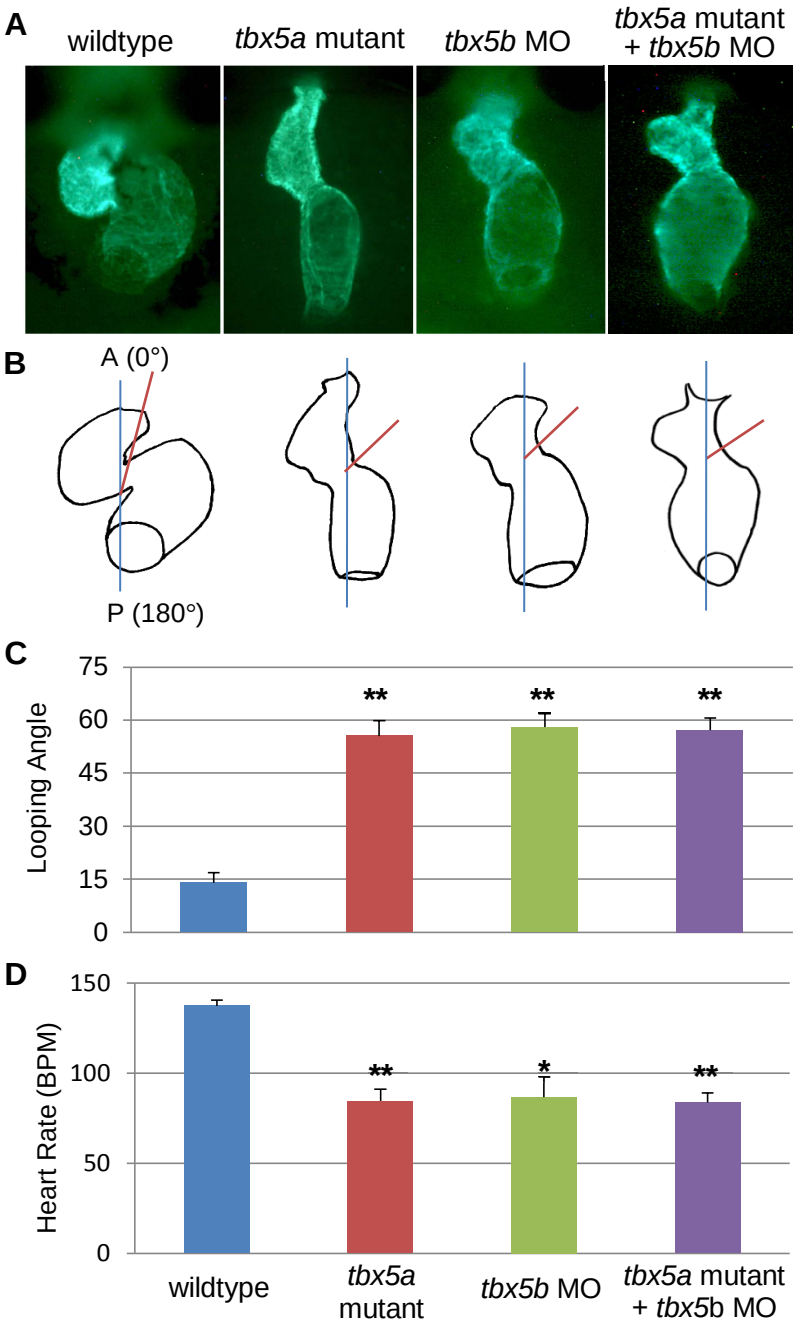

Fig. 4.5: *tbx5* deficient embryos display similar cardiac looping angles and heart rates at 48 hpf. At 48 hpf, the looping angles (defined as the angle created between the plane of the cardiac atrioventricular junction (AVJ) and the embryo A/P axis) were determined for control, *tbx5a* mutants, *tbx5b* morphants, and *tbx5b* MO-injected *tbx5a* mutant embryos. (**A**) GFP-expressing hearts imaged in the *Tg(myl7:EGFP-HsHRAS)* transgenic line. (**B**) Diagram of the looping angle as measured for the hearts in (A). (**C**) The average looping angle determined from at least 14 embryos per genotype. **, relative to controls, mutants and morphants exhibited a statistical difference of $p<0.001$. (a= anterior, defined here as 0°, p= posterior of the embryo).

Comparative analysis of phenotypes based on molecular markers of cardiac differentiation

We next employed several molecular markers to determine whether cardiac differentiation proceeded in a parallel fashion in *tbx5a* versus *tbx5b*-depleted embryos. In order to determine the effects of *tbx5b* knock-down on chamber specification, we assayed for the expression of cardiac-specific markers by whole mount *in situ* hybridization. As seen by *atrial myosin heavy chain* (*amhc*) and *ventricular myosin heavy chain* (*vmhc*) expression, chamber specification had occurred normally in both *tbx5a* mutants and *tbx5b* morphant embryos by 42 hpf (Fig. 4.6). In all cases, the expression of both markers was precisely restricted to the expected chambers, with no evidence of ectopic expression. We next examined expression of *natriuretic peptide precursor A (nppa),* a known target of zebrafish Tbx5a (Camarata *et al.* 2010) as well as a conserved Tbx5 target for other vertebrates (Bruneau *et al.* 2001, Garg *et al.* 2003, Habets *et al.* 2002, Hiroi *et al.* 2001, Stennard *et al.* 2003). At 36 hpf, *nppa* was expressed throughout both chambers of control embryos, but expressed only in the anterior portion of the ventricle in *tbx5a* mutant embryos (Fig. 4.7A-C). Expression of *nppa* was present in both chambers in *tbx5b* morphants, similar to controls.

Next, we next investigated *bmp4* expression to investigate the process of AVJ and sinus venosus (SV) patterning. By 42 hpf in wildtype *bmp4* expression was restricted to the AVJ and was also present in the SV region of the inflow tract (Fig. 4.7D, Walsh and Stainier 2001). As previously shown (Garrity *et al.* 2002), *tbx5a* mutants at 42 hpf continued to display expanded *bmp4* expression throughout the heart tube (Fig.

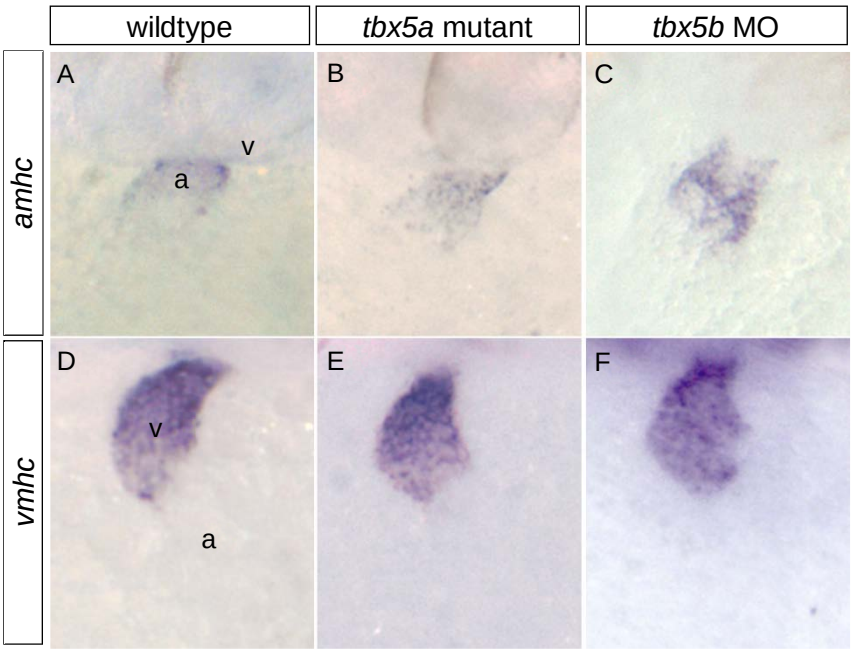

Fig. 4.6: Chamber-specific gene expression is normal in *tbx5a* mutant and *tbx5b* morphant embryos. (**A-C**) At 33 hpf, *amhc* is expressed only in the atrium of wildtype, *tbx5a* mutant, and *tbx5b* morphant embryos. (**D-F**) By 42 hpf, vmhc is expressed exclusively in the for both *tbx5a* mutants and *tbx5b* morphants. (a: atrium, v:ventricle).

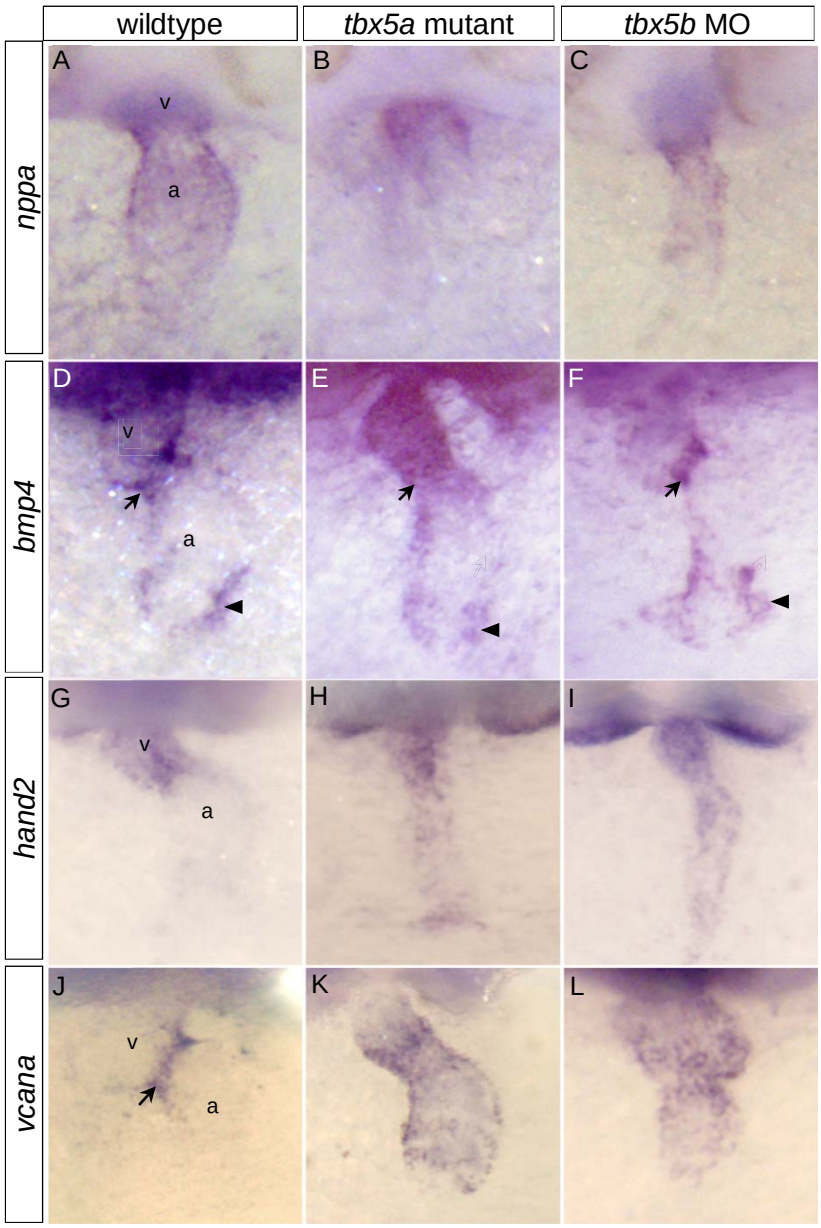

Fig. 4.7: Differential expression of putative target genes in *tbx5a* mutants versus *tbx5b* morphants. (**A-C**) At 36 hpf, expression of *nppa* (a conserved Tbx5 target) was reduced in the atrium of *tbx5a* mutant embryos, but expressed throughout both chambers in *tbx5b* morphant embryos. (**D-F**) At 42 hpf, *bmp4* was misexpressed throughout the ventricle of homozygous *tbx5a* mutant embryos. In *tbx5b* morphant embryos, *bmp4* expression was similar to wildtype. (**G-I**) At 42 hpf, soon after looping has begun, wildtype embryos primarily expressed *hand2* in the ventricle, but *tbx5a* mutant and *tbx5b* morphant embryos showed expanded expression encompassing both chambers. (**J-L**) At 42 hpf, wildtype embryos showed *vcana* expression restricted to AVJ boundary, but mutant and morphant embryos showed expanded expression throughout the ventricle and atrium. Arrow: AVJ boundary, arrowhead: sinus venosus.

4.7E). In contrast, expression in *tbx5b* morphant embryos restricted normally to the AVJ and SV (Fig. 4.7F). *bmp4* expression in the SV at this time occurs concurrently with the addition of cells derived from the second heart field to the venous pole of the heart, and *bmp4* expression in the SV is missing in mutants such as *isl-1* that that lack this addition (de Pater *et al*. 2009). Thus, this data suggests that second heart field cells are differentiating normally within the SV in *tbx5b* morphants.

We next looked at expression of the transcription factor *hand2*, a gene that plays a role in the differentiation and polarization of myocardial precursors as well as in cardiac extracellular matrix assembly (Barnes *et al.* 2011, Trinh *et al.* 2005). Just after looping has initiated, control embryos expressed *hand2* only in the ventricle (Fig. 4.7G). In contrast, *tbx5a* and *tbx5b*-depleted embryos displayed expanded expression encompassing both chambers (Fig. 4.7H, I). We also assayed for *versican a* (*vcana)*, a structural protein involved in cell adhesion and migration that interacts directly with the extracellular matrix (Matsumoto *et al.* 2003). *vcana* expression is normally restricted to the AVJ boundary by 42 hpf in wildtype embryos (Fig. 4.7J) (Walsh and Stainier 2001), but was expanded throughout the ventricle and atrium in both *tbx5a* mutant embryos and *tbx5b* morphant embryos (Fig. 4.7K,L). Proper assembly of cardiac extracellular matrix ("cardiac jelly") is important for proper cardiomyocyte precursor migration and restriction of the cardiac cushion formation (Barnes *et al.* 2011, Lagendijk *et al.* 2011). Therefore, ectopic expression of *hand2* and *vcana* in both *tbx5a* and *tbx5b* depleted embryos may point to a possible pathway for regulation of the cardiac jelly formation. Because we observe proper restriction of *bmp4* signal, but not *vcana*, to the AVJ in *tbx5b*

morphants, we hypothesize that each *tbx5* paralog regulates a unique subset of target genes, while also maintaining regulatory function over a shared target group.

Together this data demonstrates that although the cardiac phenotypes of *tbx5a* and *tbx5b* morphant embryos were similar morphologically, distinct differences exist in the way these morphants express molecular markers of cardiac differentiation. We therefore suggest that the two morphants differ in regard to the processes affected in each heart. Moreover, the fact that each morphant displays a fairly severe cardiac phenotype suggests that the remaining endogenous function of the paralog is not sufficient to rescue the defect, and argues against substantial genetic redundancy in the cardiac functions governed by these two genes.

Comparative analysis of phenotypes based on gene expression using qPCR

The Tbx5 transcription factor has several well-characterized target genes in mammals, many of which are conserved in other species (Greulich *et al.* 2011, Naiche *et al.* 2005, Stennard and Harvey 2005). If *tbx5a* and *tbx5b* share an recent evolutionary history and redundant functions in development, one would expect that they share a subset of the same target genes. To determine if *tbx5b* also regulates some of the same genes normally targeted by *tbx5a*, we selected six well-characterized Tbx5 target genes, and quantified their expression in zebrafish whole embryos using quantitative real-time PCR (qPCR). We compared mRNA expression levels for the six candidate genes in wildtype, *tbx5a* mutant (*hst*), and *tbx5b* morphant embryos. We tested two stages in development: 30 hpf (prior to overt cardiac phenotypes observed in *tbx5a* mutant and *tbx5b* morphant

embryos) and 36 hpf (after the onset of the looping and contractile phenotypes but before the severe degeneration of the heart). Therefore, this experiment will also test the hypothesis that *tbx5a* and *tbx5b* signaling is required in the heart tube even before the onset of overt cardiac phenotypes.

The six candidate target genes were: *tbx5a, tbx5b, nppa, bmp4, hey2* and *tbx2b*. We selected *tbx5a* and *tbx5b* to determine if depletion of one paralog spurred compensatory up-regulation of the alternate paralog. We chose *nppa* because this gene is directly regulated by Tbx5 in mammals (Bruneau *et al*. 2001) and *nppa* expression is reduced in *tbx5a* mutant embryos (Camarata *et al*. 2010). We selected *bmp4* because Tbx5 acts cooperatively with the Nkx2.5 transcription factor in mammals to directly regulate *bmp4* expression (Puskaric *et al*. 2010). The fifth candidate, *hey2*, is a transcription factor involved in cardiac septation, proliferation inhibition, and cardiomyocyte differentiation (Plageman and Yutzey 2006). The last candidate, *tbx2b,* is known to be directly regulated by Tbx5a together with Pdlim7 or Foxn4 (Camarata *et al*. 2010, Chi *et al*. 2008) and *tbx5a* mutant embryos showed a total absence of *tbx2b* expression at the AVJ (Camarata *et al*. 2010). For each of the candidate genes, we identified at least one conserved Tbx5 Binding Element (TBE) within 2 Kb of upstream sequences of the zebrafish gene, as would be expected if these genes were directly regulated by a T-box factor (see Appendix II, Fig. AII.2). For the *hey2* gene, no T-box Binding Element (TBE) had been found in the proximal 10Kb upstream sequence of mouse, human, or chick (Rutenberg *et al*. 2006), but we did identify a single TBE within 2 Kb of the zebrafish *hey2* start codon. A known zebrafish housekeeping gene, *ef1a*, was used as a standard control for this assay.

We found no difference in *ef1a* expression levels between the between wildtype, *tbx5a* mutant, or *tbx5b* morphants at 30 or 36 hpf by ANOVA analysis (p=0.99), indicating consistent mRNA quantity and integrity among all reactions. . In *tbx5a* mutant embryos, all of the candidate genes displayed significant decreases in mRNA copy number (Fig. 4.8A-F), reinforcing our expectation that *tbx5a* functions as a transcriptional activator, and that it would regulate these conserved vertebrate Tbx5 targets. In some cases, *tbx5a* mutant embryos showed a difference in target gene expression by 30 hpf and 36 hpf (Fig. 4.8A,C,D), but for other genes the regulation was only apparent by 36 hpf (Fig. 4.8B,E,F), consistent with some functions of *tbx5a* arising later in embryogenesis. The depletion of *tbx5a* did not result in a statistical increase in *tbx5b* expression (Fig. 4.8B), suggesting that no compensatory upregulation of the *tbx5b* paralog occurred in *tbx5a* mutant embryos.

Previous ISH studies indicated *tbx5a* transcripts were detectable in *tbx5a* mutants, even at 48 hpf (Garrity *et al*. 2002). Here, *tbx5a* transcripts were detected in *tbx5a* mutants, but were reduced relative to wildtype (Fig. 4.8A). Our data support the hypothesis that *tbx5a* contributes to regulation of *tbx5b* at 36 hpf (Fig. 4.8B), but *tbx5b* does not regulate its own expression, or that of its paralog. As opposed to the *tbx5a* mutants, the *tbx5b* morphant embryos showed no differences from wildtype in transcript levels of any of the tested genes, either at 30 or 36 hpf (Fig. 4.8), suggesting that *tbx5b* does not regulate any of these candidate genes at the timepoints tested. Based on these collective data, the *tbx5a* and *tbx5b* genes show non-overlapping profiles of gene regulation.

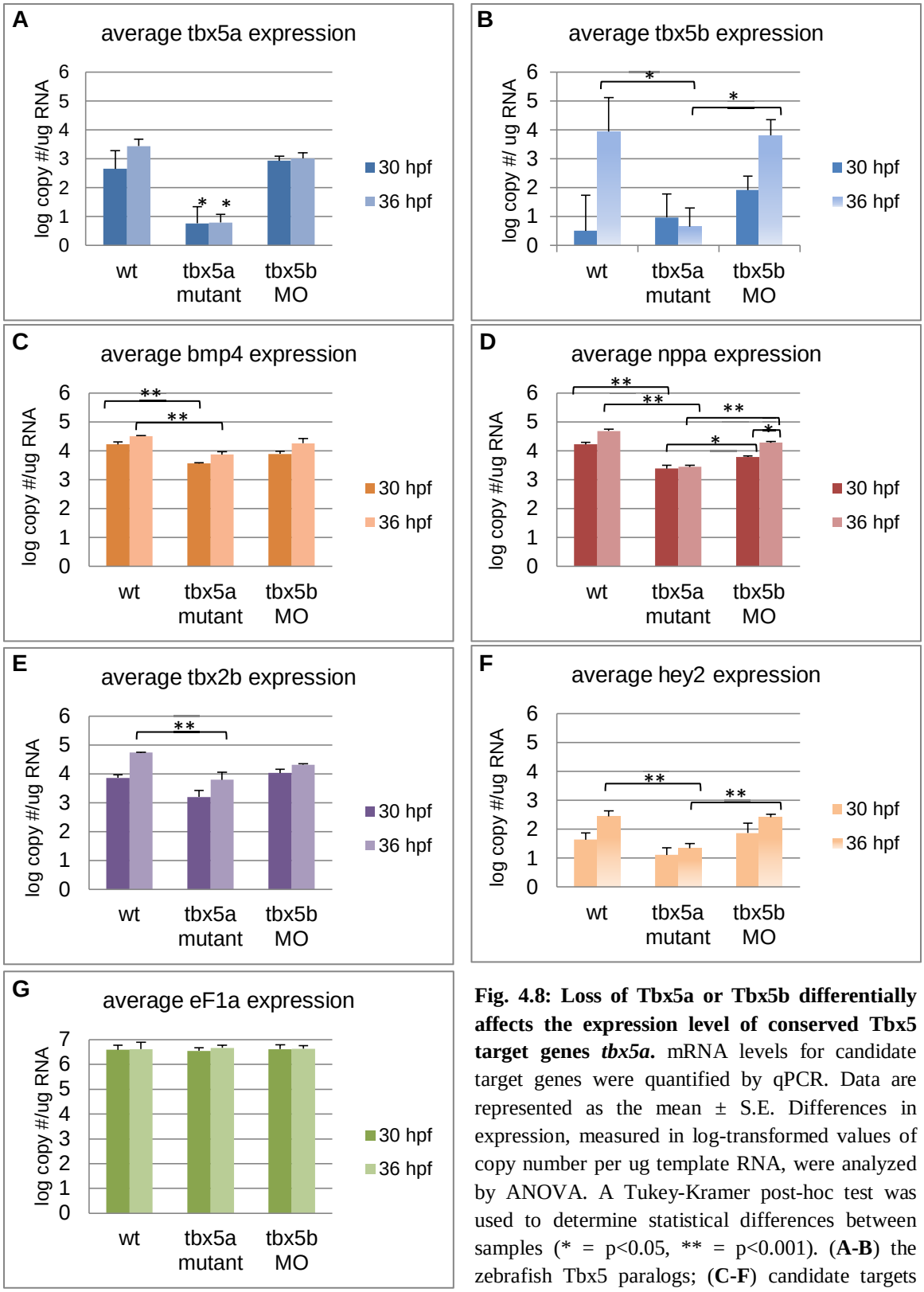

Fig. 4.8: Loss of Tbx5a or Tbx5b differentially affects the expression level of conserved Tbx5 target genes *tbx5a*. mRNA levels for candidate target genes were quantified by qPCR. Data are represented as the mean ± S.E. Differences in expression, measured in log-transformed values of copy number per ug template RNA, were analyzed by ANOVA. A Tukey-Kramer post-hoc test was used to determine statistical differences between samples (* = $p<0.05$, ** = $p<0.001$). (**A-B**) the zebrafish Tbx5 paralogs; (**C-F**) candidate targets based on conservation among vertebrates; (**G**) a house-keeping gene used as a standard control.

Tbx5b depletion results in altered pectoral fin morphology

We previously observed that injection of 12.4 ng of *tbx5a*MO caused lethal heart defects and blocked initiation of pectoral fin outgrowth (Garrity *et al*. 2002). In contrast, injection of a lower *tbx5a*MO dose (1.7 ng) resulted in fin deformities including up-turned fins, delayed fin outgrowth, or development of only one fin. While Tbx5a has a known function in forelimb initiation (Bruneau *et al*. 2004), the lack of detectable *tbx5b* expression in the zebrafish pectoral fin fields (Albalat *et al*. 2010) at first suggested that fin phenotypes would be unlikely in *tbx5b*-depleted embryos. However, in our hands the *tbx5b* ISH probe generated a broad, low level staining in several regions of the embryo (including the pectoral fins) that was difficult to distinguish from background, suggesting that *tbx5b* transcripts might be present in the fin fields at low levels, and therefore difficult to detect by ISH. Indeed, injection of *tbx5b*MO generated malformations in pectoral fin formation in 86% of *tbx5b* morphant embryos by 72 hpf (n= 282) (Fig. 4.9A, B). Injection of *tbx5b*MO also resulted in upturned (6.2% of embryos) or unilateral (10.3%) pectoral fins (Fig. 4.9B). Upturned or unilateral fin phenotypes are rather unusual, but these phenotypes can also be produced by modest reduction of *tbx5a* through low-dose morpholino injection (Garrity *et al*. 2002, data not shown). To further determine how fin bud initiation or patterning was affected, we quantified pectoral fin development from initiation through 72 hpf (Fig. 4.9). Although fin bud swellings should be apparent by 28 hpf (Hoffman *et al*. 2002), 71% of morphant embryos lacked any morphologically detectable fin buds at 30 hpf. However, fin bud formation was merely delayed, rather than absent as observed in *tbx5a* mutants, because scoring embryos at later timepoints indicated that smaller find buds eventually formed in nearly all embryos

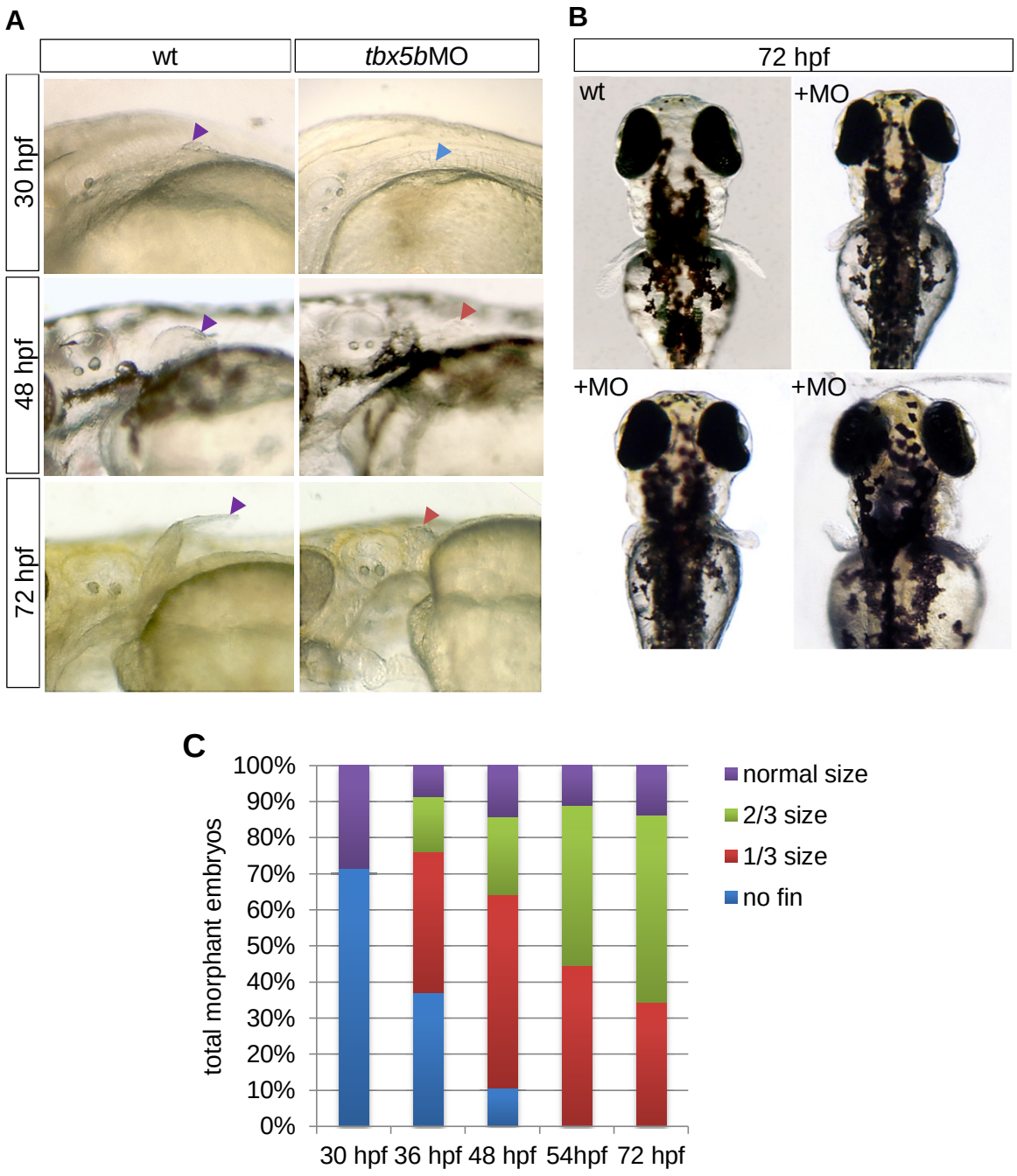

Fig. 4.9: Depletion of *tbx5b* delays pectoral fin initiation and reduces fin outgrowth. (**A**) Lateral brightfield images of pectoral fin area taken of control or *tbx5b*MO-injected embryos; anterior is oriented to the left. Arrowheads denote the tip of the pectoral fin and are color-coded based on size (see B). (**B**) Dorsal brightfield images of wildtype (wt) and *tbx5b*MO injected embryos at 72 hpf demonstrating altered pectoral fin morphology in morphant embryos. (**C**) Quantification of pectoral fin size for *tbx5b* MO-injected embryos at 30, 36, 48, 54, and 72 hpf. *n*=21-46 embryos per timepoint.

(Fig. 4.9C). Fewer than 15% of morphant embryos developed a normal pectoral fin by 72 hpf, whereas the majority of morphants developed stunted, up-turned, or otherwise abnormal pectoral fins (Fig. 4.9B). No defects were observed in the tail fins of the *tbx5b* morphants. Therefore, *tbx5b* is dispensable for pectoral fin bud initiation, but is essential for fin bud outgrowth and patterning.

tbx5b *affects apical fin fold (AF) specification*

To investigate the patterning and differentiation of the fin bud on a molecular level, we performed *in situ* hybridization with a panel of markers indicative of differentiating ectoderm (apical fold) or mesenchyme. Zebrafish pectoral fin bud development begins with mesenchyme formation by 28 hpf which is covered by an apical fold (AF, analogous to apical ectodermal ridge in tetrapods) by 31 hpf (Grandel and Schulte-Merker 1998, Neumann *et al.* 1999). Control embryos expressed *hand2* in the pectoral fin bud mesenchyme at 36 hpf (Fig. 4.10A). In contrast, *tbx5a* mutant embryos do not express *hand2* or other fin field markers consistent with the observation that pectoral fin buds never develop in these embryos (Fig. 4.10B,F,I) (Garrity *et al.* 2002). The normal expression of *hand2* in the pharyngeal arches, or *vcana and bmp4* in the otic placdoes, provided internal controls to assure probe quality in these experiments. In contrast, *tbx5b*-depleted embryos did express *hand2*, but the region of expression was reduced, consistent with the smaller fin buds that later developed (Fig. 4.10C). Therefore, *tbx5b* morphant embryos were beginning to differentiate fin bud mesenchyme. To investigate AF differentiation, we assayed for *bmp4* and *vcana*, which are normally expressed in the AF by 36-40 hpf (Rothschild *et al.* 2009, Thisse *et al.* 2005*)*. In control embryos, expression

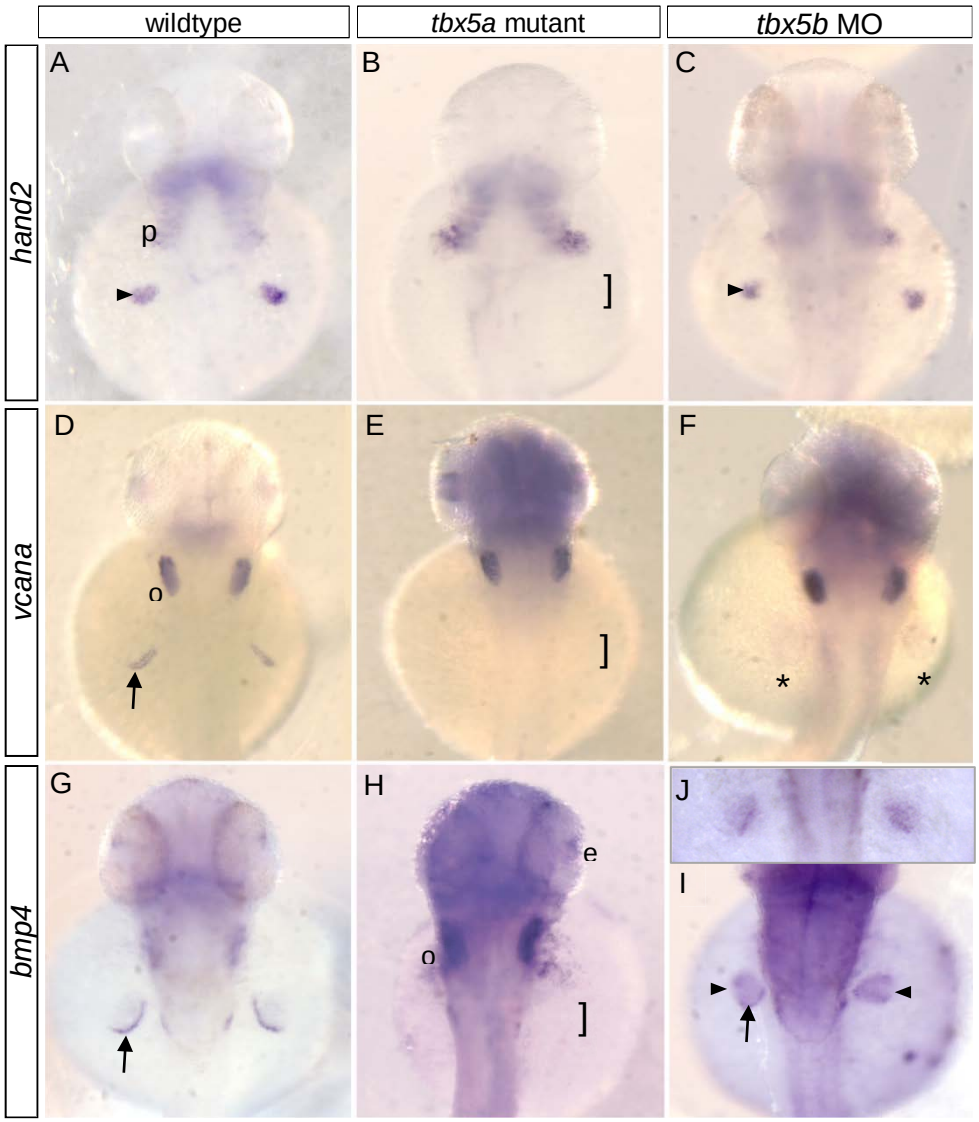

Fig. 4.10: Differential phenotypes observed in fin differentiation in *tbx5a* mutants and *tbx5b* morphants. Embryos at (**A-C**) 40 hpf; (**D-F**) 42 hpf; (**G-I**) 46 hpf; (**J**) **36** hpf. (**A**) *hand2* is expressed in the mesenchyme of the wildtype finbud. (**B**) In *tbx5a* mutant embryos, no pectoral fins develop; *hand2* expression was absent in fin buds (brackets indicate region of expected expression) although present in the pharyngeal arches. (**C**) In *tbx5b* morphants, fin buds expressed *hand2* in the mesenchyme in proportion to fin bud size. (**D**) *vcana* expression in the apical fold (AF) and otic placode (o). (**E**) *vcana* expression missing in region of expected fin buds. (**F**) *vcana* expression missing or barely detectable (*) in fin buds. (**G**) *bmp4* expression in the eye, otic placode and the AF of the pectoral fin. (**H**) No *bmp4* expression in fin bud region. (**I**) *bmp4* expression can occur in AF (arrow); additional expression in the mesenchyme of the finbud. (**J**) In younger embryos bmp4 is present in the mesenchyme and beginning in the AF. (e= eye, o= otic placode, p= pharyngeal arches, arrowhead = finbud mesenchyme, arrow = AF, * missing AF expression, brackets = region of missing finbud).

of *vcana* was present in the AF of the fin bud by 42 hpf (Fig. 4.10D). Although *tbx5b* morphants did initiate the outgrowth of pectoral fins, *vcana* expression remained absent or barely detectable even in embryos with morphological fin bud swellings at 42 hpf (Fig. 4.10F). Assays for *vcana* in 36 hpf and 54 hpf embryos similarly failed to exhibit fin bud expression (data not shown). These data suggested that the AF was not properly specified in *tbx5b* morphants. In the wildtype fin, *bmp4* expression occurred in the AF by 42 hpf and was faintly visible in the mesenchyme (Fig. 4.10G). In *tbx5b* morphants, *bmp4* expression was detectable in the mesenchyme but usually absent from the AF, although in a small minority of cases it was observed in one developing pectoral fin but not the other (Fig. 4.10I). This mesenchymal expression pattern was similar in a 36 hpf pectoral fin (Fig. 4.10J), further supporting the hypothesis that the pectoral fins of *tbx5b* morphants have initiated but are developmentally delayed.

Heart and pectoral fin development are sensitive to altered levels of tbx5

Previous studies have revealed that vertebrate cardiac and forelimb development are sensitive to transcription factor dose (Bruneau *et al.* 2001, Mori *et al.* 2006, Rallis *et al.* 2003, Seidman and Seidman 2002). In zebrafish, varying the amount injected morpholino similarly indicated that both cardiac and pectoral fin formation are sensitive to *tbx5a* dose (Garrity *et al.* 2002, Ng *et al.* 2002). To investigate cardiac and pectoral fin dose sensitivity, we increased *tbx5* dose through injection of *tbx5a* or *tbx5b* mRNA (Fig. 4.11). By 3 dpf, control hearts demonstrated normal cardiac looping, rigorous blood flow, and pectoral fins that were angled posteriorly along the body axis (Fig. 4.11A,D). Overexpression of *tbx5a* by injection of 800 ng/µl mRNA into wildtype embryos resulted

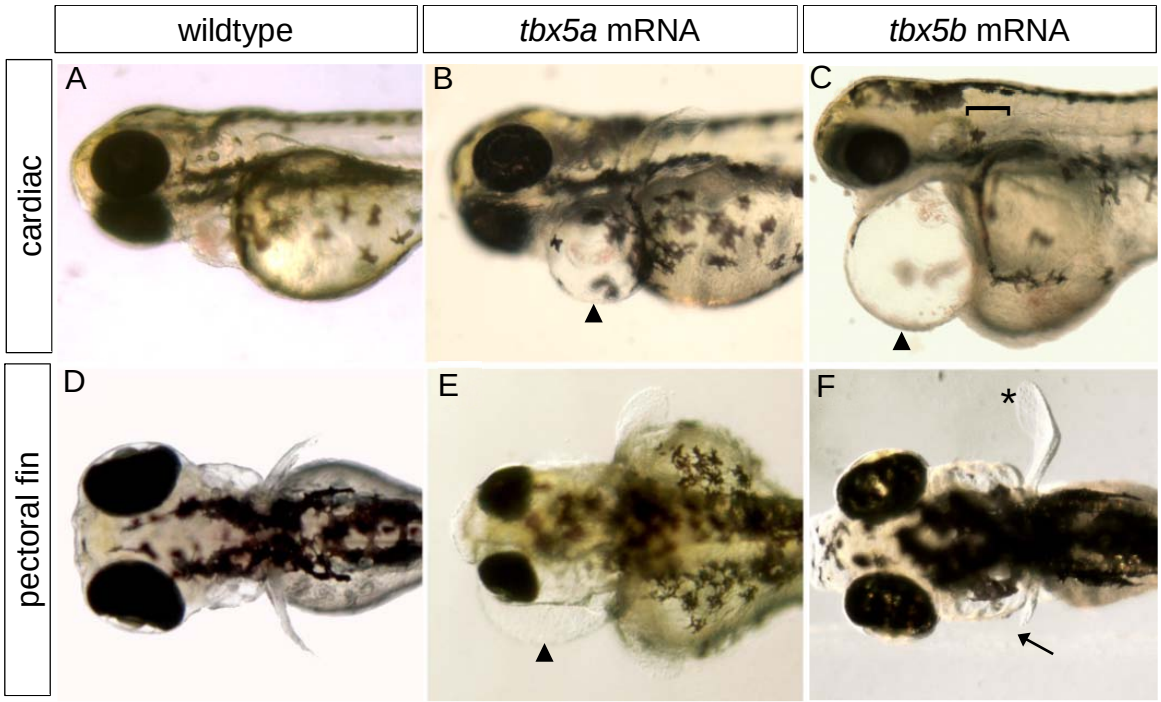

Fig. 4.11: Cardiac and pectoral fin development are sensitive to *tbx5a* and *tbx5b* overexpression. (A,D) Brightfield images of wildtype**,** (**B**,**E**) *tbx5a* mRNA-injected, or (**C,F**) *tbx5b* mRNA-injected larvae. Arrowheads denote pericardial edema; bracket represents missing pectoral fin; arrows denote pectoral fins of reduced size, * denote upturned pectoral fin.

*tbx5b*MO also resulted in upturned (6.2% of embryos) or unilateral (10.3%) pectoral fins in cardiac phenotypes (pericardial edema, lack of looping, and eventual lethality), whereas pectoral fin development was always normal (n= 75) (Fig. 4.11B,E). Overexpression of *tbx5b* by injection of 1000 ng/µl mRNA into wildtype embryos generated phenotypes similar to *tbx5a* mutants, including cardiac edema and a dysmorphic, unlooped heart (Fig. 4.11C) as well as stunted, upturned, or unilateral pectoral fins (Fig. 4.11F). These data are additional confirmation that both *tbx5a* and *tbx5b* are functionally required within the developing heart and pectoral fins, and that dose is related to the wildtype function.

tbx5a *and* tbx5b *are not functionally redundant*

Knockdown of either the *tbx5a* or *tbx5b* gene still generated phenotypes, indicating that these two genes are not fully compensatory in function. However, they both affect cardiac and pectoral fin formation (Fig. 4.4) and show similar expression of a subset of genes (Fig. 4.7), which suggests some redundancy could exist. As a further test for overlap in function, we attempted to rescue the *tbx5a*-depletion phenotypes by overexpression of *tbx5b* mRNA and vice versa (Fig. 4.12). For these "cross rescue" experiments, cardiac and pectoral fin phenotypes were scored separately. As a method to track the integrity of injected mRNAs, we created constructs encoding the *tbx5a* or *tbx5b* open reading frame fused with green fluorescent protein (GFP). The presence of GFP in injected fish will serve to confirm the stability and translation of injected mRNAs. To avoid the possibility that fusion of GFP would interfere with Tbx5a or Tbx5b function, a viral 2A (v2A) peptide sequence was inserted between the open reading frames of *tbx5*

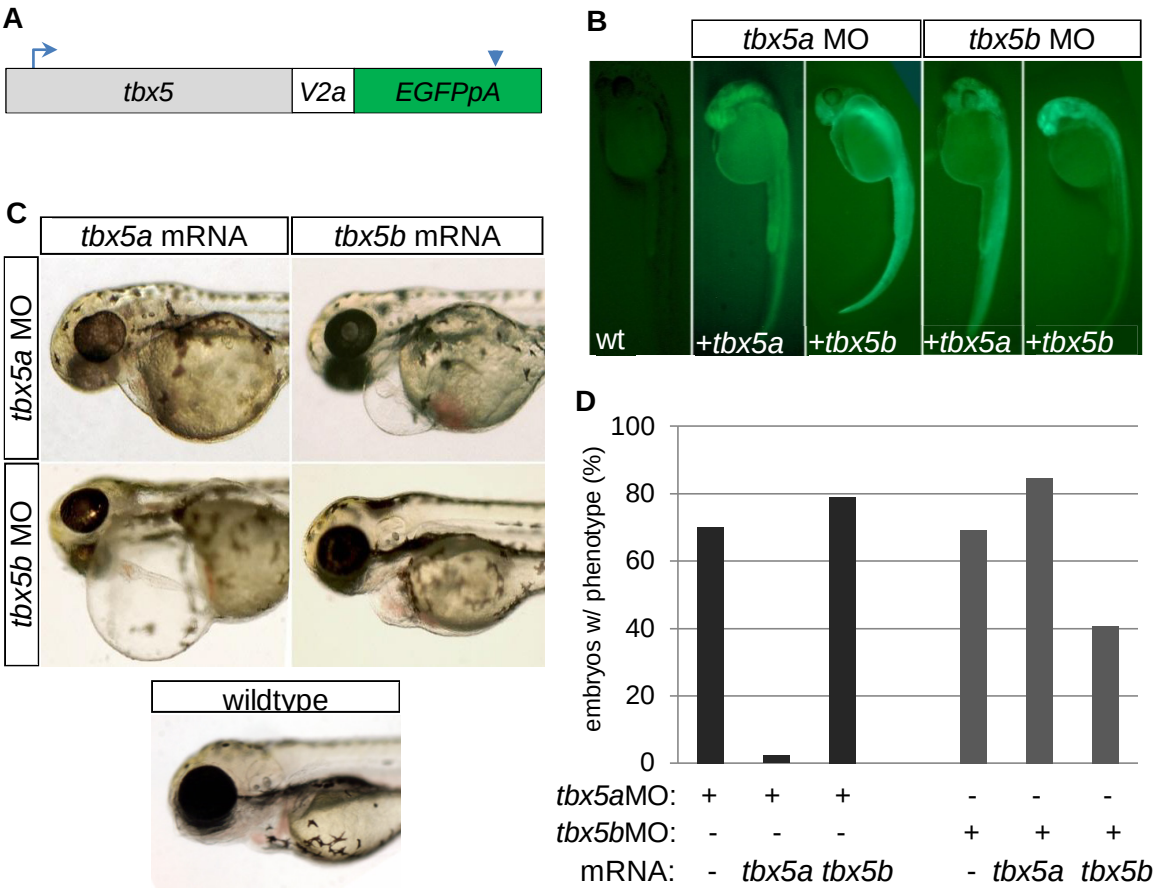

Fig. 4.12: mRNA injection rescue studies suggest *tbx5a* and *tbx5b* are not functionally redundant in cardiac development. (**A**) Schematic of mRNA structure of rescue constructs, in which the coding sequence for *tbx5a* or *tbx5b* was connected to EGFP (with accompanying poly-adenylation signal) via a viral 2A peptide. The v2A peptide cleaves subsequent to translation, allowing two separate proteins to be produced from a single mRNA transcript. Blue arrow indicates location of translation start site. Blue arrowhead indicates termination signal. (**B**) Fluorescent images of 26 hpf embryos previously injected with combinations of either buffer (in wildtype, wt), *tbx5a*MO or *tbx5b* MO, and *tbx5a* or *tbx5b* mRNA to evaluate mRNA integrity and translation through GFP. (**C**) Brightfield images of 72 hpf embryos showing representative cardiac phenotypes for each group of injected embryos. (**D**) Quantification of morpholino injected embryos displaying a cardiac morphology phenotype at 54 hpf. (*tbx5a*MO 82.4% *n*=91; *tbx5a* MO+*tbx5a* mRNA 2.4% *n*= 84; *tbx5a* MO+*tbx5b* mRNA 78.9% *n*= 133; *tbx5b* MO 69.1% *n*= 220; *tbx5b* MO+*tbx5a* mRNA 84.6% *n*= 65, *tbx5b* MO+*tbx5b* mRNA 40.6% *n*= 69).

and GFP (Fig. 4.12A). v2A is a small, “self-cleaving” peptide, first described by Ryan *et al.* (1991) as a domain of the foot-and-mouth disease (FMD) virus. Effectively, insertion of the V2A peptide allows bicistronic expression from a single transcript because the ribosome skips the synthesis of the glycyl-prolyl peptide bond at the C-terminus of the v2A peptide, but still continues its translation of downstream codons. This process ultimately results in the production of two separate proteins (Tbx5-v2A peptide and GFP) from sequences on the single transcript (de Felipe *et al.* 2010, Donnelly *et al.* 2001).

As expected, embryos injected with rescue mRNAs consistently showed fluorescence associated with the GFP reporter protein, indicating the mRNAs were stable and appropriately translated (Fig. 4.12B). Injection of *tbx5a*MO generated embryos with the expected cardiac and fin phenotypes in 82.4% of embryos (Fig. 4.12C,D). Co-injection of *tbx5a*MO along with 600 ng/µl *tbx5a* mRNA reduced the number of embryos with cardiac phenotypes to 2.4%, thereby demonstrating an efficient rescue of the phenotype. Co-injection of *tbx5b* mRNA into *tbx5a* morphants resulted in 78.9% of embryos with cardiac defects, showing that *tbx5b* mRNA could not rescue *tbx5a* morphant cardiac defects. In the converse experiment, injection of *tbx5b*MO generated cardiac phenotypes in 69.1% of embryos. Co-injection of 775 ng/µl *tbx5b* mRNA into *tbx5b* morphants decreased the incidence of cardiac defects to 40.6%, demonstrating a partial rescue of cardiac phenotypes (Fig. 4.12C,D). These experiments demonstrate that while zebrafish *tbx5a* and *tbx5b* mRNAs were capable of rescuing the cardiac phenotypes of their cognate morpholino, they were not sufficient to compensate for the cardiac function of the paralog gene. Thus, *tbx5a* and *tbx5b* have evolved separate roles in cardiac development.

Because both Tbx5a and Tbx5b are required for pectoral fun outgrowth, we also used the rescue approach to investigate potential overlap in pectoral fin function. To evaluate pectoral fin rescue we quantified fin outgrowth at 72 hpf, by which time delayed fin buds should have initiated some outgrowth. As a control, embryos were injected first with 600 ng/µl *tbx5a* or 775 ng/µl *tbx5b* (25% less than for overexpression experiments), fewer than 5% of embryos showed any detectable phenotype (data not shown). When embryos were co-injected with *tbx5a*MO and 600 ng/µl *tbx5a* mRNA, we found that 65% of embryos had no pectoral fin and only 16% of embryos had a stunted pectoral fin (Fig. 4.13). Thus, although *tbx5a* mRNA efficiently rescued heart development, it did not have a large ability to rescue fin initiation or fin outgrowth at this concentration. Higher concentrations of *tbx5a* mRNA resulted in non-specific body-axis defects or death at pre-gastrulation stages (data not shown). In the "cross-rescue" experiment, injection of 775 ng/µl *tbx5b* mRNA into *tbx5a* morphants showed 79% of total embryos failed to initiate pectoral fin initiation, showing that *tbx5b* mRNA likewise could not rescue pectoral fin initiation. As previously shown, injection of *tbx5b*MO resulted in a majority (86%) of embryos with stunted pectoral fins at 72 hpf. Injection of *tbx5b* mRNA with *tbx5b*MO decreased the percentage of embryos with stunted pectoral fin phenotypes to 23%, with the remainder of embryos showing normal fins. Thus, *tbx5b* mRNA did substantially rescue fin phenotypes produced by *tbx5b*MO. In the "cross-rescue" experiment, injection of *tbx5a* mRNA into *tbx5b* morphants resulted in 76% of embryos that completely lacked pectoral fin bud initiation, indicating no ability of Tbx5a to function in the stead of Tbx5b in the fin. In fact, injection of *tbx5a* mRNA into *tbx5b* morphants made the fin phenotype more severe, because most embryos now failed even to initiate pectoral fins. In summary,

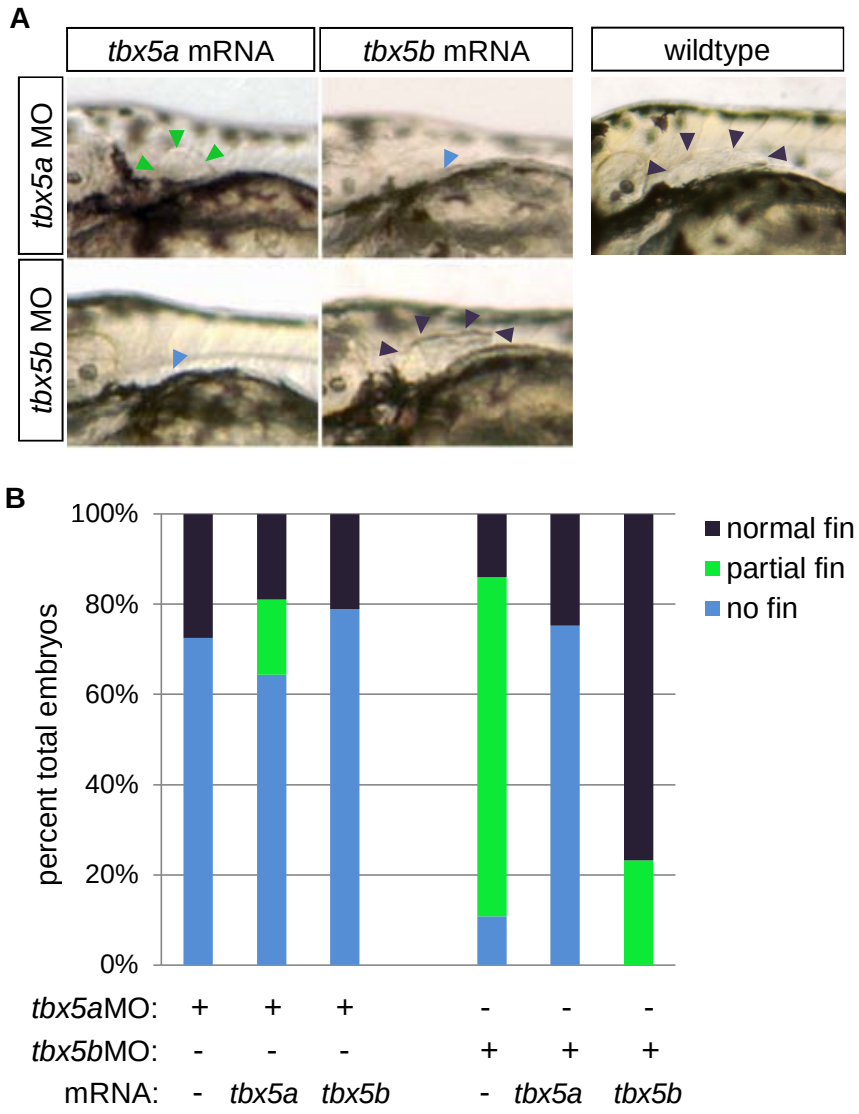

Fig. 4.13: *tbx5a* and *tbx5b* are not functionally redundant in pectoral finbud outgrowth. (**A**) Brightfield images of lateral pectoral fin region at 54 hpf. Arrowheads outline the buds and are color-coded according to legend (see B). (**B**) Percent of embryos exhibiting each phenotype (normal, partial or no pectoral fin outgrowth) at 54 hpf. (*tbx5a* MO 82.5% *n*= 91; *tbx5a* MO + *tbx5a* mRNA 78.6% *n*= 84; *tbx5a* MO + *tbx5b* mRNA 89.5% *n*= 133; *tbx5b* MO 79.1% *n*= 220; *tbx5b* MO + *tbx5a* mRNA *n*= 65, *tbx5b* MO + *tbx5b* mRNA *n*= 69).

we note that in all cases of morphants coinjected with the paralogous mRNA, no rescue occurred for either cardiac or fin phenotypes. Indeed, both phenotypes were at least slightly increased in severity and numbers. We suspect that not only are the coinjected mRNAs ineffective in compensating for the paralogous tbx5-depletion, but that their presence along with the endogenous *tbx5a* and *tbx5b* mRNA in the embryo may confer a low level of overexpression that provides a small additive effect to the morpholino phenotypes. Overall, these experiments are consistent with our other data indicating no substantial redundancy exists in the functions of Tbx5a or Tbx5b in the heart or fin.

Tbx5 is does not regulate total cardiomyocyte number in zebrafish

In various species, Tbx5 function impacts the numbers of cardiomyocytes as development proceeds. To evaluate cardiomyocyte numbers in zebrafish, we first crossed *tbx5a* heterozygous adults with a transgenic line in which the heart-specific *myl7* (formerly *cmlc2*) promoter drives expression of the nuclear DsRed reporter gene (*Tg(myl7:nDsRed2/myl7:EGFP)* (Mably *et al*., 2003)). Cardiomyocytes were quantified in 48 hpf transgenic fish of several genotypes, including: homozygous wildtype, homozygous mutant *tbx5a*^{m21}, *tbx5a* morphant, *tbx5b* morphant, *tbx5a+b* double-morphant, or *tbx5b*MO into *tbx5a* mutant embryos (Fig. 4.14). We observed no significant differences in total cardiomyocyte numbers at 48 hpf among any of these fish ($p=0.4$), suggesting that normal cardiac cell numbers had developed for all genotypes. Collectively, this data suggests that neither zebrafish *tbx5a* nor *tbx5b* has any independent or functionally redundant role in regulating cardiac cell number in the heart

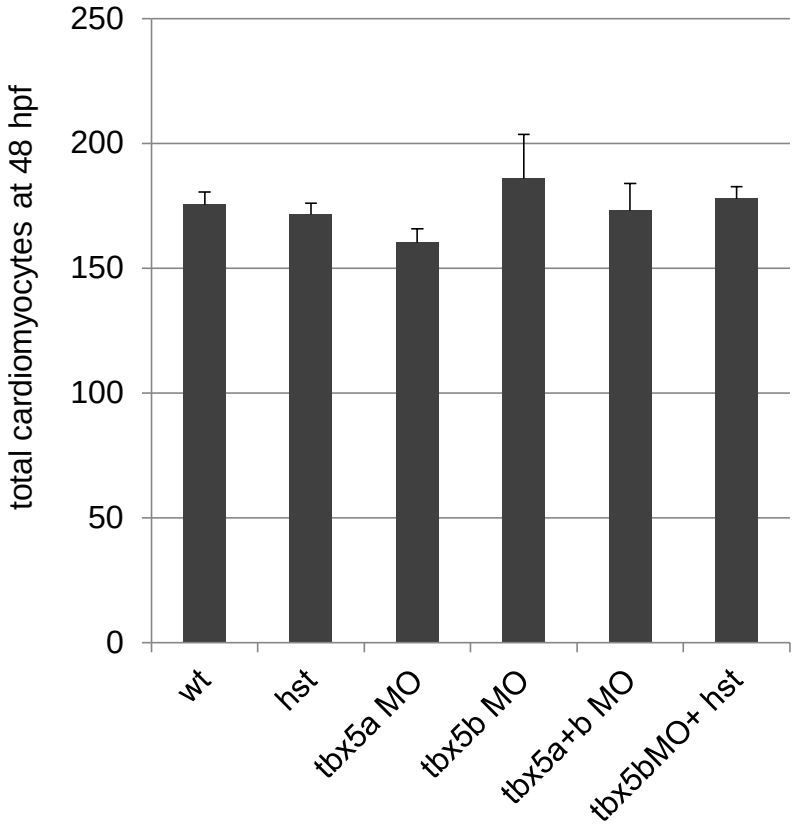

Fig. 4.14: Cardiac proliferation is not affected by a lack of functional Tbx5a or Tbx5b. Quantification of total cardiomyocyte number in wildtype (wt) and tbx5-deficient embryos at 48 hpf. Data are expressed as means ± S.E. and there were no statistically significant differences among these treatments (*p>0.05). For the columns listed, left to right, n=20, 11, 17, 11, 20, 14 embryos.

tube through early chamber morphogenesis stages (48 hpf), and further supports our premise that *tbx5a* and *tbx5b*show non-redundant functions in the heart.

Discussion

The two primary conclusions of this study are that the zebrafish T-box transcription factor *tbx5b* is essential for cardiac development and pectoral fin morphogenesis, and secondly that the *tbx5a* and *tbx5b* paralogs have distinct and non-redundant functions in development of the heart and pectoral fins. Multiple lines of evidence support these conclusions. First, knock-down of *tbx5b* via morpholino injection results in lethal deficiencies in cardiac morphogenesis that ultimately affect looping morphogenesis, contractility and blood flow. In addition, reduction of *tbx5b* causes a resolvable delay in the onset of pectoral fin initiation, followed by irresolvable defects in fin patterning and outgrowth. Second, overexpression studies indicate that the dose of both *tbx5a* and *tbx5b* can impact morphology and function in the developing heart and fin. Third, although *tbx5a* and *tbx5b* depletion results in some overt morphological similarities, ISH studies evaluating several markers of differentiation indicate that both the heart and fin show distinct phenotypic differences. Fourth, qPCR studies support this finding, indicating that whereas *tbx5a* depletion decreases mRNA levels of *tbx5b*, *nppa*, *hey2*, *bmp4* and *tbx2b*, the depletion of *tbx5b* does not alter mRNA levels for any of these genes, of *tbx5a* or of itself. Thus, *tbx5b* does not regulate the same cohort of genes as does *tbx5a*. Fifth, dual depletion of both *tbx5a* and *tbx5b* by morpholinos does not result in more severe or additive cardiac phenotypes, such as severe depletion or lack of cardiac tissue, nor does it

affect cardiomyocyte cell numbers more adversely than does single gene knockdown. Finally, the inability of each *tbx5* paralog to "cross-rescue" the knock-down phenotype of the other paralog demonstrates minimal redundancy in function exists between the two paralogs.

We are in the process of addressing several questions. First we will analyze the conservation within the T-box as compared to the whole gene of *tbx5a*, *tbxb*, human TBX5, and closely related zebrafish T-box genes *tbx4*, *tbx2*, and *tbx3*. This genomic analysis will be used to confirm that *tbx5b* is truly a *tbx5* paralog. We are also investigating which *tbx5* is evolving more quickly in zebrafish, and whether one of these *tbx5b* is evolving faster than the expected rate for this gene, as compared to other fish species.

Approximately 300 million years ago, teleost genomes underwent a duplication event (Taylor *et al*. 2001, Hurley *et al*. 2007). Since *tbx5* paralogs are present in several teleost genomes, *tbx5a* and *tbx5b* may have arisen at this time (Albalat *et al*. 2010). Following a duplication event, in many cases one gene tends to accumulate degenerative mutations over time, and ultimately becomes non-functional or devolves into a pseudogene (van Noort *et al*. 2003). In other cases, the two paralogous genes undergo 'subfunctionalization'; that is, they evolve separable patterns of expression or separable functions, so that both genes remain intact within the genome. In the case of the zebrafish *tbx5* paralogs, the regions of embryonic expression appear highly similar, and the organs of embryonic function are the same. Yet, a more detailed analysis examining the

expression of putative targets for these transcription factors suggests that mechanistically, the functions of these two genes have already diverged. We propose therefore that the *tbx5a* and *tbx5b* genes have undergone or are currently undergoing subfunctionalization.

Functional studies of Tbx5 in human, mouse, chick, frog and zebrafish have emphasized that embryos are sensitive to Tbx5 dosage. Alterations leading to decreased Tbx5, relative to the endogenous amount, are associated with phenotypes (Bruneau *et al*. 2001, Garrity *et al*. 2002, Ng *et al*. 2002). Haploinsufficiency of Tbx5 can cause HOS, a human congenital disease characterized by cardiac and forelimb defects (Basson *et al*. 1997, Li *et al* .1997). Mutations in mouse Tbx5 are also dominant, and studies show that Tbx5-null embryos die by E11 because of the severity of heart defects (Bruneau *et al*. 2001). Similarly, a conditionally-induced homozygous deletion of Tbx5 in the developing mouse forelimb resulted in a complete lack of forelimb bud formation (Rallis *et al*. 2003). Tbx5 is required not only for forelimb initiation, but also for continued limb outgrowth. As shown in the chick model, expression of dominant-negative Tbx5 after forelimb bud initiation produced a severely truncated limb. This reduction of Tbx5 solely in the bud mesenchyme was sufficient to alter *Fgf8* signaling in the AER required for continued limb outgrowth (Rallis *et al*. 2003). Alterations leading to increased Tbx5 dose are likewise associated with phenotypes. In mouse embryonic stem cells and *Xenopus* embryos, overexpression of Tbx5 mRNA led to a decrease of *Bmp4* and *Hand2* (Hermann *et al.* 2011). In chick, overexpression of constitutively-active Tbx5 causes forewing enlargement, particularly in the anterior portion of the limb (Rallis *et al*. 2003), and could lead to formation of extra limb buds (Ng *et al*. 2002). Increase and decrease of

tbx5 expression prevents migration of the chick proepicardium, a progenitor cell population that gives rise to multiple cell types in the adult heart, including the epicardium and coronary vasculature (Hatcher *et al*. 2004). We demonstrate here that zebrafish cardiac and pectoral fin bud formation are sensitive to the over- or under-expression of either *tbx5a* or *tbx5b*. Therefore, for many species, the functions of Tbx5-family genes appear to be intimately connected to dose.

An important cellular function for Tbx5 in the heart concerns its effect on cardiomyocyte cell number. Depletion of TBX5 by morpholino in *Xenopus* resulted in a ~30-40% decrease of total cardiac cells in hearts undergoing early chamber formation (stage 37), indicating that TBX5 in frogs positively regulates cardiomyocyte proliferation in this system (Brown *et al.* 2005, Goetz *et al.* 2006). On the other hand, overexpression of wildtype TBX5 in chick (beginning at HH 17-18, early cardiac looping stages) also reduced cardiomyocyte proliferation by 40% (Hatcher *et al.* 2001). These data support a model in which TBX5 functions in chick as a growth arrest signal that negatively regulates cardiomyocyte proliferation. However, the timing of depletion or over-expression of Tbx5 may affect the phenotypic outcome, especially if Tbx5 has a dual role as an activator in early stages and a growth arrest signal in later stages, as has been proposed (Goetz *et al.* 2006). Previously, we reported that in zebrafish Tbx5a is dispensable for cardiomyocyte cell number during early chamber morphogenesis, but necessary for growth of cardiomyocyte size during early-chamber morphogenesis stages (Parrie *et al*. in press). A role for Tbx5 regulation of cell growth has recently been defined for mice as well (Georges *et al*. 2008). As a caveat to our findings on cell

number, we hypothesized that the zebrafish *tbx5b* paralog might share a redundant function with *tbx5a* in modulating cardiac cell number in early chamber morphogenesis stages, and that this function could mask a cell proliferation phenotype in *tbx5a* mutants. However, we here demonstrate that reduction of both *tbx5* paralogs together did not alter total cardiomyocyte number at mid chamber morphogenesis stages, providing no support for the above hypothesis. Instead, our data suggests that reduction of cardiomyocyte cell number is not a primary defect contributing to the cardiac phenotypes by chamber morphogenesis stages. Additionally, regulation of cell proliferation by *tbx5* may reflect a role specific to tetrapods, perhaps contributing to the development of additional cardiac chambers, while the zebrafish *tbx5* genes retain more ancestral functions.

Proper assembly of cardiac extracellular matrix ("cardiac jelly") is important for proper cardiomyocyte precursor migration and restriction of the cardiac cushion formation (Barnes *et al*. 2011, Lagendijk *et al*. 2011). Therefore, ectopic expression of *hand2* and *vcana* in both *tbx5a* and *tbx5b*-depleted embryos may point to a possible pathway for regulation of the cardiac jelly formation. Because we observe proper restriction of *bmp4* signal, but not *vcana*, to the AVJ in *tbx5b* morphants, we hypothesize that each *tbx5* paralog regulates a unique subset of target genes, while also maintaining regulatory function over a shared target group.

Despite the probable low levels of *tbx5b* expression in the fin fields, we find that *tbx5b* function is indeed required for the correct timing of pectoral fin bud initiation, and for the normal outgrowth and patterning of fins. Importantly, the *tbx5b* morphant fin phenotypes

are a specific outcome of *tbx5b* gene knockdown, since they can be rescued by co-injection of *tbx5b* mRNA. Although fin bud initiation was delayed in *tbx5b* morphants, this defect was resolvable by 72 hpf when 85% of morphant embryos had developed at least a small fin bud. In contrast, the complete loss of *tbx5a* function definitively eliminates (rather than delays) pectoral fin initiation (Ahn *et al*. 2002, Garrity *et al*. 2002). A similar feature between the *tbx5b* and hypomorphic *tbx5a* loss-of-function phenotypes is that pectoral fin outgrowth (if initiated) remains stunted, and buds can later develop abnormal morphologies such as upturned fins. Nevertheless, several differences in the expression of molecular markers in pectoral fins suggest that different mechanisms may be impaired when Tbx5b versus Tbx5a is depleted. In particular, our results pinpoint a requirement for *tbx5b* function in differentiation of the AF, since embryos lacking *tbx5b* fail to express two markers for the AF. In contrast, at least one marker of the fin bud mesenchyme appeared to be expressed normally in the smaller morphant fin bud. Interestingly, *bmp4* expression was missing or highly downregulated in the AF but potentially expanded within the fin bud mesenchyme, relative to controls (Fig. 9). A similarly altered *bmp4* expression pattern combined with stunted and/or asymmetrical pectoral fin morphology was reported for embryos depleted of CaMK-II by morpholino injection (Rothschild *et al*. 2009). CaMK-II is a type II multifunctional Ca^{2+}/calmodulin-dependent protein kinase. Rothschild *et al*. determined that CaMK-II acts downstream of *tbx5a* in zebrafish. Whether *tbx5b* similarly regulates CaMK-II is currently unknown. In sum, Tbx5b now joins the cohort of several Tbx-family transcription factors with roles in limb patterning.

In conclusion, although the *tbx5b* gene is expressed in similar tissues to *tbx5a*, including the embryonic heart, eye and the pectoral fin buds, it differs from its paralog on several levels, including genomic organization, sequence, and function. We find little evidence to postulate a mechanistic overlap or redundancy in function between these two genes. The paralogs appear to fit the evolutionary model of duplication followed by subfunctionalization. Although both genes function in the embryonic heart and forelimb, as does human *TBX5*, the zebrafish Tbx5a protein appears to demonstrate a closer parallel to humans in its conserved regulation of mammalian Tbx5 target genes than does Tbx5b. However, transcriptional network studies for both genes may be required to fully comprehend the range of functions carried out by T-box genes during organogenesis.

Materials and Methods

Zebrafish husbandry

Zebrafish were raised and staged as described previously (Westerfield 1995; Nusslein-Volhard and Dahm 2002) and as per Colorado State University Animal Care and Use Protocols. Developmental time at 28.5°C was determined from the morphological features of the embryo as described by Kimmel (1990).

Zebrafish Imaging

Live larvae (48 and 72 hpf) were immobilized using tricaine anesthetic (i.e. MESAB) and placed on agarose injection plates for imaging. All samples were visualized using an Olympus SZX12 Fluorescent stereo-dissecting microscope. Photographs were taken

using a microscope-mounted Olympus U-CMAD3 digital camera and captured using SPOT software imaging (Diagnostic Instruments, Inc.). Post-processing was done using Adobe Photoshop software to correct white balance and image sizes.

Tbx5b WIK allele cloning and sequencing

Wildtype *tbx5b* mRNA was extracted from WIK embryos using the Trizol method (see below), reverse transcription and polymerase chain reaction was performed as described (Garrity *et al.* 2002, Ebert *et al.* 2008) using primers described by Albalat *et al.* (2010). Resulting cDNA was TA-cloned into the pCRII vector (Invitrogen) and sequenced using m13 universal primers. Alignments were prepared using ClustalW and Jalview (Larkin *et al.* 2007, Waterhouse *et al.* 2009).

RNA extraction

Total RNA was extracted from 30-42 hpf embryos by a modified Trizol method. Samples were collected and immediately immersed in Tri-Reagent (Invitrogen) that had been equilibrated to room temperature. Tissue did not exceed 10% of the Tri-Reagent volume. Embryos were homogenized slowly on ice until cloudy. The sample was pelleted in a refrigerated centrifuge at maximum speed for 10 minutes. The supernatant was removed to a new 1.5 ml eppendorf tube, 200 ul of chloroform was added, and the sample was shaken vigorously. The sample was incubated on ice for 3 minutes and then spun for 15 minutes, 4° C at maximum speed. The upper phase was removed to a new 1.5 ml eppendorf tube, being careful to not remove the interphase. This aqueous phase is used for RNA extraction. The original 1.5 ml eppendorf tube and sample can be kept for

DNA extraction (DNA and protein are in the interphase). To reduce phenol contamination the upper aqueous phase was spun for an additional 10 minutes at maximum speed at 4° C, and the upper phase of this was removed to a new 1.5 ml eppendorf tube. 500 ul of isopropanol was added and the sample was incubated on ice for 10 minutes. This sample was pelleted at 4° C for 10 minutes. The supernatant was discarded, the RNA pellet was washed with 1 ml cold 75% ethanol, and spun again at half speed for 5 minutes at 4° C. The pellet was air dried and resuspended in RNase/DNase-free water or DEPC-treated water. RNA samples were stored at -80° C after assessing quantity and purity by nanospec analysis.

Plasmid DNA Purification

Following transformation, white colonies were transferred to 5 ml LB broth containing 5 µl ampicillin (1:1000 dilution) and incubated overnight in a 37°C shaker. The broths were then purified using Promega Wizard® Plus SV Miniprep solutions and protocol. The concentrations of the purified plasmid samples and their purity were measured on nanospec.

Morpholino Injections

Translation blocking morpholino (*tbx5b*MO: GGATTCGCCATATTCCCGTCTGAGT) was designed against the region of *tbx5b* encoding the translational start site, and synthesized by Genetools (California). The translation blocking *tbx5a* morpholino (*tbx5a*MO: GCCTGTACGATGTCTACCGTGAGGC) was selected because it targets sequences slightly upstream of the initiation codon, thus making it possible to use with

mRNA for rescue experiments. This morpholino was designed by Lu *et al.* (2008), modified from Ahn *et al.* (2002), and the efficacy and specificity are described therein. 1-4 cell embryos were injected with 100 µM *tbx5b*MO, 150 µM *tbx5a*MO, or coinjected with 75 µM *tbx5b*MO and 100 µM *tbx5a*MO together.

Prior to injection, embryos were transferred from petri dish to an injection plate using a fire-polished Pasteur pipette. Morpholino was injected into 1-2 cell embryos using a Femtojet (Eppendorf). Injection needles were pulled from 0.75mm inner diameter borosilicate capillary tubes (World Precision Instruments, Sarasota, FL) on a Sutter P97 Flaming/Brown Micropipette puller using the following program: Heat: 715, Pull: 60, Vel: 80, Time: 200. Needles were backfilled with a mixture of 2-3 ul of rhodamine (to identify well-injected embryos) and 150uM Tbx5-ATG morpholino.

At this stage of development, although the animal and vegetal poles are easily distinguishable, it is not possible to determine the dorsal-ventral position, or longitude of a cell. Nevertheless, if the embryo is allowed to free-fall from the Pasteur pipette, it is likely to land with the lateral margin facing the surface, and the dorsal (0°) and ventral (180°) poles positioned at the edges (Stainier *et al.* 1993).

Cardiac Morphology

48 hpf larvae were immobilized using MESAB and placed in agarose-containing petri dishes for imaging. To quantify cardiac looping, wildtype and mutant lines were crossed with *Tg(myl7:EGFP-HsHRAS)* to image cardiac-specific fluorescence. Looping angles

were determined by measuring the angle of the AV junction relative to the anterior/posterior axis of the embryo. All samples were visualized using a Spot Insight IN1120 digital camera on an Olympus SZX12 fluorescent stereo-microscope. Post-processing was completed with Adobe Photoshop software.

Whole Mount **In situ** ***Hybridization***

Embryos were fixed in 4% paraformaldehyde solution in PBS (PFA) (1:10 dilution of 40% paraformaldehyde (Electron Microscopy Sciences, Hatfield, PA) at room temperature for 2 hours or at 4° C overnight and stored in 100% methanol at -20° C. Samples were prepared for whole mount *in situ* hybridization as described (Thisse *et al.* 1993). The digoxigenin-labled riboprobe for Tbx5 was synthesized using the T3 RNA polymerase. The digoxigenin-labled riboprobe for *tbx5b* was prepared as described (Albalat *et al.* 2009) with the following additions: the cDNA was cloned into pCRII (Invitrogen), linearized for probe synthesis with the ApaI restriction enzyme, and synthesized using the T7 RNA polymerase. Other RNA probes used include *amhc*, *vmhc*, *vcana*, *bmp4*, and *dhand*, and synthesized as described previously (Ebert *et al.* 2008).

Phenol/Chloroform Extraction and Overnight Ethanol Precipitation

If purity of DNA was low, or to remove restriction digest enzymes the following protocol was used:

The reaction volume was increased to 300ul with nuclease-free water. An equal volume (300ul) of phenol/chloroform was added, shaken hard for 1 minute, and spun for 2 minutes at full speed. The top aqueous layer was removed into a clean 1.5 ml eppendorf

tube and an equal volume (300 ul) of chloroform was added to extract, shaken and re-spun. The top aqueous layer was removed again and 1/10th the total reaction volume of 3mM sodium acetate (pH 5.2), 1ul glycogen, and 2.5 volumes (750ul) cold 100% ethanol was added. This mixture was precipitated at -80˚C 2 hours to overnight. The tube was spun at full speed in the 4 ˚C refrigerated centrifuge for 30 minutes to pellet the DNA. The supernatant was decanted and the pellet was washed with cold 70% ethanol and spun for 5 minutes, repeated 2 to 3 times. The pellet was then air dried and re-suspended in 20ul RNase/DNase free water and stored at -20˚C.

Quantitative Real-time PCR

Total RNA was isolated using TRIzol reagent (Invitrogen, Carlsbad, CA, USA) according to the manufacturer's protocol. Briefly, total RNA was treated with DNase I (Invitrogen) to remove genomic DNA. After DNase treatment, total RNA was subjected to phenol:chloroform extraction, followed by precipitation of RNA to remove DNase, salts and digested DNA. Total RNA was precipitated with 1 volume of isopropanol and resuspended in 30 µl of nuclease-free water. Nucleotide concentration was determined by absorbance at 260 nm and 3 µg was used for 20 µl cDNA synthesis reaction using AMV reverse transcriptase (Fisher Scientific) and Oligo$(dT)_{12\text{-}18}$ primer (Invitrogen). Resulting cDNA was treated with RNase H (New England Biolabs, Ipswich, MA, USA) to remove any residual complementary RNA.

Quantitative analysis of *tbx5b* [GenBank Accession HQ822122], *tbx5a* [GenBank NM_130915 (Tamura *et al.* 1999)], *tbx2b* [GenBank NM_131051 (Ruvinsky *et al.*

2000)], *hey2* [GenBank NM_131622 (Zhong *et al.* 2000)], *bmp4* [GenBank NM_131342 (Strausberg *et al.* 2002)], *nppa* [GenBank NM_198800], and *eF1-alpha* [GenBank NM_131263 (Gao *et al.* 1997)] was conducted using LightCycler FastStart DNA Master Plus SYBR Green I reaction mix and a LightCycler 480 thermal cycler (Roche Applied Science, Indianapolis, IN, USA). Triplicate reactions consisted of 1 μl first strand cDNA, 5 μl 2× SYBR Green Master Mix, 0.5 μl each of forward primer and reverse primer (10 μM each, sequences in Table 4.1), and 3 μl PCR-grade water.

Table 4.1: Quantitative PCR primer sequences.

tbx5a	85(f3)	5'-GGA ATT TAA GGC CTC ACG GTA-3'
tbx5a	272r	5'-GAT TTG CTG ACG GCT GCA TTC TGT-3'
tbx5b	323F	5'-ATT CAG GAC ATC ACG GAC GGA ACA-3'
tbx5b	338R	5'-TTT GTA GCT GGG AAA CAT GCG TCG-3'
tbx2b	196f	5'-GTC CCT TTC CCT TTC ATC TGT CTC -3'
tbx2b	197r	5'-CTG GGA GCT GAT AAG GGT TGA ATC-3'
nppa	204f	5'-CAG ACA CAG CTC TGA CAG CAA CAT -3'
nppa	205r	5'-CTC TGT GTG TCA AAT CCA TCC GAG -3'
hey2	206f	5'-GAA AGA AGC GGA GAG GGA TCA TTG -3'
hey2	207r	5'-AGA AGT CCA TGG CCA GAG AAT GAG -3'
bmp4	208f	5'-CAC AGT ATC TGC TCG ACC TCT A-3'
bmp4	208r	5'-GAT ATG AGT TCG TCC TCT GGG ATG -3'
ef1a	48F2	5'-CGG TGA CAA CAT GCT GGA GG-3'
ef1a	49R2	5'-ACC AGT CTC CAC ACG AC CA-3'

PCR conditions included an initial denaturation at 95°C for 5 min, followed by 45 cycles of denaturation at 95°C for 10 seconds, annealing at 55°C for 15 seconds, and extension at 72°C for 15 seconds. At the end of each run, an analysis of the PCR product melting temperature was conducted. Amplicon specificity was also verified by sequencing. Transcript concentrations were calculated with LightCycler 480 software (Roche; version 1.2) using standards curves produced by serial dilution of purified PCR product (10 zg/μl

to 10 ng/μl). Use efficiencies for all reactions were confirmed to be between 1.86 and 1.96 and transcripts were confirmed by sequencing. Statistical analysis was performed using JMP software v9.0.2 (SAS Institute, Inc., Cary, NC, USA). qRT-PCR data were log transformed prior to analysis to reduce differences in variance from the mean. Means for transcript abundance were compared between wildtype, *tbx5a*, and *tbx5b* MO embryos using analysis of variance (ANOVA). Post-hoc multiple comparisons were made using Tukey–Kramer HSD tests. All data not plotted as individual points are presented as mean ± S.E. and the level of significance was set at α=0.05 for all statistical analyses.

Capped mRNA Synthesis and Injection

For creation of the Tester mRNA the *tbx5b*MO recognition site was fused to EGFP via PCR amplification with the following primers: #331TbMOGFPF 5'-ACT CAGACGGGAATATGGCGAATCAGGTGAGCAAGGGCGAGGAGCTGTTC-3' and #304GFPR 5'-AAAAAAGGGCCCCCCGGGAAAAAACCTCCCACAC-3'. The resulting amplicon was TA-cloned into pCRII and confirmed by DNA sequencing. For the rescue mRNAs the v2A peptide sequence was inserted 5' of EGFP using a two-step PCR reaction and the following primers: #316F 5'-AAGTCTGCTAACATG CGGTGACGTCGAGGAGAATCCTGGCCCAACCATGGTGAGCAAG-3', #317F2 5'-GGCGGCCGCTTGGCAGTGGAGAGGGCAGAGGAAGTCTGCTAACATG-3'. The #366 3'EV plasmid from the Chien Lab Gateway kit, which contains EGFP, was used as template for amplification using the EGFP-specific reverse primer and a forward primer contained a portion of the v2A and a portion of the 5' end of GFP (primer #316F). The resulting band was gel-extracted and used as template for the second PCR using the same

GFP-specific reverse primer and a second forward primer contained the remainder of the v2A sequence *(*primer #317F2). This primer set contained SmaI, ApaI, and NotI restriction sites to facilitate cloning in frame with *tbx5a* and *tbx5b.* The resulting amplicons were TA-cloned into pCRII (Invitrogen). The full-length constructs containing the *tbx5* gene, v2A peptide sequence, and EGFP sequence were confirmed by DNA sequencing and were termed pCRII-tbx5a-v2A-EGFP or pCRII-tbx5b-v2A-EGFP. Full-length mRNAs were prepared using mMessage Machine kit (Ambion) according to the manufacturer's instructions. mRNA was injected into the one-celled embryo at the following concentrations: *tbx5b*MOsite-GFP tester mNRA (1000 ng/µl), *tbx5a*v2A-GFP (800 ng/µl), and *tbx5b*v2A-GFP (1000 ng/µl).

Cardiomyocyte Quantification

The number of cardiomyocytes in the heart was quantified in wildtype and mutant embryos crossed into a *Tg(myl7:nDsRed2/myl7:EGFP)* homozygous background (Mably *et al.* 2003). At 48 hpf, embryos were pressed between a glass coverslip and slide to gently flatten the heart. Intact flattened hearts were immediately imaged using a Leica 5500 microscope.

References

Abramoff MD, Magalhaes PJ, Ram SJ. 2004. Image Processing with ImageJ. Biophotonics International. 11:36-42.

Agarwal P, Wylie JN, Galceran J, Arkhitko O, Li C, Deng C, Grosschedl R, Bruneau BG. 2003. Tbx5 is essential for forelimb bud initiation following patterning of the limb field in the mouse embryo. Development. 130: 623-633.

Agulnik SI, Bollag RJ, Silver LM. 1995. Conservation of the T-box gene family from *Mus musculus* to *Caenorhabditis elegans*. Genomics. 25:214-219.

Agulnik SI, Garvey N, Hancock S, Ruvinsky I, Chapman DL, Agulnik I, Bollag R, Papaioannou V, Silver LM. 1996. Evolution of mouse T-box genes by tandem duplication and cluster dispersion. Genetics. 144:249-254.

Ahn DG, Kourakis MJ, Rohde LA, Silver LM, Ho RK. 2002. T-box gene tbx5 is essential for formation of the pectoral fin bud. Nature. 417:754-758.

Albalat R, Baquero M, Minguillion C. 2010. Identification and characterization of the developmental expression pattern of tbx5b, a novel tbx5 gene in zebrafish. Gene Expr Pat. 10:24-30.

Agarwal P, Wylie JN, Galceran J, Arkhitko O, Li C, Deng C, Grosschedl R, Bruneau BG. 2003. Tbx5 is essential for forelimb bud initiation following patterning of the limb field in the mouse embryo. Development. 130: 623-633.

Arrenberg AB, Stainier DYR, Baier H. Huisken J. 2010. Optogenetic Control of Cardiac Function. Science. 330: 971-974.

Auman HJ, Coleman H, Riley HE, Olale F, Tsai HJ, Yelon D. 2007. Functional Modulation of Cardiac Form through Regionally Confined Cell Shape Changes. PLoS Biol. 5:604-611.

Bagatto B, Francl J, Liu B, Liu Q. 2006. Cadherin2 (N-cadherin) plays an essential role in zebrafish cardiovascular development. BMC Dev Bio. 6:23-29.

Bakkers J. 2011. Zebrafish as a model to study cardiac development and human cardiac disease. Cardiovas. Res. 91:279–288.

Bamshad M, Lin RC, Law DJ, Watkins WC, Krakowiak PA, Moore ME, Franceschini P, Lala R, Holmes LB, Gebuhr TC, Bruneau BG, Schinzel A, Seidman JG, Seidman CE, Jorde LB. 1997. Mutations in human TBX3 alter limb, apocrine and genital development in ulnar-mammary syndrome. Nat Genet. 16:311-315.

Barnes RM, Firulli BA, Vandusen NJ, Morikawa Y, Conway SJ, Cserjesi P, Vincentz JW, Firulli AB. 2011. Hand2 loss-of-function in Hand1-expressing cells reveals distinct roles in epicardial and coronary vessel development. Circ Res. 108:940–949.

Bartman T, Walsh EC, Wen KK, McKane M, Ren J, Alexander J, Rubenstein PA, Stainier DY. 2004. Early myocardial function affects endocardial cushion development in zebrafish. PLoS Biol. 2(5):673-681.

Basson CT, Bachinsky DR, Lin RC, Levi T, Elkins JA, Soults J, Grayzel D, Kroumpouzou E, Traill TA, Leblanc-Straceski J, Renault B, Kucherlapati R, Seidman JG, Seidman CE. 1997. Mutations in human cause limb and cardiac malformation in Holt-Oram syndrome. Nat Gen. 15:30-35.

Basson CT, Cowely GS, Solomon SD, Weissman B, Poznanski AK, Traill TA, Seidman JG, Seidman CE. 1994. The clinical and genetic spectrum of the Holt-Oram syndrome (heart-hand syndrome). New Engl J Med. 330:885-891.

Basson CT, Huang T, Lin RC, Bachinsky DR, Weremowicz S, Vaglio A, Bruzzone R, Quadrelli R, Lerone M, Romeo G, Silengo M, Pereira A, Krieger J, Mequita SF, Kamisao M, Morton CC, Pierpont ME, Muller CW, Seidman JG, Seidman CE. 1999. Different TBX5 interactions in heart and limb defined by Holt-Oram Syndrome mutations. Proc Natl Acad Sci USA. 96:2919-2924.

Begemann G, Ingham PW. 2000. Developmental regulation of Tbx5 in zebrafish embryogenesis. Mech Dev. 90:2919-2924.

Beis D, Bartman T, Jin SW, Scott IC, D'Amico LA, Ober EA, Verkade H, Frantsve J, Field HA, Wehman A, Baier H, Tallafuss A, Bally-Cuif L, Chen JN, Stainier DYR, Jungblut B. 2005. Genetic and cellular analyses of zebrafish atrioventricular cushion and valve development. Devel. 132: 4193-4204

Berdougo E, Coleman H, Lee DH, Stainier DY, Yelon D. 2003. Mutation of weak atrium/atrial myosin heavy chain disrupts atrial function and influences ventricular morphogenesis in zebrafish. Devel. 130:6121-6129.

Bimber B, Dettman RW, Simon HG. 2007. Differential regulation of Tbx5 protein expression and sub-cellular localization during heart development. Dev Biol 302: 230–242.

Blechingera SR, Evansa TG, Tanga PT, Kuwadac JY, Warren Jr JT, Kronea PH. 2002. The heat-inducible zebrafish hsp70 gene is expressed during normal lens development under non-stress conditions. Mech Devel. 112:213–215.

Borozdin W, Bravo Ferrer Acosta AM, Bamshad MJ, Botzenhart EM, Froster UG, Lemke J, Schinzel A, Spranger S, McGaughran J, Wand D, Chrzanowska KH, Kohlhase J. 2006. Expanding the spectrum of TBX5 mutations in Holt-Oram syndrome: detection of two intragenic deletions by quantitative real time PCR, and report of eight novel point mutations. Hum Mutat. 27:975–976.

Brittijn SA, Duivesteijn SJ, Belmamoune M, Bertens LF, Bitter W, de Bruijn JD, Champagne DL, Cuppen E, Flik G, Vandenbroucke-Grauls CM, Janssen RA, de Jong IM, de Kloet ER, Kros A, Meijer AH, Metz JR, van der Sar AM, Schaaf MJ, Schulte-Merker S, Spaink HP, Tak PP, Verbeek FJ, Vervoordeldonk MJ, Vonk FJ, Witte F, Yuan H, Richardson MK. 2009. Zebrafish development and regeneration: new tools for biomedical research. Int J Dev Biol. 53:835-850.

Brown DD, Martz SN, Binder O, Goetz SC, Price BMJ, Smith JC, Conlon FL. 2005. Tbx5 and Tbx20 act synergistically to control vertebrate heart morphogenesis. Devel. 132:553-563.

Brown LA, Rodaway AR, Schilling TF, Jowett T, Ingham PW, Patient RK, Sharrocks AD. 2000. Insights into early vasculogenesis revealed by expression of the ETS-domain transcription factor Fli-1 in wild-type and mutant zebrafish embryos. Mech. Dev. 90: 237-252.

Bruneau BG, Logan M, Davis N, Levi T, Tabin CJ, Seidman JG, Seidman CE. 1999. Chamber-specific cardiac expression of Tbx5 and heart defects in Holt–Oram syndrome. Dev. Biol. 211: 100–108.

Bruneau BG, Nemer G, Schmitt JP, Charron F, Robitaille L, Caron S, Conner DA, Gessler M, Nemer M, Seidman CE, and Seidman JG. 2001. A Murine Model of Holt-Oram Syndrome Defines Roles of the T-Box Transcription Factor Tbx5 in Cardiogenesis and Disease. Cell. 106:709-721.

Bryant PJ, Simpson P. 1984. Intrinsic and extrinsic control of growth in developing organs. Q Rev Biol. 59:38-415.

Bryson-Richardson RJ, Currie PD. 2008. The genetics of vertebrate myogenesis. Nat Rev Genet. 8:632-46.

Burns CG, Milan DJ, Grande EJ, Rottbauer W, MacRae CA, Fishman MC. 2005. High-throughput assay for small molecules that modulate zebrafish embryonic heart rate. Nat Chem Biol. 1:263–264.

Carreira S, Dexter TJ, Yavuzer U, Easty DJ, Goding CR. 1998. Brachyury-related transcription factor Tbx2 and repression of the melanocyte-specific TRP-1 promoter. Mol Cell Biol. 18:5099-108.

Chang YF, Imam JS, Wilkinson MF. 2007. The Nonsense-Mediated Decay RNA Surveillance. PathwayAnnu. Rev. Biochem. 76:51–74.

Chapman DL, Agulnik I, Sarah Hancock S, Silver LM, Papaioannou VE. 1996a. Tbx6, a Mouse T-Box Gene Implicated in Paraxial Mesoderm Formation at Gastrulation. Devel Biol. 180:534-542.

Chapman DL, Garvey N, Hancock S, Alexiou M, Agulnik SI, Gibson-Brown JJ, Cebra-Thomas J, Bollag RJ, Silver LM< Papaioannou VE. 1996. Expression of the T-box family genes, *Tbx1-Tbx5*, during early mouse development. Dev Dyn. 206:37-390.

Chen JN, van Eeden FJ, Warren KS, Chin A, Nüsslein-Volhard C, Haffter P, Fishman MC. 1997. Left-right pattern of cardiac BMP4 may drive asymmetry of the heart in zebrafish. Development. 124:4373-82.

Chen, JN, van Bebber F, Goldstein AM, Serluca FC, Jackson D, Childs S, Serbedzija GN, Warren KS, Mably JD, Lindahl P, Mayer A, Haffter P, Fishman MC. 2001. Genetic steps to organ laterality in zebrafish. Comp Funct Genomics. 2:60-68.

Cheng J, Belgrader P, Zhou X, Maquat LE: Introns are cis effectors of the nonsense-codon-mediated reduction in nuclear mRNA abundance. Mol Cell Biol 1994, 14:6317-6325.

Chernyavskaya Y, Ebert AM, Milligan E, Garrity DM. 2012. The voltage gated calcium channel β2 protein is required in the heart for control of cell proliferation and heart tube integrity. Dev Dyn. Epub ahead of print.

Chi NC, Shaw RM, De Val S, Kang G, Jan LY, Black BL, Stainier DYR. 2008. Foxn4 directly regulates tbx2b expression and atrioventricular canal formation. Genes Dev. 22:734–739.

Chien KR, Domian IJ, Parker KK. 2008. Cardiogenesis and the complex biology of regenerative cardiovascular medicine. Science. 322:1494-7.

Ching YH, Ghosh TK, Cross SJ, Packham EA, Honeyman L, Loughna S, Robinson TE, Dearlove AM, Ribas G, Bonser AJ, Thomas NR, Scotter AJ, Case LSD, Tyrrell GP, Newbury-Ecob RA, Munnich A, Bonnet D, Brook JD. 2005. Mutation in myosin heavy chain 6 causes atrial septal defect. Nat Gen. 37:423-428.

Chocron S, Verhoeven MC, Rentzsch F, Hammerschmidt M, Bakkers J. 2007. Zebrafish Bmp4 regulates left-right asymmetry at two distinct developmental time points. Devel Biol. 305:577-588.

Chomczynski P, Sacchi, N. 1987. Single-step method of RNA isolation by acid guanidinium thiocyanate phenol chloroform extraction. Analyt Biochem. 162:156-159.

Chopra A, Tabdanov E, Patel H, Janmey PA, Kresh JY. 2011. Cardiac myocyte remodeling mediated by N-cadherin-dependent mechanosensing. Am J Physiol-Heart Circul Physiol. 300:H1252-H1266.

Christoffels VM, Habets PE, Franco D, Campione M, de Jong F, Lamers WH, Bao ZZ, Pamer S, Biben C, Harvey RP, Moorman AFM. 2000. Chamber formation and morphogenesis in the developing mammalian heart. Dev Biol. 223:266-278.

Clark KL, Yutzey KE, Benson DW. 2006. Transcription factors and congenital heart defects. Annu Rev Physiol. 68:97-121.

Conlon I, Raff M. 1999. Size control in animal development. Cell. 96:235-244.

Connors SA, Tucker JA, Mullins MC. 2006. Temporal and spatial action of Tolloid (Mini fin) and Chordin to pattern tail tissues. Dev Biol. 293:191-202.

Culp P, Nusslein-Volhard C, Hopkins N. 1991. High-frequency germ-line transmission of plasmid DNA sequences injected into fertilized zebrafish eggs. Proc Natl Acad Sci. 88:7953–7957.

Dabiri GA, Turnacioglu KK, Sanger JM, Sanger JW. 1997. Myofibrillogenesis visualized in living embryonic cardiomyocytes. Proc Natl Acad Sci. 94:9493-9498.

Dahme T, Katus HA, Rottbauer W. 2009. Fishing for the genetic basis of cardiovascular disease. Dis Model Mech. 2:18-22.

Day SJ, Lawrence PA. 2000. Measuring dimensions: the regulation of size and shape. Devel. 127:2977-2987.

Deacon DC, Nevis KR, Cashman TJ, Zhou Y, Zhao L, Washko D, Guner-Ataman B, Burns CG, Burns CE. 2010. The miR-143-adducin3 pathway is essential for cardiac chamber morphogenesis. Devel. 137:1887-1896.

DeBenedittis P, Jiao K. 2011. Alternative splicing of T-box transcription factor genes. Biochem Biophys Res Commun. 412:513-517.

de Felipe P, Luke GA, Brown JD, Ryan MD. 2010. Inhibition of 2A-mediated 'cleavage' of certain artificial polyproteins bearing N-terminal signal sequences. Biotechnol J. 5:213–223.

De Pater E, Clijsters L, Marques SR, Lin YF, Garavito-Aguilar ZV, Yelon D, Bakkers J. 2009. Distinct phases of cardiomyocyte differentiation regulate growth of the zebrafish heart. Devel. 136:1633-1641.

Dobrzynski H, Boyett MR, Anderson RH. 2007. New insights into pacemaker activity - Promoting understanding of sick sinus syndrome. Circulation. 115:1921-1932.

Dooley KA, Fraenkel PG, Langer NB, Schmid B, Davidson AJ, Weber G, Chiang K, Foott H, Dwyer C, Wingert RA, Zhou Y, Paw BH, Zon LI, Tubingen 2000 Screen Consortium. 2008. *montalcino,* A zebrafish model for variegate porphyria. Exp Hematol. 36:1132-1142.

Donnelly ML, Luke G, Mehrotra A, Li X, Hughes LE, Gani D, Ryan MD. 2001. Analysis of the aphthovirus 2A/2B polyprotein 'cleavage' mechanism indicates not a proteolytic reaction, but a novel translational effect: a putative ribosomal 'skip'. J Gen Virol. 82:1013–1025.

Dutta SPS. 1993. Food and feeding habits of *Danio rerio* (Ham. Buch.) inhabiting Gadigarh stream, Jammu. J Freshwater Biol. 5:165–168.

Ebarasi L, Oddsson A, Hultenby K, Betsholtz C, Tryggvason K. 2011. Zebrafish: a model system for the study of vertebrate renal development, function, and pathophysiology. Curr Opin Nephrol Hypertens. 20:416-424.

Ebert AM, Hume GL, Warren KS, Cook NP, Burns CG, Mohideen MA, Siegal G, Yelon D, Fishman MC, Garrity DM. 2005. Calcium extrusion is critical for cardiac

morphogenesis and rhythm in embryonic zebrafish hearts. Proc Natl Acad Sci. 102: 17705-17710.

Ehler E, Rothen BM, Hammerle SP, Komiyama M, Perriard JC. 1999. Myofibrillogenesis in the developing chicken heart: assembly of Z-disk, M-line and the thick filaments. J Cell Sci. 112:1529-1539.

Esengil H, Chang V, Mich JK, Chen JK. 2007. Small-molecule regulation of zebrafish gene expression. Nat Chem Biol. 3 154-155.

Forouhar AS, Liebling M, Hickerson A, Nasiraei-Moghaddam A, Tsai HJ, Hove JR, Fraser SE, Dickinson ME, Gharib M. 2006. The embryonic vertebrate heart tube is a dynamic suction pump. Science. 312:751-753.

Gao D, Li Z, Murphy T, Sauerbier W. 1997. Structure and transcription of the gene for translation elongation factor 1 subunit alpha of zebrafish (*Danio rerio).* Biochim Biophys Acta. 1350:1-5.

Garavito-Aguilar ZV, Riley HE, Yelon D. 2010. Hand2 ensures an appropriate environment for cardiac fusion by limiting Fibronectin function. Development. 137:3215–3220.

Garg V, Kathiriya1 IS, Barnes R, Schluterman MK, King IN, Butler CA, Rothrock CR, Eapen RS, Hirayama-Yamada K, Joo K, Matsuoka R, Cohen JC, Srivastava D. 2003. GATA4 mutations cause human congenital heart defects and reveal an interaction with TBX5. Nature. 424:443-447.

Garrity DM, Childs S, Fishman MC. 2002. The heartstrings mutation in zebrafish causes heart/fin Tbx5 deficiency syndrome. Dev. 129(19):4635-45.

Georges R, Nemer G, Morin M, Lefebvre C, Nemer M. 2008. Distinct Expression and Function of Alternatively Spliced Tbx5 Isoforms in Cell Growth and Differentiation. Molec Cell Biol. 28:4052–4067.

Ghosh TK, Song FF, Packham EA, Buxton S, Robinson TE, Ronksley J, Self T, Bonser AJ, Brook JD. 2009. Physical Interaction between TBX5 and MEF2C Is Required for Early Heart Development. Mol Cell Biol. 29:2205-2218.

Gibert Y, Gajewski A, Meyer A, Begemann G. 2006. Induction and prepatterning of the zebrafish pectoral fin bud requires axial retinoic acid signaling. Devel. 133: 2649-2659.

Goetz SC, Brown DD, Conlon FL. 2006. TBX5 is required for embryonic cardiac cell cycle progression. Devel. 133:2575-2584.

Govoni KE, Linares GR, Chen ST, Pourteymoor S, Mohan S. 2009. T-box 3 negatively regulates osteoblast differentiation by inhibiting expression of osterix and runx2. J Cell Biochem. 106:482-90.

Grandel H, Schulte-Merker S. 1998. The development of the paired fins in the zebrafish (*Danio rerio*). Mech Dev. 79:99-120.

Greulich F, Rudat C, Kispert A. 2011. Mechanisms of T-box gene function in the developing heart. Cardiovasc Res. 91:212-222.

Habets PE, Moorman AF, Clout DE, van Roon MA, Lingbeek M, van Lohuizen M, Campione M, Christoffels VM. 2002. Cooperative action of Tbx2 and Nkx2.5 inhibits ANF expression in the atrioventricular canal: implications for cardiac chamber formation. Genes Dev. 16:1234-1246.

Hami D, Grimes AC, Tsai HJ, Kirby ML. 2011. Zebrafish cardiac development requires a conserved secondary heart field. Devel. 138:2389-2398.

Harvey W. 1889. On the Motion of the Heart and Blood in Animals. London: George Bell and Sons.

Hasson P, Del Buono J, Logan MPO. 2007. Tbx5 is dispensable for forelimb outgrowth. Devel. 134:85-92.

Hatcher CJ, Goldstein MM, Mah CS, Delia CS, Basson CT. 2000. Identification and localization of TBX5 transcription factor during human cardiac morphogenesis. Dev Dyn. 219:90-95.

Hatcher CJ, Basson CT. 2001. Getting the T-box dose right. Nat. 7:1185-1186.

Hatcher CJ, Kim MS, Mah CS, Goldstein MM, Wong B, Mikawa T, Basson CT. 2001. TBX5 Transcription Factor Regulates Cell Proliferation during Cardiogenesis. Dev Biol. 230:177-188.

Hatcher CJ, Diman NYSG, Kim MS, Pennisi D, Song Y, Goldstein MM, Mikawa T, Basson CT. 2004. A role for Tbx5 in proepicardial cell migration during cardiogenesis. Physiol Genomics. 18:129-140.

He M, Wen L, Campbell CE, Wu JY, Rao Y. 1999. Transcription repression by *Xenopus* ET and its human ortholog TBX3, a gene involved in ulnar-mammary syndrome. Proc Natl Acad Sci. 96:10212-10217.

Heinritz W, Shou L, Moschik A, Froster UG. 2005. The human TBX5 gene mutation database. Hum Mutat. 26:397.

Hentze MW, Kulozik AE. 1999. A Perfect Message: RNA Surveillance and Nonsense-Mediated Decay. Cell. 96:307-310.

Herrmann BG, Kispert A. 1994. The T-genes in embryogenesis. Trends Genet. 10:280-286.

Herrmann F, Bundschu K, Kühl SJ, Kühl M. 2011. Tbx5 overexpression favors a first heart field lineage in murine embryonic stem cells and in *Xenopus laevis* embryos. Dev Dyn. 240:2634-45.

Hiroi Y, Kudoh S, Monzen K, Ikeda Y, Yazaki Y, Nagai R, Komuro I. 2001. Tbx5 Associates with Nkx2-5 and Synergistically Promotes Cardiomyocyte Differentiation. Nat Genet. 28:276-280.

Ho RK, Kane DA. 1990. Cell-autonomous action of zebrafish spt-1 mutation in specific mesodermal precursors. Nature 348: 728–730.

Hoffman L, Miles J, Avaron F, Laforest L, Akimenko MA. 2002. Exogenous retinoic acid induces a stage- specific, transient and progressive extension of Sonic hedgehog expression across the pectoral fin bud of Zebrafish. Int J Dev Biol. 46: 949-956.

Holland PWH, Koschorz B, Holland LZ, Herrmann BG. 1995.Conservation of Brachyury (T) genes in amphioxus and vertebrates: developmental and evolutionary implications. Development. 121:4283-4291.

Hoogaars WMH, Barnett P, Moorman AFM, Christoffels VM. 2007. T-box factors determine cardiac design. Cell Mol Life Sci. 64:646-660.

Horb ME, Thomsen GH. 1999. *Tbx5* is essential for heart development. Dev. 126:1739-1751.

Hove JR, Köster RW, Forouhar AS, Acevedo-Bolton G, Fraser SE, Gharib M. 2003. Intracardiac fluid forces are an essential epigenetic factor for embryonic cardiogenesis. Nature. 421:172-7.

Huang CJ, Tu CT, Hsiao CD, Hsieh FJ, Tsai HJ. 2003. Germ-line transmission of a myocardium-specific GFP transgene reveals critical regulatory elements in the cardiac myosin light chain 2 promoter of zebrafish. Dev Dyn. 228:30-40.

Huang W, Zhang R, Xu X. 2010. Myofibrillogenesis in the developing zebrafish heart: A functional study of tnnt2. Dev Biol. 331:237-249.

Hurley IA, Mueller RL, Dunn KA, Schmidt EJ, Friedman M, Ho RK, Prince VE, Yang Z, Thomas MG, Coates MI. 2007. A new time-scale for ray-finned fish evolution. Proc Biol Sci. 274:489-98.

Ieda M, Fu JD, Delgado-Olguin P, Vedantham V, Hayashi Y, Bruneau BG, Srivastava D. 2010. Direct Reprogramming of Fibroblasts into Functional Cardiomyocytes by Defined Factors. Cell. 142:375-386.

Isogai S, Horiguchi M, Weinstein BM. 2001. The vascular anatomy of the developing zebrafish: an atlas of embryonic and early larval development. Dev Biol. 230:278-301.

Jacobs JJ, Keblusek P, Robanus-Maandag E, Kristel P, Lingbeek M, Nederlof PM, van Welsem T, van de Vijver MJ, Koh EY, Daley GQ, van Lohuizen M. 2000. Senescence bypass screen identifies TBX2, which represses Cdkn2a (p19(ARF)) and is amplified in a subset of human breast cancers. Nat Genet. 26:291-299.

Jacquier A, Dujon B. 1985. An intron-encoded protein is active in a gene conversion process that spreads an intron into a mitochondrial gene. Cell. 41:383–394.

Jaillon O, Aury JM; Brunet F, Petit JL, Stange-Thomann N, Mauceli E, Bouneau L, Fischer C, Ozouf-Costaz C, Bernot A, Nicaud S, Jaffe D, Fisher S, Lutfalla G, Dossat C, Segurens B, Dasilva C, Salanoubat M, Levy M, Boudet N, Castellano S, Anthouard V, Jubin C, Castelli V, Katinka M, Vacherie B, Biémont C, Skalli Z, Cattolico L, Poulain J, De Berardinis V, Cruaud C, Duprat S, Brottier P, Coutanceau JP, Gouzy J, Parra G, Lardier G, Chapple C, McKernan KJ, McEwan P, Bosak S, Kellis M, Volff JN, Guigó R, Zody MC, Mesirov J, Lindblad-Toh K, Birren B, Nusbaum C, Kahn D, Robinson-Rechavi M, Laudet V, Schachter V, Quétier F, Saurin W, Scarpelli C, Wincker P, Lander ES, Weissenbach J, Roest Crollius H. 2004. Genome duplication in the teleost fish *Tetraodon nigroviridis* reveals the early vertebrate proto-karyotype. Nature. 431:946-957.

Jerome LA, Papaioannou VE. 2001. DiGeorge syndrome phenotype in mice mutant for the T-box gene, Tbx1. Nat Genet. 27:286-291.

Jiao K, Kulessa H, Tompkins K, Zhou Y, Batts L, Baldwin HS, Hogan BLM. 2003. An essential role of Bmp4 in the atrioventricular septation of the mouse heart. Gen Devel. 17:2362-2367.

Kilic N, Feldhaus S, Kilic E, Tennstedt P, Wicklein D, Wasielewski R, Viebahn C, Kreipe H, Schumacher U. 2011. Brachyury expression predicts poor prognosis at early stages of colorectal cancer. Eur J Cancer. 47:1080-5.

Kimmel CB. 1989. Genetics and early development of zebrafish. Trend Gen. 5:283–288.

Kimmel CB, Warga RM, Schilling TF. 1990. Origin and organization of the zebrafish fate map. Devel. 108:581–594.

Kimmel CB, Ballard WW, Kimmel SR, Ullmann B, Schilling TF. 1995. Stages of embryonic development of the zebrafish. Devel Dyn. 203:253–310.

Kirk EP, Sunde M, Costa MW, Rankin SA, Wolstein O, Castro ML, Butler TL, Hyun C, Guo G, Otway R, Mackay JP, Waddell LB, Cole AD, Hayward C, Keogh A, Macdonald P, Griffiths L, Fatkin D, Sholler GF, Zorn AM, Feneley MP, Winlaw DS, Harvey RP. 2007. Mutations in cardiac T-box factor gene TBX20 are associated with diverse cardiac pathologies, including defects of septation and valvulogenesis and cardiomyopathy. Am J Hum Genet. 81:280-91.

Kispert A, Herrmann BG. 1993. The Brachyury Gene Encodes a Novel DNA-Binding Protein. EMBO J. 12:3211-3220.

Kispert A, Koschorz B, Herrmann BG. 1995. The T-Protein Encoded by Brachyury is a tissue-specific transcription factor. EMBO J. 14:4763-4772.

Kochanek KD, Murphy SL, Anderson RN, Scott C. 2004. Deaths: Final Data for 2002. Natl Vital Stat Rept. 53(5):1-115.

Kopp R, Schwerte T, Pelster B. 2005. Cardiac performance in the zebrafish breakdance mutant. J Exptl Biol. 208:2123-2134.

Koshiba-Takeuchi K, Takeuchi JK, Arruda EP, Kathiriya IS, Mo R, *et al.* 2006. Cooperative and antagonistic interactions between Sall4 and Tbx5 pattern the mouse limb and heart. Nat Genet 38: 175–183.

Lagendijk AK, Goumans MJ, Burkhard SB, Bakkers J. 2011. MicroRNA-23 restricts cardiac valve formation by inhibiting Has2 and extracellular hyaluronic acid production. Circ Res. 109:649-57.

Larkin MA, Blackshields G, Brown NP, Chenna R, McGettigan PA, McWilliam H, Valentin F, Wallace IM, Wilm A, Lopez R, Thompson JD, Gibson TJ, Higgins DG. 2007.Bioinformatics. 23: 2947-2948.

Latacha KS, Remond MC, Ramasubramanian A, Chen AY, Elson EL, Taber LA. 2005. Role of actin polymerization in bending of the early heart tube. Dev Dyn. 233:1272-1286.

Lazic S, Scott I. 2011. Mef2cb regulates late myocardial cell addition from a second heart field-like population of progenitors in zebrafish. Devel Biol. 356:172-172.

Le Hir H, Izaurralde E, Maquat LE, Moore MJ. 2000. The spliceosome deposits multiple proteins 20-24 nucleotides upstream of mRNA exon–exon junctions. EMBO J. 19:6860-6869.

Lee JS, a von der Hardt S, Rusch MA, Stringer SE, Stickney HL, Talbot WS, Geisler R, Nüsslein-Volhard C, Selleck S, Chien CB, Roehl H. 2004. Axon Sorting in the Optic Tract Requires HSPG Synthesis by *ext2* (*dackel*) and *extl3* (*boxer*). J. Neuron. 44: 947-960.

Li QY, Newbury-Ecob RA, Terrett JA, Wilson DI, Curtis AR, Yi CH, Geburh T, Bullen PJ, Robson SC, Strachan T. 1997. Holt-Oram Syndrome is caused by mutations in TBX5, a member of the Brachyury (T) gene family. Nat Genet. 15:21-29.

Liberatore CM, Searcy-Schrick RD, Yutzey KE. 2000. Ventricular expression of tbx5 inhibits normal heart chamber development. Dev Biol. 223(1):169-80.

Lindsay EA, Vitelli F, Su H, Morishima M, Huynh T, Pramparo T, Jurecic V, Ogunrinu G, Sutherland HF, Scambler PJ, Bradley A, Baldini A. 2001. Tbx1 haploinsufficiency in the DiGeorge syndrome region causes aortic arch defects in mice. Nature. 410:97-101.

Liu J, Stainier DY. 2010. Tbx5 and Bmp signaling are essential for proepicardium specification in zebrafish. Circ Res. 106:1818-28.

Lu JH, Lu JK, Choo SL, Li Y-C, Yeh HW, Shiue JF, Yeh VC. 2008. Cascade effect of cardiac myogenesis gene expression during cardiac looping in tbx5 knockdown zebrafish embryos. J Biomed Sci. 15:779–787.

Lyons GE. 1996. Vertebrate heart development. Curr Opin Genet Dev. 6:454-460.

Mably JD, Mohideen M-APK, Burn CG, Chen JN, Fishman MC. 2003. *heart of glass* regulates the concentric growth of the heart in zebrafish. Curr Biol. 13:2138-2147.

Manasek FJ, Burnside MB, Waterman RE. 1972. Myocardial cell shape change as a mechanism of embryonic heart looping. Dev Biol. 29:349-371.

Mandel EM, Kaltenbrun E, Callis TE, Zen XXI, Marques SR, Yelon D, Wang DZ, Conlon FL. 2010. The BMP pathway acts to directly regulate *Tbx20* in the developing heart. Devel. 137:1919-1929.

Marcellini S, Technau U, Smith JC, Lemaire P. 2002. Evolution of Brachyury proteins: identification of a novel regulatory domain conserved within Bilateria. Devel Biol. 260:352-361.

Marques SR, Lee Y, Poss KD, Yelon D. 2008. Reiterative roles for FGF signaling in the establishment of size and proportion of the zebrafish heart. Dev Biol. 321:397–406.

Marques SR, Yelon D. 2009. Differential requirement for BMP signaling in atrial and ventricular lineages establishes cardiac chamber proportionality. Dev Biol.327:83-96.

Matsumoto K, Shionyu M, Go M, Shimizu K, Shinomura T, Kimata K, Watanabe H. 2003. Distinct interaction of versican/PG-M with hyaluronan and link protein. J Biol Chem. 278:41205-12.

Mayden RL, Tang KL, Conway KW, Freyhof J, Chamberlain S, Haskins M, Schneider L, Sudkamp M, Wood RM, Agnew M, Bufalino A, Sulaiman Z, Miya M, Saitoh, K, He S. 2007. Phylogenetic relationships of *Danio* within the order Cypriniformes: a framework for comparative and evolutionary studies of a model species. J. Exp. Zool. (Mol. Dev. Evol.) 308B: 642–654.

Meilhac SM, Esner M, Kerszberg M, Moss JE, Buckingham ME. 2004. Oriented clonal cell growth in the developing mouse myocardium underlies cardiac morphogenesis. J Cell Biol. 164:97-109.

Merscher S, Funke B, Epstein JA, Heyer J, Puech A, Lu MM, Xavier RJ, Demay MB, Russell RG, Factor S, Tokooya K, Jore BS, Lopez M, Pandita RK, Lia M, Carrion D, Xu H, Schorle H, Kobler JB, Scambler P, Wynshaw-Boris A, Skoultchi AI, Morrow BE, Kucherlapati R. 2001. TBX1 is responsible for cardiovascular defects in velo-cardio-facial/DiGeorge syndrome. Cell. 104:619-629.

Merzlyak EM, Goedhart J, Shcherbo D, Bulina ME, Shcheglov AS, Fradkov AF, Gaintzeva A, Lukyanov KA, Lukyanov S, Gadella TW, Chudakov DM. 2007. Bright monomeric red fluorescent protein with an extended fluorescence lifetime. Nat Methods. 4(7):555-557.

Mesbah K, Harrelson Z, Théveniau-Ruissy M, Papaioannou VE, Kelly RG. 2008. Tbx3 is required for outflow tract development. Circ Res. 103:743-50.

Milan DJ, Macrae CA. 2008. Zebrafish genetic models for arrhythmia. Prog Biophys Mol Biol. 98:301-308.

Minguillon C, Del Buono J, Logan MP. 2005. Tbx5 and Tbx4 Are Not Sufficient to Determine Limb-Specific Morphologies but Have Common Roles in Initiating Limb Outgrowth. Devel Cell. 8:75–84.

Mizuno Y, Thompson TG, Guyon JR, Lidov HG, Brosius M, Imamura M, Ozawa E, Watkins SC, Kunkel LM. 2001. Desmuslin, an intermediate filament protein that interacts with alpha-dystrobrevin and desmin. Proc. Natl Acad. Sci. 98:6156–6161.

Mommersteeg MT, Dominguez JN, Wiese C, Norden J, de Gier-de Vries C, Burch JB, *et al.* 2010. The sinus venosus progenitors separate and diversify from the first and second heart fields early in development. Cardiovasc Res. 87:92-101.

Moorman AFM, Christoffels VM. 2003. Development of the cardiac conduction system: amatter of chamber development.Wiley, Chichester. p. 25-43.

Moorman A, Webb S, Brown NA, Lamers W, Anderson RH. 2003. Development of the heart: (1) formation of the cardiac chambers and arterial trunks. Heart. 89:806-814.

Mori AD, Bruneau BG. 2004. TBX5 mutations and congenital heart disease: Holt-Oram syndrome revealed. Curr Opin Cardiol. 19:211-215.

Mori AD, Zhu Y, Vahora I, Nieman B, Koshiba-Takeuchi K, Davidson L, Pizard A, Seidman JG, Seidman CE, Chen XJ, Henkelman RM, Bruneau BG. 2006. Tbx5-dependent rheostatic control of cardiac gene expression and morphogenesis. Dev Biol. 297:566-86.

Muller CW, Herrmann BG. 1997. Crystallographic structure of the T domain DNA complex of the Brachyury transcription factor. Nature. 389:884-888.

Naiche LA, Harrelson Z, Kelly RG, Papaioannou VE. 2005. T-box genes in vertebrate development. Annu Rev Genet. 39:219-239.

Neumann CJ, Grandel H, Gaffield W, Schulte-Merker S, Nusslein-Volhard C. 1999. Transient establishment of anteroposterior polarity in the zebrafish pectoral fin bud in the absence of sonic hedgehog activity. Development. 126:4817-4826.

Newbury-Ecob RA, Leanage R, Raeburn JA, Young ID. 1996. Holt–Oram syndrome: A clinical genetic study. J Med Genet. 33:300–307.

Ng JK, Kawakami Y, Büscher D, Raya Á, Itoh T, Koth CM, Rodríguez-Esteban C, Rodríguez-León J, Garrity DM, Fishman MC, Izpisúa-Belmonte JC. 2002. The limb identity gene Tbx5 promotes limb initiation by interacting with Wnt2b and Fgf10. Devel. 129:5161-5170.

Nguyen PV. 2001. Zebrafish neurophysiology: ‘swimming’ in sync with gap junctions. Trends Neurosci. 24:633-634.

Niederreither K, Vermot J, Messaddeq N, Schuhbaur B, Chambon P, Dollé P. 2001. Embryonic retinoic acid synthesis is essential for heart morphogenesis in the mouse. Dev.128(7):1019-31.

Noorman M, van der Heyden MAG, van Veen TAB, Cox M, Hauer RNW, de Bakker JMT, van Rijen HVM. 2009. Cardiac cell-cell junctions in health and disease: Electrical versus mechanical coupling. J Mol Cell Cardiol. 47:23-31.

Nusselein-Volhard C, Dahm R. 2002. *Zebrafish: a Practical Approach*. Oxford University Press, New York, NY.

Offield MF, Hirsch N, Grainger RM. 2000. The development of *Xenopus tropicalis* transgenic lines and their use in studying lens developmental timing in living embryos. Development. 127:1789–1797.

Olson EN. 2006. Gene regulatory networks in the evolution and development of the heart. Science. 313:1922-1927.

Ono S. 2010. Dynamic regulation of sarcomeric actin filaments in striated muscle. Cytoskeleton. 67:677-692.

Papaioannou VE. 2001. T-box genes in development: From hydra to humans. Int Rev Cytol. 207:1–70.

Palstra AP, Tudorache C, Rovira M, Brittijn SA, Burgerhout E, van den Thillart GE, Spaink HP, Planas JV. 2010. Establishing zebrafish as a novel exercise model: swimming economy, swimming-enhanced growth and muscle growth marker gene expression. PLoS One. 5:e14483.

Parrie LE, Renfrew EM, Neavin DR, De Miranda MA, Scott IC, Garrity DM. Zebrafish Tbx5a is dispensable in the heart for cell normal cardiomyocyte number but required for cardiomyocyte growth. Submitted to Int J Dev Biol. Jan 2012.

Patra C, Diehl F, Ferrazzi F, van Amerongen MJ, Novoyatleva T, Schaefer L, Mühlfeld C, Jungblut B, Engel FB. 2011. Nephronectin regulates atrioventricular canal differentiation via Bmp4-Has2 signaling in zebrafish.

Pavlidis M, Sundvik M, Chen YC, Panula P. 2011. Adaptive changes in zebrafish brain in dominant-subordinate behavioral context. Behav Brain Res. Epub.

Piacentini G, Digilio MC, Sarkozy A, Placidi S, Dallapiccola B, Marino B. 2007. Genetics of congenital heart diseases in syndromic and non-syndromic patients: new advances and clinical implications. J Cardiovasc Med. 8:7-11.

Pizard A, Burgon PG, Paul DL, Bruneau BG, Seidman CE, Seidman JG. 2005. Connexin 40, a target of transcription factor Tbx5, patterns wrist, digits, and sternum. Mol Cell Biol. 25:5073-5083.

Postma AV, van de Meerakker JBA, Mathijssen IB, Barnett P, Christoffels VM, Ilgun A, Lam J, Wilde AAM, Lekanne Deprez RH, Moorman AFM. 2008. A Gain-of-Function TBX5 Mutation Is Associated With Atypical Holt–Oram Syndrome and Paroxysmal Atrial Fibrillation. Circ Res. 102:1433-1442.

Prall OWJ, Menon MK, Solloway MJ, Watanabe Y, Zaffran S, Bajolle F, Biben C, McBride JJ, Robertson BR, Chaulet H, Stennar FA, Wise N, Schaft D, Wolstein O, Furtado MB, Shiratori H, Chien KR, Hamada H, Black BL, Saga Y, Robertson EJ, Buckingham ME, Harvey RP. 2007. An Nkx2-5/Bmp2/Smad1 negative feedback loop controls heart progenitor specification and proliferation. Cell. 128:947-959.

Puskaric S, Schmitteckert S, Mori AD, Glaser A, Schneider KU, Bruneau BG, Blaschke RJ, Steinbeisser H, Rappold G. 2010. Shox2 mediates Tbx5 activity by regulating Bmp4 in the pacemaker region of the developing heart. Hum Mol Genet. 19:4623-4633.

Qu XH, Jia HB, Garrity DM, Tompkins K, Batts L, Appel B, Zhong TP, Baldwin HS. 2008. *ndrg4* is required for normal myocyte proliferation during early cardiac development in zebrafish. Dev Biol. 317:486-496.

Rallis C, Bruneau BG, Del Buono J, Seidman CE, Seidman JG, Nissim S, Tabin CJ, Logan MP. 2003. Tbx5 is required for forelimb bud formation and continued outgrowth. Development. 130:2741-51.

Reiter JF, Alexander J, Rodaway A, Yelon D, Patient R, Holder N, Stainier DYR. 1999. Gata5 is required for the development of the heart and endoderm in zebrafish. Gene Devel. 13:2983-2995.

Reiter JF, Verdake H, Stainier DYR. 2001. Bmp2b and Oep promote early myocardial differentiation through their regulation of *gata5*. Dev Biol. 234:330-338.

Rutenberg JB, Fischer A, Jia H, Gessler M, Zhong TP, Mercola M. 2006. Developmental patterning of the cardiac atrioventricular canal by Notch and Hairy-related transcription factors. Development. 133:4381-4390 .

Ruvinsky I, Oates AC, Silver LM, Ho RK. 2000. The evolution of paired appendages in vertebrates: T-box genes in the zebrafish. Dev Genes Evol. 210:82-91.

Ryan MD, King AM, Thomas GP. 1991. Cleavage of foot-and-mouth disease virus polyprotein is mediated by residues located within a 19 amino acid sequence. J Gen Virol. 72: 2727–2732.

Saka Y, Smith JC. 2001. Spatial and Temporal Patterns of Cell Division during Early *Xenopus* Embryogenesis. Dev Biol. 229:307-318.

Sakata Y, Kamei CN, Nakagami H, Bronson R, Liao JK, Chin MT. 2002. Ventricular septal defect and cardiomyopathy in mice lacking the transcription factor CHF1_Hey2. Proc Natl Acad Sci. 99:16197–16202.

Samarel AM. 2005. Costameres, focal adhesions, and cardiomyocyte mechanotransduction. Am J Physiol – Heart Cir Physiol. 289:H2291-2301.

Schott J, Benson D, Basson C, Pease W, Silberbach G, Moak J, Maron B, Seidman C, Seidman J. 1998. Congenital heart disease caused by mutations in the transcription factor NKX2–5. Science. 281:108–111.

Sedletcaia A, Evans T. 2011.Tissue Regeneration After Injury in Adult Zebrafish: The Regenerative Potential of the Caudal Fin. Dev Dyn. 240:1271-1277.

Seidman JG, Seidman C.2002. Transcription factor haploinsufficiency: when half a loaf is not enough. J. Clin Invest. 109:451–455.

Serluca FC. 2008. Development of the proepicardial organ in the zebrafish. Dev Biol. 315:18-27.

Shao JP, Chen DY, Ye QJ, Cui JL, Li YH, Li L.2011. Tissue regeneration after injury in adult zebrafish: the regenerative potential of the caudal fin. Dev Dyn. 217:401-414.

Shirai M, Imanaka-Yoshida K, Schneider MD, Schwartz RJ, Morisaki T. 2009. T-box 2, a mediator of Bmp-Smad signaling, induced hyaluronan synthase 2 and Tgfbeta2 expression and endocardial cushion formation. Proc Natl Acad Sci. 106:18604-18609.

Showell C, Binder O, Conlon FL. 2004. T-box genes in early embryogenesis. Dev. Dyn. 229:201-218.

Simon H. 1999. T-box genes and the formation of vertebrate forelimb- and hind-limb specific pattern. Cell Tissue Res. 296:57-66.

Singh MK, Christoffels VM, Dias JM, Trowe MO, Petry M, Schuster-Gossler K, *et al.* 2005. Tbx20 is essential for cardiac chamber differentiation and repression of Tbx2. Development.132:2697-2707.

Sirbu IO, Zhao XL, Duester G. 2008. Retinoic acid controls heart anteroposterior patterning by down-regulating Isl1 through the Fgf8 pathway. Dev Dyn. 237:1627-1635.

Smith J. 1997. Brachyury and the T-box genes. Curr Opin Genet Dev. 7:474–480.

Smith J. T-box genes: what they do and how they do it. Trend Genet. 15:154-158.

Soufan AT, Van Den Berg G, Ruijter JM, De Boer PAJ, Van Den Hoff MJB, Moorman AFM. 2006. Regionalized sequence of myocardial cell growth and proliferation characterizes early chamber formation. Circul Res. 99:545-552.

Spence R., Fatema MK., Ellis S, Ahmed ZF, Smith C. 2007. The diet, growth and recruitment of wild zebrafish (*Danio rerio*) in Bangladesh. J Fish Biol. 71:304–309.

Spence R, Gerlach G, Lawrence C, Carl Smith C. 2008. The behaviour and ecology of the zebrafish, *Danio rerio*. Biol. Rev. 83:13–34.

Stainier DYR, Fishman MC. 1992. Patterning the zebrafish heart tube: Acquisition of anteroposterior polarity. Dev Biol. 153:91-101.

Stainier DYR, Lee RK, Fishman MC.1993. Cardiovascular development in the zebrafish I. Myocardial fate map and heart tube formation. Dev. 119:31-40.

Stainier DYR. 2001. Zebrafish genetics and vertebrate heart formation. Nat Rev Gen. 2:39-48.

Strausberg RL, Feingold EA, Grouse LH, Derge JG, Mammalian Gene Collection Program Team, *et al*. 2002. Generation and initial analysis of more than 15,000 full-length human and mouse cDNA sequences. Proc Natl Acad Sci USA. 99:16899-16903.

Streisinger G, Walker C, Dower N, Knauber D, Singer F. 1981. Production of clones of homozygous diploid zebra fish (Brachydanio rerio). Nature. 291:293–296.

Stennard FA, Harvey RP. 2005. T-box transcription factors and their roles in regulatory hierarchies in the developing heart. Dev. 132:4897-4910.

Stennard F, Zorn AM, Ryan K, Garrett N, Gurdon JB. 1999. Differential expression of VegT and Antipodean protein isoforms in *Xenopus*. Mech Dev, 86:87-98.

Strausberg RL, Feingold EA, Grouse LH, Derge JG, Mammalian Gene Collection Program Team, *et al*. 2002. Generation and initial analysis of more than 15,000 full-length human and mouse cDNA sequences. Proc Natl Acad Sci USA. 99:16899-16903.

Su TT, Sprenger F, DiGregorio PJ, Campbell SD, O'Farrell PF. 1998. Exit from mitosis in Drosophila syncytial embryos requires proteolysis and cyclin degradation, and is associated with localized dephosphorylation. Genes Dev. 12:1495-1503.

Sultana N, Nag K, Hoshijima K, Lair DW, Kawakami A, Hirose S. 2008. Zebrafish early cardiac connexin, Cx36.7/Ecx, regulates myofibril orientation and heart morphogenesis by establishing Nkx2.5 expression. PNAS. 105:4763-4768.

Sun G, Lewis LE, Huang X, Nguyen Q, Price C, Huang C. 2004. *TBX5*, a gene mutated in Holt–Oram syndrome, is regulated through a GC box and T-box binding elements (TBEs). J Cell Biochem. 92:189-199.

Suzuki H, Yamashiro K, Takeda H, Nojima T, Usui M. 2011.Extra-axial soft tissue chordoma of wrist. Pathol Res Pract. 207:327-31.

Taber LA. 2006. Biophysical mechanisms of cardiac looping. Int J Dev Biol. 50:323-332.

Taguchi K, Ishiuchi T, Takeichi M. 2011. Mechanosensitive EPLIN-dependent remodeling of adherens junctions regulates epithelial reshaping. J Cell Biol. 194:643-656.

Takeuchi JK, Bruneau BG. 2009. Directed transdifferentiation of mouse mesoderm to heart tissue by defined factors. Nature. 459:708-U112.

Tamai S-I, Sanada K, Fukada Y. 2008. Time-of-Day-Dependent Enhancement of Adult Neurogenesis in the Hippocampus. PLoS ONE 3,12: e3835.

Tamura K, Yonei-Tamura S, Belmonte JC. 1999. Differential expression of Tbx4 and Tbx5 in zebrafish fin buds. Mech Dev. 87:181-184.

Taylor JS, Van de Peer Y, Braasch I, Meyer A. 2001. Comparative genomics provides evidence for an ancient genome duplication event in fish. Philos Trans R Soc. 356:1661-1679.

Technau U, Bode HR. 1999. HyBra1, a Brachyury homologue, acts during head formation in Hydra. Development. 126:999-1010.

Thermes V, Clemens G, Ristoratore F, Bourrat F, Choulika A, Wittbrodt J, Joly J. 2002. I-SceI meganuclease mediates highly efficient transgenesis in fish. Mech Devel. 118: 91-98.

Thisse, C., Thisse, B., Schilling, T. F. and Postlethwait, J. H. 1993. Structure of the zebrafish snail1 gene and its expression in wild-type, spadetail and no tail mutant embryos. Dev. 119: 1203-1215.

Thisse C, Zon LI. 2002. Organogenesis – Heart and Blood Formation from the Zebrafish Point of View. Science. 295: 457-462.

Thomas NA, Koudijs M, van Eeden FJ, Joyner AL, Yelon D. 2008. Hedgehog signaling plays a cell-autonomous role in maximizing cardiac developmental potential, Devel. 135:3789–3799.

Tokuyasu KT, Maher PA. 1987. Immunocytochemical studies of cardiac myofibrillogenesis in early chick embryos. I. Presence of immunofluorescent titin spots in premyofibril stages. J. Cell Biol. 105:2781-2793.

Trichas G, Begbie J, Srinivas S. 2008. Use of the viral 2A peptide for bicistronic expression in transgenic mice. BMC Biol. 6:40-53.

Trinh LA, Stainier DY. 2004. Fibronectin regulates epithelial organization during myocardial migration in zebrafish. Dev Cell. 6:371–382.

Trinh LA, Yelon D, Stainier DY. 2005. Hand2 regulates epithelial formation during myocardial differentiation. Curr Biol. 15:441–446.

Udvadia AJ, Linney E. 2002. Windows into development: historic, current, and future perspectives on transgenic zebrafish. Dev Biol. 256:1-17.

van Noort V, Snel B, Huynen MA. 2003. Predicting gene function by conserved co-expression. Trends Genet. 19:238-42.

van Wijk B, Moorman AFM, van den Hoff MJB. 2007. Role of bone mophogenetic proteins in cardiac differentiation. Cardiovas Res. 74:244-255.

Vance KW, Carreira S, Brosch G, Goding CR. 2005. Tbx2 is overexpressed and plays an important role in maintaining proliferation and suppression of senescence in melanomas. Cancer Res 65:2260–2268.

Vaughan CJ, Basson CT. 2000. Molecular determinants of atrial and ventricular septal defects and patent ductus arteriosus. Am. J. Med. Genet. 97:304–309.

Walsh EC, Stainier DY. 2001.UDP-glucose dehydrogenase required for cardiac valve formation in zebrafish. Science. 293:1670-1673.

Wang D, Chang PS, Wang Z, Sutherland L, Richardson JA, *et al.* 2001. Activation of cardiac gene expression by myocardin, a transcriptional cofactor for serum response factor. Cell 105: 851–862.

Wang C, Cao D, Wang Q, Wang DZ. 2011. Synergistic Activation of Cardiac Genes by Myocardin and Tbx5. PLoS One. 6:e24242.

Waterhouse AM, Procter JB, Marine DMA, Clamp M, Barton GJ. 2009. Jalview Version 2 – a multiple sequence alignment editor and analysis workbench. Bioinfo. 25:1189-1191.

Wattler S, Russ A, Evans M, Nehls M. 1998. A combined analysis of genomic and primary protein structure defines the phylogenetic relationship of new members of the T-box family. Genomics. 48:24-33.

Weinhold F. 2001. Chemistry. A new twist on molecular shape. Nature. 411: 539–541.

Westerfield M. 1995. The Zebrafish Book, A guide for the laboratory use of zebrafish (*Danio rerio*). 3rd Ed. University of Oregon press.

Wilson V, Conlon F. 2002. The T-box family. Genome Biol. reviews3008.1–reviews3008.7.

Wu YL, Pan X, Mudumana SP, Wang H, Kee PW, Gong Z. 2008. Development of a heat shock inducible gfp transgenic zebrafish line by using the zebrafish hsp27 promoter. Gene. 408(1-2):85-94.

Xu DJ, Bu JW, Gu SY, Xia YM, Du JL, Wang YW. 2011. Celecoxib impairs heart development via inhibiting cyclooxygenase-2 activity in zebrafish embryos. Anesthesiology. 114:391-400.

Yelon D, Horne SA, Stainier DY. 1999. Restricted expression of cardiac myosin genes reveals regulated aspects of heart tube assembly in zebrafish. Dev Biol. 214(1):23-37.

Yelon D. 2001. Cardiac Patterning and Morphogenesis in Zebrafish. Dev Dyn. 222: 552-563.

Yelon D, Weinstein BM, Fishman MC. 2002. Cardiovascular system. Results Probl Cell Differ. 40:298-321.

Yin C, Kikuchi K, Hochgreb T, Poss KD, Stainier DY. 2010. Hand2 regulates extracellular matrix remodeling essential for gut-looping morphogenesis in zebrafish. Dev Cell. 18:973–984.

Yutzey KE, Bader D. 1995. Diversification of cardiomyogenic cell lineages during early heart development. Circ Res. 77:216–219.

Zaffran S, Frasch M. 2002. Early signals in cardiac development. Circul Res. 91:457-469.

Zhang J, Sun X, Qian Y, LaDuca JP, Maquat LE. 1998. At least one intron is required for the nonsense-mediated decay of triosephosphate isomerase mRNA: a possible link between nuclear splicing and cytoplasmic translation. Mol Cell Biol. 18:5272-5283.

Zhong TP, Rosenberg M, Mohideen MA, Weinstein B, Fishman MC. 2000. *gridlock*, an HLH gene required for assembly of the aorta in zebrafish. Science. 287:1820-1824.

Zhou B, Ma Q, Rajagophal S, Wu SM, Domain I, Rivera-Feliciano J, Jiang DW, von Gise A, Ikeda S, Chien KR, Pu WT. 2008. Epicardail progenitors contribute to the cardiomyocyte lineage in the developing heart. Nature. 454:109-U105.

WEB CITATIONS

Fishbase: www.fishbase.org.

Integrated Taxonomic Information System. www.itis.gov. Accessed June 16, 2009

Tol2Kit wiki page: http://chien.neuro.utah.edu/tol2kitwiki/index.php/Main_Page.

rVista TBE location software: http://rvista.dcode.org/

Zebrafish Information Network (ZFIN), The Zebrafish International Resource Center, University of Oregon: http://zfin.org/

APPENDIX I: DETERMINING CRITICAL TBX5 EXPRESSION IN EARLY CARDIAC DEVELOPMENT

Introduction

I hypothesize that for optimal function, the Tbx5 protein must be expressed in a restricted spatial and temporal pattern, and that the amount of Tbx5 expressed within the cell must be within a restricted, optimal range. Two lines of evidence support a requirement for spatial regulation of the Tbx5 protein. First, in several vertebrate species, *tbx5* expression within the heart tube occurs as a gradient, with highest expression at the atrial end of the heart and with lower levels of expression in the ventricular end (Liberatore *et al.*, 2000; Yelon, 2001; Stennard and Harvey, 2005). Second, Liberatore *et al.*, (2000) noted that overexpression of *tbx5* throughout the linear heart tube of chick embryos caused a loss of chamber-specific gene expression and a delay in ventricular chamber morphogenesis. Several lines of evidence suggest that the dose of Tbx5 within the cell is critical. In this context, "dose" refers both to the number of functional copies of an allele present, as well as overexpression by mRNA injection or knock-down by morpholino injection. First, injection of a low tbx5-MO dose (17 ng) into *hst* siblings is sufficient to convert *hst* heterozgyotes to a *hst* cardiac phenotype (Garrity *et al.* 2002). This was also observed by Lu *et al.* (2008), where a partial- to full-knockdown of *tbx5a* using increasing doses of *tbx5a* morpholino resulted in increased severity of cardiac phenotypes. Second,

haploinsufficiency of Tbx5 in both mice and humans results in non-embryonic lethal cardiac defects, while mice homozygous for Tbx5 mutations die at gestation day 10 (E10) due to the severity of the heart defects (Bruneau *et al.* 2001). Furthermore, increased TBX5 dosage, such as chromosome 12q2 duplication, is reported to also result in HOS (Vaughan and Basson, 2000; Hatcher and Basson, 2001). Finally, experiments performed in Chapter IV also demonstrate that zebrafish cardiac development is sensitive to altered *tbx5b* dose.

In contrast to above, the existing evidence in support of the idea that Tbx5 is temporally regulated is not clear, as the following data indicate. First, the onset of *tbx5* expression in the hearts of vertebrates is early and clearly precedes the onset of recognized phenotypes in cardiac morphology. In zebrafish, *tbx5a* expression first occurs in the bilateral cardiac progenitor cells (11 hours post fertilization (hpf)), prior to formation of the heart tube (24-26 hpf) (Camarata *et al.* 2010). However, when assayed prior to heart tube formation, *tbx5a* homozygous mutant embryos showed no difference in expression of several cardiac markers, or in the timing or morphology of heart tube formation (Garrity *et al.* 2002, Parrie *et al.* submitted), suggesting these early events were all normal in zebrafish. Morphological defects in the *tbx5a* mutant *heartstrings (hst)* hearts first appear at mid-cardiogenesis stages (~48 hpf; chamber morphogenesis), and are followed in the subsequent 24 hours by substantial deterioration of cardiac morphology, weakening contractility, and loss of circulation. These data suggest Tbx5a is dispensable for early morphogenic events including cardiac specification and migration of bilateral cardiac precursors to the midline to create the heart tube. However, once the heart tube has

formed, cells undergo differential gene expression that contributes to cell fate and regional differentiation. I hypothesize that the degeneration of *hst* embryos at 48-72 hpf is the consequence of an earlier requirement for *tbx5a* in patterning of the heart tube (24-30 hpf), but that *tbx5a* expression in cardiac precursors prior to heart tube formation is dispensable for survival and normal cardiac morphogenesis.

The aim of this project is to directly test whether *tbx5a* expression in the linear heart tube (but not earlier) is sufficient for normal cardiac development. The zebrafish system offers an excellent opportunity to assay for phenotypes resulting from altered *tbx5a* expression because they develop *ex utero*, in transparent eggs, which facilitate experimental access, especially to the heart, throughout development. In order to study the timing of Tbx5 function, we utilize several powerful genetic tools, including the *tbx5a* mutant *hst*, *tbx5* morpholino knock-down, and new transgenic lines that induce *tbx5a* expression in cardiac tissue. My strategy is to restore expression of wildtype *tbx5a* in *hst* mutant embryos at selected times in cardiac development by inducing a temporally controllable *tbx5a* transgene. Following timed induction of *tbx5a* expression, I will assay whether *tbx5* deficient embryos then develop normally or with *hst* cardiac phenotypes. I will assay cardiac phenotypes by in situ hybridization or morphological assays to investigate cell shape, adhesion, differentiation and proliferation. A number of well-defined markers of cardiac development will help me assess the effects of manipulating *tbx5a* dose. In particular, I will assay several chamber-specific markers, to determine whether uniform high expression of *tbx5a* throughout the heart tube results in a “caudalization” of the rostral (anterior) regions of the heart. The primary strategy for this set of experiments is

to “rescue” (i.e. restore to normal development, in varying degrees) the wildtype phenotype upon induction of *tbx5* expression in transgenic *hst* or *tbx5b* morphant embryos. Previous experiments (see Chapter 4) provide proof in principle that rescue of mutant and morphant phenotypes is possible via injection of wildtype mRNAs. This project therefore extends previous work by defining more precisely the critical expression of *tbx5* required for cardiac development, by examining both dose and timing.

This work will test two hypotheses related to the critical timing and dose of Tbx5 function in the developing heart. First, we will test the hypothesis that Tbx5 activity is required in the linear heart tube (24 -30 hpf) for normal differentiation and morphogenesis, but dispensable at earlier stages (7 -24 hpf) including initial cardiac specification. Second, we will test the hypothesis that the differentiation of cardiomyocytes within the heart tube is responsive to the level (“dose”) of *tbx5* mRNA present within cardiomyocytes. Defining the critical timing for Tbx5 function in the heart is a logical prerequisite to understanding the significance of its cellular functions.

Results / Discussion

This project is divided into three stages: 1) Construction of the transgene cassettes (see Figs. AI.1,3,5,6). 2) Generation of stable transgenic lines (Figs. AI.7,10,11). 3) Execution of the induction experiments on transgenic *hst* mutant embryos of various ages, followed by analysis of heart function and morphology by biochemical and molecular biological techniques. At the time of my defense I have not successfully finished stage 2 (generation

of stable transgenic lines). Therefore, these Results will primarily discuss the troubleshooting involved in this project, briefly touching on future work, assuming we are ultimately able to generate these lines.

Project design:

For this project I have employed three general approaches to create the transgene cassettes for injection into zebrafish embryos (see Fig. AI.8). The first approach was to sub-clone the *tbx5a* coding sequences into a vector containing meganuclease restriction sites (pI-SceIhspMCSpa), which could then be used as a substrate for the *I-SceI meganuclease Method* for generating genomic insertions (Thermes *et al.* 2002), described below. The second approach was to employ the Tol2 Gateway system (Invitrogen), which relies upon DNA recombination to create transgenes and Tol2 transposable elements to generate genomic insertions (Kwan *et al.*, 2007). My third approach was to use a newly created modified Gateway system (termed "vSlick" and "vSlack") developed by Drs Ashok Srinivasan and Ken Kramer, which is currently unpublished. For all three methods, the goal was to create a transgenic construct encompassing the coding regions of wildtype *tbx5* (either *a* or *b*) adjacent to green fluorescent protein (GFP) reporter, and to obtain transgenic fish carrying this construct. Within the construct, inducible expression of *tbx5* would be driven by either 1) the zebrafish heat-shock protein (*hsp70/1*), 2) cardiac-specific (*cmlc2*) regulatory elements, or 3) a cardiac-specific ecdysone responsive Gal4-UAS element.

Integration of the various transgenes would occur when the prepared DNA was co-injected into the one-celled embryo, along with either I-SceI meganuclease or Tol2 transposase mRNA to facilitate integration. The primary method of identifying germ-line transgenic founder adults is by breeding, and visually detecting the fluorescent transgene marker in resulting offspring. Alternatively, I test adult founder fish by screening tail fin genomic DNA by PCR to detect the presence of the transgene in at least some cells (see Fig. AI.2).

The following is a detailed description of each of these methods and the associated results.

Method 1: I-SceI meganuclease

Initially, researchers hoping to generate transgenic fish simply injected the linearized gene of interest into a one-celled embryo and screened these founder fish or their progeny for those with transgene insertion (Culp *et al.* 1991). The drawback of this method is the low frequency of mosaic expression in the injected embryo and the extremely low rate of germ-line transgenesis (<5%). In 2002, a new protocol, using a rare-cutting mega-endonuclease was described for fish (Thermes *et al.* 2002). This endonuclease, called I-SceI, was isolated from the yeast *Saccharomyces cerevisiae* by Jacquier and Dujon (1985). I-SceI has an 18 bp recognition site that statistically is expected to occur only once in 7×10^{10} bp of random sequence. Therefore, this site is not likely to be found in the $7x10^{8}$ bp sized *Danio rerio* genome, and thus is not likely to fraction it if I-SceI is used in transgenic injections. When investigators co-injected plasmids containing meganuclease

recognition sites flanking the gene of interest along with the I-SceI meganuclease they observed an increase in the number of mosaic founder embryos (F0 generation) (76% as compared to 26% without the meganuclease) (Thermes *et al.* 2002). They also reported an efficient rate of stably transfected lines (i.e. the F1 offspring that were germline transgenic) with single copy integrations (approximately 30%).

Therefore, my initial approach was to design a construct consisting of the *tbx5a* gene flanked by I-SceI sites that could be used with the I-SceI meganuclease method. I created two constructs with different promoters driving expression of a *tbx5a*-GFP fusion product. First, to engineer uniform *tbx5a* expression solely within the heart, I selected the cardiac-specific *myl7* promoter (referred to as its previous name "*cardiac myosin light chain 2* (*cml2c*)" for clarity) to drive *tbx5a* expression (Fig. AI.1). This construct is referred to as "pI*cmlc2:tbx5a*-GFP," where pI refers to the plasmid that contains the transgene, and *cmlc2* is the minimal promoter, and *tbx5a-GFP* is the encoded fusion protein. As previously reported, *cmlc2* drives robust expression in cardiac precursors by 18 hpf (Huang *et al.*, 2003, Burns *et al.*, 2005), is expressed throughout the heart tube at 26 hpf, and within the atrial and ventricular myocardium and atrioventricular canal at later stages (Yelon *et al.*, 1999). Thus, the *cmlc2* promoter is suitable for driving high-level whole-heart *tbx5a* expression (i.e. obliterating the normal graded expression of *tbx5a* in the heart), without the potentially confounding effects of ectopically expressing the gene throughout the entire embryo. My second construct was designed to determine the developmental timepoints in which *tbx5a* is required for normal cardiac development. For this construct I utilized the *heat-shock70* (*hsp70*) promoter (Fig. AI.1), in order to

induce expression of *tbx5a*-GFP throughout the embryo by heat-shock at 37° C. This construct is named "pI*hsp70:tbx5a*-GFP." These, and all subsequent constructs, were confirmed by a mixture of restriction digest and sequencing.

To create germ-line transgenic embryos, I co-injected 10ng/ul of either pI*cmlc2:tbx5a*-GFP or pI*hsp70:tbx5a*-GFP plasmid with the I-SceI enzyme (NEB). I screened 260 pI*cmlc2:tbx5a*-GFP (C12 – see lab notebook) and 156 pI*hsp70:tbx5a*-GFP (H4) F0 adult founders by breeding and/or PCR genotyping either the tailfin DNA or offspring. A large number of clutches had 10-50% of embryos perish prior to gastrulation, the same percent of offspring one would expect to see from a stable germ-line founder fish (Anne Handschy, personal communication). Therefore, I extracted DNA from batches of decling embryos from clutches that had previously demonstrated this early lethality immediately after fertilization and used PCR to screen for the transgene (Fig. AI.2). This experiment demonstrated the perfect correlation of declinging embryos with the presence of the transgene. Therefore, these data stongly suggest that the presence of the wildtype *tbx5a* fused with GFP transgene was embryonic-lethal. This lethality is most likely due to problems associated with integration (either location or loss of promoter specificity), since we know that the transgene was present in some F1 offspring. As additional laboratories have attempted to use the I-SceI method, researchers have found that I-SceI meganuclease is extremely unstable and therefore seriously problematic for its intended use in these experiments (Dr. Hazel Sive, Semil Choksi personal communication). In view of these two intractable issues, we decided to abandon this technique in favor of the Tol2 Gateway method for creating transgenic zebrafish.

Method 2: Tol2Gateway (Constructs 1 & 2)

This method involves a series of plasmids that was originally created by Invitrogen and subsequently modified by Koichi Kawakami and Chi-Bin Chien with promoters and reporters suitable for use in the zebrafish (Kwan *et al.* 2007). Components from each of these plasmids (promoters, reporter genes, etc.) can be combined to suit the needs of the researcher. This method uses proprietary recombinase enzymes (Invitrogen) which provide extremely high cloning and transgenesis efficiencies. For detailed information on plasmids, methodology, etc. please see the page maintained by the Chien Lab: http://chien.neuro.utah.edu/tol2kitwiki/index.php/Main_Page.

I generated two constructs for use in the Tol2 Gateway method, which I named *hsp701:tbx5a*-GFP (Gateway construct #1; Figure 5.8) and *cmlc2:tbx5a*-GFP (#2) (Fig.5.3). These constructs were generated using plasmids obtained in the "starter kits" provided by Dr. Chi-Bin Chien and/or Dr. Nathan Lawson or were generously provided by others as noted in text. Plasmid numbers that begin with "c" refer to those from the Chien kit, while the plasmids that begin with "L" originated in the Lawson kit. First, I amplified plasmids containing the *cmlc2* promoter (plasmid "Lister p5E"; generously provided by Dr. James Lister) or the *hsp701* promoter (plasmid c222). I cloned the *tbx5a*-GFP module from Method 1 into the c237 middle entry vector (MEV) using restriction enzymes. Utilizing 2-way multisite LR recombination with the L465 Destination plasmid, I created the final Injection Constructs (Fig. AI.8 constructs 1, 2). In the Tol2Gateway technique, circular plasmid DNA is co-injected with mRNA of the final transposase (synthesized from plasmid c396) that will recombine the cassette of interest into the

zebrafish genome. I therefore injected 75 pg plasmid DNA/embryo (either construct #1 or #2), along with 50 pg transposase mRNA/embryo, rhodamine for determining injection success, and danieaus embryo medium. Use of nuclease-free water results in a high rate of death in injected embryos, thus we use danieaus embryo medium. Injected embryos were raised to adult breeding age and pproximately 100 founders of each injection type were screened for presence of the transgene. Transgenesis was determined by breeding injected fish and screening offspring for the presence GFP.

I observed an approximately 50% death rate in injected (F0) embryos, which resembles that seen by others (Kwan *et al.*, 2007). The high rate of death is most likely due to the trauma incurred when injecting the cell itself, as opposed to the yolk. Transient expression of the *hsp701:tbx5a*-GFP (#1) construct was observed in mosaic-F0 founder fish at a much higher rate (~70%) than observed with the I-SceI meganuclease (~45%) (Fig. AI.4). The Tol2 Gateway method has a reported germline transgenesis rate of 30-50% (Kwan *et al.*, 2007). However, in my hands the germline transgenesis rate was 0% (0 out of the ~200 founders screened). I hypothesize that we did not observe stable germ-line transgenesis due to integration problems, most likely due to the vector L465 backbone. In contrast, the lab has obtained transgenic lines with the c394 Destination vector; therefore, I would recommend this Destination vector in the future.

Around this time, Dr. Ashok Srinivasan and Ken Kramer had begun developing a Gateway-compatible Destination vector termed “vSlick” for use with an ecdysone-dependent (EcR) induction method developed for use in zebrafish by Esengil *et al.*

(2007). This vector offered two substantial improvements over our Gateway constructs, described in detail below. We therefore began a collaboration with these researchers to create *tbx5* fusion constructs using their methodology.

EcR agonist regulation of zebrafish gene expression.

A substantial advantage offered by the EcR Method is the potential for combining cardiac-specific expression with the ability to conditionally induce the construct. Esgengil and colleagues were the first to adapt the arthropod-specific ecdysone receptor (EcR) dependent Gal4 system used in *Arabidopsis* as new tool in an inducible gene expression system for use in zebrafish (Esengil *et al.* 2007). The EcR regulates gene transcription in a small molecule-dependent manner (Esengil *et al.* 2007). One benefit of this inducible system is that vertebrate genomes do not encode an EcR analog, and several EcR agonists including the pesticide Tebufenozide were tested and found to have no apparent abnormal effects on zebrafish development (Esengil *et al.* 2007). Although EcRs normally heterodimerize with retinoid X receptors (RXRs) in the cell, and are therefore dependent on endogenous RXR levels, Esengil *et al.* modified a chimeric transactivator that included a viral activation peptide to generate an RXR-independent expression system.

The overall scheme works as follows (Fig. AI.9): the transactivator construct, known as GVEcR, is comprised of three main components: the yeast transcription activator protein Gal4 (G), the activation domain of the herpes simplex virus regulatory protein VP16 (V), and the ligand-binding domain of the *Bombyx mori* EcR. To obtain tissue-specificity,

tissue-specific promoters are used to drive expression of GVEcR. In this system we use the minimal *myl7* promoter (formerly *cmlc2*). Once translated, the GVEcR transactivator protein is inactive unless EcR agonist is provided. Thus, temporal inducibility is provided by adding EcR agonist to the embryo at the desired time. I used Tebufenozide as the EcR agonist since it is inexpensive and effective in zebrafish (Esengil *et al.* 2007). The Gal4 portion of GVEcR recognizes the Upstream Activation Sequence (10xUAS, because the sequence in our construct includes a 10x tandem repeat), which can be fused to the target gene of choice. Therefore, once GVEcR has been activated by addition of Tebufenozide, transcription of the target construct proceeds and reporter or target protein will be produced. My target construct consisted of the 10xUAS promoter fused to Tbx5a and GFP codons. With this method, described below, the GVEcR and 10xUAS:*tbx5a*-GFP cassettes can be cloned into the same Destination plasmid for use in injections.

Method 3: vSlick/vSlack GVEcR Gateway (Constructs 3 & 4)

The basic approach was based on the Tol2Gateway technology, but now included the vSlick Destination vector provided by Dr. Srinivasan as well as the cardiac-specific GVEcR construct. The benefits of this method were twofold. First, GVEcR allows for exquisite control of our transgene, both spatially *and* temporally, which up to now has not been widely available in the world of zebrafish transgenics. This dual level of control will reduce secondary effects produced by whole-embryo transgene expression. Second, the vSlick (and second generation vSlack) Destination vector contains "insulators" that reduce self-recombination and therefore increases the probability of integration into the zebrafish genome.

This transgenesis scheme required the generation of two transgenes (Figs 5.5, 5.6, 5.8 construct 4). The first was a "Driver" cassette which contains the *myl7*:GVEcR cassette, cloned into a 5' entry vector. The second transgene included *tbx5a*-GFP under the control of a 10xUAS promoter. For this construct I cloned the 10xUAS promoter, *tbx5a*-GFP gene, and bovine growth hormone (BGH) poly-A signal into the pCRII TA cloning vector (Fig. AI.5). It is important to note that during this sub-cloning process, I re-amplified *tbx5a* from wildtype cDNA and that sequencing showed this new sequence to be identical to that published for wildtype *tbx5a*. Next, using primers that contained Gateway BP recombination att sites, I PCR amplified the entire transgene and immediately performed a BP recombination to place this cassette in the 3'EV (plasmid c220). The next step involved simultaneously recombining the GVEcR Driver 5'EV, bi-directional β–globin polyA signal (in a MEV), and the 10xUAS:*tbx5a*-GFP modules in the 3'EV into the vSlick Destination vector. I used the bi-directional poly-A sequence in the MEV to facilitate a 3-way LR recombination into the vSlick destination vector, and to ensure proper expression of the GVEcR gene.

As a backup approach, we simultaneously generated a *tbx5a*-GFP cassette under the control of the *hsp701* promoter, also cloned into vSlick (Fig. AI.8 construct #3). This construct also contained a fluorescent protein under the control of its own promoter as a reporter for transgenesis. Dr. Srinivasan suggested the use of TurboRFP under the control of the *Crystallin* (*Cry)* promoter to drive expression exclusively in the lens of the eye. TurboRFP (tRFP) is a dimeric red/orange fluorescent protein originally isolated from the sea anemone *Entacmaea quadricolor*. It is a short, 231 aa (26.1 kDa) protein that is

excited at 553 nm and emits at 574 nm. TurboRFP has several advantages over DsRed, including reduced maturation time, increased fluorescence intensity, and no abnormal aggregations or localization. Also, TurboRFP matures rapidly; fluorescence is detectable 8 hours after introduction of DNA (Merzlyak *et al.*, 2007). The use of this reporter in our constructs facilitates screening of founders since it is expressed continuously in the lens after 36 hpf. Therefore, it does not need to be induced in order to identify germ-line transgenic animals, and it has the added benefit of not interfering with our tissue of interest.

Following their creation through multi-recombinant events, injection construct (3 & 4) sequences were confirmed by restriction digestion and sequencing. Plasmid DNA was co-injected with transposase mRNA according to our standard procedure to generate founder fish with the transgene integrated into somatic cells and potentially, into germ cells. Mosaic embryos (i.e. F0 fish with transgene integrations into one or more somatic cells) were raised to adulthood, bred, and their offspring were screened either by Tebufenozide treatment or for presence of the tRFP reporter in the lens. Previous reports using the Gateway system for zebrafish transgenesis suggested this method should produce approximately 50% of F0 founders showing germline transgenesis (Kwan *et al.* 2007). In our hands, the dual transgene construct (*tbx5a*-GFP under GVEcR #4) resulted in 0% transgenesis (of ~188 founders screened) based on detection of GFP after Tebufenozide treatment. As for the second, *hsp701:tbx5a*-GFP (#3) construct, we observed expression of tFRP in F1 offspring of 15% (6/40) of the F0 mosaic embryos. While much lower than the reported 50%, this is very feasible for use in our laboratory. Although we were not

able to utilize this transgenic line for our experiments (explained below), it provided us with some much needed insight during the trouble-shooting process.

The major discovery I made while working on this aspect of the project was that fusion of wildtype *tbx5a* with GFP resulted in unexpected steric effects that eliminate the fluorescence of the GFP. Steric effects occur when atoms from molecules that do not normally associate interfere with each other's preferred shape (Weinhold 2001). In the *Tg(hsp701:tbx5a-GFP)g1* (#3) transgenic fish, we expected to see heat-shock inducible expression of *tbx5a*-GFP. In actuality, we did not even observe GFP in the retina at 48 hpf (where *hsp701* is endogenously expressed), indicating that although the transgene had integrated (as seen by tRFP reporter expression in the lens and confirmed by PCR amplification) any GFP that was produced was apparently not functional (Fig. AI.7). Additionally, although the *hsp701* promoter should have also produced high levels of *tbx5a* expression throughout the embryo, including in the heart, fins, and eye, these fish did not reproduce the overexpression phenotype observed in other experiments (see Fig. 4.10). Similarly, injection of the original pI*hsp70:tbx5a*-GFP and *hsp701:tbx5a*-GFP (#1) constructs, which both produced GFP expression, did not produce *tbx5a*-overexpression phenotypes either. Together, this data indicates that Tbx5a function was altered in these constructs.

We hypothesize that the lack of overexpression phenotype in the pI*hsp70:tbx5a*-GFP and Gateway #1/2 injected embryos was most likely due to the presence of a single-base pair mutation in *tbx5a*, which we discovered upon re-sequencing of the plasmid DNAs. This

mutation resulted in an asparagine (N) to serine (S) substitution at residue 32 (both small polar amino acids), one apparently severe enough to alter *tbx5a* function and/or tertiary structure. Upon discovery of this mutation, I re-amplified wildtype *tbx5a* and used this non-mutated gene in all future constructs. Direct fusion of wildtype *tbx5a* with GFP (such as used in Gateway constructs #3 and #4) ultimately resulted in a lack of detectable GFP fluorescence. We know that GFP was also negatively affected by this fusion, due to the lack of fluorescence. This fusion may also result in inability of *tbx5a* to fold into its functional tertiary structure, but our inability to easily screen for transgenics (due to a lack of GFP) makes testing this hypothesis more difficult. Because this question was not one of the main goals of this project, we did not pursue this line of investigation.

Second attempt using an improved vSlick GVEcR Gateway method (constructs 5-8)

Next, my collaborators and I made two improvements to vSlick approach. The first improvement involved generating two separate transgenic lines (see Fig. AI.8, #5), one containing the GVEcR driver, and the other containing a 10xUAS:*tbx5a*-GFP with the *Cry*:tFP cassette as a marker of transgenesis. This approach provided the advantage that we would have a dedicated "Driver line" that could be used to drive cardiac-specific expression of any UAS-containing transgenic lines we chose to create, and we would also have a separate transgene reporter for our gene of interest. Construct #5 was made with these improvements during the time I was confirming that fusion of *tbx5a* directly with GFP does not work. While it was useful to confirm our steric hindrance hypothesis, we quickly moved on from this construct.

The second improvement was utilization of a viral 2A peptide, a "self-cleaving" peptide, at the recommendation of Dr. Hazel Sive (personal communication). Effectively, insertion of the the 18 aa v2A peptide between two genes allows bicistronic expression from a single transcript because the ribosome skips the synthesis of the glycyl-prolyl peptide bond at the C-terminus of the v2A peptide. This skip ultimately results in the "cleavage" of the Tbx5-v2A peptide from the GFP peptide encoded by downstream residues (de Felipe *et al.* 2010, Donnelly *et al.* 2001, Trichas *et al.* 2008). Therefore, presence of GFP would be indicative of Tbx5 protein in the cell, but this independent reporter protein would not specify the intracellular location of Tbx5.

To begin generation of construct #6 the v2A peptide sequence was PCR amplified using primers containing the v2A nucleotide sequence as well as a portion of the 5' end of GFP and the c366 plasmid. The amplicon was then TA-cloned into pCRII, and the 10xUAS:*tbx5a* coding sequence was then cloned in frame into the multiple cloning site using restriction enzymes. After cloning the 10xUAS:*tbx5a*-v2A-GFP cassette into a middle entry vector (plasmid c237), an LR reaction was performed with plasmids c228, c302, and vSlick to create the final injection construct (Fig. AI.8 construct #6).

Once the injection construct was sequenced to confirm the expected recombination events had occurred, I co-injected *myl7:*GVEcR Driver mRNA (because we did not yet have a germline Driver line), transposase mRNA, and the 10xUAS:*tbx5a*-v2A-GFP #6 injection plasmid. After 2.5 uM Tebufenozide treatment (addition of 10 µl of 10 mM Tebufenoxide to petri dishes containing 24 hpf embryos) I was able to confirm cardiac-

specific GFP expression in mosaic founder fish. This result indicated several things: first, both the *myl7*:GVEcR Driver and 10xUAS:tbx5a-v2ApGFP (#6) constructs translated functional products; second, the Tebufenozide drug treatment was adequate to stimulate the EcR portion of GVEcR; third, that GVEcR bound the UAS promoter and produced a functional GFP at levels easily detected by eye (see Fig. AI.10). Unfortunately, the 10xUAS:*tbx5a*-v2A-GFP construct did not integrate into the genome, resulting in 0% transgenesis (of ~60 fish screened). At the time I was confirming the practicality of the v2A fusion, Dr. Srinivasan created a germline transgenic "Driver line" using vSlack and *Cry*:tFP to confirm the integration of the *myl7*:GVEcR cassette. Two lines, generated from two separate integration events of this construct, are now maintained in our system.

Because I did not identify any germ-line transgenic fish using the construct #6, I made two final constructs (Fig. AI.8 constructs 7 and 8). I decided to create these lines because: 1) there was no reporter for integration of the 10xUAS:*tbx5a*-v2A-GFP construct; 2) I had not identified any germ-line transgenic founders from construct #6 injections; 3) I had recently cloned and sequenced the full-length *tbx5b* from zebrafish and thought I could easily add this gene to my cloning scheme. For these constructs I put *tbx5a*- v2A-GFP (construct 7) or *tbx5b*-v2A-GFP (construct 8) under the control of the 10xUAS promoter, as well as the *hsp701* promoter. In this scenario, either heat-shock or Tebufenozide-induction could be used to stimulate production of the separable *tbx5*-v2A-GFP transgene. Transgenic animals could be easily identified by screening for the non-induced (endogenous) *hsp701* expression in the lens. Experimentally, either heat-shock or EcR-induction could be used to elicit timed expression of Tbx5a or Tbx5b, and could be

used to test both original hypotheses. To create constructs 7 & 8 I directly sub-cloned *hsp701*:10xUAS:*tbx5[a/b]*-v2a-GFP into vSlick to circumvent LR clonase issues. In mosaic founders, I was able to obtain very robust, specific expression of GFP in the heart (Fig. AI.10,11). 95 founders were screened. Unfortunately these constructs did not integrate into the genome (~200 founders screened to date).

Future Work:

Our original experimental question of temporal requirement for cardiac Tbx5a function was answered in part by Liu and Stainier (2010). They generated a heat-shock inducible dominant-negative *tbx5a* transgenic line and used it to determine that *tbx5a* is required in early somite stages for normal cardiac development. However, this series of constructs may still be useful for generation of other constructs. Because we have a stable Driver line, it would be fairly easy to generate other UAS-fused lines. I would recommend utilizing the c394 Destination vector when creating any injection constructs, as we have successfully generated two stable transgenic lines using this vector, whereas we have not had any success with L444, L465, or vSlick.

If one were to continue with this project, there are several experiments that would still be worthwhile. With transgenic embryos in hand, a future researcher will first need to optimize conditions of induction. For the first pilot experiment, one would need to titrate the duration and concentrations of Tebufenozide to obtain maximal gene activation (i.e. *tbx5a* mRNA expression) without inducing secondary defects (such as altered body axis). This could be carried out by Tebufenozide-treating embryos for a period of 5 to 120

minutes and then assessing body shape versus GFP expression every hour up to 48 hpf (protocol based on Connors *et al.,* 2006; Wu *et al.,* 2008). Both the magnitude and the duration of the Tbx5a-v2A-GFP response to a given heat-shock regime would be tracked and optimized. In the second pilot experiment, one would determine the lag time between heat-shock and the appearance of GFP (indicative of Tbx5a-v2A-GFP proteins present in the cardiomyocytes). These pilot experiments should give a clear idea of whether our system achieves a robust expression of the transgene, and how long it persists in the embryo. Understanding these two parameters will help the researcher carefully interpret future results.

Once the pilot studies have been completed, the next step would be to characterize the timepoint(s) at which conditional activation of Tbx5a function is sufficient for proper cardiac development. To do this, one should chemically induce expression in batches of *hst* embryos (~40 per batch), using optimal protocols based on the pilot experiments, at regular intervals between 16 hpf and 48 hpf. These ages represent the period from the onset of endogenous *tbx5a* expression and the beginning of the *hst* cardiac phenotype. Additional stages should be tested as needed. Experiments should be performed on entire clutches of embryos, in order to include the non-*hst* transgenic embryos as internal controls for possible gain-of-function or non-specific phenotypes. Parameters of cardiac function (heart rate, cardiac output, stroke volume) could be assessed by analysis of short video clips of heart motion, as described (Bagatto *et al.*, 2006; Ebert *et al.,* 2005, Kopp *et al.,* 2005). Where appropriate, one should perform statistical analysis (ANOVA or Student's t-test) to assess for significant differences. Cardiac morphology can be

assessed by visualizing transgenic hearts, as described in previous chapters. To evaluate patterning and differentiation in the heart, one would use our standard panels of *in situ* hybridization probes. Pertinent probes include *vcana*, *hand2* and *bmp4*, as well as chamber- and atrioventricular (AV) canal-specific probes (Marques *et al.*, 2008). A careful analysis of chamber-specific markers would be important, because "caudalization" of the heart tube would potentially expand the presumptive atrium at the expense of the presumptive ventricular domain.

Materials and Methods

Staging of Embryos

Developmental time at 28.5°C was determined from the morphological features of the embryo as described by Kimmel (1990): somitogenesis starts around 10 hours post-fertilization (hpf), reaches the 18-somite stage around 18 hpf and the 26-somite stage around 22 hpf. At 24 hpf, embryos have between 29 and 30 somites (Stainier *et al*. 1993).

Generation of transgene cassettes

pI-SceI

The *tbx5a* open reading frame was cloned into the pG1 plasmid, which includes the minimal *cmlc2* promoter and mGFP. The two final injection constructs were obtained through subcloning into the pI-SceIhspMCSpa plasmid. For *cmlc2*:*tbx5a*-mGFP, I used restriction enzymes Sac/lI and NotI, while for *hsp70*:*tbx5a*-GFP I used XhoI. Both constructs are flagged by the I-SceI recognition site TAGGGATAACAGGGTAAT to

facilitate integration into the 1-celled embryonic genome. Injection mix was as follows: plasmid DNA: 10 µg/µl; commercial I-SceI meganuclease buffer (New England Biolabs): 0.5×; I-SceI meganuclease: 1 units/µl; 0.1% rhodamine.

Transformation:

For routine cloning, chemically competent *Escherichia coli* were transformed with at least 10ng of plasmid DNA. Typically 2-5 µl of plasmid were added to 25 µl of the *E. coli* and placed for thirty minutes on ice. Following a 45 second heat shock at 37°C, the transformation mixture was incubated in 250 µl SOC medium in a 37°C shaking incubator for one hour. The cells were then plated on LB plates containing the appropriate antibiotic (usually ampicillin, kanamycin, and/or chloramphenicol) along with 40 µl of 40 mg/ml X-Gal (5-bromo-4-chloro-3-indolyl-beta-D-galactopyranoside), and incubated overnight at 37°C. X-gal was added to the plates if LacZ –mediated color screening was possible, to ensure that colonies did indeed have the gene of interest.

Tol2Gateway

See http://chien.neuro.utah.edu/tol2kitwiki/index.php/Protocols for detailed protocols and information on the structure and sequence of plasmids. The particular plasmids I used are in mentioned by number in the text.

Capped Tol2 transposase mRNA synthesis

The c396 plasmid (pCS2FA-transposase) was linearized using NotI for 1 hour and purified using the Qiagen PCR Purification Kit. A minimum of 1 µg of linearized DNA

was used in each transcription reaction (2 μg is preferable). Capped transposase mRNA was synthesized in vitro using the Ambion mMessage mMachine SP6 Kit (catalog #1340). In vitro transcribed RNA was purified using lithium chloride precipitation, subsequently ethanol precipitated, and resuspended in a final volume of 20 μl of RNase, DNase-free Danieaus solution.

vSlick/vSlack

The methodology for this was nearly identical to that of the other Gateway method, with the following exception: the "Driver" line was produced by the Ken Kramer Lab (NIH, Bethesda, MD).

Screening for germ-line transgenic zebrafish

Heat-shock

Mosaic-injected embryos were raised to sexual maturity (approximately 3 months) and outcrossed to wildtype fish in order to identify stable transgenic carriers. F1 offspring were heat-shocked for 1 hr at 37° C, by incubating the entire clutch in their original petri dish, and observed for the presence of GFP. It was essential to place the dish on the top shelf of the incubator, as well as place it on a rack, to prevent overheating and death of the embryos. Alternatively, F1 embryos could be allowed to mature to 48 hpf at 28° C and scored for the presence of GFP in the eye. The basis for this is that the *hsp70/1* promoter is active under non-heatshock conditions in the lens; thus, transcription from hsp70/1:tbx5-GFP transgenes, if present in the genome, generates a small amount of GFP protein in this tissue.

PCR amplification

To detect the transgene using PCR, genomic DNA was extracted from the tail-fin or whole embryo using a modified Trizol method (see Chapter II) with an additional "back-extraction" step. This back-extraction allows you to isolate DNA out of the aqueous phase. Primers against *tbx5a* (246F), *tbx5b* (323F), and EGFP (254R) were selected to amplify the transgene but not the endogenous *tbx5* gene. Reactions to amplify the usual positive control, *eF1a* (primers 47, 48), were included to ensure that DNA extraction had been successful.

Tebufenozide treatment

10 µl of 10mM Tebufenozide (Sigma) was added to embryos in their existing E3 media. Embryos were screened for fluorescence 3-6 hours after addition of the drug.

I-SceI Meganuclease Method:

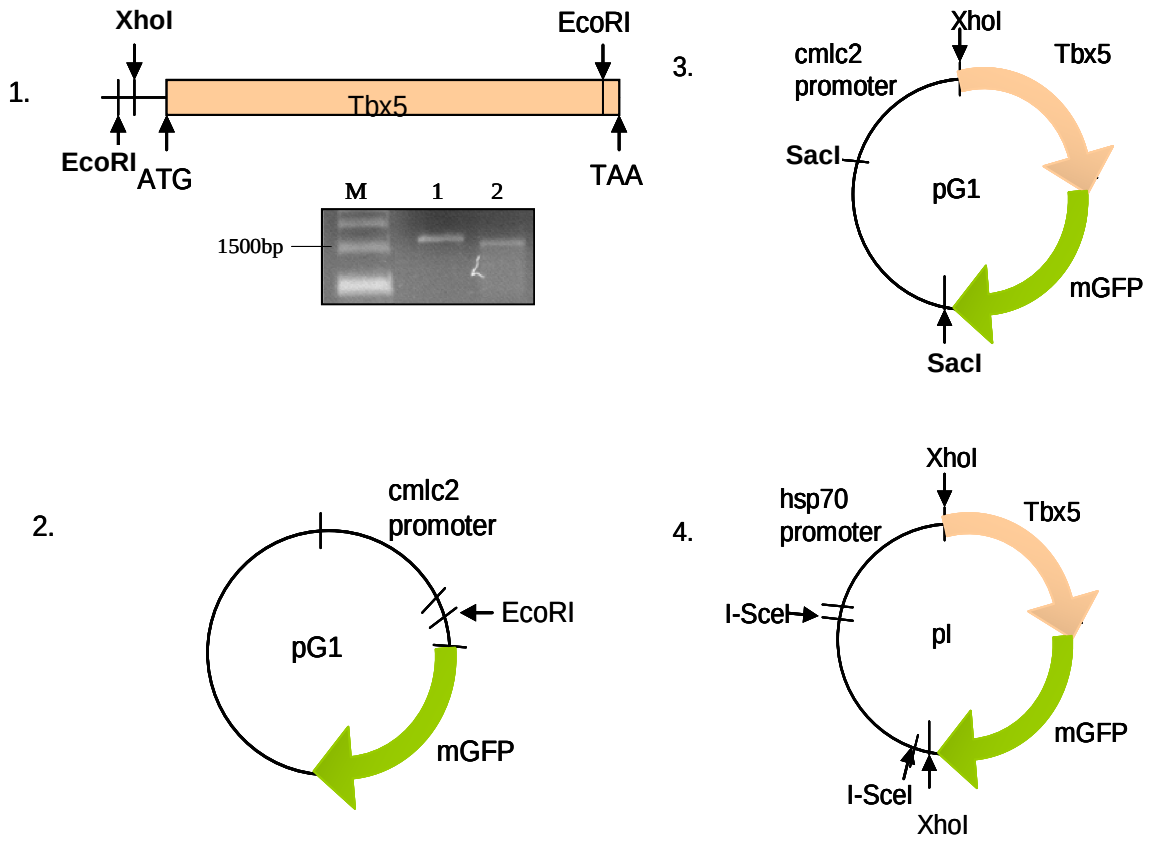

Fig. AI.1: First method of creating transgenic zebrafish embryos via I-SceI meganuclease. I-SceI Method: (**1**) Schematic of full-length wildtype *tbx5a* to include additional restriction sites. Lane 1: Amplified full-length wildtype Tbx5, Lane 2: wt *tbx5a* amplified with primers introducing restriction sites. (**2, 3**) Digested *tbx5a* and pG1 plasmids with EcoRI, ligated, and checked for direction. (**4**) Sub-cloned *tbx5a*-GFP into the pI-SceI plasmid, thereby putting the cassette under the control of the *hsp70* or *cmlc2* promoter, as well as positioning it between the two I-SceI restriction sites. These constructs were then used for I-SceI digestion and microinjection into one-celled zebrafish embryos.

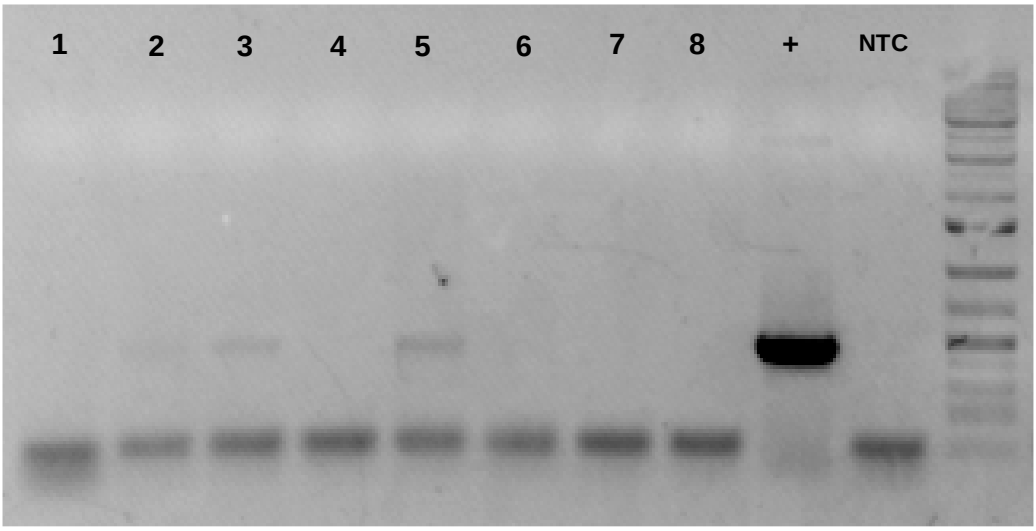

Fig. AI.2: Genotyping *hsp701:tbx5a*-GFP F1 generation by PCR amplification. Embryos with irregular development were collected at 2 hpf and screened for the tbx5-GFP transgene. Samples 2, 3, and 5 have the transgene in dying embryos, suggesting a correlation of transgene and lethality. The surviving siblings did not fluoresce after heat-shock (i.e. GFP was not inducible, suggesting by this second method that these embryos were non-transgenic). + lane: positive control amplification off of p*Ihsp70tbx5a*GFP plasmid. NTC lane: no template control amplification.

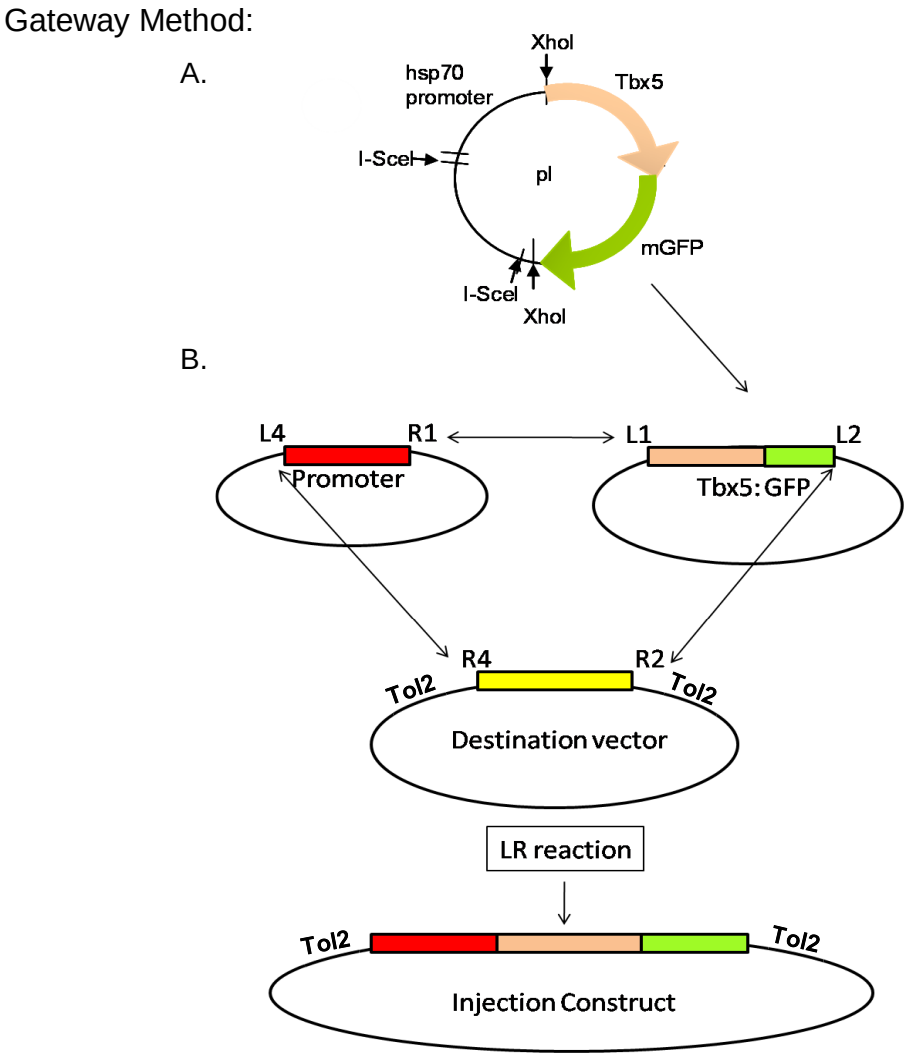

Fig. AI.3: Second method for creating transgenic zebrafish: the Gateway approach. (**A**) The initial pI*hsp70:tbx5a*-GFP plasmid with *tbx5a* cloned in frame with GFP. (**B**) To create the Gateway transgene constructs: 1) The XhoI-digested *tbx5a*-GFP segment (from A) was sub-cloned into Gateway middle entry (ME) vector c237, containing L and R recombination sites. 2. Inserts from the c222 (*hsp701* promoter) or Lister5' (*cmlc2* promoter) and the tbx5a-GFP c237 were combined in an "LR" reaction with the L465 Destination vector using recombinase enzyme. This placed the *tbx5a*-GFP cassette under the control of either the *hsp701* or *cmlc2* promoters and the entire transgene is now flanked by Tol2 recombination sites. 3. This final injection constructs [#1 *hsp701:tbx5a*-GFP or #2 *cmlc2:tbx5a*-GFP] were co-injected with RNA for the Tol2 recombinase enzyme into one-celled embryos. Recombinase should catalyze a recombinant event, mediated at the Tol2 sites, that inserts the transgene into the genome at a random Tol2-containing site.

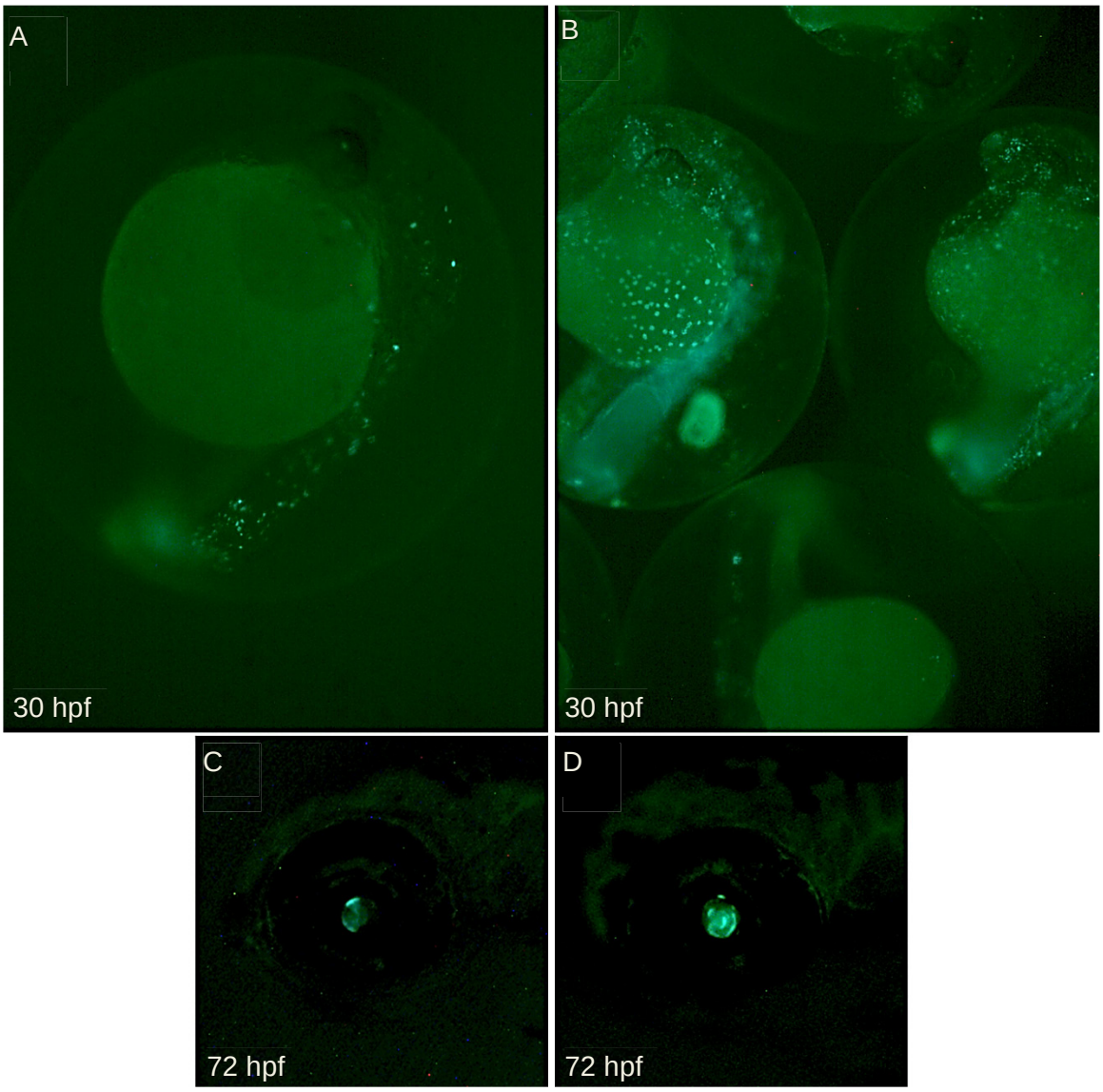

Fig. AI.4: The pI*hsp70:tbx5a*-GFP and *hps701:tbx5a*-GFP (#1) constructs both express GFP and are inducible. When injected at the one-cell stage the Gateway transgene (**B**, construct #1) was expressed more robustly than the same DNA in the pI meganuclease plasmid (**A**). Mosaic-transgenic embryos at 30 hpf were 5-6 hours post-heatshock (phs) and exhibit the strongest *tbx5a*-GFP expression at this phs interval. (**C**, **D**) Endogenous induction of the hsp701 protein in the retina also drives *tbx5a*-GFP expression. This retinal expression is used as an indication of integration into the genome. There is less retina GFP expression in pI*hsp70:tbx5a*-GFP mosaic embryos (C), indicating less efficient integration.

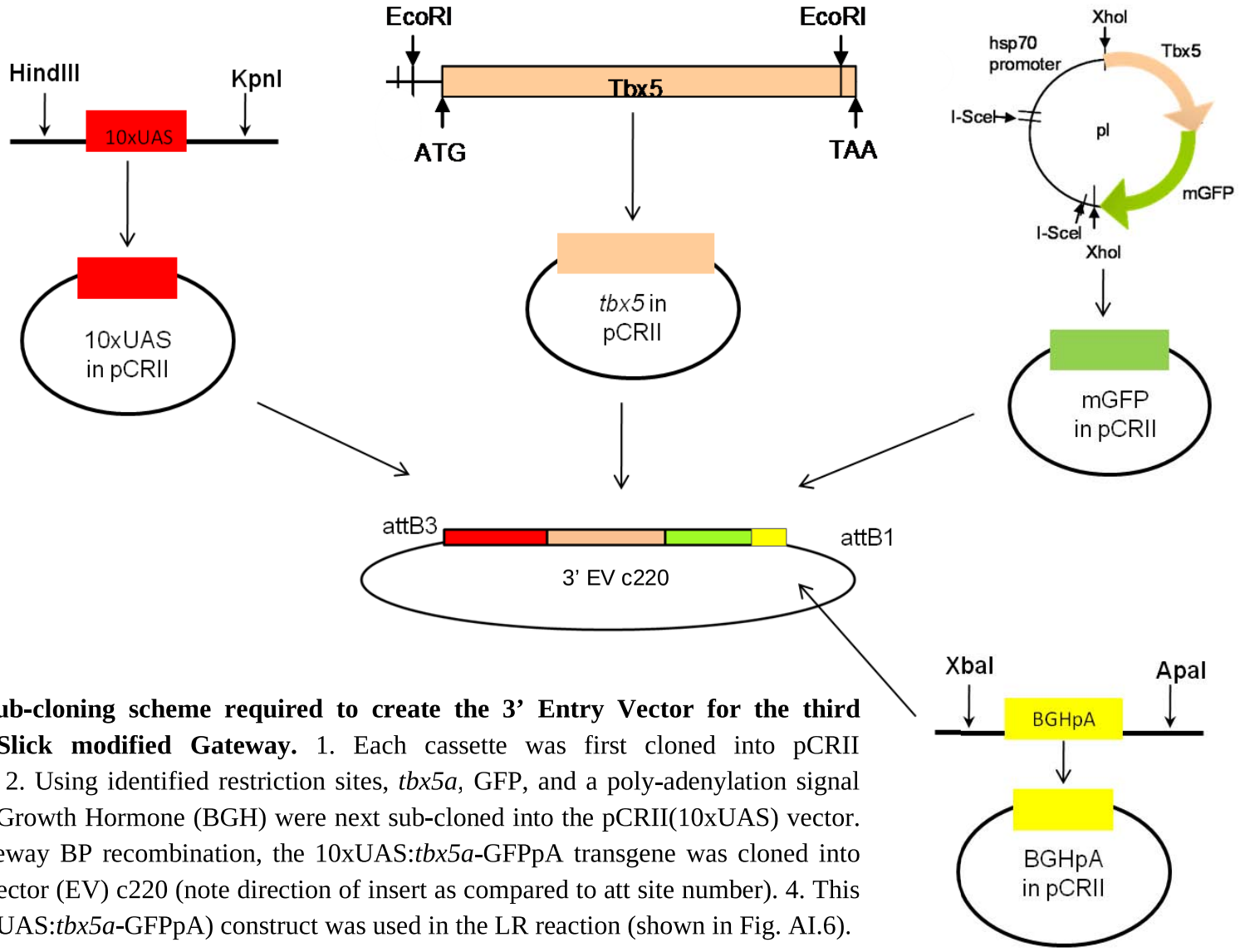

Fig. AI.5: Sub-cloning scheme required to create the 3' Entry Vector for the third method: vSlick modified Gateway. 1. Each cassette was first cloned into pCRII (Invitrogen). 2. Using identified restriction sites, *tbx5a*, GFP, and a poly-adenylation signal from Bovine Growth Hormone (BGH) were next sub-cloned into the pCRII(10xUAS) vector. 3. Using Gateway BP recombination, the 10xUAS:*tbx5a*-GFPpA transgene was cloned into the 3' entry vector (EV) c220 (note direction of insert as compared to att site number). 4. This full c220(10xUAS:*tbx5a*-GFPpA) construct was used in the LR reaction (shown in Fig. AI.6).

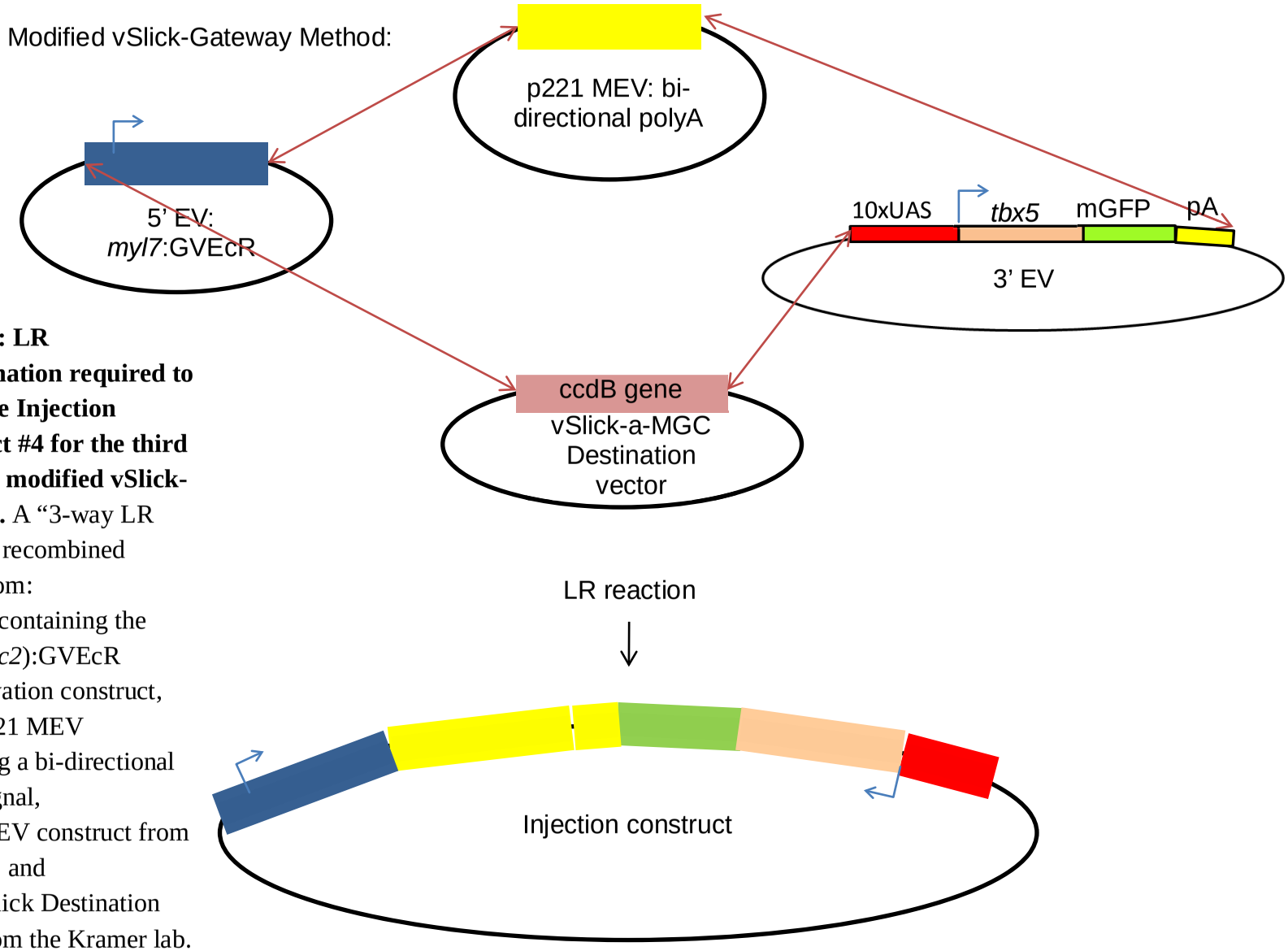

Fig. AI.6: LR recombination required to create the Injection Construct #4 for the third method: modified vSlick-Gateway. A "3-way LR reaction" recombined inserts from:
1) 5' EV containing the *myl7*(*cmlc2*):GVEcR transactivation construct,
2) the p221 MEV containing a bi-directional polyA signal,
3) the 3' EV construct from Fig. AI.5, and
4) the vSlick Destination vector from the Kramer lab.

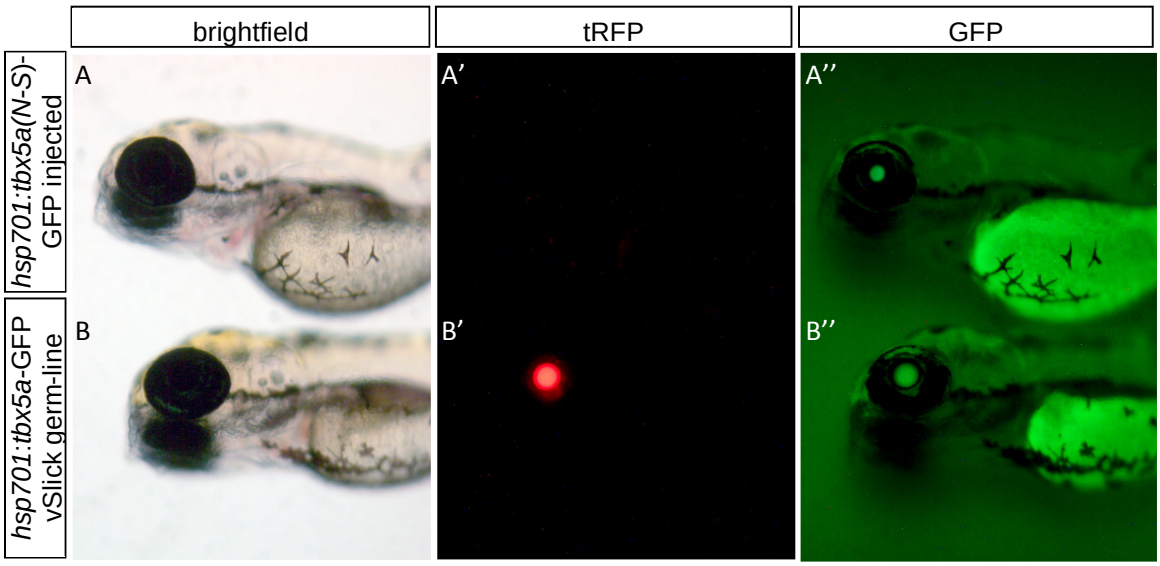

Fig. AI.7: Wildtype *tbx5a* fused with GFP does not fluoresce. (**A**) Top panels show a mosaic-founder embryo injected with the *hsp701*:*tbx5a*(N-S)-GFP (#1) construct. This construct contains a mutant *tbx5a* transgene where asparagine (N) mutated to serine (S) at residue 32. (**A'**) Construct #1 does not contain *Cry*-tFP, therefore this embryo did not have lens-specific tRFP expression. (**A''**) True lens-specific GFP expression at 72 hpf as a result of endogenous *hsp701* induction (note: this embryos was not heat-shocked). (**B**) The bottom panel shows an *hsp701*:*tbx5a*-GFP (#3) germline embryo 5 hr phs. (**B'**) For easier founder screening, *Cry*-tRFP was subcloned in Construct #3 and presence of tRFP in the lens shows that this embryo contains the *hsp701:tbx5a*-GFP transgene. (**B''**) When the *tbx5a* mutation was corrected, the *tbx5a*-GFP fusion protein no longer fluoresces as seen by the absence of GFP in any area of the embryo. The "GFP" in the eye is only bleed-over from the tRFP channel, and the green yolks are autofluorescence of yolk lipids.

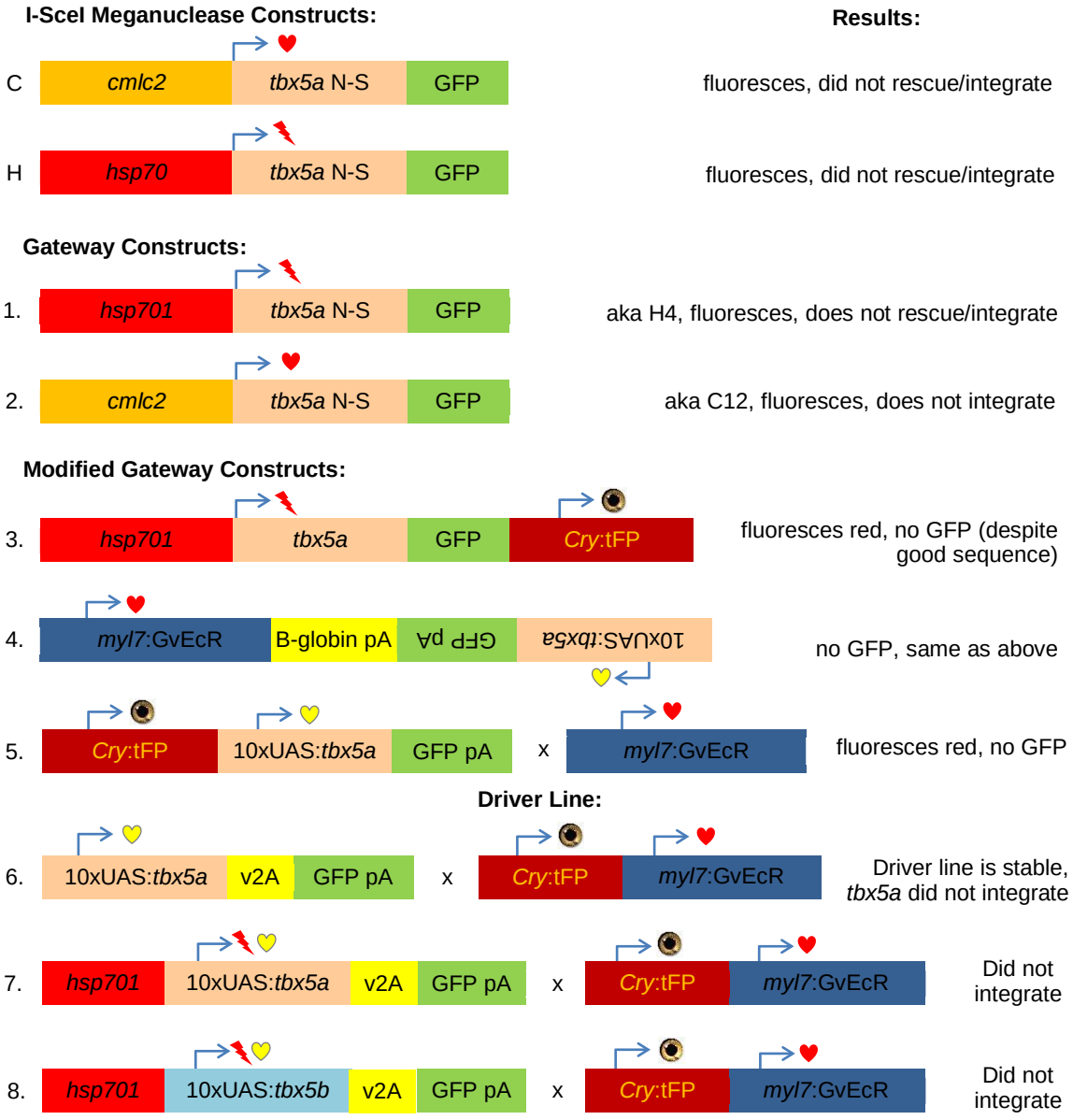

Fig. AI.8: Schematics of Injection Constructs used in attempts at creating viable transgenic animals. The Gateway constructs (**1-3**) were made using components from I-SceI constructs as well as Tol2 kit components. Constructs (**4-6**) were made using components the Tol2 kit as well as "vSlick" and "vSlack" Destination vectors that containing insulators, created by the Dr. Srinivasan in Dr. Kramer's lab at the NIH. Constructs 5-8 require the generation of two separate transgenic lines, which need to be intercrossed to "drive" expression of *tbx5*-GFP in the heart. Red heart: heart specific expression; lightning bolt: heat shock-induced whole-embryo expression (with endogenous eye expression); eye: eye-specific expression; yellow heart: Gal4 Tebufenozide-induced cardiac expression.

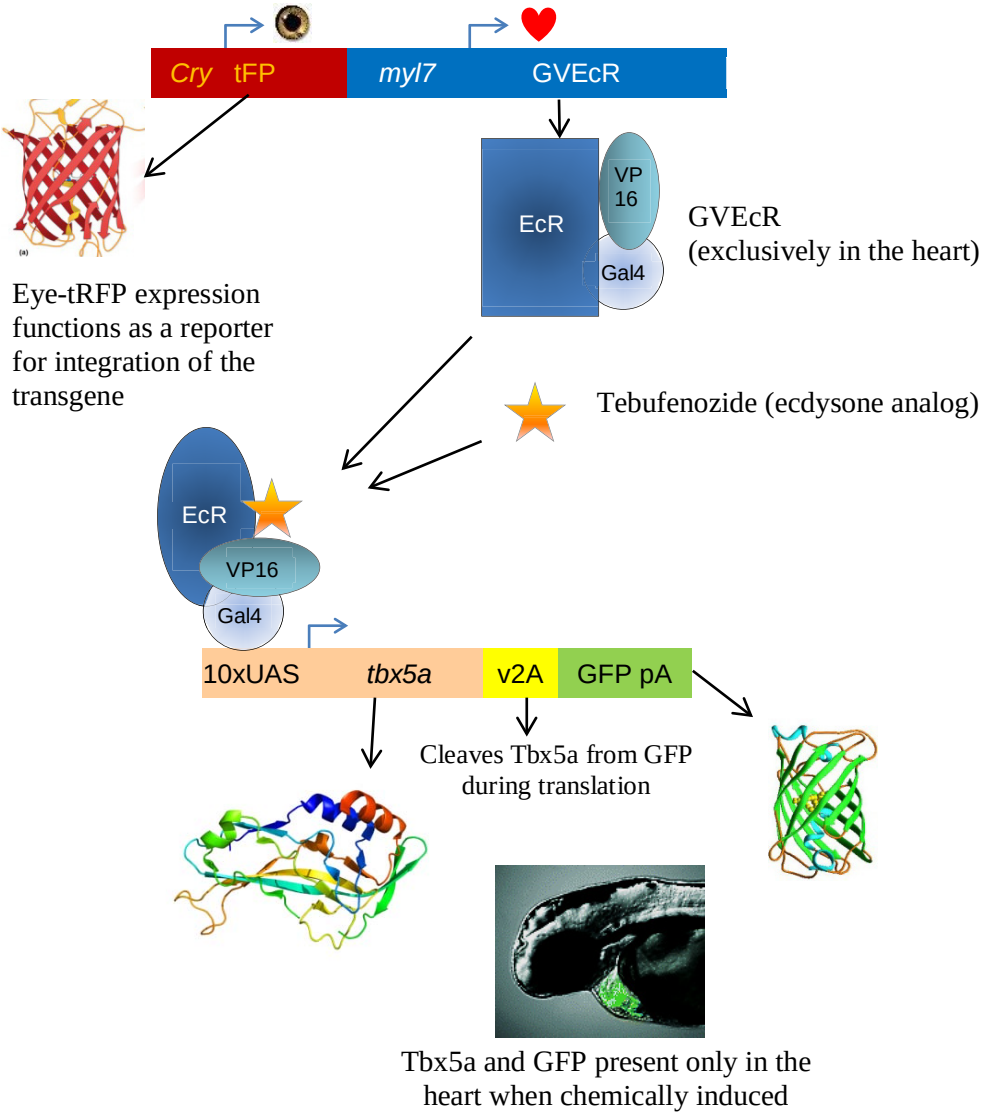

Fig. AI.9: Schematic of construct #6 cardiac-specific induction system. Schematic diagram of the interaction between the two #6 transgenes to generate Tbx5 expression solely in the heart following Tebufenozide induction. Photograph from Esengil *et al.* 2007). Protein structures from:
(http://zeiss.magnet.fsu.edu/articles/probes/anthozoafps.html, http://www-bioc.rice.edu/Bioch/Phillips/Papers/gfpbio.html).

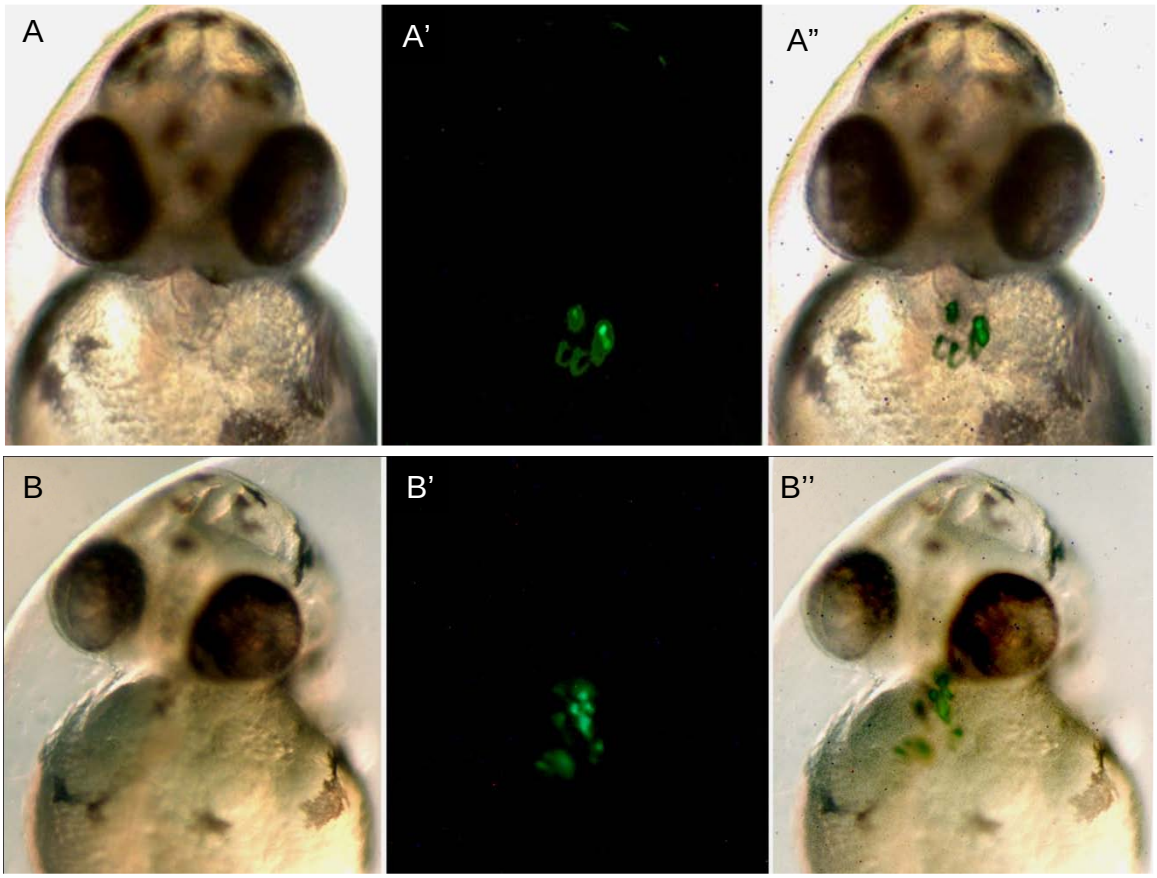

Fig. AI.10: Confirmation that the Drive Line construct is inducible and stimulates construct #6 to encode cardiac specific GFP (vSlick Method). Embryos were co-injected with (*tbx5a*-v2A-GFP, construct #6) DNA, (*myl7*-GVEcR/*Cry* tRFP, Driver Line) mRNA and transposase mRNA. At 28 hpf, the injected embryos were treated with 2.5 µM tebufenozide to induce *tbx5a*-v2A-GFP expression solely within the heart (i.e. wherever GVEcR protein is made). Two examples (siblings) are shown. (**A**, **B**) Brightfield of 36 hpf mosaic-embryos; (**A', B'**) several cardiac cells expressing *tbx5a*-v2A-GFP; (**A'', B''**) overlay.

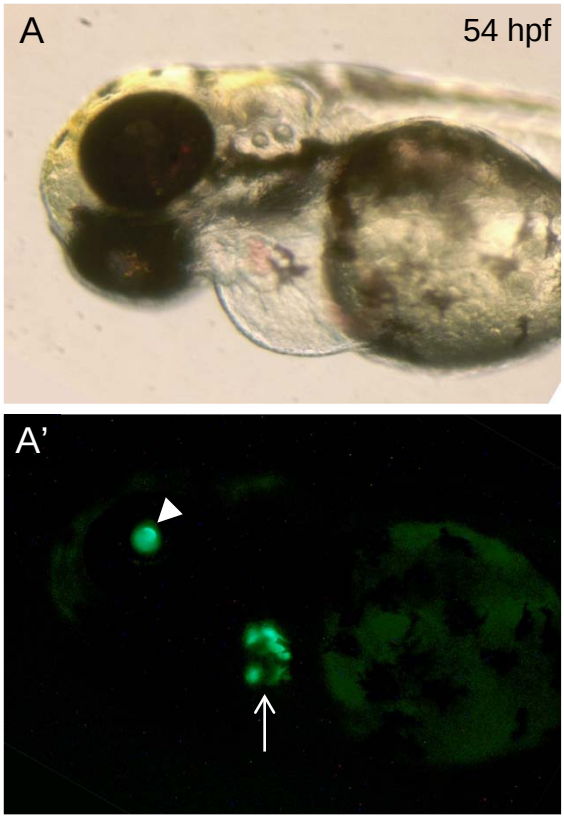

Fig. AI.11: Confirmation of doubly- inducible *tbx5b*-v2a-GFP (construct #8), demonstrating cardiac- and lens-specific GFP expression. vSlick(*hsp701*-10xUAS:*tbx5a*-v2A-GFP, construct #8) DNA was injected into vSlack(*cmlc2*-GVEcR/Cry-tRFP, Driver Line) embryos at the one-celled stage. At 48 hpf, embryos were then treated with 2.5 µM Tebufenozide. (**A**) Brightfield image of an injected embryo. (**A'**) tbx5a-v2AGFP expression. GFP expression is present in the eye (**arrowhead**) as a result of endogenous activation of *hsp701* in the lens from 48 hpf to 76 hpf. Cardiac GFP expression (**arrow**) is a result of the Tebufenozide induction through the *myl7*-GVEcR Driver Line.

APPENDIX II: ALTERNATIVE *TBX5* mRNA SPLICING AND PROMOTER ELEMENT SEARCH.

Introduction

The T-box transcription factor *tbx5* is one of the earliest genes to be expressed in cardiac development and has several known functions in the heart (Stennard and Harvey, 2005; Hatcher and McDermott, 2006). The regulation of *tbx5* is still not completely understood, and the identification of the targets, regulators, and cofactors of Tbx5 would provide a mechanistic framework for researchers to utilize when investigating mutant phenotypes including human HOS and zebrafish *heartstrings*. One surprising regulator of *tbx5* may be Tbx5 itself – a phenomenon described as "autoregulation." One intriguing line of evidence that *tbx5* undergoes autoregulation is found in chick forelimb formation, in which ectopic *Tbx5* expression induced *Tbx5*, *Wnt2b*, and *Fgf10* expression (Ng *et al.* 2002). In cell culture Sun *et al.* (2004) demonstrated the ability of human TBX5 to regulate its own promoter, and further demonstrated direct DNA-protein interactions with potential T-box Binding Elements (TBEs) within the putative Tbx5 promoter. Finally, our lab has found evidence of autoregulation using *in situ* hybridization in the zebrafish *hst* mutant embryo (Krista Lewiki, unpublished). Understanding the mechanisms underlying regulation is important because not all HOS patients have mutations within

the coding region itself (Borozdin *et al.* 2006, Heinritz *et al.* 2005), raising the possibility that mutations in promoter elements could also cause HOS phenotypes.

The aim of this project was to elucidate the cis-regulatory elements that are necessary and sufficient for *tbx5a* expression in the developing zebrafish heart. The work of this chapter was completed by myself and undergraduate researchers Anne Handschy, Kara McCoy and Krista Lewicki. To directly assess cis-regulatory control of cardiac-specific expression, we cloned and sequenced regions of the zebrafish *tbx5a* upstream regulatory region (UPR) and assayed their ability to drive expression of a GFP reporter in the embryonic heart. We show that 5.5 Kb of genomic sequence located 5' to the *tbx5a* coding region is sufficient to drive GFP expression in the heart. No consistent expression was observed in the other sites of endogenous *tbx5a* expression, namely the dorsal retina and pectoral fins, suggesting *tbx5a* expression in these tissues is controlled by separate regulatory modules.

Here, I summarize our findings that although alternative *tbx5a* mRNA transcripts exist in zebrafish, with evidence of 5' alternative splicing. Furthermore, I reveal the presence of TBEs in the enhancer regions of several known and putative Tbx5 target genes. Finally, I provide an update on our *tbx5a* promoter search and demonstrate that use of the Tol2 Gateway system of transgenesis increases specificity of transient GFP expression in these experiments.

Results and Discussion

5’ RACE reveals the presence of additional exons in the UTR of tbx5a *mRNA*

We hypothesized that zebrafish encodes variant *tbx5a* transcripts using alternative first exons. Human TBX5 has three alternatively spliced first exons, with one isoform used predominantly (Basson *et al.* 1999). Because the start codon is present in the second exon, substitution for any these first exons would not affect the protein composition, rather it may affect regulation of *tbx5a* expression. To assay for alternative splicing in zebrafish, I continued work in our lab initiated by Anne Handschy. I amplified *tbx5a* transcripts from 5’ RACE-ready cDNA provided by Dr. Srinivasan and cloned three variants. At least three clones from each transcript variant were sequenced. Comparison of these transcript sequences, combined with those found by Anne, to the zebrafish genome revealed additional exons existed at the 5’ end of the *tbx5a* mRNA (Fig. AII.1). Variation existed in sequences at the 5' end, although all transcripts (with the exception of transcript variant 2) were identical from exon 4 onward. Comparison of the 5' mRNA sequence found matches within the genome, with the exception of exon 2, which suggested these sequences were in fact zebrafish *tbx5a* exons. They were located in *cis* with the *tbx5a* coding sequence on chromosome 15, upstream of the published first exon (labeled as "exon 3" in figure 6.2). The genomic sequence, available on the Ensembl and UCSC Genome Browsers, between exon 1 and exon 3 contained gaps, which may account for the inability to find a match for exon 2 in the zebrafish genome. Exon 2 did not match sequences from the vector database (VecScreen, at NCBI) either. However,

exon 2 was identified independently in clones sequenced by both Anne and myself, which lends strength to the argument that it is a true exon.

An additional anomaly is that exon 3 varied in size between the different transcripts. That is, while the 3'-most exon 3 basepair always aligned with genomic basepair 74125422, the 5'-most exon 3 basepair matched several different genomic basepairs, such that the apparent size of exon 3 ranged from 327 to 440 basepairs in transcripts that also contained an exon 2. Since this sequence is contiguous in the genome, it does not appear to represent additional alternative exons. In addition, we noted transcript variant 2 had exon 2 spliced directly to exon 7, indicating the potential to splice out exon 3 entirely. Potentially, this variation may be due to an artifact in the RACE reaction (i.e. incomplete reverse transcription) or during cloning. Alternatively, these mRNAs suggest the presence of alternative exon acceptor sites, which would then create transcripts with exon 3's of different sizes.

Mice demonstrate two Tbx5 protein isoforms, encoded either by a long transcript with the standard cardiac transcription factor function or a transcript truncated in the activation domain of the C-terminus that has roles in negatively regulating cell proliferation (Georges *et al.* 2008). Our immunoblot studies, which were performed using an antibody against the first 15 translated amino acids (encoded in exon 4) (Anaspec, zebrafish tbx5(NT)) do not support the existence of C-terminus truncated splice variants in zebrafish (Fig. 2.6) because we observed a darkly stained, Tbx5a-specific band at the expected size of 54 kDa. There were several smaller, faint bands, but they were not

present in all wildtype protein preparations and most likely represent degradation products due to the presence of potent proteases in zebrafish embryos. The other, darker bands are not Tbx5a, as they are still present in the immunizing peptide lane. However, this antibody cannot be used to identify alternatively spliced Tbx5a products that do not include the exon 4 start site, because the zebrafish antibody is against the first 15 amino acids of the known protein. There is a second, zebrafish-specific antibody available (Anaspec) that recognizes C-terminal resudes that could be used to look for the presence of these isoforms, including variant 2.

Defining the minimal tbx5a *cardiac promoter*

To complement the above experiments, I initiated a second approach to identify enhancer elements that are necessary and sufficient for cardiac-specific *tbx5a* expression. One of the elements we were looking for was TBEs that would provide evidence for Tbx5a autoregulation. The conserved TBE sequence for Tbx5 is (A/G)GGTGT(C/G/T)(A/G) (Ghosh *et al.* 2001). Using the rVista program (rvista.dcode.org), I identified TBEs in the zebrafish *tbx5a* enhancer region as well as in promoter regions of known and putative downstream targets (Fig. AII.2). To begin fine-mapping of the full 5.5 Kp upstream region of *tbx5a*, we selected 500 bp fragments to sublcone in frame with a GFP reporter and tested them *in vivo* for *tbx5a*-like cardiac-specific expression. The specific constructs we investigated were GFP1, GFP2, GFP3, GFP5, GFP7, and GFP15 (Fig. AII.3). The ultimate goal of these experiments was to narrow down the location of cardiac-specific enhancer elements within a ~500 bp region, similar to the approach taken to identify the minimal *myl7* promoter (Huang *et al.* 2003). This fine mapping will

involve cloning these 5 fragments into the Tol2 Gateway system to drive expression of a GFP reporter (provided by a 3' Entry Vector (EV)).

To create the Gateway clones, Anne cloned "GFP1," the full 5.5 Kb fragment, into plasmid c237 (note: this construct does not contain GFP. "GFP1" originally referred to a plasmid that contained the 5.5 Kb fragment cloned into the pG1 (GFP-containing) plasmid, and the nomenclature became synonymous with the size of the *tbx5a*-promoter fragment being investigated). [Note: plasmid numbers beginning with "c" refer to plasmids received in the starter kit from Dr. Chi-Bin Chien while those beginning with "L" refer to those from the kit from Dr. Nathan Lawson. A full description of all plasmid sequences and components can be found online at http://chien.neuro.utah.edu/tol2kitwiki/index.php/Main_Page]. Anne named this plasmid c237J. The next step was to perform an LR reaction with the c237J plasmid and the c366 plasmid (a 3'EV that contains GFP), confirm the recombination reaction, and perform injections to assay for transient gene expression in F0 mosaic animals. I found that injection of this GFP1-LR construct resulted in expression of GFP predominantly in the developing heart tube at early (24 hpf) and late (48 hpf) timepoints (Fig. AII.4). This was dramatically different from injection of linearized GFP1 in the pG1 plasmid (see Fig. AII.4 top panels) in which GFP is ectopically expressed in cells of the yolk, trunk, and head. This increased specificity in expression is most likely due to earlier integration of the entire transgene when using the transposase in the Tol2Gateway system. GFP expression was not consistently observed in the dorsal retina or pectoral fin, indicating that the 5.5 Kb region was not sufficient to drive expression in those tissues. One possible pectoral fin-specific

module was found by Ng *et al.* (2002), who reported a transcription factor binding site 7.3 Kb upstream of the *tbx5a* start codon that was necessary for *wnt* regulation of *tbx5a* expression in pectoral fin. Transient expression of both GFP1 constructs diminished rapidly after 48 hpf. Surviving embryos were placed in to our system for rearing and screening for stable, germ-line transgensis. Unfortunately, there were no instances of germ-line transmission in the approximately 80 fish screened.

In the process of generating the remaining five promoter constructs various technical issues arose. LR reactions to combine GFP2 and GFP3 with plasmid c366 (which contains EGFP) were unsuccessful, even with new LR clonase II reagents. Sequencing and restriction digest analysis demonstrated that the 3'EV typically did not recombine with the middle entry vector. This appears to be a problem associated with the att sites. There is only a 1 basepair difference between the att site on the 3' EV and the destination vector, which may allow for preferential omission of 3' EV vectors. This phenomenon was observed in other LR reactions (observed in experiments for Appendix I and John Fitts, personal communication). It may also be due to deficiencies in the proprietary LR clonase mix, which contains several recombinases.

In addition to the difficulties with the LR reactions, the limited number of restriction sites in the Gateway vectors made the creation of the smaller promoter fragments difficult. PCR amplification of smaller fragments also proved difficult. Ultimately, attempting to troubleshoot all of these technical issues proved logistically unfeasible due to remaining time constraints, and the project is waiting for a more intrepid investigator.

Promoter collaboration

Our collaborator Ashok Srinivasan at the NIH also hoped to create three "minimal promoter" constructions for use with his vSlick transgenes. The rationale for these constructs was that the *tbx5a* gene is expressed considerably earlier in the developing heart than is *myl7*, the most commonly used promoter available for cardiac-specific transcription studies. The three regions we wished to test were the whole 5.5 Kb fragment, and the two halves, either the distal 3.1Kb or proximal 2.8 Kb length fragments, fused with the GFP reporter. Our lab provided the 5.5 Kb and 2.8 Kb fragments, but we encountered difficulty in regenerating the 3.1 fragment from our stocks. I was to inject the Gateway constructs once they were made and screen for germline transgenesis. However, the project was put on hold when Dr Srinivasan moved to a new position.

Future studies:

Although this series of experiments has proved technically challenging, not only for our lab but also for our collaborators, I would recommend this as a project only to someone who is experienced with various cloning techniques and has a significant amount of time to contribute to it. Because use of the Tol2 Gateway kit increased specificity and strength of the transient expression, I would recommend continuing with this technique, but utilizing plasmids that have previously worked in our lab (c366, c394, etc). I would also recommend determining a more efficient method of inserting promoter fragments in to the Gateway vectors, as restriction digestion/ligation appears to be very inefficient.

Once the ability of genomic fragments to drive GFP expression in mosaic embryos has been established, it will be important to determine whether conserved transcription factor binding sites (such as TBEs) within the promoter fragments are necessary for cardiac expression *in vivo* expression or for luciferase *in vitro*. To identify candidate binding sites, the regulatory elements that displayed the most consistent GFP expression in transient transgenics (i.e mosaic embryos) would be analyzed for conserved (or cardiac-specific) transcription factor binding sites using the rVista program (Fig. AII.2). These sites would be mutated using site-directed mutagenesis (Strategene Quikchange kit) to alter 1 to 3 base-pairs to effectively destroy transcription factor binding and determine if these sites are functionally relevant to *tbx5a* expression in the developing heart. This experiment would also allow us to definitively address *tbx5a* autoregulation in zebrafish cardiac development.

In conclusion, our studies to date suggest that there is no single, cardiac-specific enhancer region that independently drives robust *tbx5a* expression. Instead, we observed that the degree of cardiac expression correlated with the length of the enhancer fragments, where longer portions correlated with increased frequency of cells showing cardiac GFP expression. This result is consistent with a potential requirement for multiple interacting regulatory elements that collectively drive *tbx5a* cardiac expression. In contrast, the 5.5 Kb fragment provided no consistent expression of GFP in the eye or pectoral fin, suggesting *tbx5a* expression in these tissues is controlled by separate regulatory modules.

Materials and Methods

RACE amplification and sequencing

5' RACE-Ready cDNA was prepared by Dr. Ashok Srinivasan. Using Advantage 2 polymerase, primers 239F (UPM) and 238R, 5' RACE was performed as recommended by the manufacturer (Clontech). Resulting bands were gel extracted, purified (Qiagen) and sent to the Proteomics and Metabolomics Facility at CSU. Sequences were then blasted against the zebrafish genome to assign exon-intron boundaries.

Creation and analysis of transient transgenics

The original pG1 vector containing the 5.5 Kb of *tbx5a* promoter/enhancer region fused upstream the green fluorescent protein (GFP) gene was kindly provided by Dr. Chi-Bin Chien (University of Utah). This construct, designated pG1-5.5Kb, also contains an ampicillin resistance gene. This 5.5 Kb fragment was sub-cloned to create all subsequent constructs. See the notebook of Anne Handschy for methods on creating the First Generation constructs. For the Gateway clones, we performed EcoRI restriction digests of "GFP1" to insert the fragment into c237. This clone was called c237J by Anne (and it is important to note that it does not contain GFP) and was used in an LR recombination reaction with c366 for insertion into the L444 backbone. This is a "2-way" recombination reaction. This construct was injected into wildtype embryos at the one-celled stage and the resulting mosaic embryos were quantified for presence of cardiac-specific GFP expression before being reared to adulthood.

Microinjection

All injections were performed using a Femtojet micro-injector (Eppendorf). Injection volumes ranged from approximately 30 picoliters to 5 nl. Borosilicate microinjection needles were pulled using 0.74 mm capillaries (World Precision Instruments) on a Sutter P97 Flaming/Brown Micropipette puller. Settings were: Heat (715), Pull (60), Velocity (80), Time (200).

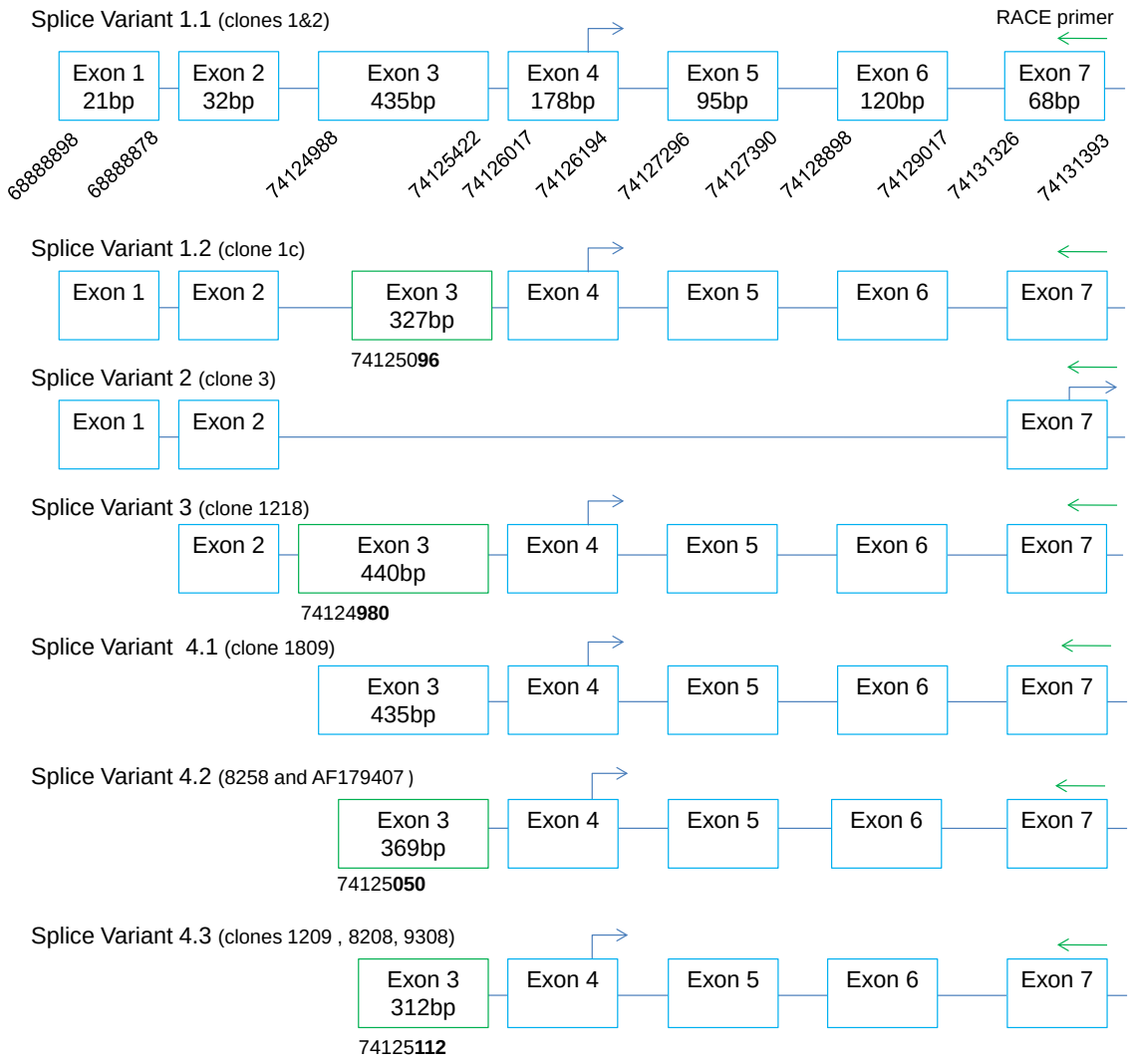

Fig. AII.1: Alternative splicing occurs in the 5' region of *tbx5a*. The largest transcript variant was designated as Splice Variant 1.1. Our numbering of the exons in this figure represents new nomenclature, as published reports denote that transcription begins in "Exon 2," which is equivalent to Exon 4 in this diagram. All exons except the new Exon 2 matched sequences found on the 15th chromosome. Exon 2 was present in multiple different clones, but did not find any match in a genome blast search. Splice variant 4.2 matches the published sequence (accession number provided).

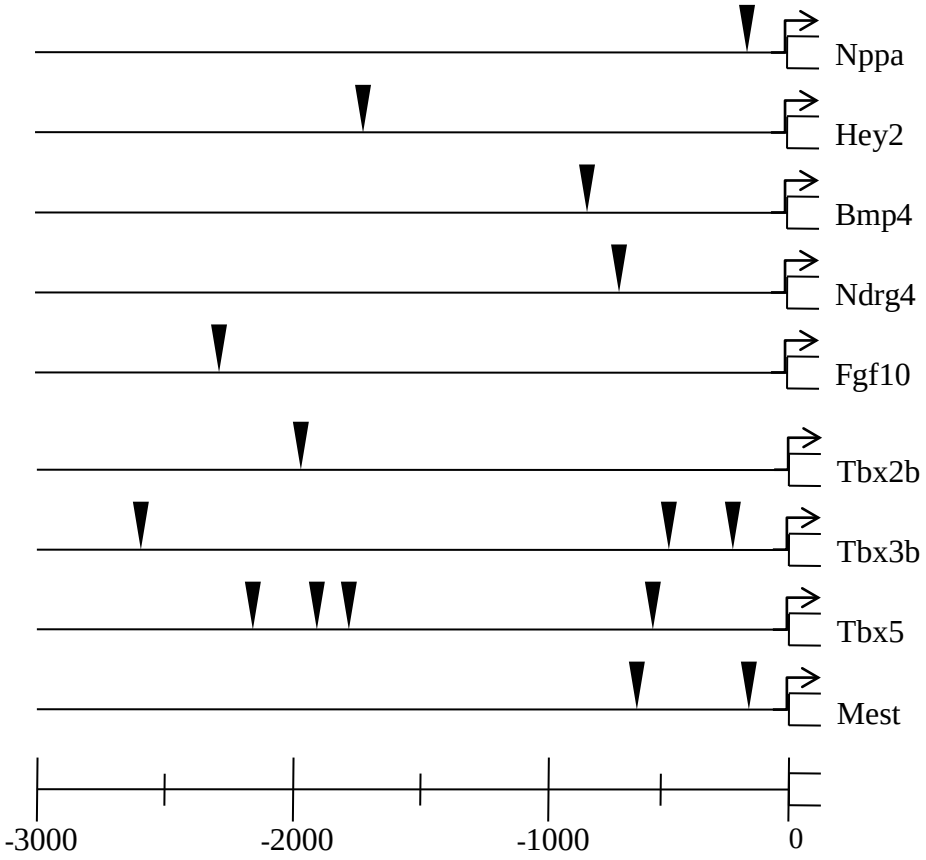

Fig. AII.2: T-box Binding Elements (TBEs) are present in the promoter regions of candidate downstream target genes. Arrowheads denote the presence of TBE(s) in the upstream promoter sequence of both known and candidate Tbx5a target genes. The list was compiled using rVista software.

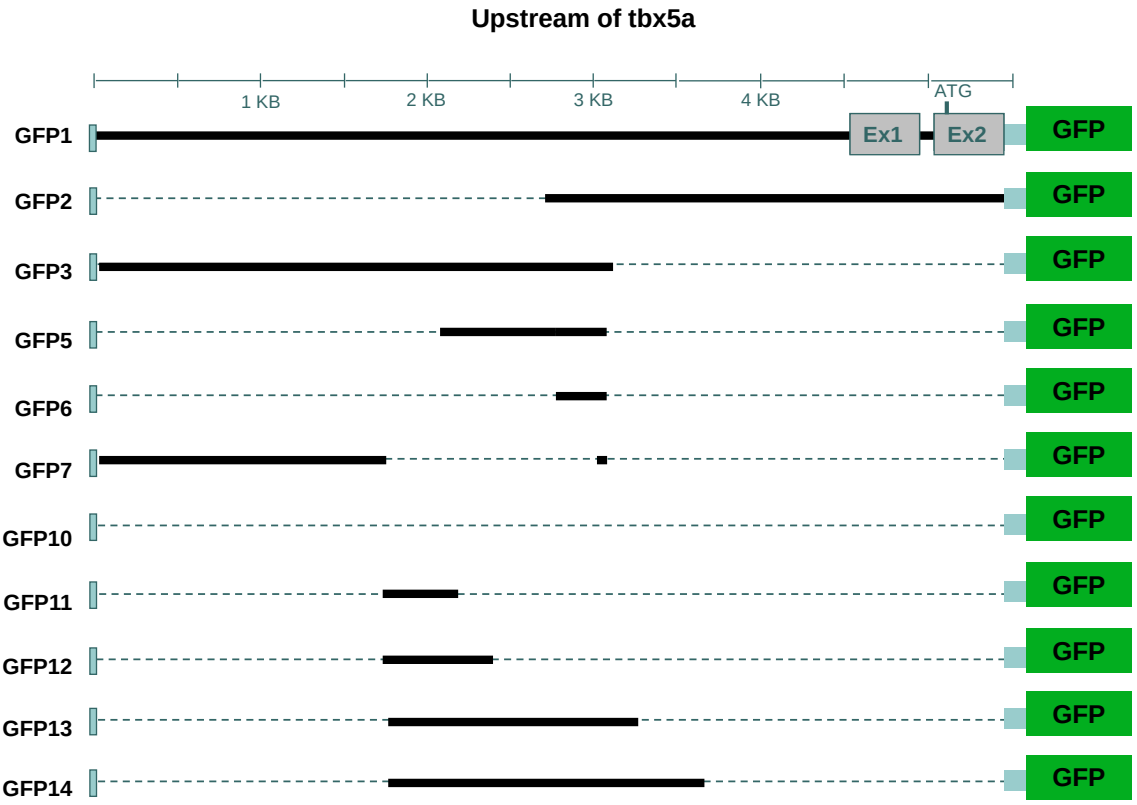

Fig. AII.3: Identifying the necessary *cis*-regulatory domains upstream of *tbx5a*. Diagram showing 5.5Kb of upstream non-coding sequence, as well as the first two exons (Ex, gray boxes). Black bars represent portions of genomic fragments cloned in frame with GFP coding sequence. Dotted lines represent excised sequence. Blue boxes represent pG1 plasmid sequence.

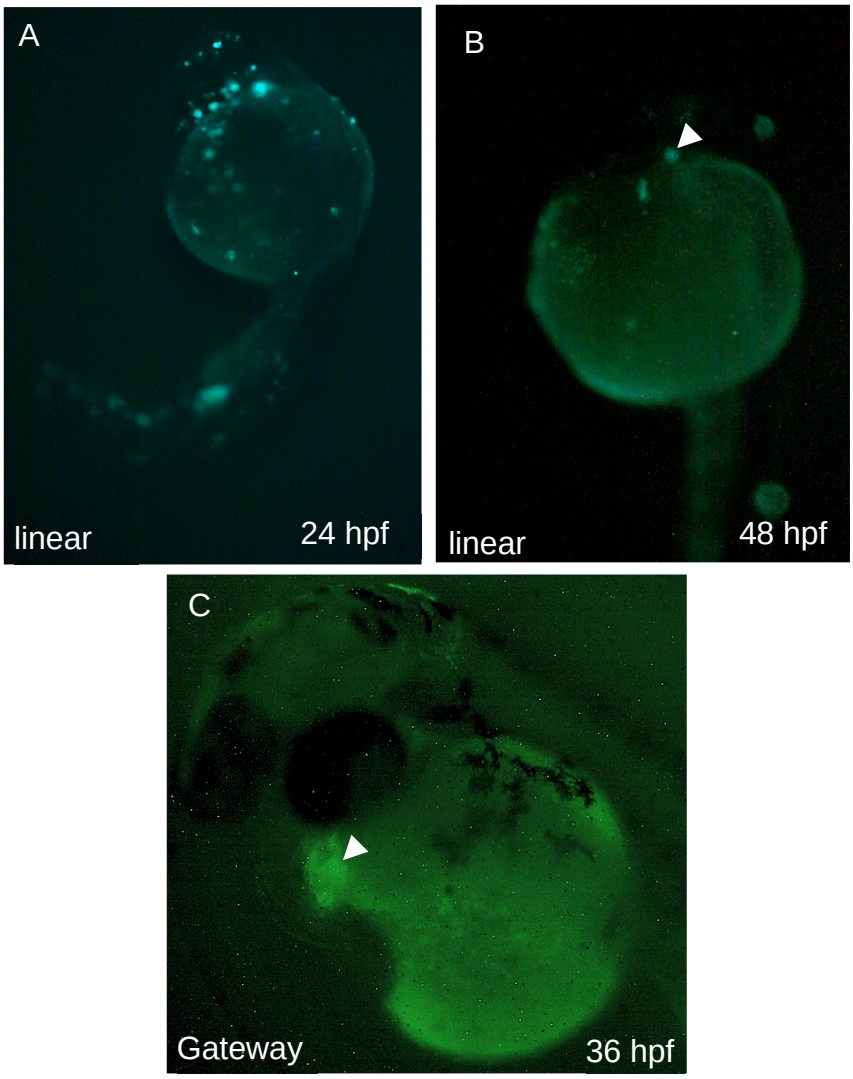

Fig. AII.4: Use of Gateway technology increases level and specificity of transient expression of *tbx5a*UE-GFP transgenes. Transiently transgenic fish expressing GFP, injected with GFP1 DNA that was either linearized (**A**, **B**) or co-injected with transposase mRNA (**C**) at the one-celled stage. Arrowheads = cardiac-specific GFP.

List of Abbreviations:

AP	anterior-posterior (refers to fish axis)
BCIP	5-bromo-4-chloro-3-indolyl-phosphate
BSA	bovine serum albumin
DEPC	diethyl pyrocarbonate
dH_2O	distilled water
DIG	digoxigenin
DMSO	dimethyl sulphoxide
dpf	days post fertilization
D-V	dorso-ventral
E3	embryonic medium
EDTA	ethylenediaminetetraacetic acid
EtOH	ethanol
EV	entry vector, used in the Tol2Gateway system (designated 5', ME, or 3')
GFP	green fluorescent protein
GVEcR	Gal4- Virus regulatory protein- Ecdysone Receptor transactivator
hpf	hours post fertilization
hst	*heartstrings*, *tbx5* mutant line
HRP	horseradish peroxidase
HS	heat shock
hst	*heartstrings* (Tbx5a.1 homozygous mutant embryos)
ME	middle entry vector, used in the Tol2Gateway cloning system
MeOH	methanol

MESAB	ethyl-*m*-aminobenzoate methanesulphonate
NaAc	sodium acetate
NBT	4-nitroblue tetrazolim chloride
NFDM	non-fat dry milk
PBS	phosphate-buffered saline
PCR	polymerase chain reaction
PTU	1-phyenyl-2-thiourea
RT	reverse transcription
TBS	Tris buffered saline
TE	Tris, EDTA
WIK	wildtype strain of zebrafish
YSL	yolk syncytial layer